Cloning of two neurally expressed genes found adjacent to P[GAL4]307, a marker of the giant fibre circuit, in *Drosophila melanogaster.*

A thesis submitted for the degree of
Doctor of Philosophy
at the University of Warwick.

by

James A. Drummond, B.Sc. (Hons).

Department of Biological Sciences
University of Warwick

January 1999

For Rosalind.

List of Figures.

List of Tables:

Acknowledgements.

I would like to thank, first and foremost, Dr Marcus Allen for his excellent friendship, help and collaboration. My thanks also go to all the other members of the group and department who have made my time at Warwick so memorable and enjoyable. In particular I would like to thank Jane, Gav, Phil, Dylan, Stu , Tricky and Ahmet. For funding and support thanks has to go to my parents and Dr Moffat.

Mostly I would like to thank Ros for her unending patience with me and for her unfailing support.

Declaration.

I hearby declare that all the work reported in this thesis is my own unless stated otherwise in the text. None of this work has been previously submitted for any other degree or at any other institution. All sources of information used in the preparation of this thesis are indicated by reference.

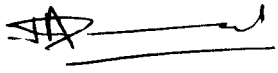

James A Drummond.

Summary.

The enhancer trap line P[GAL4]307 was isolated on the basis of expression in the giant fibres. It has proved to be an elegant marker of giant fibres in adult *Drosophila*. The giant fibres (GFs) are part of a simple circuit in the fly's central nervous system (CNS) that mediate a light-off escape response involving a jump and wing beat.

Detailed analysis of the adult expression pattern, using antibodies to the products of the genetic elements used in enhancer trapping, has revealed that all the major components of the escape circuit are clearly detectable. Subsequently, the development of this circuit has been traced using the same antibody staining techniques, revealing the timing of circuit establishment and the developmental profiles of each component neuron. To complete this profile the birthdating of the GFs has been attempted. The overall aim of this section of work was to map the circuit from the first cell division producing the major neurons in embryos, through establishment of the circuit in pupae to full development of the active circuit in adults.

The second major section of work has been the cloning of genes from DNA surrounding the P-element insertion. An important facet of P-element design is the ability to use it to remove the genomic DNA from around the site of insertion. A probe created from a fragment of this genomic DNA has been used to screen a library. This yielded a cDNA that, in combination with subsequently isolated cDNAs, forms a contiguous stretch of DNA approximately 4Kb in length. A translation of the cDNA has revealed homology with proteins from a range of eukaryotes from yeast to humans. These may form a family of elongation initiation co-factors. On the basis of homology with an *Arabidopsis thaliana* gene *argonaute*, this new *Drosophila* gene has been named *diomedes*.

The genomic region has also been sequenced, revealing another gene close to *diomedes*. This new gene, LD07701, appears to be full length, and is unusual because it may be a non-coding RNA.

Both genes isolated have neural expression in embryos, larvae and pupae, although it appears neither is the gene whose expression is reflected by the enhancer trap pattern.

Abbreviations:

ABD: abdominal region of the ventral nerve cord.

AEL: after egg laying.

ALH: after larval hatching.

Amp^{R}: ampicillin resistance gene.

APF: after pupa formation.

APS: ammonium peroxidisulphate.

AS-C: acheate-scute complex.

BDA: biotin labelled dextran amine.

BDGP: Berkeley *Drosophila* Genome Project.

ben: *bendless*.

BLAST: basic local alignment search tool.

BrdU: 5-bromo-2-deoxyuridine.

BSA: bovine serum albumen.

CAM: cell adhesion molecule.

cDNA: complementary deoxyribonucleic acid.

Ci: curie.

CNS: central nervous system.

Comm: Commissureless.

CyO: Curly of Oster.

D: deuterocerebrum.

DAB: diamino benzoate.

dATP: deoxyadenosine triphosphate.

dCTP: deoxycytidine triphosphate.

DGI: dorsal giant interneuron.

dGTP: deoxyguanosine triphosphate.

dH_2O: distilled water.

Dig: digoxygenin.

Dl: Delta.

Dlg: Discs-large.

DLM: dorsal longitudinal muscle.

DLMn: dorsal longitudinal motorneuron.

DMD: dorsal medial dendrite.

DNA: deoxyriobonucleic acid.

DNAse: deoxyribonuclease.

dNTP: deoxynucleotide triphosphate.

dock: *dreadlocks.*

dpp: *decapentaplegic.*

dTTP: deoxythymidine triphosphate.

dTTP: deoxythymidine triphosphate.

dUTP: deoxyuricil triphosphate.

E(SPL)-C: *Enhancer of Split Complex.*

ECM: extracellular matrix.

EDTA: ethylene diamine tetra acetic acid.

eIF2: elongation initiation factor 2.

eIF2C: eIF2 co-factor (also called Co-eIF-2A).

en: *engrailed.*

EST: end sequence tagged cDNA.

EtOH: ethanol.

eve: *even-skipped.*

GCI: giant commissural interneuron.

gcm: *glial cells missing.*

GF: giant fibre.

GFCB: giant fibre cell body.

GFP: green fluorescent protein.

GFS: giant fibre system.

GMC: ganglion mother cell.

HRP: horseradish peroxidase.

IB: inframedial bridge.

insc: *inscuteable.*

l(1)ogre: *lethal (l) optic ganglion reduced.*

L1: first instar larva.

L2: second instar larva.

L3: third instar larva.

LB: Luria-Bertani medium.

LTR: long terminal repeat.

M: molar.

MAGUK: membrane-associated guanylate kinase.

MCS: multiple cloning site.

mM: millimolar.

MOPS: 3-[N-morpholino] propane sulphonic acid.

mRNA: messenger RNA.

N: Notch.

NB: neuroblast

NBT: nitro blue tetrazolium.

ncRNA: non-coding RNA.

NICD: Notch intracellular domain.

NMJ: neuromuscular junction.

NTP: nucleotide triphosphate.

NZYM: 1%(w/v) NZ amine/ 0.5%(w/v) NaCl/ 0.5% (w/v) yeast extract / 0.2% (w/v) $MgSO_4$.

OD: optical density.

OPUS family: *l(1)ogre*, *passover/shaking-B*, *unc-7*.

ORF: open reading frame.

ori: plasmid origin of replication genes.

P: protocerebrum.

P1-12: pupal stages 1-12.

Pas: Passover.

PAT: PBS/BSA 1%/Triton X-100.

PBS: phosphate buffered saline.

pBSK: pBluescript vector.

PBS-Tw: phosphate buffered saline with 0.1% Tween 20.

PBS-TX: phosphate buffered saline with 0.1% Triton X-100.

Pc1: central procephalic neuroblast 1.

PCR: polymerase chain reaction.

PEG: poly ethylene glycol.

pfu: plaque forming units.

Pgc: *polar granule component.*

pGH4.2: genomic *Hin*dIII fragment cloned into pGEM-72f (+).

pKpnI: *Kpn*I plasmid rescue clone.

PLD: posterior lateral dendrite.

PNE: procephalic neurectoderm.

PNS: peripheral nervous system.

pros: *prospero.*

PSI: peripherally synapsing interneuron.

repo: *reverse potential.*

rRNA: ribosomal RNA.

RNA: ribonucleic acid.

RNAse: ribonuclease.

Robo: Roundabout.

rpm: revolutions per minute.

RPTK: receptor protein tyrosine kinase.

RPTP: receptor protein tyrosine phosphotase.

RT-PCR: reverse transcription PCR.

ry: *rosy.*

SDS: sodium dodecyl sulphate.

Shak-B: Shaking-B.

snRNA: small nuclear RNA.

snoRNA: small nucleolar RNA.

sog: *short gastrulation.*

SSC: salt/ sodium citrate buffer.

SuH: Supressor of Hairless.

T: tritocerebrum.

T1: prothoracic neuromere.

T2: mesothoracic neuromere.

T3: metathoracic neuromere.

TBE: 0.9M Tris.borate pH 8.3, 20mM EDTA.

TE: 10mM Tris.HCl pH 7.5, 1mM EDTA.

Tris:	tris(hydroxymethyl)aminomethane.
TRITC:	tetramethylrhodamine isothiocyanate.
tRNA:	transfer RNA.
TTM:	tergotrochanteral muscle.
TTMn:	tergotrochanteral motorneuron.
TTMnCB:	tergotrochanteral motorneuron cell body.
U.V.:	ultraviolet.
UAS:	upstream activating sequence.
UAS:	upstream activating sequence.
UBC:	ubiquitin conjugating enzyme.
VLD:	ventral lateral dendrite.
VNC:	ventral nerve cord.
VNE:	ventral neuroectoderm.
WCS:	white Canton specials.
wg:	*wingless*.
WPP:	white pre-prepupa.
X-gal:	5-bromo-4-chloro-indolyl-β-D-galactosidase.
X-phosphate:	4-chloro-3-indoyl phosphate.
(v/v):	volume / volume.
(w/v):	weight / volume.

1. Introduction.

The central theme of this thesis is developmental neurobiology of *Drosophila melanogaster*. This introductory chapter aims to give a brief overview of the major stages in the development of a fly's nervous system, from specification of a neurogenic region to establishment of neural connectivity. Enhancer trapping will be introduced, as will its use in studying particular facets of neural development. A specific model neural circuit (the giant fibre circuit) the central feature of this study, is also presented here.

1.1 Neurogenesis.

Drosophila is a holometabolous insect and as such neurogenesis proceeds in two stages; embryonic and postembryonic. The first stage produces the larval nervous system, whilst the second transforms the larval nervous system into the adult nervous system. These stages include many of the same processes, such as axon guidance and synaptogenesis. However, production of the adult central nervous system (CNS) transforms a CNS adapted for one body form to a CNS suitable for a very different body plan, with correspondingly different sensory and behavioural requirements. Consequently the metamorphosis includes the disassembly of the larval CNS and the construction of the adult CNS.

This section of the introduction will introduce the processes involved in both stages of CNS formation. CNS development throughout the life of a *Drosophila* is presented in figure 1.1 (Hartenstein 1993).

1.1.1 Embryonic neurogenesis.

1.1.1.1 Staging embryonic development.

Drosophila embryos develop to larvae in 17 distinguishable stages that cover approximately 18-24 hours (Bownes 1975,1982, Campos-Ortega & Hartenstein 1985, Hartenstein 1993). Stage 1 blastoderm embryos are syncitial and cellularise to form the cellular blastoderm by stage 5. Gastrulation proceeds from stage 6 to stage 7 (forming the germ layers) with germ band extension

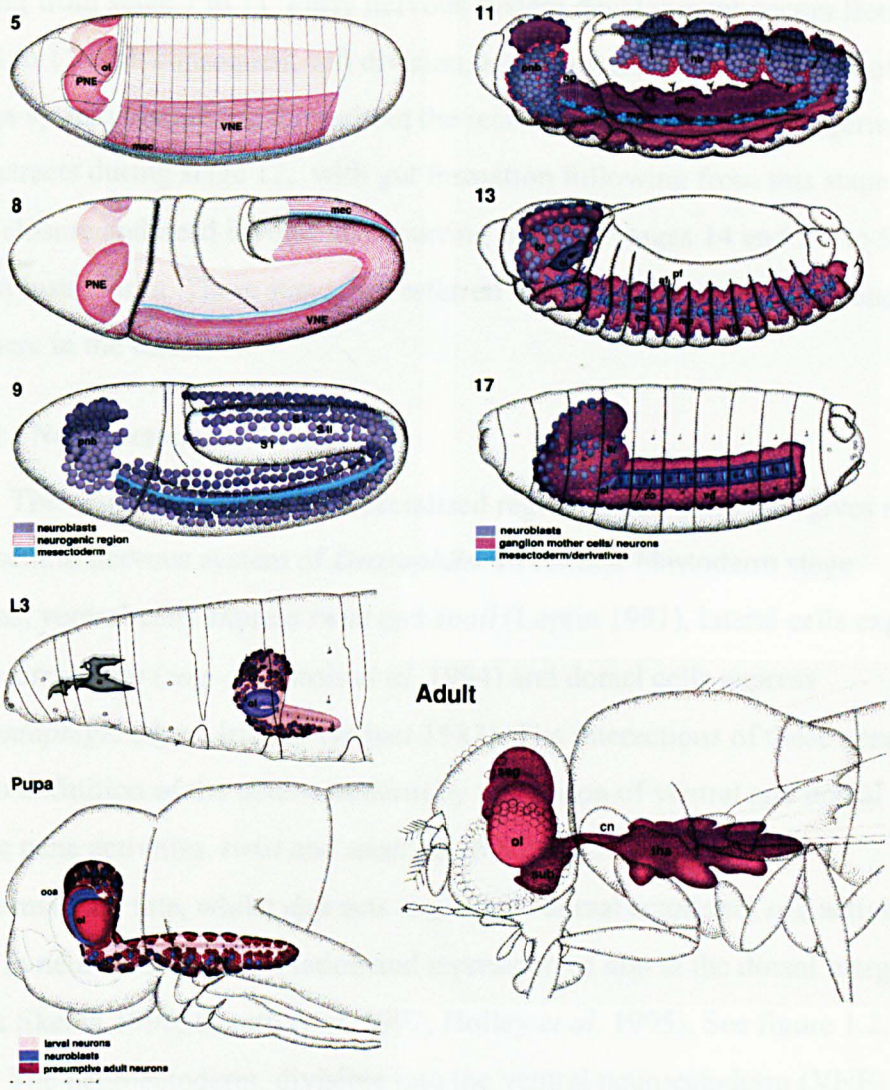

Figure 1.1: Diagrams of the developing *Drosophila* CNS throughout development.
The neuroblasts are the precursors of the nervous system derived from the neurogenic ectoderm. This is apparent in 2 regions : the ventral neurogenic (VNE) and the procephalic neurogenic region (PNE) – Stages **5** and **8**. The mesectoderm (mec) is a single row of cells that gives rise to some neuronal precursors. The optic lobe anlage (ol) develops differently to the rest of the PNE. The first 2 waves of neuroblast delamination, starting at stage **9**, are shown forming 3 rows of neuroblasts (S1 and S2). Procephalic neuroblasts also delaminate in a cluster (pnb).
The neuroblasts (nb) divide asymmetrically to produce ganglion mother cells (gmc) that then produce the neurons. The mitosis taking place in stage **9** to **11** produce a nerve cord that is the length of the germ band extended embryo. This then retracts at stage **13**, condensing until the end of embryogenesis producing a compact and complex nervous system, with features such as connectives (cn), commissures (co) and fascicles (af/pf) in the ventral ganglia (vg).
The optic lobe precursors (op) form a vesicle (ol) attached to the basal surfaces of the brain hemispheres (br).
The morphogenetic changes can be seen as the CNS develops further in the third larval instar (**L3**) and **pupa**. Neuroblast divisions produce new neurons whilst cell death trims away the elements of the CNS that were used in the larva but are not required for the **adult**. The CNS resulting differs greatly from the larval form with a distinct head region (with supraesophageal ganglion (seg), subesophageal ganglion (sub) and optic lobes (ol)), connected to the large thoracic ganglia (tha) located in the thorax by a connective (cn). From Hartenstein (1993).

occuring from stage 7 to 11. Early nervous system development occurs from stage 8 to 11 with consequent cell division, elaboration and condensation of the nervous system continuing throughout the rest of embryogenesis. The germ band retracts during stage 12, with gut formation following from this stage and dorsal closure and head involution occurring between stages 14 and 17, to form the first instar larva. These stages are referred to throughout this chapter and elsewhere in the thesis.

1.1.1.2 Neuroectoderm formation.

The neuroectoderm is the specialised region of ectoderm that gives rise to the central nervous system of *Drosophila*. In cellular blastoderm stage embryos, ventral cells express *twist* and *snail* (Leptin 1991), lateral cells express *short gastrulation* (*sog* - Francois *et al.* 1994) and dorsal cells express *decapentaplegic* (*dpp* - Irish & Gelbart 1987). The interactions of these genes leads to definition of the neuroectoderm by repression of ventral and dorsal specific gene activities. *twist* and *snail* act to repress *sog*, leading to a mesodermal cell fate, whilst *dpp* acts to produce dorsal ectoderm, *sog* activity results in neuroectoderm formation and repression of *dpp* at the dorsal margin (Doe & Skeath 1996, Skeath *et al.* 1992, Holley *et al.* 1995). See figure 1.2.

The neuroectoderm, divisible into the ventral neuroectoderm (VNE) and the procephalic neuroectoderm (PNE), differentiates at stage 5 of embryogenesis (Hartenstein 1993). The VNE forms 2 neurogenic regions along the ventro-lateral faces of the embryo, dorsal to the mesectoderm. These VNE regions give rise to the ventral nerve cord. The PNE forms anterior to the VNE, running dorso-ventrally in the embryo, and gives rise to the brain.

The development of the neuroectoderm to form the nervous system is reliant on zygotically transcribed genes of 2 groups; the proneural genes and the neurogenic genes. Neuroblasts, the neuronal stem cells that produce neurons and glia, form from the neuroectoderm via the Notch pathway. This pathway has been pieced together in a variety of experiments in several organisms ranging from mammals to *Caenorhabditis elegans*, all of which have homologs of the pathway components (Artavanis-Tsakonas *et al.* 1995). Notch is a ligand

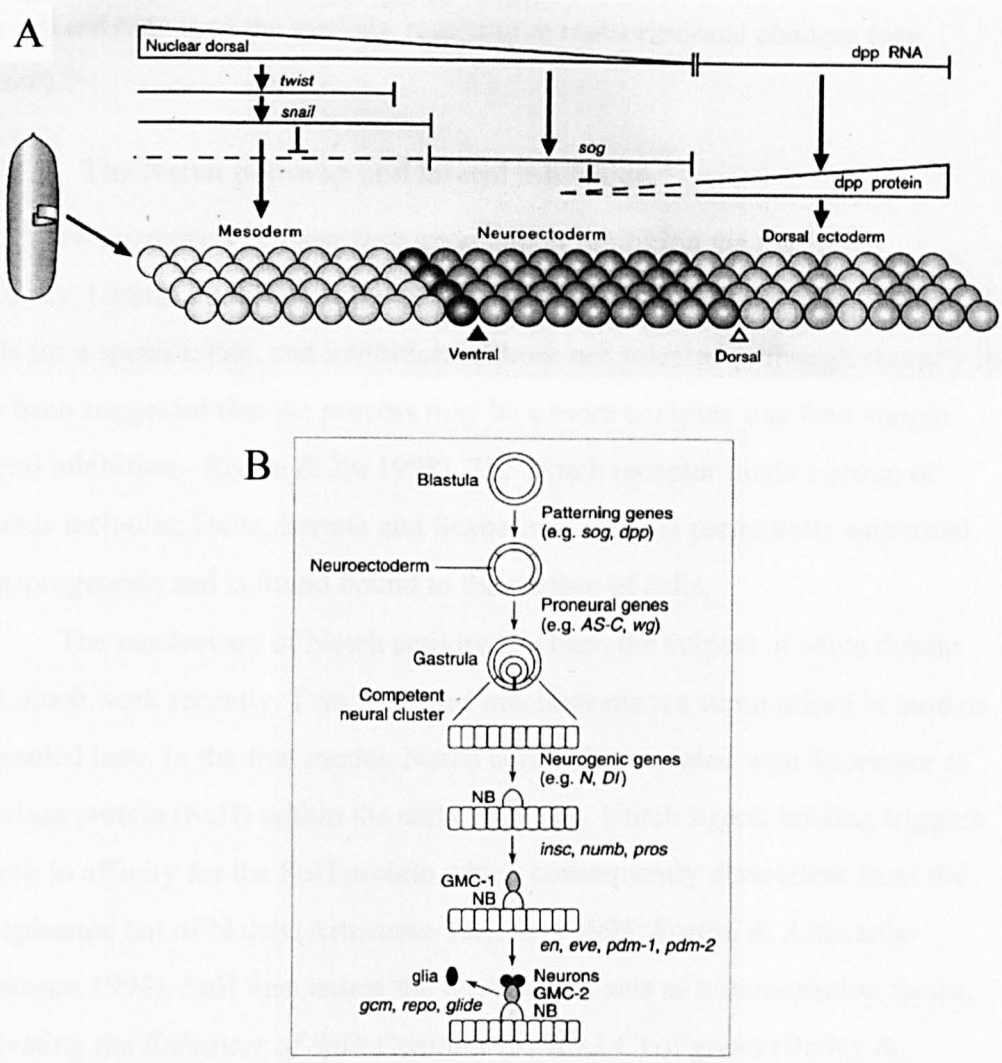

Figure 1.2: Establishment of the neuroectoderm, formation of neuroblasts and subsequent neuroblast division.

A: Establishment of the neuroectoderm. The cartoon on the left depicts a highlighted hemisegment of a blastoderm stage embryo. The scheme on the right shows gene expression along the dorsal-ventral axis in such a hemisegment. The ventral and dorsal edges of the neuroectoderm are marked with triangles (black and white, respectively). The mesoderm is light grey, the midline CNS is very dark grey, the neuroectoderm is dark grey and the dorsal ectoderm is medium grey. Figure from Doe & Skeath (1996).

B: The formation and subsequent divisions of the neuroblast and its progeny. Shaded regions signify neurogenic potential. Genes involved in each stage of neurogenesis are in italics. Abbreviations: *AS-C, Acheate-scute Complex; Dl, Delta; dpp, decapentaplegic; en, engrailed; eve, even-skipped; gcm, glial cells missing;* GMC, ganglion mother cell; *insc, inscuteable; N, Notch;* NB, neuroblast; *pros, prospero; repo, reverse potential; sog, short gastrulation; wg, wingless.* Figure from Lin & Schagat (1997).

activated transmembrane receptor that, upon activation, transduces signals from the cell membrane to the nucleus, resulting in transcriptional changes (see below).

1.1.1.3 The Notch pathway and lateral inhibition.

Neurogenesis is dependent upon lateral inhibition via the Notch pathway. Lateral inhibition is the process of singling out a cell from a cluster of cells for a specific fate, and inhibition of those not selected (although recently it has been suggested that the process may be a more complex one than simple lateral inhibition - Rooke & Xu 1998). The Notch receptor binds a group of ligands including Delta, Serrate and Scaberous. Delta is particularly important in neurogenesis and is found bound to the surface of cells.

The mechanism of Notch activity has been the subject of some debate and much work recently. Two proposed mechanisms are summarised in models presented here. In the first model, Notch is found associated with Supressor of Hairless protein (SuH) within the cell cytoplasm. Notch ligand binding triggers a drop in affinity for the SuH protein which consequently dissociates from the cytoplasmic tail of Notch (Artavanis-Tsakonas 1995, Fortini & Artavanis-Tsakonas 1994). SuH then enters the nucleus and acts as a transcription factor, activating the *Enhancer of Split Complex* (*E(SPL)-C*) of genes (Bailey & Posakony 1995, Lecourtois & Schweisguth 1995).

In the second proposed model, the signal transduction involves up to 3 independent proteolytic cleavage events of the Notch protein (Weinmaster 1998). The initial event would be ligand independent and may occur in the trans-Golgi network, to produce a functional cell surface Notch receptor (Blaumueller *et al.* 1997). Following ligand binding, the second proteolytic event, mediated by the metalloproteinase Kuzbanian, would cleave the Notch receptor extracellularly (Rooke et al. 1996, Pan & Rubin 1997). Subsequent to this the third cleavage event would produce a soluble cytoplasmic form of Notch (the Notch intracellular domain - NICD). This form moves to the nucleus to interact directly with SuH (Schroeter *et al.* 1998, Lecourtois & Schweisguth 1998, Kopan *et al.* 1996, Lieber *et al.* 1993, Jarriault *et al.* 1995).

The interaction between SuH and the cytoplasmic domain of Notch drives the transcription of the *E(SPL)-C* genes.

SuH in *Drosophila* is part of a larger family of DNA binding proteins, the CSL family (from CBF1, SuH and Lag-1 homologs in mammals, *Drosophila* and *C.elegans* respectively). *Notch*, *Delta*, *Serrate*, *scaberous*, *Supressor of hairless* and the *E(SPL)-C* genes are all termed neurogenic genes. *E(SPL)-C* is a family of transcriptional repressors encoding 8 genes over 50 Kb on chromosome 3 (Schrons *et al.* 1992). When these genes are expressed they repress the *Achaete Scute Complex* (*AS-C*). *AS-C* covers 90Kb, and contains 4 genes, *achaete*, *scute*, *lethal of scute* and *asense*, all of which are basic helix-loop-helix DNA binding proteins (Garcia-Bellido 1979, Campuzano & Modolell 1992). The *AS-C* genes are termed proneural, because they promote neuroblast differentiation, hence their repression leads to the repression of neuroblast differentiation. In this manner, cells expressing Notch ligand (i.e. Delta) become neuroblasts by inhibiting those around them. Proneural genes influence neuronal type, probably by controlling the expression of neuron-type selector genes (Jarman *et al.* 1993).

Lateral inhibition also has a cell migration component. The interaction of Notch and Delta leads to cell adhesion as both are attached to the cell surface, and as already discussed are receptor and ligand, respectively (Fehon 1990). Cell adhesion allows cell migration. Cells expressing high levels of Delta can therefore adhere and migrate, in addition to causing repression of the proneural genes of surrounding cells (see above). Thus lateral inhibition via the Notch pathway singles out the neuroblasts from the neuroectoderm and causes them to move medially, out of the surrounding neuroectodermal layer of cells, a process known as delamination.

1.1.1.4 Neuroblast delamination.

Larvae and adults each require a central nervous system (CNS) that is both very different and specific to their locomotor and sensory needs. Essentially, the larval CNS is produced in embryonic development whilst the adult CNS is produced in larval and pupal life. Two types of neuroblast exist to

produce these nervous systems; the first divides and produces only embryonic progeny, whilst the second produces embryonic progeny and then becomes mitotically silent until postembryonic stages when it resumes division (Prokop & Technau 1991). Essentially all neuroblasts are produced embryonically.

Delamination of neuroblasts from the neuroectoderm occurs in 5 phases (S1- S5), between embryonic stages 8 and 11 (Hartenstein 1993). In the ventral nerve cord, delaminating neuroblasts form 3 longitudinal columns in medial, intermediate and lateral positions, either side of the ventral midline (S1- S3). The position of S1, S2 and S3 columns are regulated by the genes defining the dorso-ventral axis, for example *twist* and *snail* (as previously mentioned above). The last 2 columns of neuroblasts (S4 & S5) form in intermediate positions between the existing 3 columns.

Within the ventral nerve cord, neuroblasts can be divided into groups, based on their positions within a segment of the embryo (a segment is the basic division of the body, each embryo being made up of 14). Progressing from anterior to posterior within a segment each neuroblast can be assigned a row number from 1 to 7. The rows are perpendicular to the columns so each neuroblast can be mapped in 2 dimensions (rows and columns). Per hemisegment (half a segment), there are 35 neuroblasts producing a total of 350 progeny neurons and 30 glial cells during embryonic development. Different segmental fates of the neuroblasts are determined by the homeotic genes. Much work has been done to study neuroblast lineages and to date more than 90% of lineages in the embryonic ventral nerve cord (the most accessible region of the central nervous system) have been mapped (Bossing *et al.* 1996, Schmidt *et al.* 1997).

Whilst harder to study there is some information on brain development (Younossi-Hartenstein *et al.* 1996, Younossi-Hartenstein *et al.* 1997 - see also chapter 5). The neuroblasts that give rise to the brain delaminate from the procephalic neuroectoderm to form 3 neuromeres, the protocerebrum (P), the deuterocerebrum (D) and the tritocerebrum (T). The neuromeres of P and D are further subdivisible into anterior, central and posterior. In the P, D and T neuromeres there are 75 to 80 neuroblasts that delaminate between stages 9 and

11 from the centre of the neuromeres outwards, these are subdivided accordingly: 51 in P, 22 in D and 6 in T. The control of early neurogenesis is achieved by the head gap genes (*tailless*, *orthodentical*, *empty spiracles* & *buttonhead*).

1.1.1.5 Neuroblast division patterns.

Following their delamination neuroblasts start dividing with 8 waves of mitosis between stages 9 and 13. Mitotic activity is most intense between the fifth and ninth hour but drops off dramatically with the onset of germ band retraction. The ventral nervous system is apparently devoid of activity after this, whilst some mitosis is still visible in the posterior of the brain (Campos-Ortega & Hartenstein 1985).

Each neuroblast (NB) divides asymmetrically to form a small ganglion mother cell (GMC) and leaving a slightly reduced neuroblast. The ganglion mother cells divide symmetrically to produce two ganglion cells (neurons). Embryonically, the neuroblasts in the VNC can each produce up to 9 ganglion mother cells and therefore up to 18 neurons. In most studied insects these divisions produce new progeny that displace the older progeny sequentially one cell diameter further from the neuroblast (for example grasshopper - Doe & Goodman 1985). This gives rise to a chain of progeny, attached to the basal neuroblast surface, in direct topographical relationship to the dividing neuroblast. However, in *Drosophila*, although the pattern of proliferation is the same, these chains are not always apparent (Younossi-Hartenstein *et al.* 1996). The derivatives of a given neuroblast can be arranged irregularly in its neighbourhood, possibly intermingled with the derivatives of other neuroblasts. Procephalic ganglion mother cells are arranged, as in other insects, in elongated vertical chains attached to the basal neuroblast surface, whereas in the ventral nerve cord there can be 3 or 4 ganglion mother cells side by side all contacting the neuroblast. This results in a comparatively thick cortex in the brain hemispheres measuring, in some places, 5 to 8 cell diameters in thickness.

1.1.1.6 Asymmetric neuroblast division.

Post specification and delamination, neuroblasts next undergo divisions to produce GMCs that subsequently divide once resulting in 2 neurons. GMCs are distinguishable from the NBs as they are smaller, have reduced mitotic potential (one division) and an altered pattern of gene expression. Neuroblasts have a stereotypic mechanism for division with cell fate determinants localised asymmetrically, consequently resulting in their unequal distribution between the daughter cells. Genetic analysis has revealed several proteins that segregate differentially during division of the neuroblasts, including the proteins, Numb (Rhyu *et al.* 1994), Prospero (Spana & Doe 1995, Hirata *et al.* 1995) and Inscuteable (Kraut & Campos-Ortega 1996). Prospero (Pros) and Numb seem to be localised cell fate determinants, with Inscuteable (Insc) a possible component of the cellular machinery responsible for their specific segregation.

Pros, a transcription factor (Vaessin et al. 1991), is found in a crescent at the basal side of the neuroblast, and upon division the protein is also exclusively localised to the ganglion mother cell and seems to be a key GMC determinant. Pros is rapidly transported to the nucleus following division and activates ganglion mother cell specific genes (Doe *et al.* 1991).

Within neuroblasts Numb is localised basally in a crescent at the cortex. Apicobasal neuroblast division segregates Numb into the ganglion mother cell solely. An example of Numb function can be found in the CNS, in the MP2 neuroblast (Knoblich *et al.* 1995). This NB is unusual as it directly produces only 2 progeny cells from a single division, the dMP2 and vMP2 neurons. Numb is localised in the dorsal cortex of the neuroblast and segregates solely to the dMP2 neuron and seems necessary and sufficient to specify dMP2 cell fate (Spana *et al.* 1995). This effect may be mediated by antagonising the extrinsic Notch-Delta pathway (Spana & Doe 1996, Guo *et al.* 1996). Extrinsic Notch-Delta signals specify the vMP2 fate, whilst Numb specifies the dMP2 fate by suppressing the Notch-Delta function.

Insc is thought to be a cytoskeletally associated protein with an SH-3 binding domain and weak homology to a known cytoskeletal adapter protein ankyrin. Insc is required for Numb and Pros localisation, but its localisation

preceeds and is opposed to that of Numb and Pros (Kraut & Campos-Ortega 1996). This pattern of localisation suggests that Insc is a blocker that stops Numb and Pros binding to the cytoskeleton at the apical region.

Therefore, the unequal segregation and distribution of these proteins leads to the specification of GMCs from NBs and, in the case of Numb, can lead to the specification of neuron cell fate.

Glial cells are not only produced by glial specific precursors but also from neuroblasts that generate mixed neuronal/glial lineages (Bossing & Technau 1994, Udolph *et al.* 1993). Glial cell fate is under the control of *glial cells missing* (*gcm* - Jones *et al.* 1995, Horsoya *et al.* 1995). Glia have several defined and essential roles in the CNS. They appear to play a role in axon guidance (Jones *et al.* 1995) as well as providing a scaffold to physically support neurons. Glia also provide nutrients and growth factors which influence neuronal survival (Xiong & Montell 1995) and secrete proteins that regulate NB proliferation (Ebens *et al.* 1993).

1.1.2 Larval neurogenesis.

Larval life proceeds through 3 stages (larval instars), discernable by characteristic mouthpart morphology, that take approximately 100 hours (all times given are for development at 25^0C). After the third instar the puparium forms and persists for around another 100 hours, during which time metamorphosis occurs. The adult emerges 220 to 230 hours after the fertilised egg was laid.

The larval CNS contains persistent embryonic neuroblasts (i.e. those arrested after embryonic divisions), which resume division subsequently (dividing as embryonic NBs do). These NBs are found both in the ventral nerve cord (Prokop & Technau 1991) and in the brain (Younossi-Hartenstein *et al.* 1996).

In the ventral nerve cord each thoracic neuromere has 47 neuroblasts, whilst the abdominal neuromere has 6. This indicates the subsequent alteration of body plan away from abdominal control of locomotion to thoracic (See figure 1.1). The neuroblasts begin enlarging at 18 to 26 hours of larval life and DNA

synthesis proceeds from 31 to 36 hours. The first mitotic division of the neuroblasts occurs after this and mitosis is apparent throughout the rest of larval life. By 12 hours after the start of pupation each neuroblast has produced around 100 cells of progeny in a discrete cluster. These progeny accumulate in an immature arrested state and finish differentiation some time in the following metamorphosis. Most abdominal proliferation occurs at 50 to 90 hours of larval life (Trueman & Bate 1988).

In the brain there is less data about neuroblast proliferation, with respect either to patterns, numbers or timing. The following description is constructed from several accounts (White & Kankel 1978, Truman & Bate 1988, Ito & Hotta 1992). At larval hatching, the larval brain already has 5 pairs of fully enlarged neuroblasts. Four of these are in the anteromedial region of each hemisphere (the mushroom body NBs), whilst the fifth is in the posterolateral region (lateral NB). These neuroblasts are in mitosis in the newly hatched larvae and proliferate throughout larval life. The optic lobe neuroblasts enlarge by 8-12 hours after larval hatching (ALH), with DNA synthesis occurring by 13 hour ALH. Optic lobe analagen proliferation ensues subsequently, and this region is one of the most strikingly proliferative in the brain, during larval life. Other scattered brain neuroblasts start enlarging and then DNA synthesis at around 13 hours ALH. By 20 hours ALH all the central brain complex is covered with 20-30 neuroblasts per hemisphere. The number of proliferating neuroblasts then increases between 20-30 hours ALH, reaching a plateau of about 85 neuroblasts per hemisphere. In all these neuroblasts mitotic activity is maintained at a high rate through the remainder of larval life until white puparium formation. At this time mitotic activity wanes, but is still detected in limited areas of the brain and optic lobes until 25-30 hours after puparium formation.

Programmed cell death is used to remove un-needed larval neurons from the CNS, in production of the adult CNS (Truman 1990).There are 2 bouts of cell death, the first 12 to 18 hours after puparium formation, and the second soon after adult emergence (removing neurons involved in eclosion specific behaviours - Kimura & Truman 1990). In addition to cell death, segment specific morphogenetic movements, neuron-glia interactions and the structural

and functional modification of persistent embryonic neurons all help to shape the adult CNS postembryonically (Levine *et al.* 1995).

1.1.3 Summary of neurogenesis.

In summary, all the neuroblasts required during the fly's life are formed during embryogenesis, some are immediately used, whilst others proliferate in embryogenesis, subsequently arrest and then become activated again in larval life to produce adult-specific neurons. Neurons produced during larval life account for more than 90% of the cells found in the adult (data from the ventral nerve cord), indicating the origins of the adult CNS are largely larval.

Once produced (either embryonically or postembryonically), the neurons must form specific and complex interactions to form a functioning nervous system. This is the central topic of the next section.

1.2 Formation of a functioning CNS – axon growth and guidance.

It is a fundamental aim of developmental neurobiology to identify mechanisms that generate patterns of neuronal connectivity. The normal and correct functioning of any nervous system is dependent on the underlying patterns of connectivity. A vast array of neurons project axons that traverse huge distances and are confronted by many different environments exposing a multitude of different choices to the specialist sensory tip of the axon, the growth cone. Via mechanisms that are not fully understood yet, the axons correctly navigate in an amazingly consistent manner to contact a specific target, thereby forming a circuit (reviewed Goodman & Shatz 1993, Tessier-Lavigne & Goodman 1996, Goodman 1996).

Some headway has been made into determining mechanisms that allow for this stereotyped connectivity between specific neurons. Firstly, the mechanisms that give rise to this specificity take place in 2 distinct phases :

1) Activity independent - initial steps of axon guidance and pathfinding occurring prior to the neuron becoming functionally active. This, in turn, can be split into:

I) Pathway selection - growth cones traverse specific pathways to

reach the correct neighbourhood.

II) Target selection - once in the neighbourhood they recognise and contact their target; usually a small set of localised neurons.

III) Synapse formation.

2) **Activity dependent** - a later process that takes place when the neurons are functionally active. This is largely a "fine tuning" process further refining the connections a neuron makes within the target area, via a process of synaptic plasticity. This mechanism of synaptic plasticity continues throughout the lifetime of the organism and is thought to be responsible for learning and memory - "cells that fire together wire together" (Goodman & Shatz 1993).

Pathway and target selection, are topics that have been intensively studied from several different perspectives all of which are tightly interlinked. The different disciplines used to study nervous system formation include neuroanatomy, experimental embryology, cell culture, classical genetics and molecular biology. These have allowed progress towards understanding specific steps in neural development to be achieved down to a molecular level. It has emerged from this that there is extensive molecular conservation amongst components regulating development in vertebrates and invertebrates.

1.2.1 The two principles of axon guidance.

The focus of this section will be a brief summary of the activity independent steps of nervous system development as these are the most relevant to this project. Two main principles have emerged from the study of axon pathway development (Varela-Echavarria & Guthrie 1997, Tessier-Levigne & Goodman 1996, Cook *et al.* 1998, Van Vactor 1998, Stoeckli & Landmesser 1998). The first is the use of intermediate targets in axon trajectories, so the axon does not traverse the entire distance between cell body and target in one step. Rather, the axon utilises structural targets en route. These "choice points" can be guidepost cells or more complex regions of tissue such as the embryonic CNS midline (see 1.2.6).

The second principle is that the first, early growing "pioneer axons"

provide a substrate for later axons to traverse (forming axon bundles or "fascicles"). This reduces the complexity of the pathfinding task (the axon growth cones are consequently smaller) and growth is much faster.

1.2.2 The Growth Cone.

During axon pathfinding the growth cone (the tip of the advancing nerve projection), a structure first identified and named by Ramon y Cajal in 1892, plays a vital role. Growth cones have a diverse set of behaviours that underlie the complex processes of neurite elongation, pathfinding and selective synaptogenesis.

A typical growth cone projects many fine processes called filopodia that rapidly extend and retract, with the ability to contact substrates tens of microns away. In addition, the growth cone can express ruffling, membranous veils or lamellae around its perimeter.

The structure of the growth cone is supported internally by the cytoskeleton (Bentley & O'Conner 1994, Challacombe *et al.* A&B 1996, Rehder & Kater 1996, Lin *et al.* 1994, Lin & Forscher 1995, reviewed in Suter & Forscher 1998). In the filopodia and lamellipodia, that constitute the periphery of the growth cone, this is predominantly composed of actin. It is the polymerisation, depolymerisation and translocation of actin that is primarily responsible for the motile activity that drives axonal growth. There is a soluble pool of tubulin in the growth cone and much microtubule polymerisation occurs here. A few microtubules are present in the proximal regions of the filopodia and lamellipodia, but the majority of the microtubular axonal cytoskeleton extends from the central part of the growth cone through the axon to the cell body (figure 1.3). During interactions between the growth cone and the environment, the mirotubules reorient and extend towards positive interactions and away from less favourable substrates.

Growth cones can simultaneously be exposed to a plethora of attractive and repulsive cues and their complex behaviours reflect a tight regulation of their responsiveness to these cues (Dodd *et al.* 1988, Bastiani *et al.* 1987, Hall *et al.* 1987, Cohen *et al.* 1989). Two recent reviews (Cook *et al.* 1998, Stoeckli &

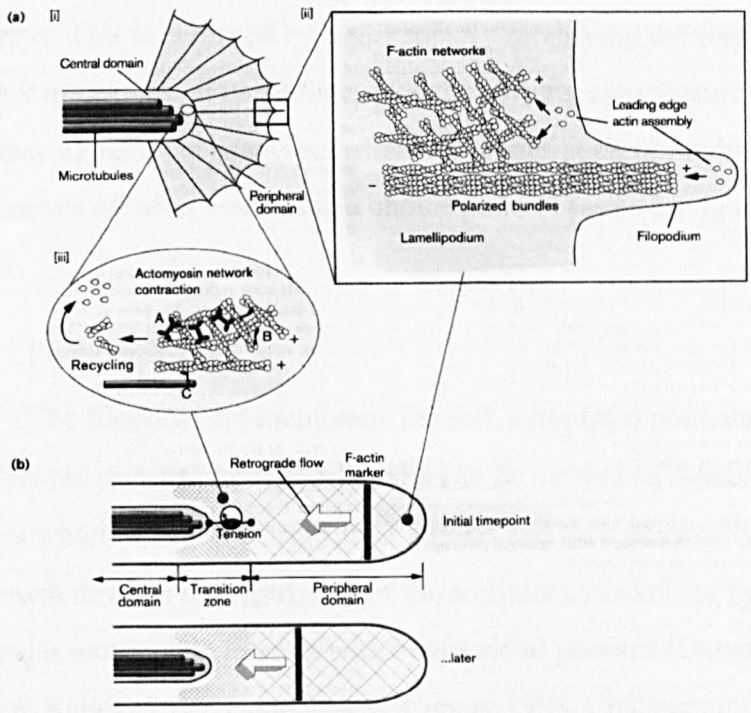

Figure 1.3: Cytoskeletal organisation and actin dynamics in growth cones.
(a) Distribution of the 2 major cytoskeletal components of neurites and growth cones. [i] Microtubules are localised in the neurite and central domain of the growth cone, whilst actin filaments are distributed in the peripheral domain.
[ii] Enlargement of [i] showing the organisation of actin filaments in more detail. Actin can be found in polarised bundles in the filopodia and in less polarised networks in the lamellapodia.
[iii] Retrograde translocation of actin filaments is driven by myosin motors that may be in the transition zone (see b). A-C depict possible actinomyosin combinations for tension generation. A:double headed myosin II.
B & C: single headed myosin I.
(b) Cross sections of a growth cone demonstrating the dynamic processes involved in actin based growth cone motility. Retrograde F-actin flow is indicated by a marker (black band).
The tension meter indicates low tension if actin networks are not stabilised by substrate interactions. Filament recycling occurs by the action of putative severing proteins (e.g. gelsolin).
From Suter & Forscher (1998).

Landmesser 1998) have shown that the same growth cone can rapidly change its response to the same environment by modifying its signal transduction pathways. This is achieved by either rapidly modifying the complement of receptor molecules on its surface, or by modifying cytoplasmic components. This may explain the behaviour of growth cones at choice points and how the axon moves off after contacting a choice point (Tessier-Levigne & Zipursky 1998).

1.2.3 Filopodia.

The filopodia are membrane limited, cytoplasm poor and actin rich microscopic protrusions. The filopodia can be viewed as signal transduction devices which interpret extracellular signals and then physically direct neurite outgrowth through the regulation of intracellular cytoskeletal dynamics and molecular motors that interact with cytoskeletal proteins (Davenport *et al.* 1993, Kater & Rehder 1995, Bentley & O'Conner 1994, Challacombe *et al.* A &B 1996, Rehder & Kater 1996, Lin *et al.* 1994). Therefore, pathfinding decisions as the growth cone navigates to its target are largely determined by the fan shaped array of filopodia at the leading edges of the advancing growth cone.

Growth cone behaviour can be rapidly altered when a single filopodium contacts instructive molecules, and conversely when growth cones are denuded of filopodia experimentally they often fail to navigate in the usual stereotyped manner (Davenport *et al.* 1993). Having a small diameter and a large surface to volume ratio means a change in calcium channels causes a large change in intracellular calcium concentrations (Kater & Mills 1991, Davenport *et al.* 1993, Kater & Rehder 1995). The same applies for any second messenger or locally activated enzyme - small changes intracellularly are rapidly relayed due to the small volume of cytoplasm. The information received may elicit local effects followed by a relaying to the growth cone for further processing (Kater & Rehder 1995). These must then effect the growth cone in a stimulus specific manner and to render an effect in growth cone morphology the messages must be translated into alterations of the cytoskeleton.

Filopodia, being widely spread, could integrate information from

multiple cues to arrive at a final pathfinding decision - this may be achieved by a process of information summation to overcome a threshold. The shape of growth cones radiating filopodia may also allow spatial distribution and gradients of instructive molecules to be identified.

1.2.4 Growth cone cytoskeletal studies.

Growth cone filopodia have roles as sensors, transducers and autonomous motor structures important for growth cone steering (Bentley & O'Conner 1994,Lin *et al.* 1994, Challacombe *et al.* 1996 A & B). These functions are controlled through the regulation of intracellular cytoskeletal dynamics (involving actin binding proteins such as Profilin and Gelsolin that regulate F-actin assembly and F-actin severing respectively) and molecular motors (e.g. myosins), that interact with cytoskeletal proteins (F-actin and Tubulin). Cytoskeletal linkage with the substrate may occur through a series of adaptor proteins that act as a clutch and functionally transduce F-actin flux into growth cone advance (Lin & Forscher 1995, Challacombe *et al.* 1996 A & B) - figure 1.4. Binding of extracellular cues may also affect the growth cone via intracellular signalling involving molecules such as Rho (affects Myosin contractility), Rac (affects lamellipodium structure) and Cdc42 (affects filopodial structure).

1.2.5 Guidance cues.

Embryological, tissue culture and genetic experiments indicate that axons respond to the coordinate actions of four types of guidance cues (Tessier-Lavigne & Goodman 1996, Stoeckli & Landmesser 1998, Keynes & Cook 1995) - see figure 1.5. Type 1, chemorepulsive (e.g. secreted semaphorins and netrins) and type 2, chemoattractive (e.g. netrins) are long range cues. Type 3, contact repulsive (e.g. Eph ligands, transmembrane semaphorins and extracellular matrix proteins such as the tenascins) and type 4, contact attractive (e.g. immunoglobulin superfamily cell adhesion molecules, cadherins and extracellular matrix proteins such as laminins) are short range cues. However, the molecules implicated in these cues do not easily fall into these catagories

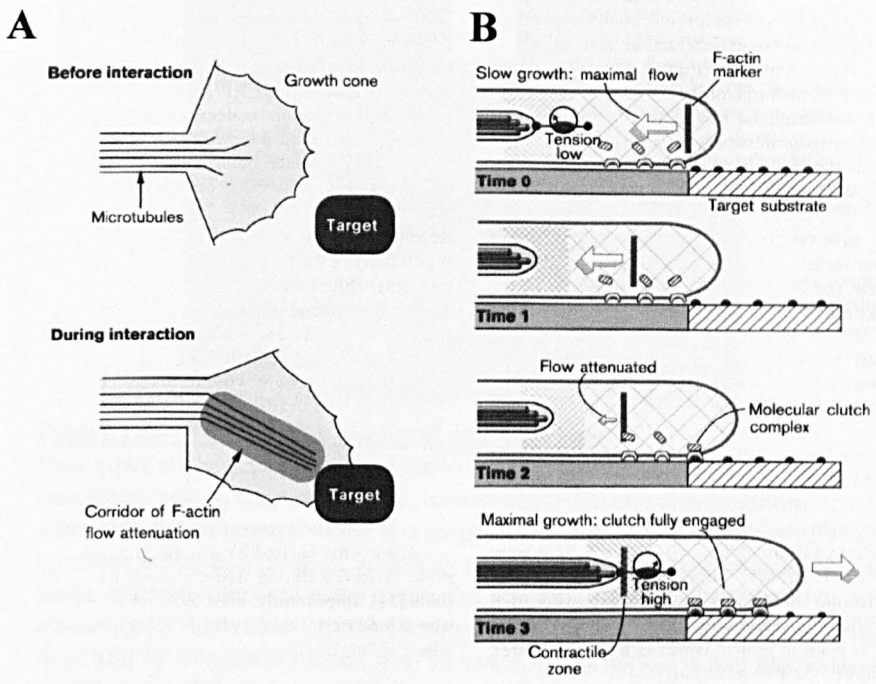

Figure 1.4A & B: Cytoskeletal rearrangements during interactions between the growth cone and a target.

A: Shows microtubule reorientation due to contact with an attractive target. Microtubule extension occurs specifically in a corridor of F-actin attenuation.

B: Timecourse cross sections demonstrate a mechanism of growth cone advance by substrate –cytoskeletal coupling (see also1.4C). Before target interaction there is maximal retrograde flow, no substrate coupling and little advance (Time 0-1). If the growth cone encounters a favourable target substrate (Time 2), molecular clutch complexes form linking the substrate and cytoskeleton. Stabilisation of peripheral actin leads to attenuation of retrograde flow and increased tension between central and peripheral domains (Time 3). Advance occurs by a combination of increased tension on the central domain and continued leading edge actin assembly. From Suter & Forscher (1998).

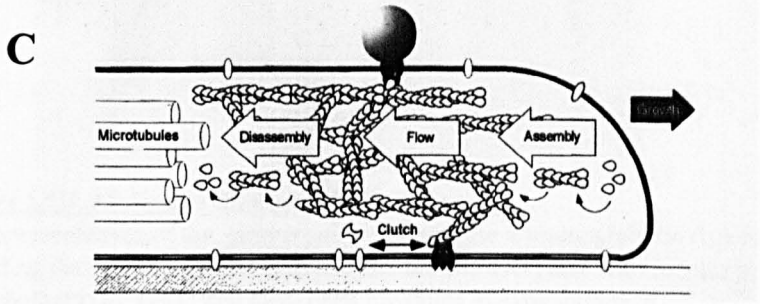

Figure 1.4C: The substratum-cytoskeleton coupling model of growth cone advance.
Actin dynamics of the lamellipodium are represented by a steady state composed of 3 processes; actin filament assembly at the leading edge, actin filament disassembly at the back of the peripheral domain, and retrograde flow of actin filaments at a rate matching assembly and disassembly. "Clutch" protein complexes may regulate the degree of mechanical coupling between the actin network and the adhesive bond between surface ligands and substrata. When the "clutch" engages the filament network to the cell-substratum contact, the retrograde flow is attenuated, while actin disassembly continues. This removes impedence and accelerates the advance of the microtubules by polymerisation and transport.
Figure from Challacombe *et al.* (1996).

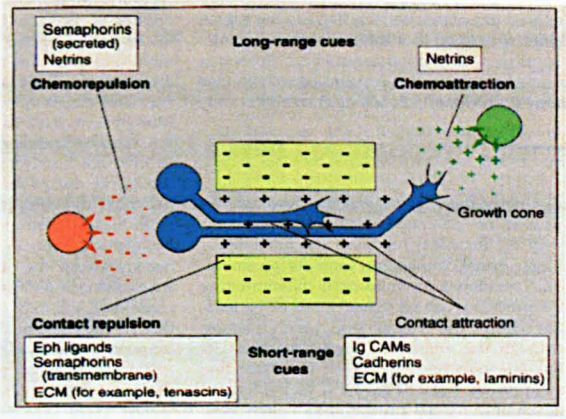

Figure 1.5A: The 4 major classes of guidance cues.
Four types of mechanisms contribute to guiding growth cones:
contact attraction, chemoattraction, contact repulsion and chemorepulsion.
Attraction in this context refers to a range of permissive and attractive effects whilst repulsion refers to a range of inhibitory and repulsive effects. Examples of each cue are listed, although there are many molecules that fall into more than one category (i.e. are bifunctional). Individual growth cones may be "pushed" by a chemorepellent, "pulled" from afar by a chemoattractant and "hemmed in" by attractive and repulsive cues. A combination of these cues and their activities ensures accurate guidance.

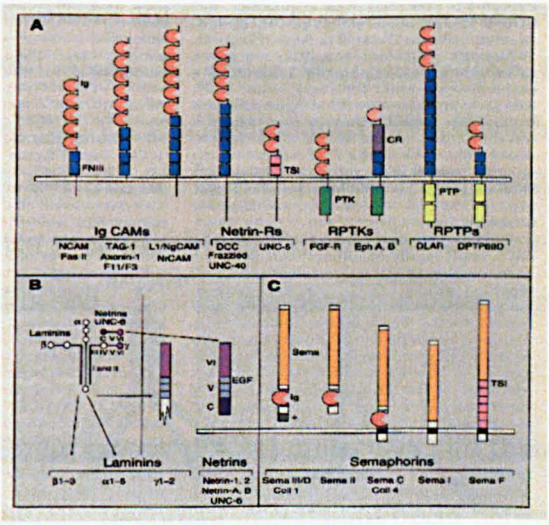

Figure 1.5B: Molecules that modulate axon growth.
A: Representatives of the various subfamilies of the immunoglobulin (Ig) superfamily, including the receptor protein tyrosine kinases (RPTKs) and the receptor protein tyrosine phosphotases (RPTPs), that have been implicate in axon guidance.
Ig = immunoglobulin repeat, FNIII = fibronectin type III domain, TSI = thrombospondin type I domain, CR = cysteine rich domain, PTK = protein tyrosine kinase domain, PTP = protein tyrosine phosphotase domain.
B & C: The laminin, netrin and semaphorin families of guidance cues.
The laminins are heterodimeric, cruciform glycoprotein complexes with constituent α, β and γ chains. The netrins are related to the amino terminus of the VI and V laminin chains. The semaphorins share a common 500 amino acid semaphorin domain and often contain an Ig domain.
All these guidance cues are conserved between nematodes, insects and vertebrates.

Both figures 1.5A and 1.5B are from Tessier-Lavigne & Goodman (1996).

because the same molecule may play more than a single role. Discussed below are the major groups of molecules, alluded to here, that are involved in axon guidance and fasciculation, and a brief description of their roles in nervous system development (often based on experiments in both vertebrates and invertebrates).

1.2.5.1 Cell Adhesion molecules (CAMs).

These largely fall into 2 groups, those of the calcium independent immunoglobulin superfamily (e.g. NCAM, MAG, L1, NgCAM, F11/Contactin & Neurofascin) and those of the calcium dependent cadherins (for example N-cadherin). They seem to fulfil roles of growth promotion and growth cone guidance via homophilic or heterophilic binding between those CAMs expressed on the growth cone (on the filopodia) and those on the underlying substrate - the extracellular matrix, glia or other axons (reviewed Uemura 1998, Bixby & Harris 1991, Hynes & Lander 1992, Stoker 1996, Rackic *et al.* 1994, Doherty & Walsh 1992, Vaughn & Bjorkman 1996, Schuch *et al.* 1989, Grenningloh *et al.*1991, Harrelson & Goodman 1988, Bastiani *et al.* 1987). There are at least ten neural CAMs in *Drosophila* and there is evidence CAMs can act as a ligand in one cell and a receptor on another (Cunningham *et al.* 1987).

1.2.5.2 Extracellular matrix (ECM) molecules and their receptors.

Many potentially important interactions occur between the growth cone and the ECM, which is a complex association of extracellular glycoproteins organised into aggregates and polymers. The ECM has components that are permissive, stimulatory and inhibitory to the growth cone. Molecules identified and implicated in these processes include Fibronectin, Tenascin, Laminin, Collagen, Thrombospondin, Perlecan, Integrin and F11 (Howe *et al.* 1998, Goodman & Shatz 1993, Goodman 1996, Letourneau *et al.*1994, Hynes & Lander 1992).

1.2.5.3 Receptor protein tyrosine kinases (RPTKs).

A variety of RPTKs modulate axon growth or regulate target invasion in

both vertebrates and invertebrates. Derailed is a *Drosophila* RPTK implicated in axon fasciculation and guidance in a subset of embryonic neurons (Callahan *et al.* 1995). Derailed is related to the vertebrate protein Ryk. In vertebrates, the largest RPTK subfamily is the Eph family who, together with their ligands the Ephrins, are implicated in fasciculation (by contact repulsion), topographic map formation and guidance to the target (Winslow *et al.* 1995, Drescher *et al.* 1995, Gao *et al.* 1996, Zhang *et al.* 1996, and reviewed by Cook *et al.* 1998). Mutations in the *Drosophila* gene *dreadlocks* (*dock*) disrupt photoreceptor axon guidance and targeting. Dock protein contains one SH2 domain and three SH3 domains, implicating it in tyrosine kinase signalling. Taken together these two points suggest Dock may be involved in tyrosine kinase signalling in the growth cone that influences axon guidance (Garrity *et al.* 1996).

1.2.5.4 Receptor protein tyrosine phosphotases (RPTPs).

Genetic analysis in *Drosophila* has implicated several RPTPs in the control of axon fasciculation and defasciculation (Desai *et al.* 1996,1997, Chien 1996 and reviewed in VanVactor 1998, Stoker & Dutta 1998). There is limited knowledge currently about RPTP ligands, although RPTPβ binds the immunoglobulin CAM Contactin/F11, functionally linking CAMs and RPTPs (Peles 1995).

1.2.5.5 Netrins and their receptors.

Netrins are a small family of bifunctional guidance cues found in both vertebrates and invertebrates, capable of attracting some axons and repelling others (Mitchell *et al.* 1996, Shirasaki *et al.* 1995, Serafini *et al.* 1994, Hedgecock *et al.* 1990, reviewed in Culotti & Kolodkin 1996, Cook *et al.* 1998). They are diffusable, although this can be effected by ECM or cell surface interactions (Serafini *et al.* 1994, Shirasaki *et al.* 1995). Immunoglobulin superfamily members (DCC/Frazzled/UNC-40) are netrin receptor components in a variety of organisms (vertebrates, *Drosophila* and *C.elegans* respectively). These mediate the attractive effects of the netrins (Chan *et al.* 1996). Within *C.elegans* another immunoglobulin superfamily member (UNC-5) mediates the

repulsive effects of the netrin UNC-6 (Hamelin *et al.* 1993). Studies of the netrins also provide evidence of the redundancy of guidance cues. Two redundant netrins (Netrin A & B) are co-expressed at the *Drosophila* midline and knockouts of netrins in several organisms have only partially penetrant phenotypes (Mitchell *et al.* 1996, Tessier-Levigne & Goodman 1996).

1.2.5.6 Semaphorins.

The semaphorins are a large family of cell-surface and secreted proteins that appear to function as chemorepellents or inhibitors (Luo *et al.* 1993, Messersmith *et al.* 1995, Matthes *et al.* 1995, reviewed in Cook *et al.* 1998, Chien *et al.* 1998). To date at least three semaphorins have been identified in *Drosophila*, two in *C.elegans*, seven in mouse and ten in humans.

Vertebrate Collapsin/Semaphorin III/D is a potent inducer of growth cone collapse. During growth cone collapse axons usually only retract the actin containing filopodia and lamellipodia. Molecules that regulate collapse are strongly implicated in axon guidance, as negative factors (Muller et al. 1996, Fawcett 1993, Fan & Raper 1995). Cell surface receptors linked to the interior through a second messenger systems are probably involved in collapse, via a G protein mediated system involving intracellular calcium (Doeherty & Walsh 1994). Beyond this it is not clear how these regulate cytoskeletal elements to collapse and retract. It could be that actin associated molecules present at the leading edge of the growth cone may be involved in collapsing, following a modification of their activities by calcium ions. Molecules likely to be affected include: cross linking molecules such as α-Actinin and Fodrin, depolymerising proteins like Gelsolin and perhaps cytoskeletal/membrane linkers Talin and Vinculin (Sydor *et al.* 1996, reviewed in Suter & Forscher 1998).

In insects, semaphorins have been implicated in many processes (Tessier-Levigne & Goodman 1996) including; influencing growth cone steering decisions, inhibiting branching of axons and inhibiting the formation of synaptic arbors. However, Sema I may act as a contact attractant.

1.2.5.7 Neurexins.

Signalling and adhesive diversity is not solely achieved by large numbers of unrelated molecules but also relies on alternate splicing producing different protein forms in different spatial and temporal patterns. Alternative gene products may also have different second messenger responses within the growth cone. An example to illustrate this, from vertebrates, is the neurexin family (Missler & Sudhof 1998). Neurexins are a family of polymorphic cell surface proteins. Thousands of neurexin isoforms are generated from 3 genes (designated I-III) by usage of alternative promoters and alternative splicing. These isoforms are displayed on the neuronal cell surface. Different classes of neurons express distinct combinations of isoforms. Neurexins probably have many ligands, some of which are isoform specific. Whilst Neurexin IV exists in *Drosophila* it is thought to actually be from a different gene family.

1.2.6 Guidepost cells and the midline – "choice points" in the CNS.

The "choice points" alluded to in section 1.2.1 are mentioned here in a little more detail. The midline of the embryonic *Drosophila* CNS represents one of the major models of axon guidance, and consequently will be mentioned here at some length. This model illustrates the integration of several of the major groups of molecules listed above to produce a stereotypically patterned CNS (reviewed in Thomas 1998, Flanagan & Van Vactor 1998).

1.2.6.1 Guidepost cells.

A single filopodial contact with a very high affinity substrate, such as a guidepost cell can reorient a growth cone, even when it is migrating on a favourable substrate (figure 1.6A). The filopodium that contacts the guidepost in this way expands in diameter until it becomes the main axon (Bentley & O'Conner 1994, Kuhn *et al.* 1995, O'Conner *et al.* 1990, Hynes & Lander 1992).

1.2.6.2 The midline.

A substantial number of neurons project axons in the CNS that will cross the midline to the contralateral side. Within *Drosophila,* neurons project their

A

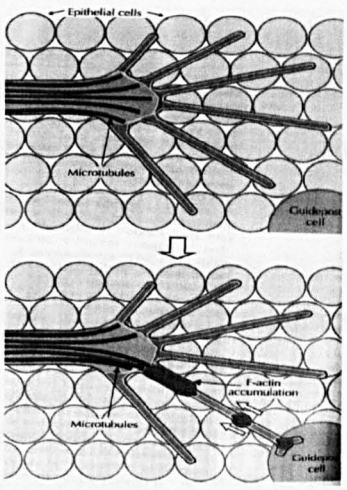

Figure 1.6A: Diagram showing the simplified growth cone response to contact with a guidepost cell.
After filopodial contact with the guidepost cell, the filopodial tip enlarges and extends secondary filopodia, whilst the base increases in diameter. F-actin increases at the tip of the filopodium and accumulates in a dense core in the base of the filopodium, possibly through retrograde transport (white arrows). Microtubules selectively accrue in the enlarging base and result in a growth cone turning event, with further growth in this new direction. From Bentley & O'Conner (1994).

B

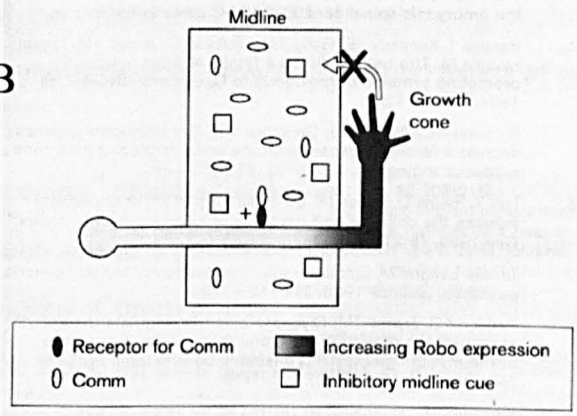

Figure 1.6B: The midline of *Drosophila* and the effect upon commissural axon guidance.
Roundabout (Robo) is upregulated after the growth cone contacts the midline. As Robo is a receptor for the inhibitory cue of the midline the upregulation can prevent axons from recrossing the midline. Commissureless (Comm), which is expressed by the midline cells and provides a positive cue for midline crossing, is removed by transfer to commissural axons as they cross the midline. Studies have shown Comm can regulate the expression of Robo. Figure from Stoeckli & Landmesser (1998).

processes in two major tracts called the longitudinal connectives, which run the length of the CNS parallel, either side of the midline. Groups of axons called commissures link these parallel connectives, connecting the two sides. The formation of the commissures requires certain axons to cross the midline and project anteriorly or posteriorly along the fascicles of the longitudinal connective. These axons do not usually cross the midline again. Glial cells at the midline are located between the connectives and are essential for commissure formation.

Initially, the midline secretes diffusible factors capable of attracting contralateral projecting axons (Netrin A & B in *Drosophila*) – (Mitchell *et al.* 1996, Harris *et al.* 1996). Controls are required at the midline to allow axons that have been attracted to cross and then leave, and to prevent them recrossing. The evidence suggests local contact mediated repulsive and attractive guidance cues operate to guide crossing. Two recent papers (Kidd *et al.* 1998 a & b), suggest two cell surface proteins are the key. These are Commissureless (Comm - Tear *et al.* 1996), a novel transmembrane protein expressed on midline cells, and Roundabout (Robo - Kidd *et al.* 1998), an immunoglobulin superfamily CAM expressed on the surface of growth cones and axons of developing neurons.

The "gatekeeping" model (Kidd *et al.* 1998a & b) derived from these studies suggests Robo acts as a guidance receptor for a repellent molecule expressed at the midline. Comm protein on the midline cells signals the neurons to down regulate the Robo on their growth cones. Robo's midline repulsion is then mitigated, allowing the axons to cross. Once across, Robo is up regulated, repelling the axons from the midline and preventing them from recrossing. However, not all axons contacting the midline subsequently cross. Choice may be dictated by the levels of Robo on the growth cones of axons contacting the midline; those with less cross, whilst those with high Robo levels would not have the repulsion overcome by Comm and would be repelled. Alternatively, neurons may possess differential sensitivity to Comm due to varying intrinsic levels of a putative Comm receptor. The mechanism of Robo and Comm may well be applicable to other organisms as Robo homologs have been found in rat,

human and *C.elegans*. The model also illustrates the importance of tight spatial and temporal control over molecules required for guidance (see figure 1.6B).

Direct cell contact may also play a role at the midline via other mechanisms. The immunoglobulin superfamily CAMs certainly have an important role in vertebrates in the analogous situation to the midline – the floorplate. AxoninI/TAG1 and NrCAM/L1 can bind one another and are expressed on commisural axons and spinal cord floor plate respectively. If blocked by NrCAM antibody the crossing is blocked (Stoeckli *et al.* 1997). As with other mechanisms of axon guidance an analogous situation may also occur during *Drosophila* development. Likewise, the possibility of repellent cues playing a role at the midline has been hinted at in vertebrates and invertebrates (Stoeckli *et al.* 1997).

1.2.7 Target selection and synaptogenesis.

Growth cone morphology varies depending on the local environment and pathfinding events are due to a variety of different types of molecule. Axon growth through the incredibly intricate and complex terrain of the developing nervous system is an almost unbelievable feat. It is not surprising then that the growth cone and underlying substrate are vastly complex and heterogeneous throughout the nervous system, making the mapping of just one pathway and all its cues, an unfulfilled task to date. Once at the target region the neuron has to select the target and synapse with it.

1.2.7.1 Target selection.

Once the neurons have projected axons to the correct target region, via the mechanisms mentioned above, they often form a topographic projection pattern (usually following defasciculation) prior to selecting appropriate synaptic partners within the target field. The invasion of the target region by axons is regulated by both pathway-derived and target-derived cues (Kennedy & Tessier-Lavigne 1995, Garrity & Zipursky 1995). In *Drosophila* this has been dissected genetically, in the embryo, to test the molecular mechanisms controlling motor axon ability to recognise the appropriate muscle target

(Winberg *et al.* 1998). Netrin A, Netrin B, Semaphorin II and Fasciclin II were all genetically added and subtracted alone or in combination in embryos. Fasciclin II and Semaphorin II are expressed in all muscles where they promote or inhibit (respectively) promiscuous synaptogenesis. Netrin B is restricted to expression in a subset of muscles where it attracts some axons and repels others. The study showed that growth cones in this system do not rely on single molecular labels on individual targets, but assess a relative balance of attractive and repulsive cues. Thus, they select their target based on combinatorial and simultaneous input of multiple cues. Other molecules implicated in target selection in *Drosophila* include Connectin (Nose *et al.* 1994, Raghavan & White 1997), Beaten path (Fambrough & Goodman 1996) and Fasciclin III (Chiba *et al.* 1995).

1.2.7.2 Synapse formation.

Target selection has been shown to be independent of synapse formation (Prokop *et al.* 1996). Once again, combined molecular and genetic studies have provided important insights into the mechanisms of synapse formation in *Drosophila*. An important model in this field is the neuromuscular junction (NMJ) and there has been much research into the mechanisms of NMJ assembly (reviewed by Broadie 1998).

A PDZ-containing protein Discs-large (Dlg) plays a central role in assembling specific components at the synapse, including the homophilic CAM Fasciclin II and the Shaker potassium channel. Dlg is a membrane-associated guanylate kinase (MAGUK) family member implicated in regulation of presynaptic function and postsynaptic structural maturation (Budnik 1996, Guan *et al.* 1996). Assembly of the NMJ presynaptic active zones occurs independently of the target cell, but synaptic localisation of the active zones requires a muscle derived Mef2 dependent retrograde signal (Prokop *et al.* 1996). Thus the basic components of pre- and post-synaptic machinery assemble independently of intercellular communication, but localise properly only in response to mutually exchanged inducing signals. Construction of the postsynaptic receptor field is induced by the presynaptic terminal.

All subsequent alterations to the synapse are activity dependent.

1.2.8 Activity-independent nervous system development - a summary.

Despite many gaps in knowledge it is starting to emerge that axon pathfinding is directed by the coordinate action of multiple guidance cues that are mediated by mechanistically and evolutionarily conserved ligand-receptor systems. The integration of the four fundamental guidance cues results in complex growth cone behaviour such as advance, turning, withdrawal (collapse) and target recognition (see figure 1.7). Even error correction during development has been reported in insects (Rajan & Denburg 1996) to ensure the stereotypy of final axon projections (particularly important in pioneer axon guidance). Complete sequencing of the genomes of the model organisms used to study nervous system development may lead to a shift in emphasis in the field from molecular phenomenology to more mechanistically based studies (as proposed by Tessier-Levigne & Goodman 1996). This may lead to a greater understanding of the precise functions of the gene products and, perhaps more importantly, how they fit together to control neural development.

Despite the major differences in organisation at the multicellular level, many of the fundamental cellular and molecular mechanisms involved are phylogenetically conserved between insects and mammals (for example the CAMs fasciclin II and NCAM respectively - Goodman 1994, Harrelson & Goodman 1988). Therefore close study of a particular circuit to a molecular level may indicate homology / similarity to mammalian nervous system components, as well as giving an insight into the evolution and conservation of molecules and genes between the two systems. A good model system in *Drosophila* is the giant fibre circuit, a simple neural circuit that mediates a reflex escape response to a shadow passing over the fly's head (thus preventing it being swatted).

1.3 Giant interneuron mediated escape responses.

Escape responses are seen in many vertebrates and invertebrates from sea anemones to rats (for a brief review see Korn & Faber 1996). These escape

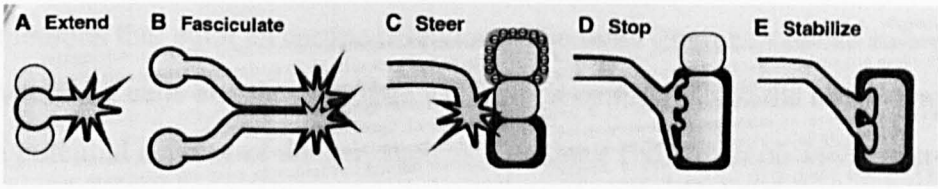

Figure 1.7a: A summary diagram revealing the many proposed roles of axon guidance cues.
A: Neurite outgrowth is promoted in a neuron expressing guidance cues.
B: Axon-axon fasciculation is mediated by guidance cues.
C: A growth cone steers away from some cells whilst turning towards others, via interactions mediated by guidance cues.
D: Growth cone stopping and initiation of synaptogenesis are caused by guidance cues.
E: Synaptic stabilisation or mobilisation is facilitated by guidance cues.
Figure from Chiba & Keshishan (1996).

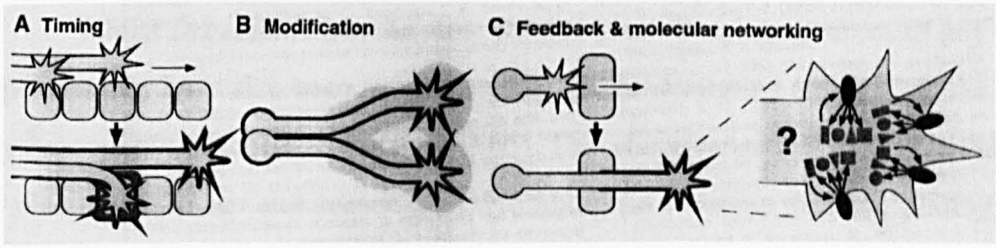

Figure 1.7b: Modes of control for membrane bound guidance cues.
A: Precise temporal control of guidance cue expression leads to specific neural recognition.
B: Alternate splicing or post-translational modification of guidance cues results in altered adhesivity and/or signal transduction.
C: A growth cone's contact with external cues activates guidance molecule receptors (black ovals), which can trigger any number of intracellular pathways and modulate the growth cone responses.
Figure from Chiba & Keshishan (1996).

responses often involve an identifiable giant fibre, especially in the invertebrate nervous system. Goldfish provide an example of a vertebrate with giant interneurons that elicit an escape behaviour. The giant interneurons are called the Mauthner cells and they mediate a C-shaped contraction of the torso away from potential sources of danger, such as a predator (Nissan *et al.* 1990, Eaton *et al.* 1995). It has been postulated, that in addition to the excitatory influence on motorneurons that initiate the escape response, the Mauthner axon size is important in rapidly spreading an inhibitory command to turn off other competing motor commands (Eaton *et al.* 1995). Within invertebrates, examples of giant interneuron mediated escape behaviours are found in cockroach (Levi & Camhi 1995), crayfish (Krasne & Teshiba 1995, Yeh *et al.* 1996) and the diptera.

1.3.1 Dipteran giant fibre escape circuits.

Whilst *Drosophila* has the most studied giant fibre interneurons of any dipteran, they have also been investigated in *Musca domestica* and *Calliphora erythrocephala* (Bacon & Strausfeld 1986). This characterisation was achieved by electrophysiology and intracellular dye filling (to visualise their morphology and characterise their dye coupling partners). Initially these techniques were easier in these larger diptera, but the genetic amenability of *Drosophila* has made it the ideal candidate to study this giant interneuron escape circuit.

1.3.2 The giant fibre circuit of *Drosophila melanogaster*.

The giant fibre circuit provides a convenient system in which to study neural development. The circuit itself mediates a reflex escape response to a light-off stimulus. As is the case with many reflex circuits, it is relatively simple, comprising just 10 neurons unilaterally, of the 200,000 or so thought to make up the CNS of *Drosophila*. The size of the cell bodies and axons of the 2 giant fibres that are the central component of this circuit meant that they were first identified in 1948 by simply silver staining the CNS (Power 1948).

More recently they have been extensively investigated. Techniques such as serial reconstructions of sections and electronmicroscopic examination of

synapses (King & Wyman 1980), electrophysiology (Thomas & Wyman 1984, Pavaldis & Tanouye 1995) and dye filling (Koto *et al*. 1981, Phelan *et al.* 1996) have been used, which take advantage of the size of the neurons. Additionally, the behavioural aspect of the circuit's function can be tested in relatively simple apparatus.

The giant fibre circuit mediates the light-off escape response by relaying excitation from the eyes to the muscles of the thorax. The neurons it is comprised of include the two large and distinctive interneurons known as the giant fibres. The circuit will be briefly described here (see figure 1.8) and elaborated upon in chapter 3.

1.3.3 Details of the circuit.

The giant fibres (GFs) are a pair of large bilaterally symmetrical interneurons with large cell bodies located close to the posterior of the brain (Koto *et al.* 1981). The main process of the neuron is connected to the cell body via a neurite, the dendritic field branches from this point, as does the axon (Koto *et al.* 1981, Phelan *et al.* 1996). The axon projects through the cervical connective to the mesothoracic neuromere. Each giant fibre axon has a lateral bend in the mesothoracic neuromere (Power 1948, King & Wyman 1980).

Just before the lateral bend each giant fibre synapses, near the inframedial bridge, with the peripherally synapsing interneuron (PSI - King & Wyman 1980). The PSI projects across the ganglion and synapses onto the five motorneurons (DLMns) of the contralateral dorsal longitudinal flight muscles (DLMs - Thomas & Wyman 1982). At the end of the lateral bend the giant fibre synapses again, this time with the large tergotrochanteral motorneuron (TTMn - King & Wyman 1980) - innervating the tergotrochanteral muscle (TTM, the "jump muscle" - Fernandes & Vijayraghavan 1993). This muscle acts as a leg extensor and wing elevator (Trimarchi & Schniederman 1993), so activity in the giant fibres results in mid-leg extension and wing opening and depression (Trimarchi & Schniderman 1994,1995 A, B & C). The TTM is the largest tubular muscle in the thorax, spanning the thorax dorsoventrally. It originates on the scutum and inserts on an apodeme in the proximal femur of the

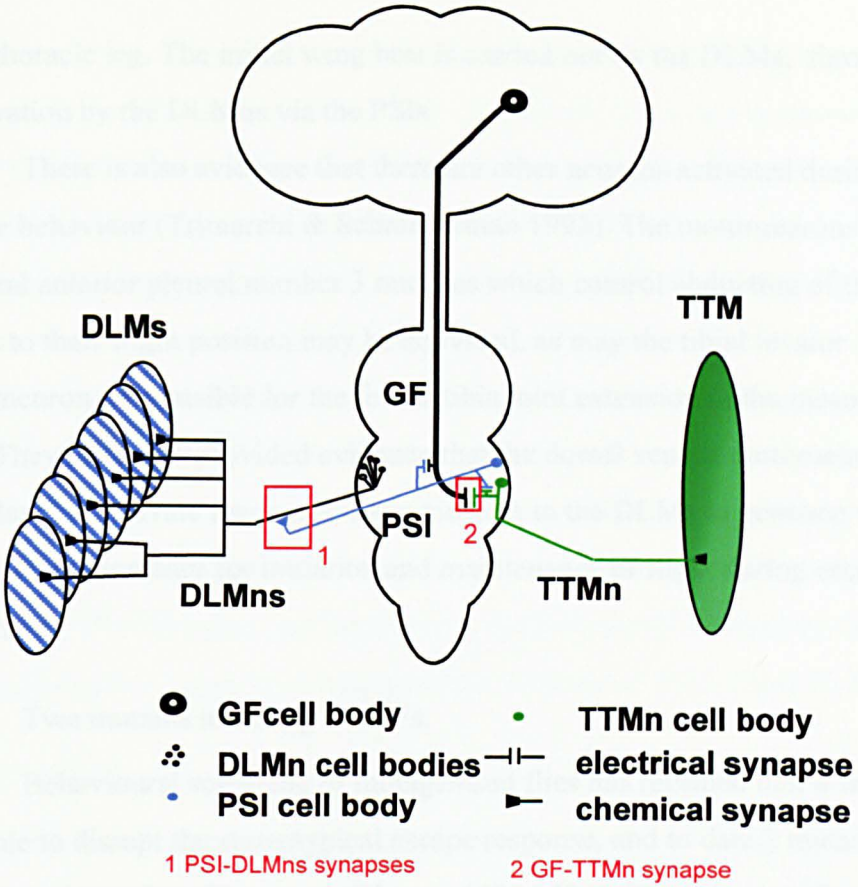

Figure 1.8A: Schematic diagram of the identified neurons and muscles of the GF circuit.
Only one half of the circuit is shown. GF= Giant Fibre, PSI= Peripherally Synapsing interneuron, TTMn= Tegotrochanteral motorneuron, TTM= Tegotrochanteral Muscle, DLMn= Dorsal Longitudinal motorneuron, DLM= Dorsal Longitudinal Muscle.

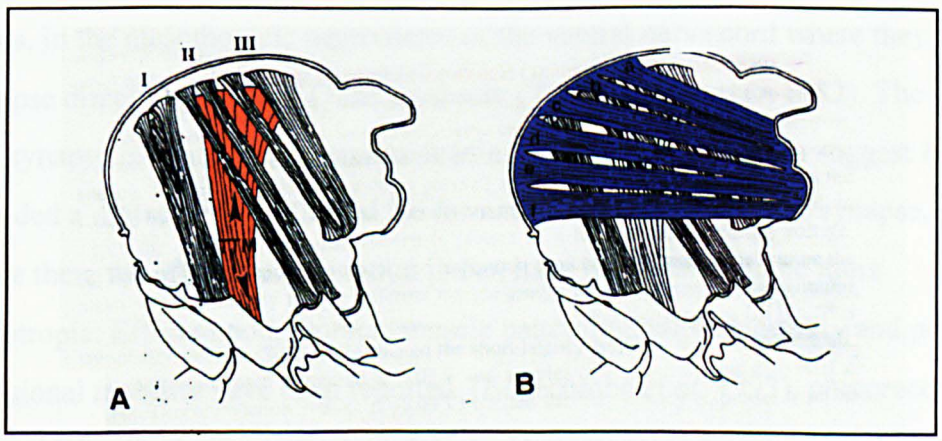

Figure 1.8B: Schematic diagrams of the muscles involved in the light-off escape response.
A: The tergotrochanteral muscle, spanning the thorax (red, labelled TTM).
B: The 6 dorsal longitudinal flight muscles (blue, labelled a-f).
Figures from Trimarchi & Schniederman (1995).

mesothoracic leg. The initial wing beat is carried out by the DLMs, through innervation by the DLMns via the PSIs.

There is also evidence that there are other neurons activated during the escape behaviour (Trimarchi & Schniederman 1993). The motorneurons for the bilateral anterior pleural number 3 muscles which control abduction of the wings to their flight position may be activated, as may the tibial levator motorneuron, responsible for the femur-tibia joint extension of the mesothoracic legs. They have also provided evidence that the dorsal ventral motorneurons are stimulated to activate the antagonistic muscles to the DLMs to generate wing movements necessary for initiation and maintenance of flight during escape behaviour.

1.3.4 Two mutants affecting the GFs.

Behavioural screening of mutagenised flies has revealed that it is possible to disrupt the stereotypical escape response, and to date 2 mutant genes have been identified (Thomas & Wyman 1983,1984). These are *bendless* and *shaking-B*.

1.3.4.1 bendless.

bendless (ben), is named because the characteristic bend of the giant fibres, in the mesothoracic neuromeres of the ventral nerve cord where they synapse directly with the TTMns, is absent (Thomas & Wyman 1982). The GF-PSI synapse is unaffected, therefore leading Thomas & Wyman to suggest *ben* encoded a molecule that affected the formation of a single specific synapse. Since then, the effects of a mutation in *ben* have been shown to be more pleiotropic. Effects upon, thoracic muscle patterning, pupal mortality and post eclosional mobility have been reported (Edgecombe *et al.* 1993), photoreceptor R7 and R8 retinal axon projection defects, photoreceptor defects, retinal lamina defects (Oh *et al.* 1994) and grooming behaviour defects (Phillis *et al.* 1993) have also been noted.

The gene has subsequently been cloned (Muralidhar & Thomas 1993, Oh *et al.* 1994) and codes for a ubiquitin conjugating enzyme (UBC). UBCs

have been shown to target proteins for degradation, and the conclusion based on the phenotype of *ben* mutant flies is that this process has a role in neural development (Oh *et al.* 1994, Muralidhar & Thomas 1993). This role must be presynaptic as mosaic analysis has revealed that the GF phenotype is determined by the genotype of the head (Oh *et al.* 1994). Data from the photoreceptor projection and GF projection phenotypes in mutant flies indicate *ben* may act to regulate the direction of growth near the postsynaptic target (and therefore may be affecting growth cone development). Specific ubiquitination of an unknown target/targets by *ben* in the GF may affect axon guidance either by stabilising adhesive interactions or by degrading inhibitory or repellent molecules. Therefore *ben* may be involved in either target recognition or stabilisation after target contact (Muralidhar & Thomas 1993, Oh *et al.* 1994).

1.3.4.2 shaking-B.

The second mutant gene is an allele of the *shaking-B* locus (Crompton *et al.* 1995). In this case, the giant fibre circuit appears intact in general morphology of the components, however the mutation disrupts transmission at the GF-TTMn synapse and probably the GF-PSI synapse (Thomas & Wyman 1982,83,84, Krishnan *et al.* 1993). The cause of this disruption has been shown to be directly due to the prevention of electrical synapse formation or maintenance (Phelan *et al.* 1996, Sun & Wyman 1996). The gap junction impairment, revealed by a lack of dye coupling in the GF synaptic partners, is not manifest in all gap junctions in mutant flies indicating some specificity for the gene in the GF circuit.

Two groups (Krishnan *et al.* 1995, Crompton *et al.* 1995) have shown that the *shaking-B* locus encodes 2 polypeptides, Shak-B^{neural} and Shak-B^{lethal}. The locus is a complicated one (Baird *et al.* 1990) with alternative splicing producing the 2 transcripts coding for Shak-B^{neural} and Shak-B^{lethal}. Combinations of the neural and lethal alleles result in the production of both proteins thereby demonstrating intracistronic complementation (Krishnan *et al.* 1995). The lethal transcript is expressed in somatic musculature, visceral mesoderm and cardioblasts in the embryo and is expressed in the pupal CNS.

The neural transcript is expressed only in the pupal CNS (within the GFs) - (Crompton *et al.* 1995).

Shaking-B (alias Passover - Pas) belongs to a family of proteins called the OPUS family (Barnes 1994). The name is derived from the initials of a group of similar proteins with sequence homology: the *Drosophila* genes, *lethal (1) optic ganglion reduced* (*l(1)ogre*), *passover*/*shaking-B* and the *C. elegans* gene *unc-7*. These are multipass transmembrane proteins and based on their mutant phenotypes are candidates for the invertebrate gap junction proteins.

Evidence for Shaking-B being an integral channel protein in gap junctions was recently provided (Phelan *et al.* 1998). Both lethal and neural proteins were expressed in paired *Xenopus laevis* oocytes. They localised to the membrane and, in the case of Shak-B^{lethal}, the presence of the protein induced the formation of functional intercellular channels. These data indicate Shak-B^{lethal} expression leads to electrical coupling via homotypic interactions. This study provided the first evidence that invertebrates have gap junction proteins that are functionally analogous to, but molecularly distinct from, the connexins in vertebrates. However, it is Shak-B^{neural} that is essential for the gap junction function at the electrical synapses of the GFs, not Shak-B^{lethal}. Shak-B^{neural} expression in *Xenopus* oocytes did not lead to the formation of intercellular channels. Both proteins are similar in molecular mass (43-44,000) and share a common C-terminus (coded for by 5 common exons), are conserved in the membrane spanning regions and therefore may be expected to function in a similar manner. It may be that, although very similar, the neural form acts in a more cell specific manner, forming heterotypic/heteromeric channels, the partners for which will not be present in the *Xenopus* oocyte system used.

1.3.5 Summary.

The giant fibre circuit of adult *Drosophila* comprises a small number of neurons and is known to be involved in escape behaviour (Thomas & Wyman 1982, Trimarchi & Schniederman 1995A & B). The circuit has also been used as a model system in which to study the effects of gene mutations on the functioning of an adult neural circuit *in vivo* (Pavaldis & Tanouye 1995, Engel

& Wu 1996,1998, Lin & Nash 1996, Schneiderman *et al.* 1993). The simplicity and its precedence of study has made the giant fibre circuit an important model system in the adult fly, with a number of basic questions remaining about its development. When are the component neurons born? What is the time course of the circuit development, and how do each of the individual neurons develop and in what order? Is there any plasticity of development? Whilst many features of embryonic development have been intensively studied, less is known about the development and underlying mechanisms involved in formation of neural connections through larval and pupal CNS development.

1.3.6 P[GAL4]307.

Enhancer trapping, using modified P-elements, provides a method of marking neuronal cells during development. One enhancer trap line, P[GAL4]307, picked out in an enhancer trap screen, marks the giant fibre circuit (figure 1.9). This thesis concerns the use of P[GAL4]307 as a molecular marker for the giant fibre circuit, therefore an introduction into enhancer trapping is required next.

1.4 The P-element.

Transposable elements are fragments of DNA with the special ability to jump from place to place within the genome. Typically they are widely scattered around the genome and there are many of them, in highly variable positions. In *Drosophila melanogaster*, transposable elements are thought to constitute between 10% to 20% of the genome. A typical individual may have as many as 50 transposon families with an average of 100 genomic copies each (Engels 1992).

The P family of transposable elements are naturally occurring genetic elements, most of which are autonomously capable of insertion into the *Drosophila* genome. It is a currently held belief that these elements were introduced through a rare horizontal transmission event, less than 100 years ago, rapidly spreading by heredity and transposition to become apparent in all natural populations within a few decades (Kidwell 1979,1983).

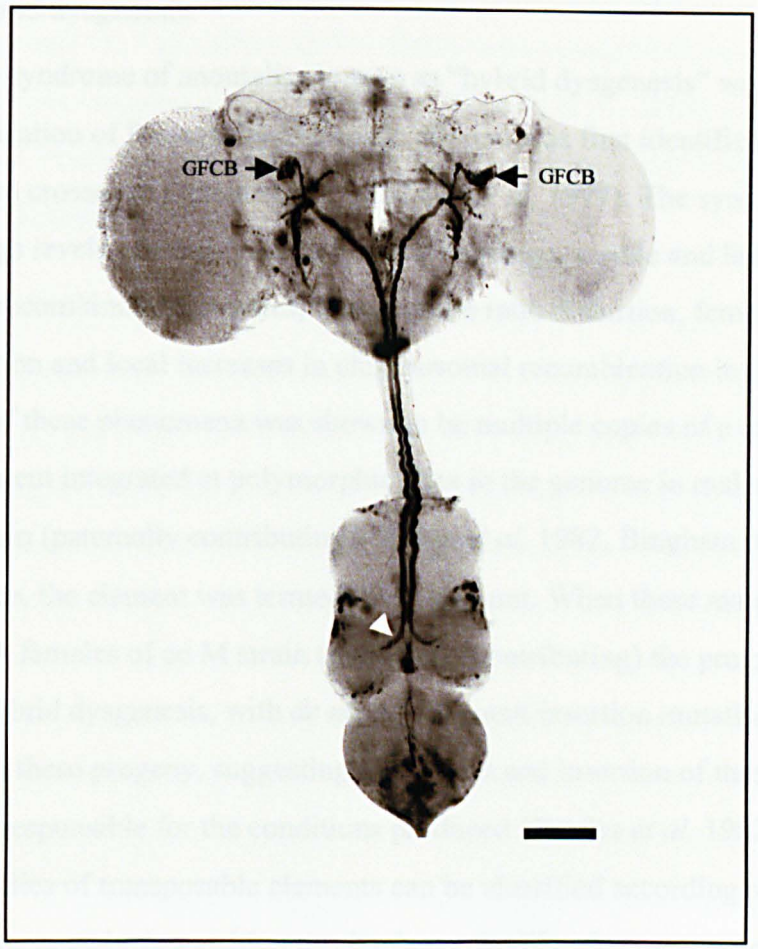

Figure 1.9: Dissected adult CNS of a fly containing P[GAL4]307and a UAS-*lacZ* reporter construct stained for β-gal protein by immunocytochemistry.
A dorsal view of the adult pattern 1-3 days post eclosion clearly showing the giant fibre cell bodies (GFCB) the large GF axons and the characteristic bend in T2 (marked with white arrowhead). Scale bar = 100μm

1.4.1 Hybrid dysgenesis.

The syndrome of anomalies known as "hybrid dysgenesis" was the earliest indication of P-elements in *Drosophila* and was first identified in F_1 hybrids from crosses of certain strains (Kidwell *et al.* 1977). The syndrome includes high levels of sterility, chromosome breakage, visible and lethal mutations, recombination in males, transmission ratio distortion, female nondisjunction and local increases in chromosomal recombination in females. The cause of these phenomena was shown to be multiple copies of a mobile genetic element integrated at polymorphic sites in the genome in males of the so called P strain (paternally contributing)-(Rubin *et al.* 1982, Bingham *et al.* 1982). Hence, the element was termed the P-element. When these males were crossed with females of an M strain (maternally contributing) the progeny exhibited hybrid dysgenesis, with *de novo* P-element insertion mutations appearing in these progeny, suggesting movement and insertion of these elements is responsible for the conditions produced (Searles *et al.* 1982).

Families of transposable elements can be classified according to their repeat structures and transposition mechanisms. Ac-like elements, named after Activator the first transposable element identified by McClintock, have inverted terminal repeats of less than 100 base pairs and are thought to transpose by DNA-only mechanisms. The P-element family of elements is the most extensively studied of the Ac-like elements in *Drosophila* (Engels 1992).

1.4.2 P-element structure.

P-elements naturally occur that are both autonomous and non-autonomous. The sequencing of autonomous P-elements has revealed important features. There are 31bp terminal inverted repeats and 11bp subterminal inverted repeats required for efficient transposition in *cis* (O'Hare & Rubin 1983) and a gene coding for transposase in four exons which is required in *trans* for transposition and regulation of transposition (Rio 1990, Rio & Rubin 1988). Non-autonomous elements tend to have internal deletions, lacking the

transposase gene, but are in other respects fully functioning and can be mobilised by the addition of a transposase source. Transposase is an 87 kD protein that binds GTP (Kaufman & Rio 1992) subsequently allowing binding to the subterminal regions of the P-element (Kaufman *et al.* 1989), causing transposition. Transposition is restricted to the germ line cells by tissue specific splicing of transposase (Laski *et al.* 1986).

1.4.3 Transposition.

Transposition is a non replicative event and does not involve an mRNA intermediate (Engels *et al.* 1990, Kaufman & Rio 1992), the element excising and reinserting itself into the genome, resulting in a target site duplication of 8bp (O'Hare & Rubin 1983). The target site is not random, however the mechanism of site selection is not fully understood. Investigations by a number of researchers has revealed several facts that are generally true of most insertion events. P-elements insert more often into euchromatic loci than heterochromatic loci (Berg & Spradling 1991), with some loci being more susceptible than others. Within genes there is a preference for non coding upstream sequences (Kelly *et al.* 1987), and regions corresponding to the consensus octamer GGCCAGAC (O'Hare *et al.*1992). If there are other P-elements present they tend to insert near them or into the terminal repeat at 19-26bp (Eggleston 1990).

1.5 Enhancer trapping.

Enhancer trapping was first devised by O'Kane and Gehring (1987), and represented a major breakthrough in rapidly producing tissue and cell specific markers and subsequent identification of genes expressed in these restricted patterns. The technique was based on a modified version of the naturally occurring mobile genetic element, the P-element, its low copy number and high transposition rate making it an ideal tool.

The enhancer trap allows the *in situ* detection of genomic elements that regulate transcription. The method is based on the fact that many regulatory sites in eukaryotes act at a distance of up to several thousand base pairs of the promoter and in either orientation (Atchison 1988).

1.5.1 First generation enhancer trapping.

The "first generation" enhancer traps (O'Kane & Gehring 1987, Bier *et al.* 1989 & Bellen *et al.* 1989) consisted of a modified transposable element, called P[lrAB]. This element had the terminal repeats of the P-element but lacked the open reading frames that code for transposase, which were replaced by the reporter gene – *E.coli lacZ* gene. This gene codes for the enzyme β-galactosidase.

These elements were introduced to flies by co-injection into precellular embryos with a second construct, a helper plasmid (pπ25.7wc), encoding P-transposase, but itself unable to transpose. Thus the transposon could integrate into the genome using the source of transposase provided by the helper plasmid. Therefore with the germ line specific activity of transposase the insertions were passed on to progeny and a stock of each incorporation event could be established.

The need for time consuming injection into embryos every time a new insertion line was to be produced, was soon removed. Strains of flies with a defective P-element transposon expressing high levels of transposase, but unable to move itself, known as "jumpstarter" strains are crossed to flies with P-elements in the genome to remobilise the element creating new enhancer trap lines (Robertson *et al.* 1988). The random insertions are the basis of new lines as they are captured in individual stocks that no longer contain the transposase source, and so remain stable (Cooley *et al.* 1988).

The dependence of expression levels on the genomic position of integrated genes have been frequently reported in eukaryotes and are termed "position effects". Therefore a promoter sensitive to the activity of adjacent genomic sequences, linked to a reporter, would allow detection of these elements in the genome that regulate transcription at a distance. The promoter required to initiate β-galactosidase production when activated needs three properties:

1) To allow easy detection of an increase in its activity, the promoter has to be relatively weak.
2) To be relatively exposed to the influences of enhancers on at least

one side of the integration site, the promoter should be at one end of the transposon.

3) To show any spatially regulated pattern of expression superimposed over the uniform, low background levels, the promoter has to be constitutively active in all cells throughout development.

A promoter which fulfilled all 3 requirements was the P-element itself, whose main transcription start site is 87bp from the 5' end of the element (O'Kane & Gehring 1987).

Onto the 3' side of the *lacZ* gene, the trailer sequences and the polyadenylation site of the *Drosophila hsp70* gene were cloned to allow functional transcription of the exogenous gene. Finally a genetic marker is required to show that the construct has successfully inserted into the genome. In this case the *rosy* gene (*ry*) was used - an eye colour marker (O'Kane & Gehring 1987).

Therefore, the transposon contained a gene that coded for a detectable product, under the control of a weak promoter. This weak promoter could not drive the gene in the absence of a transcriptional enhancer near the insertion site in the genomic DNA (hence the name - enhancer detector or trap). As the construct was incorporated into the germ line the transformed progeny would contain the transposon in all their tissues. The expression patterns vary between lines and are stable and inheritable. The genomic elements most likely to be capable of activating the promoter to produce β-galactosidase at detectable levels are enhancers. These exhibit several characteristics: they increase production by *cis* linked promoters, they operate orientation independently, they exert effects over large distances and they enhance the expression of heterologous promoters (Atchison 1988). Transposon integration near an enhancer occurs in about 65% of insertions and the *cis* acting enhancer enhances transcription from the weak promoter - see figure 1.10.

The "first generation" P-element transposons contained the *E.coli lac-Z* gene coding for the enzyme β-galactosidase which is easily detected by polyclonal antibodies to the protein or by a histochemical assay involving the breakdown of a chromogenic substrate, 5-bromo-4-chloro-3-indolyl-β-D-

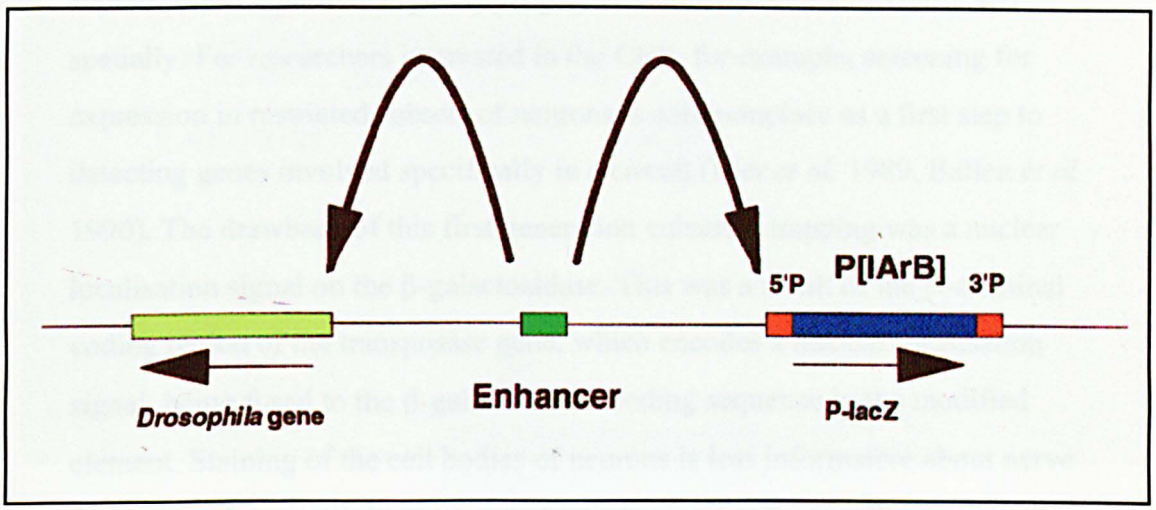

Figure 1.10: Diagram illustrating the principle of "first generation" enhancer trapping.

An endogenous enhancer element acts on the P-element reporter construct (P[lArB]), producing β-galactosidase in the nuclei of cells, in a pattern reflecting that of the gene(s) controlled by the enhancer. Diagram modified from Wilson *et al.* (1989).

galactoside (X-gal), by the enzyme to give a characteristic blue colour. Rapid screening of enhancer trap lines is done using X-gal; all the tissues can be tested for β-galactosidase activity.

Enhancers regulate the pattern of gene expression, patterns detected should reflect a particular gene(s) expression domain both temporally and spatially. For researchers interested in the CNS, for example, screening for expression in restricted subsets of neurons is commonplace as a first step to detecting genes involved specifically in a circuit (Bier *et al.* 1989, Bellen *et al.* 1990). The drawback of this first generation enhancer trapping was a nuclear localisation signal on the β-galactosidase. This was a result of the N-terminal coding region of the transposase gene, which encodes a nuclear localisation signal, being fused to the β-galactosidase coding sequence in the modified element. Staining of the cell bodies of neurons is less informative about nerve function and connectivity than visualising the axons (Kaiser 1993).

1.5.2 "Second generation" enhancer trapping.

The advent of "second generation" enhancer trapping (Brand & Perrimon 1993) has bypassed the problem of nuclear localisation by removing the original *lacZ* gene and placing a gene in the transposon coding for GAL4 protein. This yeast regulator of gene expression acts at the transcriptional level, dimers binding a yeast Upstream Activating Sequence (UAS) at four related 17bp sequences (Giniger *et al.* 1985, Marmorstein *et al.* 1992). Transcriptional activation is achieved by interaction with the GAL4 protein and another factor bound to the DNA near the transcriptional start site (Keegan *et al.* 1986) .

A second construct crossed into the flies with a yeast UAS, binds the GAL4 allowing the activation of a modified *lac-Z* gene on this construct (figure 1.11, X = *lac-Z*). The modified *lac-Z* gene product is cytoplasmically localised (Kaiser 1993). The enhancer trap lines activating UAS-*lacZ*, that is detectable cytoplasmically, allowing for elucidation of cellular architecture, including axon trajectory (Phillis *et al.* 1996) and neuronal complexity (Yang *et al.* 1995). The technique has been used recently to reveal the alteration and reconfiguration of sensory neurons from larval life to adulthood (Smith & Shepherd 1996).

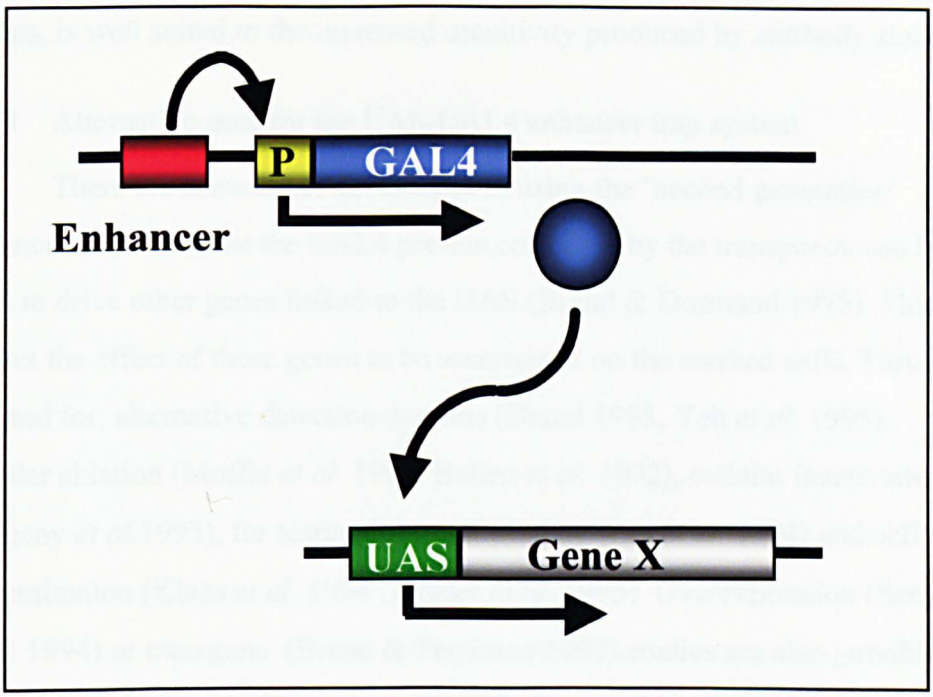

Figure 1.11: A diagram of second generation enhancer trapping.
This binary system has a primary P-element construct that responds to a local endogenous enhancer in the same manner as first generation enhancer traps. The reporter (gene X) is on a separate construct and is activated by the GAL4 product of the first construct, binding to the upstream activating sequence (UAS). See accompanying text for details.

P[GAL4]307 is a second generation enhancer trap line, cytoplasmically expressing β-galactosidase. The staining of axons, allowed for by this development of enhancer trapping, particularly those projecting from small cell bodies, is well suited to the increased sensitivity produced by antibody staining.

1.5.3 Alternative uses for the UAS-GAL4 enhancer trap system.

There are some other advantages in using the "second generation" enhancer traps because the GAL4 protein coded for by the transposon can be used to drive other genes linked to the UAS (Brand & Dormand 1995). This allows the effect of these genes to be ascertained on the marked cells. This can be used for; alternative detection systems (Brand 1995, Yeh *et al.* 1995), cellular ablation (Moffat *et al.* 1992, Bellen *et al.* 1992), cellular inactivation (Sweeny *et al.*1995), for testing axon pathfinding (Lin *et al.* 1994) and cell fate determination (Klaes *et al.* 1994 , Halder *et al.* 1995). Overexpression (Serrano *et al.* 1994) or transgene (Brand & Perrimon 1993) studies are also possible via this methodology and effects can potentially be tested in as many different patterns as there are enhancer trap lines (many of which are readily available within the *Drosophila* community via stock centres and personal collections).

1.5.4 Mutant production by imprecise excisions or flanking deletions.

Enhancer trapping as a technique has many associated benefits, including, on remobilisation of the transposable elements, imprecise excisions (Voelker *et al.*1984) leading to removal of genomic DNA surrounding the insert. One main feature of imprecise excisions is the creation of mutants - traditionally the starting point of tracking down a gene - either by interrupting an exon or by removing an important regulatory region. Alternatively, flanking deletions can be created by selection for male recombination events (Preston *et al.* 1996) that will yield deletions of several base pairs to several hundred kilobases.

1.5.5 Plasmid rescue.

Plasmid rescue of the P-elements (Wilson *et al.* 1989) is another technique associated with enhancer trapping (figure 1.11). The transposon has

within it antibiotic resistance (*Amp*^{R}) and plasmid origin of replication genes (*ori*). The genomic DNA from transformed flies is digested with a specific restriction enzyme that recognises a site in one of the transposon polylinker sequences, cleaving 5' to the *Amp*^{R} and *ori* genes. There are no further recognition sites for this enzyme within the transposon, so the fragment contains the *Amp*^{R} and *ori* genes plus an unknown length of genomic DNA, its length being dependent upon the site of the next naturally occurring restriction site for the enzyme. Subsequent ligation of this DNA circularises it, and it is then used to transform competent *E.coli* cells. Selection for antibiotic resistant colonies is followed by recovery of the genomic DNA by digestion.

Plasmid rescue of the region surrounding P[GAL4]307 has been done, yielding 25Kb of flanking genomic DNA (K.G.Moffat pers. comm.).

1.5.6 Enhancer trapping, a summary.

Enhancer trapping is based on a modified naturally occcurring mobile genetic element, the P-element. First generation enhancer trapping produced a nuclear localised detectable product with limited application in the investigation of neural projection patterns. This was solved by the introduction of a second generation, binary system of enhancer trapping allowing a variety of detection systems linked to the primary reporter construct. Enhancer trapping also allows the cloning of flanking genes, providing the opportunity to clone the genes whose pattern within a tissue are regulated temporally and spatially by the enhancer being detected. In this manner the screening of patterns within a tissue of interest may lead to the cloning of genes involved in a range of separate developmental processes. The use of this reverse genetic approach has the potential to reveal pleiotropic and redundant genes not easily detectable by traditional mutagenesis.

1.6 Aims.

Within *Drosophila* the neuroectoderm formation, embryonically, is followed by neuroblast formation (all the neuroblasts required for both larval and adult CNSs are produced embryonically), which in turn leads to the production of neurons and glia via asymmetric cell division (through defined phases of cell division). Once produced the neurons undergo a stereotypic development precisely connecting to targets to produce a functioning CNS that will subsequently be refined by activity. Post embryonically this process of CNS development is slightly different as it requires the alteration of a developed nervous system to serve a new body plan. The "wiring" of a nervous system shares processes embryonically and postembryonically requiring the action of a large number of gene products in complex and overlapping arrays. These gene products are largely subdivisible into four sets of guidance activities with any particular molecule belonging to one or more of these categories. The molecules involved tend to be highly conserved between organisms from mammals to insects. The study of genes encoding these activities has traditionally relied on mutant production and subsequent cloning of the genes involved. This has drawbacks as genes with pleiotropic effects and partially redundant functions are difficult or impossible to investigate.

The use of reverse genetic techniques such as enhancer trapping has the potential to reduce these problems. Enhancer trapping has been used previously to clone genes based on expression patterns (for example *Fasciclin III* and *Collagen type IV*, Wilson *et al.* 1989). A pattern of interest in a subset of the nervous system can be investigated by cloning of the endogenous gene whose expression is controlled by the enhancer and revealed by the enhancer trap pattern. Therefore, the potential exists to clone a gene involved in nervous system development. In this manner the pleiotropic or redundant functions of the gene are not of any immediate consequence. The giant fibre circuit represents a model circuit that is well defined and accessible to experimentation via a range of techniques, and in these respects is relatively rare in the adult CNS. The enhancer trap line P[GAL4]307 was isolated from a CNS screen of lines marking the giant fibres. P[GAL4]307 presents an opportunity to define

the extent and specificity of the expression pattern in the giant fibre circuit, to investigate the development of the circuit and clone a gene that may be involved in establishment of the circuit. To date, two giant fibre specific genes have been isolated by traditional mutagenesis techniques. The potential exists to discover a new gene that, within the CNS at least, is involved in the development of a specific neural circuit.

2. Materials & Methods

2.1 Techniques for the study of enhancer trap expression pattern and giant fibre development.

2.1.1 Staging development of *Drosophila melanogaster*:

2.1.1.1 Embryos:

Embryos were aged based on hours After Egg Laying (AEL). Staging was done morphologically based on descriptions in Campos-Ortega & Hartenstein (1985).

2.1.1.2 Larvae:

Larvae were staged based on hours after hatching (0-48 hours = 1st instar (L1), 48-72 hours = 2nd instar (L2), 72-144 hours = 3rd instar (L3)). Staging larvae by mouthpart morphology is more accurate , but is impractical for large scale experiments.

2.1.1.3 Pupae:

Pupae were staged based on morphological characteristics visible through the pupal case (based on Bainbridge & Bownes 1981).

Stages from Bainbridge & Bownes	Timing in hours APF
L3	
P1(WPP)	0-1
P2-3	1-7
P4(i)-5(i)	7-13.5
P5(i)	12.5-48
P5(i)-6	14-48
P7-9	38-78
P10-12(i)	72.5-97
P12(ii)-15(i)	75-105
Total	

APF= after puparium formation.

2.1.2 Phosphate buffers:

General lab chemicals were from Sigma except where specified.

Phosphate buffered saline (PBS) solutions:

PBS (0.1M $NaPO_4$ pH 7.3, 0.1M NaCl).

PBS-TX (0.1M $NaPO_4$ pH 7.3, 0.1M NaCl, 0.1% Triton X-100 (BDH, Poole, Dorset)).

PBS-Tw (0.1M $NaPO_4$ pH 7.3, 0.1M NaCl, 0.1% Tween 20).

2.1.3 Nervous system dissection:

Method as described in Drummond *et al.* (1997) and Allen, Drummond & Moffat (1998). Technique for removal of nervous systems from larvae, pupae and adult stages of *Drosophila melanogaster*. Dissections were performed in a petri dish (Nuncleon) half filled with Sylgard (a silicon elastomer from Dow Corning) using fine forceps (Dumont Medical).

2.1.4 Immunocytochemistry:

Method as described in Drummond *et al.* (1997) and Allen, Drummond & Moffat (1998). Technique to reveal the expression pattern of enhancer trap lines using an antibody to detect the reporter construct β-galactosidase.

2.1.5 Standard dehydration, clearing and mounting of tissues:

Tissues were dehydrated by washing for 5 minutes each in 50%, 70%, 90% and 95% ethanol. Finally they were washed three times for 5 minutes in absolute ethanol.

This was followed by clearing in xylene (BDH) or histoclear (Raymond Lamb, London) and mounting in either DePeX (BDH) for permanant preparations, or Canada Balsam (BDH). Mounting was done under a dissecting microscope (Zeiss Stemi SV6) using glass microscope slides (BDH) and coverslips (BDH).

2.1.6 Monitoring neuronal birthdates using BrdU:

2.1.6.1 Treatment with BrdU:

BrdU labelling was used to identify the timing of neuronal differentiation. Reagents for BrdU labelling were obtained from a cell proliferation kit (Amersham).

2.1.6.1.1 Larval treatment with BrdU:

Method as described in Allen, Drummond & Moffat (1998).

2.1.6.1.2 Embryonic treatment with BrdU:

Adapted from Limbourg & Zalokar (1973).

Laying cages and grape juice agar plates (see 2.5.3) are used for collection of embryos, as for antibody staining and *in situs* (see 2.1.7).

Embryos were collected in 1 hour periods covering the whole of embryogenesis rinsed in tap water, bathed in sodium hypochlorite for 3 minutes to remove the chorion and then rinsed again in tap water to remove residual sodium hypochlorite.

Perforation of the vitelline membrane, allowing the BrdU access to the developing cells and tissues, was achieved by moving the embryos into an eppendorf and washing with octane for 8 minutes on a rotator. The octane was drawn off and replaced with BrdU solution (1 mg BrdU/ml – diluted in Grace's Insect media (Gibco)) and then incubated on the rotator for half an hour or an hour. A subsequent wash in Grace's insect media removed any remaining BrdU and the embryos were transferred to concave slides and placed under halocarbon oil (KZM - series 700), in a moist chamber at 18^0C.

On hatching the survivors were transferred to Sussex fly food (see section 2.5.1) to develop to adulthood.

2.1.6.2 Detection of BrdU:

2.1.6.2.1 Detection of BrdU labelling in embryos:

To test labelling efficiency of the embryos with BrdU a number of embryos were removed pre-incubation in the high humidity chamber under halocarbon oil, and processed in the following manner.

Following treatment with the BrdU staining solution the embryos were washed in Grace's insect media. This media was then drawn off and after a brief fixation of 30 minutes (equal volumes n-heptane and 10% formaldehyde), the embryos were removed from the bottom of the eppendorf and placed in a new eppendorf.

Vitelline membranes were removed by the addition of methanol to the embryos,

followed by brief vigorous shaking (30 seconds) to mechanically aid the process. Subsequent treatments fix, permeablises and post fix the embryos. Two 2 minute washes in methanol and two 2 minute washes in equal volumes of methanol / 5% formaldehyde (diluted in PBS) were followed by fixing for 20 minutes in 5% formaldehyde (in 0.5 x PBS-TX). Rinsing occurred in three 5 minute washes with PBS-TX. Permeabilisation took place over 3 minutes at 37^0C in prewarmed proteinase K solution (Boehringer-Mannheim) at 5 mg/ml in PBS-TX. This digestion was stopped by washing twice for 2 minutes in glycine (2mg/ml - Sigma). Embryos are then washed three times for 5 minutes in PBS-TX, post fixed in 5% formaldehyde (in PBS-TX) for 20 minutes and washed again three times in PBS-TX for 5 minutes.

Following pretreatment, the incorporated BrdU was exposed by denaturing the DNA with acid treatment (2 N HCl in PBS-TX) for 30 minutes. Having washed the acid from the embryos with PBS-TX, they were incubated in bovine serum albumen (BSA) at 10% w/v, for 30 minutes to block non-specific antibody binding. After blocking, the primary antibody (mouse anti-BrdU monoclonal – Amersham) was added at 1:100 dilution in PBS-TX and left overnight at 4^0C. Following at least 5 rounds of 30 minute washes in PBS-TX the goat anti-mouse secondary antibody (from Vector) conjugated to tetramethylrhodamine isothiocyanate (TRITC) was added and allowed to incubate in the dark overnight at 4^0C. After rinsing in PBS-TX, the preparations were mounted under a coverslip using Vectashield (Vector) - an anti-quenching mountant.

2.1.6.2.2 Detection of BrdU and β-galactosidase in the adult CNS:

Method as described in Allen, Drummond & Moffat (1998).

2.1.7 Birthdating using the dye injection technique:

Method from D.William & D.Shepherd, University of Southampton.

2.1.7.1 Embryo preparation and dye injection:

A high molecular weight dye - biotin labelled dextran amine (BDA) was diluted to 25 mg/ml with 0.4M KCl and 1ml of intense blue food dye added (McCormick) to allow visualisation of the injection volume. This mixture was

then spun at 13,000 rpm in a benchtop micro centrifuge (MSE microcentaur) for 5 minutes to pellet any particulate matter in the solution. A 100µl glass capillary tube (Supracaps) was then heated over a flame and pulled to form a fine point. The injection solution was drawn into the capillary, from the top of the spun volume, by mouth pipetting (the capillary was attached to the end of a length of rubber tubing for this purpose). A prepulled fine injection needle, (sterile femtotip with 5µm opening- Eppendorf), was backfilled with the injection mix from the capillary tubing and attached to a controlled volume delivery system (Narishige) under an inverted microscope (Nikon). Prior to injection and between injection sessions the tip of the needle was kept under halocarbon oil (Voltalef 10S) on a glass microscope slide to prevent drying out.

Flies placed in a laying cage (cut away sandwich box), with an aperture for a grape juice agar plate supplemented with live yeast paste, had their embryos collected every hour (to ensure largely syncytial blastoderm stage embryos were collected). These embryos were then dechorionated by rolling on double sided sticky tape attached to a glass microscope slide. Once dechorionated the embryos were placed (end to end across the short axis of the slide) on a fine strip of double sided sticky tape placed at one end of the slide, for a maximum of 30 minutes after which the embryos were dehydrated for a further 5 minutes by incubation in a box containing a sachet of silica gel at 18^0C.

Dehydration allowed a volume of liquid to be injected into the embryos. To prevent further dehydration and to allow support of the embryos and respiration they were then covered in 10 S halocarbon oil. Injection, with an approximate volume of 50 nl injection mix, was into the centre of precellular embryos (older embryos were ruptured with the needle). Following injection the embryos were stored at 18^0C in a box containing moist tissue to ensure high humidity. They were left to develop to larvae and were transferred to normal fly media (Sussex fly food) to develop to pupal stages.

2.1.7.2 Dye detection in the pupal CNS:

Dissections of the pupal nervous systems were carried out as described in section 2.1.3.

Fixation of the CNSs with 4% paraformaldehyde for 30 minutes was followed by three 10 minute washes in PBS-TX (see section 2.1.2). Then they were washed for 45 minutes in PBS-TX containing 10μl of reagents A and B (Vector labs - Vectastain ABC kit) on a shaker at room temperature. This solution was washed off with three 10 minute rinses in PBS-TX and the DAB (diaminobenzidine - Sigma) staining solution added (0.1M Tris HCl pH 7.8 and 0.5mg/ml DAB).This was then allowed to permeate the tissue for 20 minutes in the dark, before 1ml of hydrogen peroxide (Fisher Scientific) was added and left to colour react until staining was visible. The reaction was stopped by three 10 minute washes in PBS-TX.

Following this the nervous systems were dehydrated, cleared in xylene and mounted in DePeX (as described in section 2.1.5).

2.1.8 Antibody staining to *Drosophila* embryos:

2.1.8.1 Collection of embryos for antibody staining:

Based Weichaus & Nusslein-Volhard (1986).

Approximately 50 *Drosophila,* of the required genotype, were placed in a small cage (made from a cut away sandwich box) and allowed to lay onto a grape juice agar plate.

Embryos were collected from the plate using a fine paintbrush and transferred to a collection basket that was placed into sodium hypochlorite (Fischer Scientific) dechorionated until they appeared shiny (approx. 3 minutes). The embryos were then transferred to a 1.5ml eppendorf containing a two phase mixture of equal volumes of n-heptane and 10% formaldehyde (diluted in PBS) and fixed, on a rotator at room temperature, for 20 minutes. The lower aqueous phase and some of the heptane was removed and 1ml of methanol added. The embryos were then devitellinised by shaking vigorously for 30 seconds. The devitellinised embryos (those which had sunk) were transferred to an eppendorf and washed with methanol.

These were then used immediately or stored in methanol at -20°C.

2.1.8.2 Antibody binding and detection:

Based on Jacobs *et al* . (1989).

Following the treatment described in section 2.1.8.1 the embryos were removed from -20°C. All the following steps were done at room temperature on a rotator, unless otherwise specified.

Two 2 minute washes in methanol and two 2 minute washes in equal volumes of methanol / 5% formaldehyde (diluted in PBS - see section 2.1.2) were followed by fixing for 20 minutes in 5% formaldehyde (in 0.5 x PBS-TX). Rinsing occurred in three 5 minute washes with PBS-TX. Permeabilisation took place over 3 minutes at 37^0C in prewarmed proteinase K solution at 5mg/ml . This digestion is stopped by washing twice for 2 minutes in glycine (2mg/ml). Embryos are then washed three times for 5 minutes in PBS-TX, post fixed in 5% formaldehyde (in PBS-TX) for 20 minutes and washed again three times in PBS-TX for 5 minutes.

Following the pre-treatment the embryos were blocked by washing in 10% (w/v) BSA in PBS, for 30 minutes. Primary antibody (polyclonal rabbit anti b-galactosidase from Cappel diluted 1:500 for enhancer trap pattern detection) in PBS-TX was then added and incubated either at room temperature for 4 hours or overnight at 4°C. Following this the embryos were washed three times for 5 minutes in PBS-Tw, then three times for 20 minutes in PBS-Tw.

The secondary antibody (Vector biotinylated goat anti-rabbit diluted 1:250 in PBS-TX) was added and incubated as for the primary antibody. Following this the embryos were washed 3 times for 20 minutes in PBS-Tw. ABC reagent was prepared by adding 16µl of reagent A and 16µl of reagent B (from Vectastain ABC horseradish peroxidase detection kit) to 1ml of PBS-Tw (1 hour prior to use). This was then added to the embryos and incubated for 30 minutes. The embryos were subsequently washed for 1 minute in PBS-Tw, and then washed three times for 20 minutes in PBS-Tw.

The colour reaction was performed by washing the embryos 3 times for 5 minutes in colour reaction buffer (0.1M Tris (pH 7.5); 0.12% fresh hydrogen peroxide, v/v) then placing them in a cell culture dish and adding DAB reagent

(diaminobenzidine solution (Sigma) 0.5mg/ml in colour reaction buffer). The embryos were incubated until the colour reaction was complete (typically from 30 minutes to two hours) and were then washed three times for 5 minutes in PBS-Tw.

The embryos were dehydrated, cleared in histoclear and mounted in Canada balsam (BDH) under coverslips supported by tape (see section 2.1.5).

2.1.9 Microscopy and photo microscopy:

Preparations were examined with a Zeiss Axioskop FS microscope. Slides were taken with an Olympus OM10 camera using Kodak 150T slide film. Alternatively images were captured with a JVC TK-1280E video camera attached to an Apple Power Macintosh 7100/80AV. These were subsequently montaged in Graphic Converter (shareware - Thorsten Lemke) or Canvas (Deneba), and printed through Powerpoint (Microsoft).

Nikon Optiphot microscopes were used to view the fluorescent preparations using the UV light source and a rhodamine filter (DM580). A Nikon FX-35A camera attached to a Nikon UFX-II lightmeter and exposure unit was used to capture images from this microscope on Kodak 160T slide film.

2.2 DNA manipulations:

All phenol extractions in this section were performed with Tris buffered phenol, pH7 (Fisons). All chloroform extractions used chloroform : isoamyl alcohol in a ratio of 24:1. DNA was quantified using an Ultraspec III spectrophotometer (Pharmacia) and associated software.

2.2.1 DNA isolation:

2.2.1.1 Isolation of genomic DNA from adult Drosophila:

A 15 ml homogeniser was washed and placed on ice. 100 - 200 flies were homogenised in 3mls of homogenisation buffer (10mM Tris (pH 8); 60mM NaCl; 10mM EDTA; 0.15mM spermidine; 0.5% Triton X-100 (v/v)) on ice. The homogenisation buffer containing the flies was filtered through gauze into a 15ml

plastic tube (Falcon 2059). The filtrate was centrifuged at 7,000 rpm for 7 minutes in a Beckman centrifuge (J2-21M/E) in a JS 13.1 swing out rotor at 4°C. The supernatant was removed and the pellet resuspended in 3mls of homogenisation buffer and centrifuged again at 7,000 rpm for 7 minutes (under the same conditions). The supernatant was discarded and the pellet resuspended in 1.8mls of homogenisation buffer and 200µl of 20% sarkosyl (N-Lauroyl-sarcosine 20% w/v, Sigma) added. The solution was mixed by inversion and 20µl of Proteinase K (10mg/ml) added. The solution was then incubated at 50°C for 2 to 3 hours.

Following proteinase treatment 200µl of sodium acetate (3M, pH 6.8) was added followed by 250µl phenol. The solution was vortexed for 10 seconds and centrifuged (conditions as before). The upper, aqueous layer was retained and an equal volume and chloroform / isoamyl alcohol added . This was vortexed and centrifuged again. The upper layer was transferred to a falcon tube (3059) and 3 volumes of 100% ethanol added. This was then spun at 13,000 rpm for 30 minutes in the Beckman J2-21M/E centrifuge with the JS 13.1 swing out rotor. Following this the supernatant was discarded and the pellet washed in 70% ethanol. The pellet was then air dried and resuspended in 100µl of dH_2O.

2.2.1.2 Small scale preparation of plasmid DNA:

Small scale isolation of plasmid DNA was performed in two ways. For most applications the alkaline lysis method was used, but for DNA to be sequenced the QIAprep Spin miniprep kit (Qiagen) was used.

2.2.1.2.1 Alkaline lysis method:

Described in Sambrook *et al.* (1989) - book 1, chapter 1, page 25.

2.2.1.2.2 QIAprep kit method:

This was done using a QIAprep Spin Miniprep Kit (Qiagen) according to manufacturer's manual.

2.2.1.3 Large scale isolation of plasmid DNA:

This was done using a Qiagen Plasmid maxi kit according to the manufacturer's manual.

2.2.1.4 Isolation of phage DNA from a liquid culture:

Adapted from Sambrook *et al.* (1989) - book 1, chapter 2, pages 72-73.

100 mls of an overnight culture of *E. coli* of an appropriate strain (e.g. LE392 or Y1090r$^-$) were taken and centrifuged in a Beckman centrifuge (J2-21M/E) at 2,500 rpm in the JA 14 rotor for 5 minutes. The pellet was then resuspended in 10mls 10mM $MgSO_4$. This was stored at 4°C for up to several weeks and used as required. For the phage infection; 1ml of the bacterial suspension in $MgSO_4$ was added to 1ml of CaMg mix (10mM $CaCl_2$; 10mM MgCl) and 5 x 10^8 phage particles in SM buffer (5.8g NaCl; 2g $MgSO_4$; 50ml In Tris (pH 7.5); 5mls 2% gelatine to 1l H_2O) and incubated at room temperature for 5 to 10 minutes. This was added to 500mls of NZYM (10g NZ amine; 5g NaCl; 5g Bacto yeast extract; 2g $MgSO_4$; 1l H_2O) and grown overnight in a shaking incubator at 37°C.

The following morning 2.5mls of chloroform were added along with 30g of NaCl, and placed on a magnetic stirrer until the salt had dissolved. The culture was then transferred to 250ml Beckman centrifuge pots excepting 1ml which was reserved for titreing the phage. DNAse and RNAse (both Boehringer Mannheim) were added to a final concentration of 1µg / ml each and the pots incubated for 2 hours at 37°C. 25g of PEG 8000 (Sigma) was then added to each pot, dissolved and then the mixture was left overnight at 4°C. The mixture was then centrifuged at 8,000 rpm (in a Beckman M2-21 M/E in a JA 14 rotor) for 30 minutes at 4°C and the supernatant removed by aspiration. The pellet was then resuspended in 1ml of SM buffer by vortexing and transferred to a 2ml eppendorf. To this 10µl of 10% SDS was added along with 10µl of 0.5M EDTA. This was then incubated at 68°C for 15 minutes.

Following the incubation the mixture was phenol extracted, phenol / chloroform extracted and finally chloroform extracted. An equal volume of isopropanol was added and the mixture centrifuged at 13,000 rpm in a benchtop centrifuge. The

resulting pellet was washed in 70% ethanol and then resuspended in 500µl H_2O.

2.2.2 Restriction Digestion of DNA:

This was done using buffers supplied by the manufacturer for each enzyme. The total reaction volume was between 10 and 100µl with the enzyme at 1/20 of the total volume. Enzymes were supplied by Gibco. From 200ng to 5µg of DNA was used in each reaction.

2.2.3 Size separation of DNA fragments:

Method based on Sambrook *et al.* (1989) - book 1, chapter 6, pages 3-15.

Fragments of DNA were separated on the basis of their size by electrophoresis in agarose gels by the standard method in Sambrook *et al.* (1989). For visualisation, the DNA was mixed with loading buffer containing 30% glycerol, 0.1% bromophenol blue and 0.1% xylene cyanol. The gels were run at between 20 and 150V until the DNA fragments had migrated far enough to become separated. Ethidium bromide was incorporated into the gel at 0.5µg/ml to allow visualisation of the fragments by placing the gel onto a U.V. transilluminator.

2.2.4 Transfer of DNA onto nylon membrane:

Adapted from Sambrook *et al.* (1989) - book 2, chapter 9, page 38.

DNA was transferred onto nylon membranes (Hybond N, Amersham) after gel electrophoresis for Southern hybridisation using capillary transfer. Transfer followed photography of the gel (see 2.2.3) on a U.V. transilluminator next to a ruler, to allow later estimation of DNA fragment sizes.

After electrophoresis the gel was incubated in 0.25M HCl if the fragments to be transferred were over 5Kb in length. For smaller fragments this step was omitted. The gel was then denatured by incubating in alkali buffer (0.5 M NaOH; 1.5 M NaCl) for 30 minutes and then neutralised by washing twice for 15 minutes in 1M ammonium acetate. The gel was then rinsed in 10 x SSC and the DNA was transferred to the membrane by capillary action. A piece of 3mm Whatman paper was wetted with 10 x SSC and placed on a glass plate. The gel was then inverted

and placed onto the paper. The nylon membrane was cut to size and placed on top of the gel. This was followed by three layers of Whatman (pre wetted with 10 x SSC) and finally on top of this a layer (approx. 10cm) of tissues. Another glass plate was placed on this and weight was placed on the top plate (a brick). Transfer was allowed to proceed overnight.

After transfer the membrane was removed from the stack and allowed to dry in an oven at 80^0C. The DNA was permanently fixed to the membrane by placing the membrane DNA side down on a U.V. transilluminator for 3 minutes. The membrane was then stored between Whatman paper before use.

2.2.5 Detection of labelled DNA hybridised to Southern blots:

Adapted from Sambrook *et al.* (1989)

Two methods were used for this procedure. DNA was either labelled with α^{32}P dGTP and detected with either X-ray film (Fuji) or a Molecular Dynamics Phosphor Image screen, alternatively, incorporation of digoxygenin labelled dUTP (Boehringer Mannheim) was used and detected with a colour reaction using NBT and X-Phosphate.

2.2.5.1 Preparation of radioactive probes for Southern hybridisation:

Two methods were used for probe preparation, the random priming method and the megaprime kit from Amersham. The megaprime kit also relies on random primers but uses nonamers as opposed to hexamers.

2.2.5.1.1 Random priming method:

Based on Feinberg & Vogelstein, 1983. Template was isolated from agarose gels by the QIAquick Gel Extraction Kit (see 2.2.9).

First three solutions were prepared.

Solution A: (1.25M Tris (pH 8); 0.25M $MgCl_2$; 0.018% β-mercaptoethanol; 1mM dATP; 1mM dCTP; 1mM dTTP).

Solution B: (2M Hepes pH 6.6).

Solution C: (Random hexamers (Boehringer Mannheim) at 90 OD units / ml in TE).

To make OLB these were mixed in the following ratio: Solution A : Solution B : Solution C, 100:250:150.

Approximately 50ng of template was dissolved in 32.5µl dH_2O and denatured by boiling in a water bath for 3 minutes. The template was incubated at 37°C for 5 minutes and the following ingredients added in order: 10µl OLB, 2µl BSA (10 mg/ml, Sigma), 5µl α^{32}PdGTP Amersham, 10µCi / µl), 1µl Klenow fragment of DNA polymerase (Gibco). The solution was mixed by pipetting and incubated at room temperature for 2 hours.

2.2.5.1.2 Megaprime Method:

This was done according to the manufacturer's manual except that the final incubation at 37°C was extended to 1 hour.

2.2.5.2 Separation of unincorporated nucleotides from DNA probes:

This was done using Amersham microspin columns. The column was prepared by spinning at 4,000 rpm in an MSE microcentaur benchtop centrifuge for 2 minutes and the eluent discarded. Following this the probe was added to the top of the column and again spun at 4,000 rpm for 2 minutes. Before use the probe was denatured by the addition of 1/10 total volume (typically 5µl) of 4M NaOH.

2.2.6 Hybridisation and detection of radiolabelled DNA hybridised to Southern blots:

Adapted from Sambrook *et al.* (1989) - book 2, chapter 9, pages 47-55.

The membrane onto which the DNA had been transferred was placed in a glass tube (Hybaid) and 50mls of prehybridisation solution (50% formamide (Fluka); 5 x Denhardts; 5 x SCC; 0.1% SDS, 100µg/ml denatured sonicated herring sperm DNA) preheated to 42°C was added. The tube was then incubated in a rotating oven (Hybaid) at 42°C for at least 1 hour. Most of the prehybridisation solution was then poured off and the denatured probe added. The blot was then incubated

for 12 hours at 42°C. Following incubation the probe was poured off and the membrane rinsed twice at room temperature 100mls of washing solution 1(2 x SSC; 0.1% SDS). The membrane was then washed twice in washing solution 2 (0.1 x SSC; 0.1% SDS) for 45 minutes each wash as 68°C in the rotating oven. The filter was then removed, wrapped in cling film and exposed to either X-ray film or a Phosphor imager screen.

2.2.7 Stripping radiolabelled probe from DNA blots:

To strip probe from filters to allow the re-probing the blot was washed at 70°C for 1 hour in 2mM EDTA; 0.1% SDS.

2.2.8 Hybridisation and detection of Digoxygenin labelled DNA on Southern blots:

2.2.8.1 Preparation of Digoxygenin labelled DNA:

Adapted from a Boehringer Mannheim product sheet.

50 - 60ng of template DNA was dissolved in 19µl of dH_2O and denatured by boiling for 5 minutes and then cooling on ice. To this was added 2µl of hexanucleotide mix (10 x conc., 62.5 OD_{260} units/ml, Boehringer Mannheim), 2µl of Dig DNA labelling mix (10 x conc., Boehringer Mannheim) and 1µl of Klenow. The mixture was incubated at 37°C from one hour to overnight. After labelling, the Dig DNA was precipitated by the addition of 80µl H_2O, 1µl tRNA (100 mg/ml, Sigma), 10µl of 4M LiCl and 300µl of 100% EtOH. This was centrifuged at 13,000 rpm for 30 minutes and the supernatant discarded. The pellet was washed in 70% ethanol and the pellet resuspended in 100µl formamide buffer (50% formamide (Fluka); 5 x SSC; 0.1 mg/ml sonicated and boiled herring sperm DNA; 0.1 mg/ml tRNA; 0.05 mg/ml Heparin; 0.1% Tween-20). This was then used as a 10 x stock probe for Southern blotting or *in situ* hybridisation.

2.2.8.2 Hybridisation and detection of Digoxygenin labelled probe on Southern blots using NBT and X-Phosphate:

Method from a Boehringer Mannheim product sheet.

DNA blots were prehybridised for 1 hour in 30mls prehybridisation solution (5x SSC: 1% blocking reagent (1 in 10 dilution of 10 x blocking buffer - Boehringer Mannheim); 0.1% n-Lauroyl sarcosine; 0.02% SDS) at 68°C. Digoxygenin labelled probes were denatured by boiling for 10 minutes followed by cooling on dry ice. Prehybridisation solution was poured off to leave a volume of 10mls. Single stranded probe was added (10µl) and the blot was incubated at 68°C for 12 hours.

The probe solution was poured off and the blot rinsed twice in 50mls of washing solution 1 (2 x SSC; 0.1% SDS) at room temperature. The blot was then washed twice for 45 minutes in washing solution 2 (0.1 x SSC; 0.1% SDS) at 68°C. The blot was then incubated for 2 minutes in malate buffer (100mM maleic acid, 150mM NaCl; adjusted to pH7 with NaOH) and then incubated for 30 minutes in 1% (w/v) Boehringer Blocking Reagent (Boehringer-Mannheim) in malate buffer, on a rocking platform. Anti Digoxygenin conjugate (Anti digoxygenin fab fragments conjugated to alkaline phosphatase, Boehringer Mannheim) was diluted 1:5000 in blocking solution at 10% (w/v) in malate buffer, and the blot was washed in this solution for 30 minutes.

The blot was then washed twice for 15 minutes each wash in 50mls of malate buffer containing 0.1% Tween-20 (Sigma). Next blots were washed twice for 5 minutes each wash in NMT (100mM Tris (pH 9.5); 100mM NaCl; 50mM $MgCl_2$). During these washes colour reaction solution was made by adding 90µl NBT (100 mg/ml in DMF - Boehringer Mannheim) and 45µl X-Phosphate (50 mg/ml in DMF- Boehringer Mannheim) to 10mls of NMT. The blot was then incubated with this solution until the colour reaction was complete. The reaction was stopped by washing in TE and the blot was stored in clingfilm.

2.2.9 Purification of DNA away from salts, impurities and agarose:

For this the QIAquick Gel Extraction Kits (Qiagen) were used. This was done

according to the manufacturers instructions.

2.2.10 Subcloning of DNA fragments into plasmid vectors:

The subcloning of DNA fragments into plasmid vectors can be divided into 4 stages: isolation of DNA, ligation of fragment to vector, transformation of host *E. coli* and selection of transformants. The isolation of DNA involves the restriction digestion of both vector and insert and then the purification of these away from other impurities.

This was done by agarose gel electrophoresis followed by purification of the desired DNA fragment using one of the gel extraction kits above. The vector used was pBluescript II SK+ (Stratagene)

2.2.10.1 Ligation of DNA fragments to plasmid vectors:

Based on Sambrook *et al.* (1989) - book 1, chapter 1, pages 53-67.

In the standard reaction 50ng of vector was digested with the appropriate restriction endonucleases and then treated with bacterial alkaline phosphatase (Gibco) to prevent religation of the vector. This was combined with insert DNA at a molar ratio of 1:3 and the volume made up to 17µl with dH_2O. To this 2µl of ligase buffer (Gibco) was added along with 1µl of T4 DNA ligase (Gibco). The reaction was mixed by pipetting and incubated at 14°C overnight.

2.2.10.2 Preparation of competent cells:

DNA transformations were made into DH5α cells. The method for competency was obtained from Sambrook *et al.* (1989). Competent cells were stored at -70^0C.

2.2.10.3 Transformation of Escherichia coli and selection of colonies:

Following 2.2.10.2, the ligated DNA (typically one quarter of the total reaction volume) was added and the mixture left on ice for a further 30 minutes. The bacteria were then heat shocked at 42°C for one and a half minutes and then placed on ice for a further 15 minutes. The bacteria were plated onto an LB agar plate containing Ampicillin (final conc 0.1mg/ml). Blue-white selection was used with pBluescript (pBS - Stratagene) by adding IPTG (Sigma) and X-gal

(Sigma) to the bacterial suspension to a concentration of 0.5% and 1% respectively, before plating.

2.2.11 Amplification of DNA using Polymerase Chain reaction (PCR):

2.2.11.1 Primer design:

All PCR and sequencing primers were designed using Primer Designer (Scientific & Educational Software). Primer Designer scores potential primers on the basis of a set of criteria which the sequence must fulfil in order to prime correctly under set conditions. The criteria include: primer length, GC content, melting temperature, dimers, runs of bases, annealing temperature, hairpins and stability 5' vs 3'. Primers fulfilling these standards were ordered from Gibco.

2.2.11.2 Basic PCR conditions:

Adapted from Innis *et al.* (1990).

PCR reactions were carried out using the following conditions for a 20µl reaction:

2.5µl 10 x PCR buffer (Gibco)

2µl 50mM $MgCl_2$ (Gibco)

0.5µl 10mM dNTPs (Promega)

1µl each Primer (10ng/µl)

x µl target DNA (100pg for plasmid - 1ng for genomic)

0.5µl Taq DNA polymerase (Gibco)

Made up to 20µl with dH_2O and overlaid with 2 drops of light paraffin oil.

A Hybaid Touchdown PCR cycler was used for all reactions.

PCRs using plasmid as target were preceeded by a hot start (3 minutes at 95^0C) prior to adding the Taq DNA polymerase, in order to melt the target sufficiently.

Cycle times:

15 seconds at 94^0C to melt template.

15 seconds at X^0C to anneal the primers to the template (this varies with the primers used and is listed with ordered primers).

Y seconds at 72^0C for extension (dependant on length of product : 45 seconds for 2Kb with 30 seconds extra for every additional Kb).

The number of rounds of amplification was determined by trial and error and was

usually about 30.

2.2.11.3 Reverse Transcription PCR (RT-PCR):

PCR as above (section 2.2.11.2) using DNA template produced by a reverse transcription reaction on RNA samples (isolated as in section 2.3.1). 0.5mg of total RNA was made up to 20.1µl with distilled water and heated to 75^0C for 5 minutes. Next 7.9µl of a mix (3.3mM random hexamers, 1x PCR buffer, 3mM $MgCl_2$, 500mM dNTPs and 1U/µl RNAase inhibitor) was added to each sample and heated to 37^0C for 5 minutes. Next, 2µl of MMLV reverse transcriptase (Gibco BRL, 200U/ml) was added to each sample and incubated for 1 hour at 37^0C. Controls without MMLV reverse trancriptase and with no RNA were included. Samples were heated at 95^0C for 5 minutes, with subsequent storage at -20^0C. 1µl of the reverse transcribed DNA was used in the PCR (2.2.11.2).

2.2.11.4 Phage library colony screening using PCR:

A phage pick was eluted in 500µl of SM buffer and 1µl of this was template for the PCR, carried out as in section 2.2.11.2.

2.2.11.5 PCR using "phage arm" primers:

A primer was made to the furthest 5' end of the cDNA cloned (*diomedes*) and used in a PCR with a primer to either of the lambda gt11 phage arms (depending on orientation of insert in library), to determine the size of any additional sequence in impure plaque picks (1^{st} and 2^{nd} round screens).
For details of the phage library screening see section 2.2.12.
The primers used were:
diomedes (PKout):5' CTG TCC GGC CAC AAT GTT GC 3'
gt11forward:5' GGT GGC GAC GAC TCC TGG AGC CCG 3'
gt11reverse:5' TTG ACA CCA GAC CAA CTG GTA ATG 3'
In each 20 µl PCR were the following: 1x PCR buffer, 0.25mM of each primer, 1µl W1, 1.5mM $MgCl_2$, 250mM of each dNTP, 0.2µl Taq DNA polymerase and 1µl of phage in SM buffer.
Cycling conditions were: 94^0C for 10 seconds, 60^0C for 20 seconds, 72^0C for 1.5

minutes for 35 cycles, then 72^0C for 5 minutes.

2.2.12 Screening of phage cDNA libraries:

Based on Sambrook *et al.* (1989) - book 1, chapter 2, page 108.

2.2.12.1 Plating phage:

Plates are prepared with standard LB agar (see 2.5.4.1) and warmed to 37°C. Top agarose (LB with 3.5g agarose per 500ml) was autoclaved and allowed to cool to 45°C in an oven. For library screens $22cm^2$ plates are used. 500 ml of LB agar were used per plate. Phage were added to 1 ml of LE392 or Y1090r$^-$ *E.coli* grown to stationary phase and resuspended in half the culture volume of ice cold sterile 10mM $MgSO_4$ and left at 37°C for 15 minutes. The bacterial suspension was added top agarose (20 mls for $22cm^2$ plates), mixed briefly and poured on to the plate. The plates were then incubated at 37 ° C for 8 - 10 hours and stored overnight at 4^0C before lifts were taken.

2.2.12.2 Plaque screening:

Plates were made as described above with approx. 500,000 plaques per plate and grown until the plaques are around 1mm diameter. After cooling Hybond N+ (Amersham) was cut to the size of the plate, placed on the plate and holes made in the filter using a sterile needle in an assymetric pattern to allow later orientation of the plates to the autoradiogram. After 30 seconds the filter was removed and placed,DNA side up, onto Whatman paper wetted with denaturing solution (1.5M NaCl, 0.5M NaOH) and left for 6 minutes. A replica was made and left on the plate for 2 minutes then subsequently treated as for the first lift. After denaturation the filters were placed into NaPi, pH 6.8 for 20-30 seconds and agitated, blotted on Whatman paper, baked at 80°C for 20-30 minutes in a Gallenkamp vacuum oven, then cross linked under U.V. for 3 minutes. Hybridisation was performed as for Southern hybridisation (2.2.6). Positive plaques were isolated by alignment of the replica lift autoradiographs, which were then aligned with the plate and removed with a sterile scalpel blade. The agar containing these plaques was placed in 1ml of SM buffer and incubated overnight at 4°C. This solution was then titred and used as a source of phage for further

screening. Three rounds of screening were performed to isolate a plaque pure phage clone.

2.2.13 Sequencing DNA:

2.2.13.1 Double stranded sequencing:

This technique was supplied with a dideoxy sequencing kit (the Sequenase Version 2 DNA sequencing kit from United States Biochemicals). Sequencing reactions were performed as described in the manufacturer's instructions using plasmid DNA prepared as in 2.2.1.2.2.

The method is essentially as in Sambrook (1989) - book 2, chapter 13, pages 3-10, 45-46 & 65-66. The gels were 0.4mm thick and were run in a 40 cm gel apparatus. Prior to running the gel the plates were thoroughly cleaned with detergent, cream cleaner and then ethanol, after which the inner surface of the smaller plate was treated with Acrylease (Stratagene) to facilitate later dissembly of the gel. 6% acrylamide gels were used containing acrylamide:NN-methylenebisacrylamide in the ratio 9:1, 1 x TBE and 42% urea (w/v). For a 100ml gel 800ml of 10% ammonium peroxidisulphate (APS) and 70ml of TEMED were added prior to pouring to cause polymerisation (APS provides free radicals and TEMED to start the reaction).

After setting and placement into the gel running apparatus all samples were heated to 95^0C to denature the DNA and 3.5ml of each reaction was loaded into the wells in the order ACTG. Gels were run at 1000-1500V for approximately 2 hours (until the first band of dye ran off the gel). The gel was then fixed in 10% (v/v) methanol and 10% (v/v) acetic acid, vacuum dried at 80^0C and autoradiographed.

2.2.13.2 Automatic sequencing:

Using plasmid DNA prepared as in 2.2.1.2.2 and primers designed as described in 2.2.11.1. Typically 500ng of template and 1.6pmol primer were used.

Automated cycle sequencing was carried out by L.Ward & T.Andresson, using an ABI PRISM Dye Terminator Cycle Sequencing Ready Reaction Kit with AmpliTaq DNA Polymerase, FS (Perkin Elmer) on a 373A DNA sequencer

(Applied Biosystems).

2.3 RNA manipulations:

2.3.1 Total RNA extraction from *Drosophila* tissue:

The Promega "RNAgents total RNA isolation kit" was used as per instructions.

2.3.1.1 Isolation of total RNA from Drosophila tissue:

As per Promega RNAgents total RNA isolation kit instructions.

To prevent contamination with RNAases all glassware used was washed thoroughly with distilled water and baked overnight at 250°C. All plastic ware was from freshly opened bags.

To assess the concentration and purity of the RNA, absorbance spectra were taken between 200 and 300nm. The 260nm peak was used to assess the concentration of the RNA (using the approximation that a 40μg/ml solution of RNA will have an absorbance of 1OD unit). The 260 / 280 ratio was used to assess levels of contamination from protein (a value of 1.7 or above was considered acceptable). A 260 / 280 ratio of less than 2 indicated contamination with guanidine thiocyanate. In this case the RNA was reprecipitated with sodium acetate and isopropanol, pelleted, washed thoroughly with ice cold 75% EtOH, pellet again, air dried and resuspended in RNAase free water.

2.3.1.2 Isolation of mRNA from Drosophila total RNA:

This was done using the Oligotex mRNA mini kit according to the manufacturers instructions.

2.3.2 Size fractionation of RNA:

Method based on Sambrook *et al.* (1989) - book 1, chapter 7, pages 43-45.
RNA species were size separated on formaldehyde / MOPS buffer agarose gels.

For a standard size agarose gel (11cm x 14cm) 3g of agarose was added to 30mls 10 x MOPS buffer (46.3g MOPS; 6.8g sodium acetate; 3.72g EDTA, adjusted to pH 7.0 with 4M NaOH made to 1l with H_2O) and 254mls H_2O. This was heated

in a microwave until the agarose dissolved and then allowed to cool in a fume hood to 55°C when 15.6mls of formaldehyde (37%, BDH) was added. The gel was then poured by the usual method.

After setting the gel was placed in a standard electrophoresis tank and submerged in 1x MOPS buffer. The gel was pre run for 15 mins at 120V before loading. During this time the RNA samples were diluted 1:3.5 in loading buffer (50% deionised formamide (Fluka); 1 x MOPS buffer; 6.5% formaldehyde, 0.05% bromophenol blue and 0.05% xylene cyanol) and heated to 65°C before cooling on ice to remove secondary structure. To estimate the size of the RNA species 5μg samples of RNA ladder (Promega, 1μg / μl) were included and treated in the same manner as the other RNA samples. After the gel had been pre-run the wells were flushed out with 200μl of 1 x MOPS buffer and the RNA samples loaded and the gel run at 120V.

2.3.3 Transfer of RNA to nylon membrane:

Based on Sambrook *et al.* (1989) - book 1, chapter 7, pages 49-50.
RNA species were fractionated on a 1% agarose / formaldehyde gel as described. The gel was then soaked in solution 1 (1 x SSC; 50mM NaOH) for 10 minutes to partially hydrolyse the RNA then washed twice in 0.1M ammonium acetate for 15 minutes each wash. The gel was rinsed briefly in PO_4 (Mixture of NaH_2PO_4 and Na_2HPO_4 at pH 6.8 (50mM)) and then transferred to nylon membrane as described for DNA blots. Following transfer the membrane was baked at 80°C for 30 minutes then wrapped in cling film and placed RNA side down on a UV transilluminator for 3 minutes. Membranes were stored between two sheets of Whatman paper before use.

2.3.3.1 Visualisation of RNA bound to nylon membranes:

This technique was used to visualise the RNA markers transferred to allow estimation of the size of bands hybridised during northern analysis.

To stain for RNA the region of the filter where the RNA markers had been run was cut off the main filter. This part of the filter was incubated in 5% acetic acid

for 15 minutes on an orbital shaker. The solution was then replaced with staining solution (0.5M sodium acetate; 0.04% methylene blue) and incubated for 5 to 10 minutes again on an orbital shaker. Finally the filter was washed in several changes of dH_2O until the bands became visible against the background staining. The filter was air dried and stored between two sheets of Whatman paper.

2.3.3.2 Preparation of DNA probes for hybridisation to nylon membranes:

See Southern probe production (section 2.2.5.1).

2.3.4 Hybridisation of RNA probes to nylon membranes:

The filter with RNA bound to it was prehybridised in 20mls of Quickhyb (Stratagene) with 200µl of tRNA added at 58°C for 1 hour in a rotating oven (Hybaid). The RNA probe was then added to this and the blot incubated for 1 hour at 58°C in the rotating oven. After hybridisation the probe was removed and the blot rinsed in washing solution (1x SSC; 0.1% SDS) at room temperature. The blot was then washed twice for 1 hour in washing solution again at 55°C. The blot was then removed, wrapped in cling film and either exposed to X-ray film or a phosphor imager screen.

2.3.5 Stripping of blots for reprobing:

To strip blots hybridised as described above they were washed for 1 hour at 70°C in 0.2% SDS. The blot was then rinsed in dH_2O and stored wrapped in clingfilm.

2.4 In situ hybridisations:

Based on Tautz & Pfeifle, 1989

In situ hybridisations were performed with both DNA and RNA probes incorporating Digoxygenin (Dig) labelled nucleotides. DNA probes were prepared as described for Southern blot probes (see 2.2.8.1). Before use both DNA and RNA probes were denatured by heating to 95°C for three minutes and then cooled on ice.

2.4.1 Preparation of Digoxygenin labelled RNA probe:

Template DNA was prepared (see section 2.2.1.2.) and linearised (see 2.2.2).

0.5μg of template DNA was made up to a volume of 11μl in dH_2O. To this was added 4μl of transcription buffer (Gibco), 3μl of Dig labelling mix (Boerhinger Mannheim), 1μl of RNAase inhibitor (Gibco) and 1μl of either T3, SP6 or T7 RNA polymerase (Gibco). The reaction was incubated at 37°C for 2 hours. After this 1μl was removed and set aside for later analysis. To the remaining reaction mix 1μl of RNAase free DNAase (Boehringer Mannheim) was added and the reaction was incubated for a further 10 minutes at 37°C. Following this another aliquot of 1μl was removed for analysis.

Then 80μl dH_2O, 20μl of 4M LiCl and 360μl of 100% Ethanol were added, and left at -20^0C for 20 minutes to precipitate. The RNA was pelleted by centrifugation at 13,000 rpm for 15 minutes. During this step the removed aliquots were run on a 1% agarose gel at 120V to check the efficiency of the reaction and that no DNA contamination was left. Following precipitation the supernatant was removed and the RNA resuspended in 100μl of RNAse free water. Prior to use the riboprobes were hydrolysed to create a probe size of around 150bp to facilitate entry into the preparation. This was achieved by adding 100μl of 0.2M $NaHCO_3$ and the sample placed at 60°C. The time for hydrolysis was calculated according to the following formula:

Formula for hydrolysis of RNA probes:

$$t = \frac{L_o - L_f}{(0.11)\ (L_o)\ (L_f)}$$

where L_o is the initial length of the transcript, L_f is the desired length and t is the time in minutes required for the hydrolysis. Following this the probes were precipitated with 20μl 5% acetic acid, 20μl 3m NaAc and 500μl of 100% ethanol followed by centrifugation at 13,000 rpm for 30 minutes. The pellet was then resuspended in 100μl RNAse free water and used as a 100x stock for hybridisation.

2.4.2 *In situ* hybridisation to *Drosophila* polytene chromosomes:

Adapted from Pardue (1986).

2.4.2.1 Subbed slides:

As in Pardue (1986).

2.4.2.2 Preparation of polytene squashes:

As in Pardue (1986).

2.4.2.3 Hybridisation of Dig DNA to polytene squashes:

Slides were treated in 2 x SSC at 68°C for 30 minutes then brought to room temperature in 2 x SSC for 2 minutes. The slides were dehydrated by washing twice for 5 minutes in 70% ethanol then washed for 5 minutes in 95% ethanol. The chromosomes were denatured in fresh 0.07M NaOH, pH12 for 3 minutes then washed three times in 2 x SSC for 5 minutes each wash. The slides were then dehydrated as above, air dried and then used within 24 hours for hybridisation.

For hybridisation 10µl of stock Dig DNA probe (see section 2.2.8.1) was made up to 30µl total in formamide buffer (50% formamide ; 5 x SSC; 0.1 mg/ml sonicated and boiled herring sperm DNA; 0.1 mg/ml tRNA; 0.05 mg/ml Heparin; 0.1% Tween-20), heat denatured and placed onto the chromosome spread. This was covered with a 22mm^2 cover slip which was sealed with rubber cement. The slides were placed in a sandwich box containing damp tissue paper and incubated overnight at 42°C.

After 3 rounds of washing in PBS-Tw, the slides were incubated with a 1:200 dilution of anti Dig conjugate (anti-digoxygenin fab fragments conjugated to alkaline phosphatase, Boehringer Mannheim) in PBS-Tw covered with a 22 x 50mm cover slip at room temperature for 90 minutes. The slides were then washed 3 times for 1 minute, each wash in PBS-Tw, and three times in NMTT (100mM Tris (pH 9.5); 100mM NaCl; 50mM $MgCl_2$; 0.1% Tween-20. Filtered through a 0.23µm filter and then Levamisol added to 1mM). Then 200µl of NMTT containing 4.5µl of NBT and 3.5µl of X-phosphate per ml of NMTT was

added and incubated at room temperature for 30 minutes. The slides were then washed 3 times for 3 minutes each wash in dH_2O, counter stained with aceto orcein and mounted in water under a 22 x 50mm coverslip.

2.4.3 *In situ* hybridisation to *Drosophila* embryos:

Based on Tautz & Pfeifle (1989).

Embryos collected as described for antibody staining (section 2.1.7). All washes were done in 1ml in microcentrifuge tubes on a rotastat unless stated otherwise.

Embryos were taken from the stock in ethanol and washed twice for 2 minutes in methanol and then twice for two minutes in methanol : 5% formaldehyde in PBS (1:1). The embryos were then fixed in 5% formaldehyde in 0.5 x PBS-Tw for 20 minutes. Following this the embryos were washed three times for 5 minutes in PBS-Tw and then treated for 3 minutes in proteinase K (5mg/ml in PBS-Tw) at 37°C. The embryos were then washed twice for two minutes in glycine (2mg/ml), washed twice for 5 minutes in PBS-Tw and then fixed again in 5% formaldehyde in 1 x PBS-Tw. The embryos were washed five times for 5 minutes in PBS-Tw and washed twice for 10 minutes in PBS-Tw : hybridisation solution (1:1)

The embryos were prehybridised for 2 hours at 42°C for DNA probes or 55°C for RNA probes in hybridisation solution (50% formamide (Fluka); 5 x SSC; sonicated, boiled herring sperm DNA (0.1mg/ml); tRNA (0.1mg/ml); Heparin (0.05mg/ml); Tween-20 (0.1%)). The prehybridisation solution was removed and replaced with 100µl of probe (diluted 1:10 in hybridisation solution for DNA probes or 1:100 in hybridisation solution for RNA probes). Hybridisation was allowed to proceed overnight at the same temperature as prehybridisation.

After hybridisation the embryos were washed in hybridisation solution at room temperature for 2 minutes then washed once for 20 minutes in hybridisation solution at the hybridisation temperature, once for 20 minutes in hybridisation solution : PBS-Tw (1:1) at the hybridisation temperature then 4 times for 20 minutes in PBS-Tw at the hybridisation temperature. Following this the embryos were incubated in 1 ml of anti-Dig antibody conjugate (Boehringer-Mannheim)

diluted 1:2000 in PBS-Tw for at least two hours.

The embryos were then washed once for 2 minutes, once for 10 minutes and 3 times for 20 minutes (minimum) all in PBS-Tw. The embryos were then washed twice for 5 minutes in NMTT plus levamisol (added to 1mM), then placed into NMTT in a tissue culture dish with 4.5µl of NBT and 3.5µl of X-Phosphate added per ml of NMTT. The colour reaction was then allowed to proceed (typically from 30 minutes to overnight). When complete the reaction was stopped by washing in TE.

The embryos were then dehydrated and cleared with histoclear (see 2.1.5). Embryos were mounted in Canada balsam under coverslips supported by insulating tape.

2.4.4 *In situ* hybridisation to *Drosophila* central nervous systems:

Based on Crompton *et al.* (1995)

For *in situ* hybridisation on brains Dig RNA probes were used.

Brains were dissected in PBS or PBS-TX (see section 2.1.3). Following dissection, brains were placed in fix (4% paraformaldehyde, 50mM Pipes, 0.1mM EGTA,2mM $MgSO_4$ and 0.1% sodium deoxycholate) for 60 minutes and then washed 5 times for 5 minutes in PBS-TX. Adult nervous systems were then treated with proteinase K (5mg/ml 3 minutes at 37^0C), washed twice in glycine (2mg/ml) and rinsed three times in PBS-TX.

Then they were washed twice for 10 minutes in PBS-TX : hybrix (1:1) (hybrix: 50% deionised formamide; 5 x SSC; 100µg/ml tRNA; 50µg/ml heparin; 0.1% Triton X-100). This was replaced with 500µl of hybrix then replaced again with another 500µl of hybrix. This was replaced again with 500µl of hybrix and the brains were prehybridised overnight at 55°C. The following day the prehybridisation solution was replaced with 200µl of denatured probe and hybridisation was allowed to proceed overnight at 55°C.

After hybridisation the brains were rinsed in hybrix at 55°C, washed twice for 20

minutes in hybrix at 55°C then washed in PBS-TX : hybrix (1:1) for 20 minutes at 55°C. This was then replaced with 1ml of PBS-TX and then the brains were washed 4 times for 20 minutes in PBS-TX at room temperature. The brains were then blocked for 60 minutes in PBS-TX with 0.2 mg/ml BSA and 3% normal goat serum (heat inactivated). This was then replaced with PBS-TX with 0.2mg/ml BSA, 1% normal goat serum and anti-Dig antibody conjugate diluted 1:2000. This incubation was allowed to proceed from 1 - 4 hours (or overnight in the fridge).

Following antibody binding the brains were washed once for two minutes, four times for 20 minutes and then washed overnight, all in PBS-TX. This solution was then replaced and the brains washed three times for 5 minutes in NMTT. After this the brains were transferred to a watch glass and the colour reaction started by incubating with 4.5µl of NBT and 3.5µl of X-Phosphate per ml of NMTT. After the colour reaction was complete the brains were washed in TE to stop the reaction and rinsed in PBS-TX. They were subsequently dehydrated, cleared in xylene and mounted in Depex mounting medium (see 2.1.5).

2.5 Fly food and media:

2.5.1 Sussex fly food:

Contains: 518g maize flour, 471g sugar, 93g yeast, 28g agar, 75ml Nipagen M (Philip Harris) (10% w/v in EtOH), made to 5l with water. Boiled for 10 minutes to kill the live yeast and then cooled prior to the addition of the nipagen. Once mixed well this is poured into media bottles and vials to set, and then supplemented with live yeast.

2.5.2 Rich fly food:

Contains: 100g yeast, 100g D glucose, 20g agar, 15mls Nipagin M (10% w/v in EtOH) made to 1l with water. Boiled for 10 minutes to kill the live yeast and then cooled prior to the addition of the nipagen. Once mixed well this is poured into media bottles to set and then supplemented with live yeast.

2.5.3 Grape juice agar:

Contains: 50mls grape juice, 80g sugar, 25g agar water to 1l. Boiled until the agar dissolves and poured into small petri dishes and stored at 4^0C. These were warmed prior to use and supplemented with a drop of live yeast.

2.5.4 LB broth:

Constituents: 10g NaCL, 10g tryptone, 5g yeast extract, 1l H_2O. Mixed and autoclaved. Cooled prior to use.

2.5.4.1 LB agar plates:

LB broth with 15g / l agar. Autoclaved and cooled before pouring into large petri dishes to set.

2.5.5 NZY broth:

Made of: 10g NZ amine, 5g yeast extract, 5g NaCl. Autoclaved and cooled prior to use.

2.6 Strains of bacteria and Drosophila melanogaster:

2.6.1 Bacterial Strains:

Escherichia coli (for genotypes see Sambrook et al. 1989):

DH5α (lab stock).

LE392 (lab stock).

Y1090r$^-$ (lab stock)

2.6.2 *Drosophila melanogaster* strains:

WCS (White Canton Special): w ; + ; + (lab stock).

307 (second generation enhancer trap line): w;P[GAL4]307;+ (lab stock).

ULZ (UAS-lacZ reporter line): w,ULZ;+;+ (from Brand & Perrimon 1993).

ULZ:307 (homozygous stable stock with reporter on the first chromosome and the P-element insert on the second): ULZ;307;+ (lab stock).

3. A detailed analysis of the enhancer trap pattern revealed in the adult CNS by P[GAL4]307.

This work was done in collaboration with Dr M.J.Allen.

3.1 Introduction.

As discussed in the main introduction (section 1.3), the giant fibre circuit mediates the light-off escape response by relaying excitation from the eyes to the muscles of the thorax. It comprises a small number of neurons, including the two large and distinctive interneurons known as the giant fibres (GFs).

3.1.1 Intracellular dye injection, a technique for the study of the GFs.

The study of the GF circuit was originally done in the adult by dye filling the neurons with lucifer yellow, a dye which antero- and retrogradely fills the cytoplasm of the impaled neuron and of some connected neurons (the dye travels through gap junctions and so labels only neurons which are directly coupled in this manner). This allows the detailed descriptions of the morphology of impaled neurons and that of other interconnecting neurons. This technique was first used to fill the GFs by Koto (1981). Dye filling reveals the morphology of the neurons and all their processes to a high resolution and has allowed the following description to be produced.

3.1.2 A detailed description of the GF circuit, as revealed by dye filling.

The GF circuit is summarised diagrammatically in figure 3.1A and the characteristic pattern revealed by dye filling is presented in figures 3.1C, 3.2C, E & F (from Phelan *et al.* 1996).

3.1.2.1 GF neurons in the brain region.

The giant fibres are a pair of large bilaterally symmetrical interneurons with cell bodies about 20μm in diameter. The GF cell bodies are located close to the posterior border of the brain, adjacent to the neuropile of the protocerebrum, about 30μm dorsal to the oesophageal canal. The main process of the neuron is connected to the cell body via a neurite, some 60μm long. The dendritic field,

Figure 3.1: The giant fibre system (GFS) of *Drosophila*.

A: Schematic diagram of the identified neurons and muscles of the GFS. Only one half of the bilateral circuit is shown. The giant fibre (GF) interneuron relays information from the brain to the second thoracic neuromere. Here it electrically synapses with the peripherally synapsing interneuron (PSI) and the tergotrochanteral motorneuron (TTMn). The PSI makes chemical synapses with the dorsal longitudinal motorneurons (DLMns) that drive the six wing depressor muscles (the dorsal longitudinal muscles or DLMs). The TTMn drives the jump muscle (the tergotrochanteral muscle or TTM). Figure from Allen, Drummond and Moffat (1998).

B: Adult expression pattern of P[GAL4]307. An image of a CNS stained for Lac-Z protein by immunocytochemistry (see section 2.1.4). Expression is clearly seen in the GF cells and in other identified and unidentified cells in the brain and thoracic ganglia. This image is a montage, produced on Canvas software. Dorsal view. Anterior is top. Scale bar is 100μm. Figure from Allen, Drummond and Moffat (1998).

C: The GFS as revealed by injection of lucifer yellow. This image is of a CNS that has had the GFS backfilled with lucifer yellow. The dye has been introduced into a single axon intracellularly at the site marked by an arrow (in the connective).
1= TTMn, 2= PSI, 3= GCIs.
Scale bar is 100μm. Image from Phelan *et al.* (1996) - (figure 3A in the original).

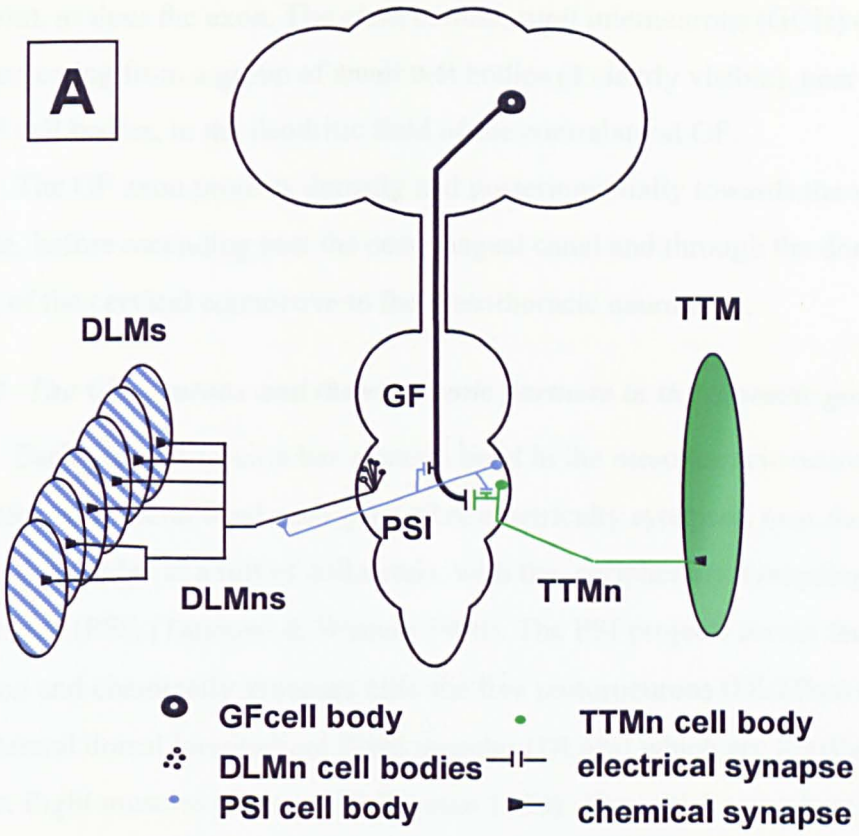
A
DLMs
GF
TTM
PSI
DLMns
TTMn
GFcell body
DLMn cell bodies
PSI cell body
TTMn cell body
electrical synapse
chemical synapse

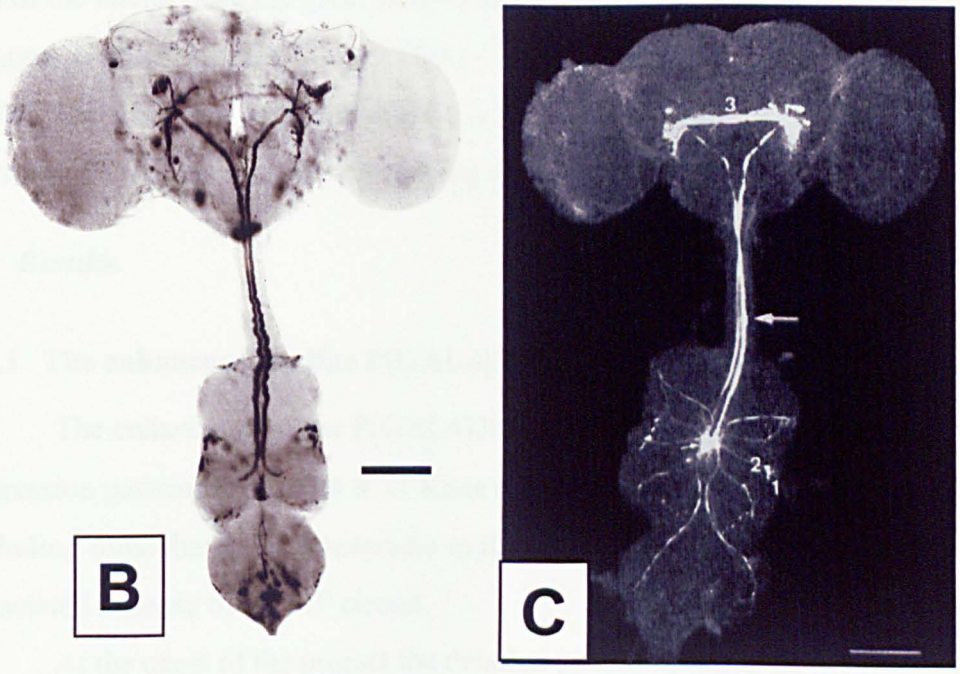
B
C
3
2
1

composed of dorsomedial, ventrolateral and posterolateral processes, branch from this point, as does the axon. The giant commissural interneurons (GCIs) can be seen projecting from a group of small cell bodies (3 clearly visible), near one of the GF cell bodies, to the dendritic field of the contralateral GF.

The GF axon projects dorsally and posteriomedially towards the ventral midline, before ascending past the oesophageal canal and through the dorsal region of the cervical connective to the mesothoracic neuromere.

3.1.2.2 The GF neurons and their synaptic partners in the thoracic ganglia.

Each giant fibre axon has a lateral bend in the mesothoracic neuromere. Just before the lateral bend each giant fibre electrically synapses, near the inframedial bridge at a tuft of collaterals, with the peripherally synapsing interneuron (PSI) (Tanouye & Wyman 1980). The PSI projects across the ganglion and chemically synapses onto the five motorneurons (DLMNs) of the contralateral dorsal longitudinal flight muscles (DLMs) which are fibrillar indirect flight muscles (Tanouye & Wyman 1980). The initial wing beat is carried out by the DLMs, through innervation by the DLMns via the PSIs. At the end of the lateral bend the giant fibre synapses again, this time with the large tergotrochanteral motorneuron (TTMn) - innervating the tergotrochanteral muscle (TTM, also known as the jump muscle or flight starter muscle) (Thomas & Wyman 1982). This muscle acts as a leg extensor and wing elevator.

3.2 Results.

3.2.1 The enhancer trap line P[GAL4]307.

The enhancer trap line P[GAL4]307, isolated in a screen for adult CNS expression patterns by Moffat & O'Kane (unpublished), marks several neurons, including some that are characteristic in their morphology of the GFs and the associated neurons of the GF circuit.

At the onset of the project the detailed pattern revealed by the enhancer trap was previously uncharacterised, although since this time the adult pattern has been described following staining with X-gal (Phelan *et al.* 1996). We have been using a polyclonal anti-β-galactosidase antibody to visualise the protein (see

Figure 3.2: Expression pattern of enhancer trap line P[GAL4]307 (as compared with the level of detail attainable with dye filling the GFS).

A, B & D: Enhancer trap pattern of P[GAL4]307. Produced by montaging serial focal planes (using Canvas software) – from Allen, Drummond and Moffat (1998).

C, E & F: Dye injection revealing the GFS. These images are from Phelan *et al.* (1996)- (Figure 3 B-D in original).

Diagram: Schematic diagram of the CNS indicating the regions of the brain or thoracic ganglia shown in A, B and D. T1 is the prothoracic neuromere, T2 the mesothoracic neuromere and T3 the metathoracic neuromere.

A & B: Montages of serial focal planes of the supraoesophageal ganglion from an anti-Lac-Z stained P[GAL4]307 CNS.

A: This shows the neurite (N) projecting from the giant fibre cell body (GFCB, white arrowhead) to the axon and characteristic GF dendritic field. This comprises the dorsal medial dendrite (DMD), the ventral lateral dendrite (VLD) and the large posterior lateral dendrite (PLD).

B: The pattern also shows the giant commissural interneurons (GCI) connecting with the GF dendritic field.

C: The supraoesophageal ganglion following lucifer yellow filling of a GF axon. The GF cell body (red arrowhead) and proximal portion of the axon (white arrowhead) of the filled GF are shown. The dye coupled GCIs cross the central commissure. Three axons can clearly be distinguished (green arrows) their cell bodies are found contralateral to the injected GF.

D: A montage of serial focal planes of the thoracic ganglia. This clearly exposes other neurons of the GFS including the peripherally synapsing interneuron (PSI) with its cell body (white asterix) projecting an axon medially to where it synapses with the GFs at the inframedial bridge (IB). The tergotrochanteral motorneuron (TTMn) can also be seen with its cell body (TTMnCB) and distinctive projections that link to the GFs.

E & F: Dye coupled neurons in the thoracic ganglia, revealed by lucifer yellow dye filling of a GF. Arrows indicate the GF axon bending laterally in the mesothoracic neuromere.

E: The intensely fluorescent, bilaterally symmetrical neurons are the PSIs. The ipsi- and contralateral portions of the axon on the filled side are visible (2 arrowheads).

F: The GF dye coupled cell is the TTMn, the arrowheads indicate the posterior and medial dendrites.

Scale bar (in **B**) = 100μm in **A** & **B**, 70μm in **C**, and 35μm in **D**, **E** & **F**. In all images anterior is top and the view is from dorsal.

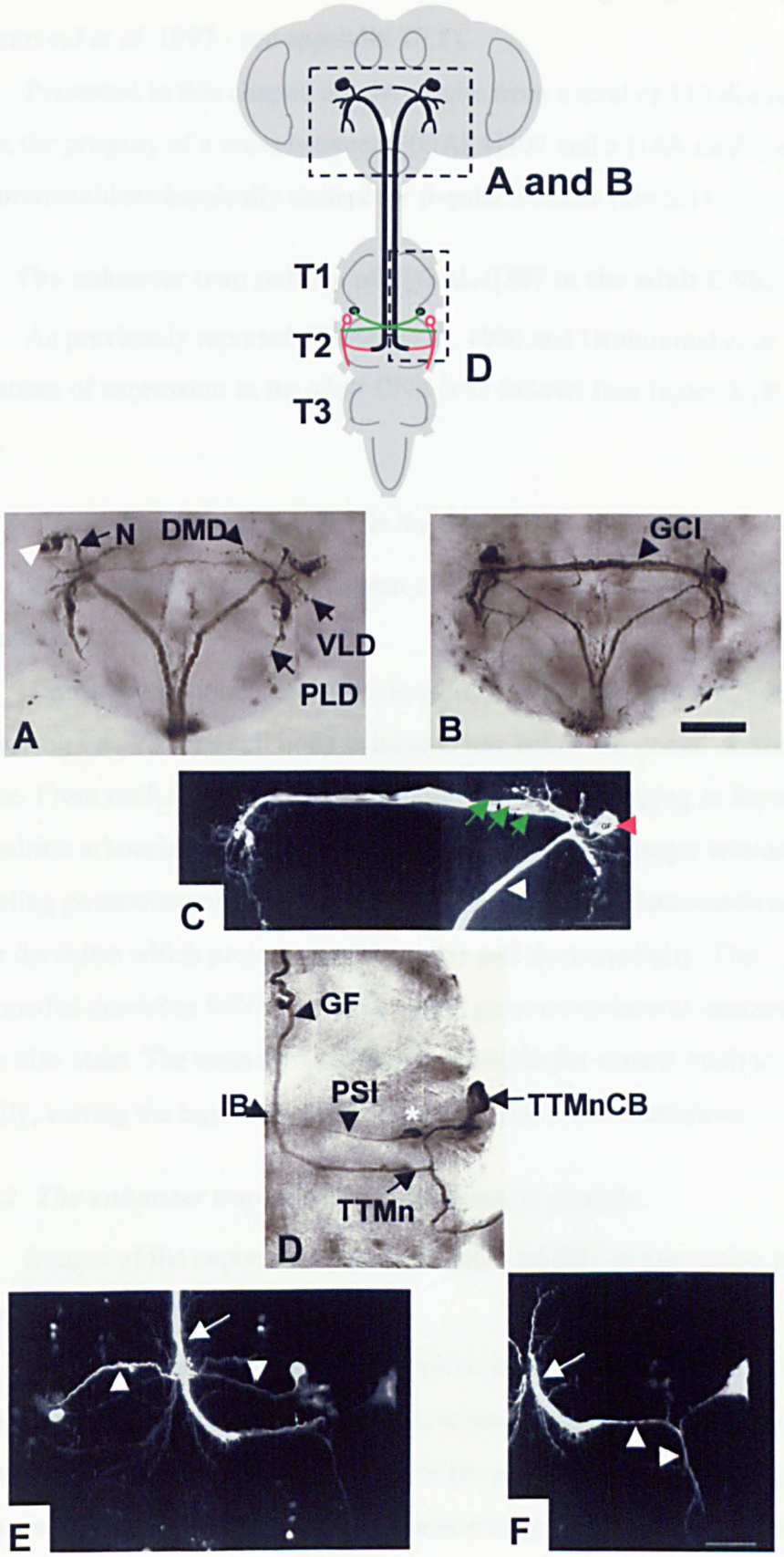
A and B
T1
T2
T3
D
N
DMD
VLD
PLD
A
GCl
B
C
GF
PSI
IB
TTMnCB
TTMn
D
E
F

section 2.1.4), with the result that we have achieved a high degree of resolution (Drummond *et al.* 1997 - see appendix 10.1).

Presented in this chapter are the results from a total of 113 dissected adult CNSs, the progeny of a cross between P[GAL4]307 and a UAS-*lacZ* "reporter" line, immunohistochemically stained for β-galactosidase (see 2.1).

3.2.2 The enhancer trap pattern of P[GAL4]307 in the adult CNS.

As previously reported (Phelan *et al.* 1996 and Drummond *et al.* 1997), the pattern of expression in the adult CNS is as follows (see figure 3.1B, 3.2A,B & D).

3.2.2.1 The enhancer trap pattern in the brain.

Images of the expression pattern of P[GAL4]307 in this region are presented in figure 3.2 A & B.

Immediately noticeable, are 2 large descending neurons clearly staining (expressing Lac-Z). The cell body is located just below the dorsal protocerebral surface. From each a neurite extends ventrally prior to enlarging to form a group of dendritic arbourisations. These can be subdivided into a major arbourisation, projecting posterolaterally and laterally, arbourising in the deutocerebrum, and minor dendrites which project ventrolaterally and dorsomedially. The dorsomedial dendrites follow the path of the giant commissural interneurons which also stain. The axon runs posteriorly towards the ventral midline, projects dorsally, exiting the brain along the dorsal midline of the connective.

3.2.2.2 The enhancer trap pattern in the thoracic ganglia.

Images of the expression pattern of P[GAL4]307 in this region are presented in figure 3.2 D.

From the connective the axon projects unbranched through the prothoracic neuromere, until it reaches the mesothoracic neuromere (T2), where it turns ventrally and laterally towards the edge of the ganglion. Two other neurons that interact with this axon are visible at the lateral edge of the mesothoracic neuromere.

The first of these neurons has a large cell body at the extreme lateral edge

of the anterior border of T2. An axon projects posteriorly from this cell body to mid T2. At this point the axon bifurcates, sending one process laterally towards the midline where it contacts the large axon that has bent ventrally and laterally. The site of contact is not clearly discernible as both axons appear the same width and where one starts and the other ends is not precisely definable with this technique. The second process proceeds to the posterior border of T2 where it projects outwards and exits the ganglion.

The second neuron has a smaller cell body that is found in a more medial position in relation to the first neuron's cell body. This projects a single fine process directly over the midline where it contacts the large axon anterior to its ventro-lateral bend in T2.

3.2.3 Identification of the neurons revealed by the enhancer trap line.

The details of size and position of the cell body, the trajectory of the axon and the characteristic bend in the mesothoracic neuromere, provide overwhelming evidence that we are visualising the GFs as previously described by Koto in 1981 (see figures 3.1C & 3.2C). Dye filling experiments have revealed that other cells marked by the enhancer trap line can be identified as the TTMn and the PSI, by their size, position and characteristic projections (Koto et al. 1981, Baird et al. 1993, Phelan et al. 1996 - see figures 3.2E & F). The GCIs are also identifiable.

3.2.4 Other neurons marked by the enhancer trap.

There are also other neurons visible that are identified. These include the dorsal giant interneurone (DGI) with projections extending dorsomedially and anteriorly in the brain (described by Ito *et al.* 1997). We also believe that a subset of projections seen in the thoracic ganglia are from sensory organs - possibly the chordatonal organs (proprioreceptors) (Shepherd & Smith 1996). Images of these neurons are presented in figure 3.3.

3.2.5 Abnormal development of the GFs.

During the course of these experiments we isolated 2 CNSs with only 1 GF. Smith *et al.* (1996) had previously shown that the ablation of 1 GF had no effect upon growth or survival of the other. Indeed, in both cases we isolated, the

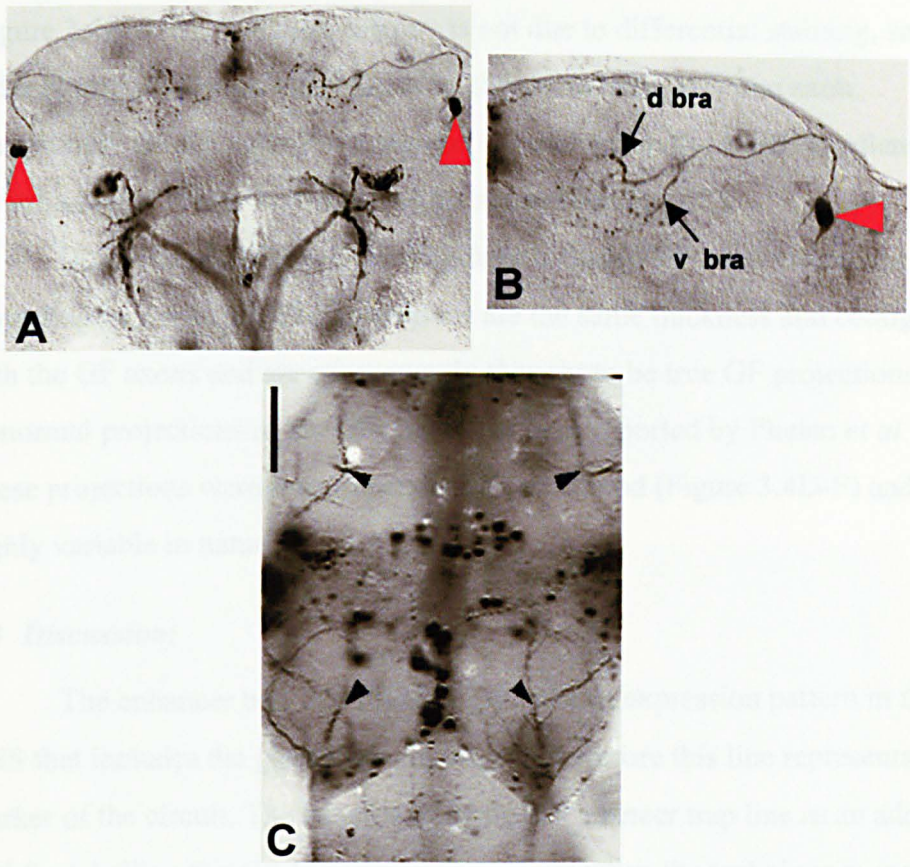

Figure 3.3: The dorsal giant interneuron (DGI) and chordatonal organ inputs are part of the enhancer trap pattern of P[GAL4]307.

A & B: Montage images of the brain showing the DGIs.

A: An image of the brain showing the giant fibre cell bodies, neurite, dendrites, and axons (out of focus) - as previously described. The DGI cell bodies are located in the anterior dorsal protocerebral region of the supraoesophageal ganglion (red arrowheads).

B: The DGI cell body (red arrowhead) can be clearly seen to project an axon that characteristically branches dorsally (d bra) and ventrally (v bra) in the terminal region.

C: The chordatonal organs input axons from the peripheral nervous system that arborise in the thoracic neuromeres (black arrowheads).

Scale bar (see **C**) = 23μm in **A**, 70μm in **B** and 50μm in **C**. All views from dorsal.

single cell body was present with normal dendritic and axonal morphology (Figure 3.4A & B). The phenomenon is not due to differential staining, since under Normarski optics the connective clearly showed only one axon. Interestingly the GF axon in T2 appears to bend normally, whilst a collateral from the inframedial bridge seems to make a second bend (3.4C).

Other abnormalities of development included GF axon extensions projecting well into T3. The projections are the same thickness and contiguous with the GF axons and are consequently thought to be true GF projections. Abnormal projections of the GFs have also been reported by Phelan *et al.* (1996). These projections were seen to persist into adulthood (Figure 3.4D-F) and were highly variable in nature.

3.3 Discussion:

The enhancer trap line P[GAL4]307 has an expression pattern in the adult CNS that includes the giant fibre circuit, and therefore this line represents a marker of the circuit. The benefits of using an enhancer trap line as an additional tool for labelling the giant fibre circuit are clear when the technique is compared to dye injection.

Firstly, the relative numbers of CNSs that can be treated and examined are much greater for enhancer trap detection as the technique is much less labour intensive and gives high quality results. As I have demonstrated here, the results are of almost equivalent resolution. Secondly, as a factor of the number you can treat, you can detect aberrations of the giant fibre circuit that only rarely occur. Thirdly, the possibility exists with an enhancer trapping system, to alter or add additional constructs under UAS control. This allows alternative detection systems (for a review of alternatives see Callahan *et al.* 1998) or the expression of toxins (for example ricin A chain - Moffat *et al.* 1992) in this circuit with a high degree of specificity to either ablate or inactivate the neurons. A *caveat* is that the enhancer trap line probably has expression patterns in other tissues not studied here which will also be affected. Finally, the marker may also label the component neurons of the circuit during development, when the GF axons would be inaccessible to dye filling and when the associated neurons in the circuit would

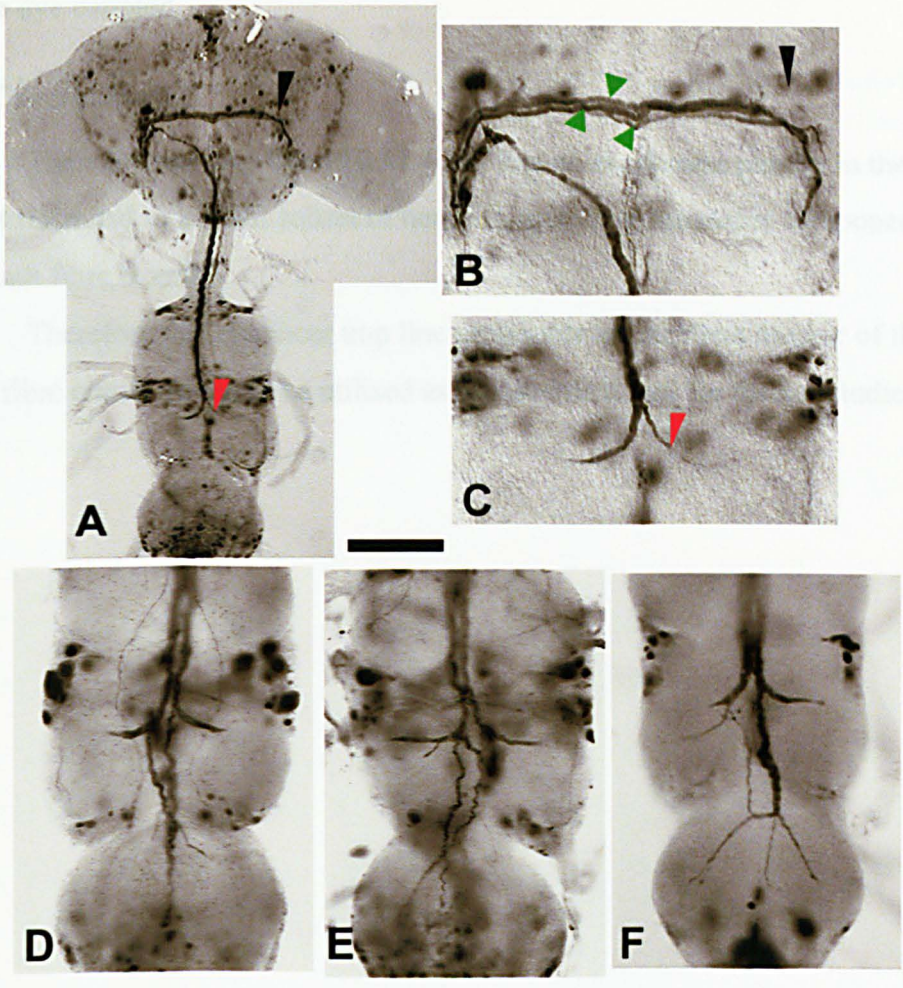

Figure 3.4: Aberrations of the giant fibre system (GFS).

Dorsal views of adult nervous systems 1-3 days post eclosion stained for Lac-Z protein by immunocytochemistry.

A,B & C: A preparation of the central nervous system (CNS) that exhibits only one giant fibre (GF). Black arrowhead shows where the GF cell body should be in the brain. At least three of the giant commissural interneurons are present and project correctly to the position of the dendritic field of the absent GF (green arrowheads - **B**).

C: In the mesothoracic neuromere the single GF appears to have connected with both tergotrochanteral motorneurons (TTMns). In focus (red arrowhead in **A** and **C**) is the TTMn whose normal GF partner is absent.

D-F: Preparations that show GF extensions into the metathoracic neuromere (T3). Anterior is top. Scale bar = 125μm in A, 45μm in B, 50μm in C and 100μm in D-F. Figures A & D-F from Allen, Drummond & Moffat (1998).

not be dye coupled.

3.4 Conclusions:

The enhancer trap line P[GAL4]307 has an expression pattern in the CNS that is restricted to a small subset of neurons, including the major components of the giant fibre circuit.

Therefore this enhancer trap line represents an excellent marker of the giant fibre circuit and may be utilised as a convenient tool for further studies.

4. Analysis of the enhancer trap pattern revealed in developing flies by P[GAL4]307.

This work was done in collaboration with Dr M.J.Allen.

4.1 Introduction.

The study of the GF morphology in the adult has been conducted in the past by the use of intracellular dye filling of the GF axons (see chapter 3). Whilst this technique has yielded excellent results in the adult, revealing both morphology and connectivity of the GFs, the approach has many drawbacks when specifically focusing on development of the GF circuit.

4.1.1 Traditional problems of studying GF development.

Injection of the GFs is usually carried out in the adult CNS, when the connective between the brain and the ventral nerve cord is present. The connective is an ideal region for visualising the GF axons as they are clearly visible due to their characteristic size and position when viewed through Normarski optics, aiding precise impaling of the axon.

Injections into stages of pupae without either clearly identifiable GF axons in a connective, or a connective, are therefore not possible. If the GFs develop during pupal life when there is a connective, and have thin axons, they may well be indistinguishable from adjacent axons and therefore cannot be dye filled. Alternatively, if the GFs develop prior to connective formation then dye filling cannot be used, and as the connective only forms after approximately 40-48 hours of pupal development (approaching mid pupation) this is a likely possibility.

Another drawback of dye filling is that it reveals nothing about the axonogenesis of associated neurons in the circuit, with dye coupling occurring only after synaptogenesis with the GFs has occurred.

These reasons preclude the injection method for easy study of the possible early development of the GF circuit.

4.1.2 Using the enhancer trap line P[GAL4]307 to study GF development.

At the time of the initiation of this study no description of the development (axonogenesis and synaptogenesis) of the GF circuit had been attempted, therefore we set out to study this using the enhancer trap line P[GAL4]307. This enhancer trap line is a clear marker of the GF circuit in the adult (Drummond *et al.* 1997 – see previous chapter), comparing favourably in the level of discernible detail with dye filling techniques.

The development of the circuit can be viewed by examining large numbers of dissected CNSs from different and sequentially arranged developmental stages from late third instar larvae and through pupation (855 in total - see table 4.1). Pupal development can be assigned stages (Table 4.1) derived from morphologically identifiable characteristics visible through the pupal case, as described in Bainbridge and Bownes (1981). This represents a more accurate approach than simple timing of development which can vary widely between individuals.

Stages from Bainbridge & Bownes	Timing in hours APF	CNSs dissected
L3		393
P1(WPP)	0-1	77
P2-3	1-7	17
P4(i)-5(i)	7-13.5	7.5
P5(i)	12.5-48	274
P5(i)-6	14-48	35.5
P7-9	38-78	18.5
P10-12(i)	72.5-97	16.5
P12(ii)-15(i)	75-105	16
Total		855

Table 4.1: Stages of pupal development, approximate timing of each stage and numbers of CNSs dissected and stained for LacZ expression.

L3 = third instar larvae, WPP = white prepupae, APF = After Pupa Formation. 0.5 of a CNS is either the brain or ventral nerve cord (rather than both halves joined by the connective).

Having established the adult enhancer trap pattern (chapter 3), a profile of development was created working backwards from this stage. As with the study

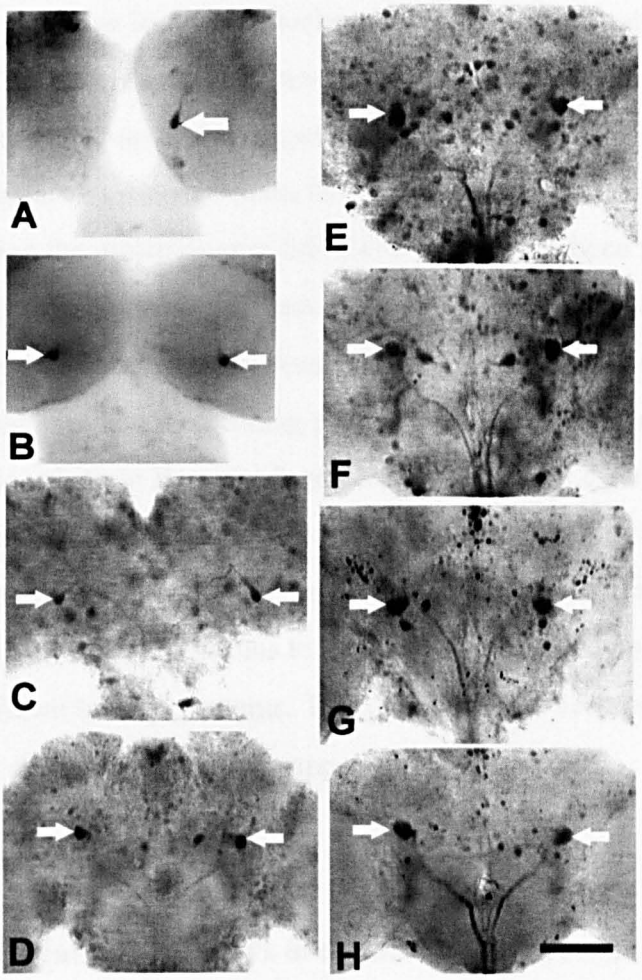

Figure 4.1: P[GAL4]307 marks the giant fibre cell bodies through late larval and pupal development.

Dorsal views of the brain region of the central nervous system at several stages through development, stained for LacZ protein by immunocytochemistry. Intense staining is seen in 2 large perikaryon (arrows) which can be identified as the GF cell bodies after pupal stage P5.

A: third larval instar (L3), **B**: white prepupal stage (WPP), **C**: P4(ii), **D**: P5(ii), **E**: P8, **F**: P11, **G**: P15, **H**: adult.

Anterior is top. Scale bar = 50μm in **A** & **B**, 100μm in **C**-**H**.

of the adult circuit an immunohistochemical approach was taken (Drummond *et al.* 1997). The CNS preparations reveal that the enhancer trap pattern is visible throughout the developmental stages studied (i.e. expression regulated by the enhancer appears consistent within these cells throughout this period).

During the preparation of this thesis a paper has been published (Phelan *et al.* 1996) that complements our data, showing P[GAL4]307 expression throughout pupal development reveals the development of the GF circuit. Their approach was based on the staining produced by the breakdown of the chromogenic substrate X-gal by β-galactosidase (the *lacZ* gene product) in the cells labelled by the enhancer trap – producing a diffuse blue coloration. The work presented here, based upon immunocytochemical detection of the LacZ protein (see section 2.1.4), seems to be more sensitive and this is reflected in a slightly different timing of events. This data has since been published (Allen, Drummond & Moffat 1998) - see appendix 10.2.

4.2 Results.

4.2.1 Identification of the GFs in the developing nervous system.

Two large bilaterally symmetrical perikaryon are seen near the dorsal surface of the protocerebrum throughout development (see figure 4.1 A-H). Following the development of these cell bodies reveals they develop into the correct size and shape, and in the correct position within the CNS, to be the GF cell bodies. These cell bodies have a characteristic pear-shape during early development (Figure 4.1 A-C). From pupal stage P5 onwards the axonal projections are clearly identifiable as those of the GFs.

4.2.2 Early stages of GF development.

In third instar larval CNSs (the earliest stage studied here due to the constraints listed in the discussion of this chapter), we see the GF cell bodies, having already projected axons into the prothoracic neuromere (T1) (Figure 4.2 A).

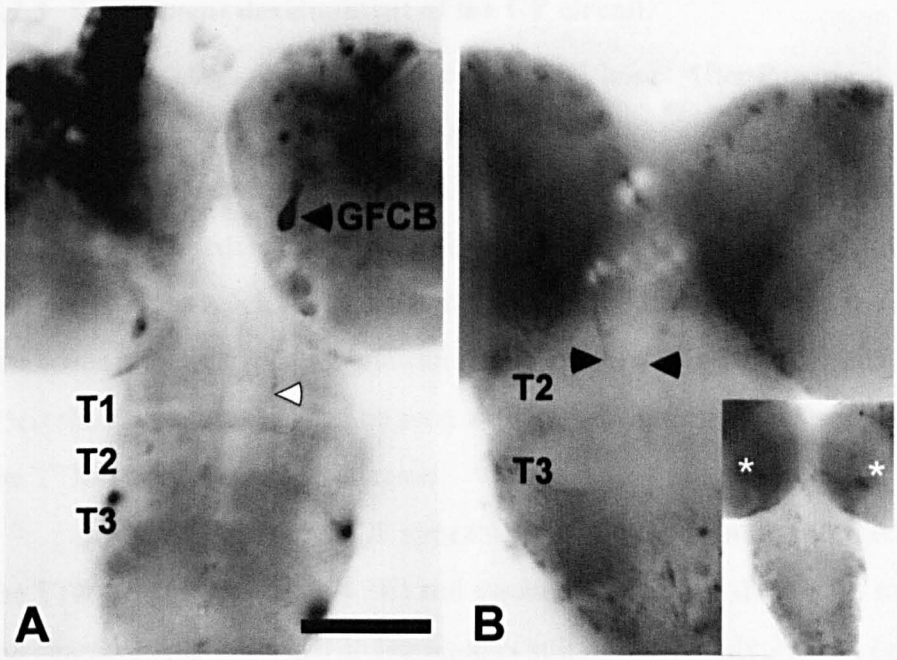

Figure 4.2: Early axonogenesis of the giant fibre neuron.

A & B: CNSs stained for LacZ protein by immunocytochemistry.

A: Third instar larval (L3) CNS. The giant fibre cell body (a distinctive pear shape) is clearly visible with an axon that is seen to have projected into the prothoracic neuromere (T1 - white arrowhead).

B: CNS from a white prepuparium (WPP). By this stage the giant fibre axons can be seen to have projected into the anterior of the presumptive mesothoracic neuromere (T2 - arrowheads). **Inset** is a more dorsal plain of focus of the same CNS showing the giant fibre cell bodies (marked with asterisks).

Views from dorsal. Anterior is top. Scale bar = 75μm (150μm in inset).

4.2.3 Subsequent development of the GF circuit.

By the stage of earliest pupal onset (0-1 hours After Puparium Formation - APF; the white prepuparium stage) the axons have extended into the mesothoracic neuromere (T2) or are at the T1/T2 border (Figure 4.2B – inset reveals the cell bodies on different focal plane). By the end of stage P3 (7 hours APF), the axons reach the mid point of T2. By the end of stage P4 the axon has thickened slightly to ~2μm, and can be clearly seen (Figure 4.3A & D). At stage P5(i) the PSI cell bodies can be seen without axonal projections and the GF and the TTMn appear to have synapsed.

By stage P5(ii) each GF appeared to be linked to both its target neurons the TTMn and PSI (Figure 4.3E) and essentially reaching their adult shape with the characteristic bend in T2. The axon is still however only 2-3 μm thick and the boundary between the GF and the TTMn is indistinguishable using this technique. During this stage the enhancer trap pattern becomes more elaborate with many cells starting to stain. The dendritic field arborises at this stage (Figure 4.3B).

Stages P7-8 see the GF axons thickening to two-thirds of adult proportions (~6μm), whilst the TTMn remains ~2μm, allowing a visualisation of the boundary between the axons (Figure 4.3F). These stages also see the further elaboration of the dendritic arborization (Figure 4.3C), and thickening of the dendrites. The rest of pupal life up to eclosion sees a further thickening of axon and dendrites to adult proportions.

This developmental data is summarised in diagrammatic form in Figure 4.4.

4.2.4 A model of development of the GF terminal connection.

To study the mechanism of formation of the terminal connection of the GF axons in T2 and the sequence of events occurring in synapse formation with the TTMn we intensively studied the period P5(i), the period identified by us as important in these events (see above). P[GAL4]307 is particularly useful for

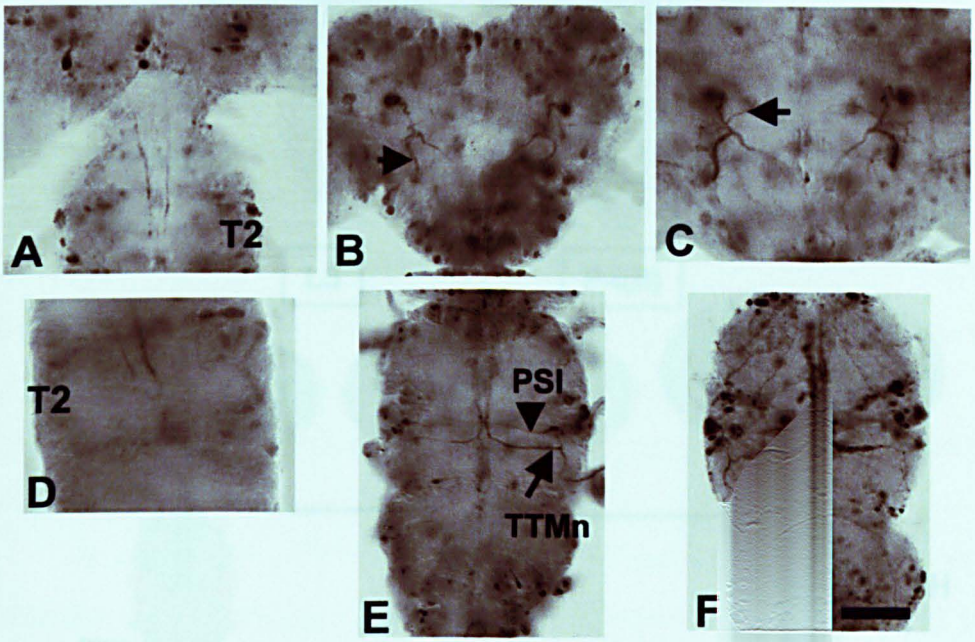

Figure 4.3: Later development of the enhancer trap pattern shows further elements of the giant fibre circuit.

Dorsal views of pupal nervous systems stained for LacZ protein by immunocytochemistry.

A & D: A pupal stage P4(ii) CNS, showing the giant fibre axons can be seen at the midpoint of the mesothoracic neuromere (T2). The distinctive cell bodies can be clearly seen but no dendritic field has formed (**A**).

B & E: CNS from a pupa at stage P5(ii). By this stage the dendritic field has started to stain, with the posterior lateral dendrite appearing first (arrowhead in **B**). The giant fibres have made both connections with their targets, the peripherally synapsing interneuron (PSI) and the tergotrochanteral motorneuron (TTMn), as shown in **E**.

C & F: Pupal stage P8 CNS. The dendritic field has increased in complexity with the ventrolateral dendrite becoming prominent (arrowhead in **C**). By this stage the giant fibre axons have thickened to approximately three quarters of their adult dimensions (approximately 6μm), whilst the TTMns remain at 2-3μm (**F**).

Anterior is top. Scale bar = 75μm.

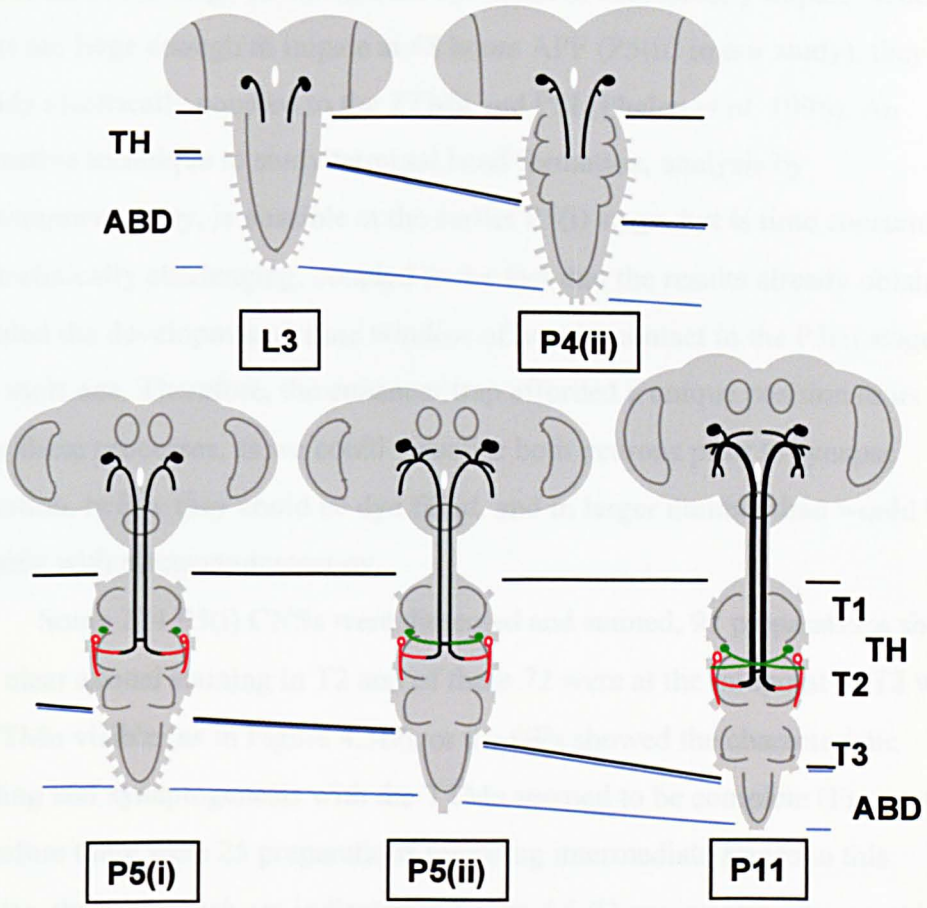

Figure 4.4: Schematic of the observed development of the giant fibre circuit highlighted by P[GAL4]307.

TH = Thoracic region of the ventral nerve cord.

ABD = Abdominal region of the ventral nerve cord.

L3: The giant fibre (GF) cell bodies (in black) have already projected fine axons into the thoracic ventral nerve cord (future prothoracic (T1) region).

P4(ii): The GF axons have reached their final position in the mesothoracic neuromere (T2).

P5(i): The dendrite of the tergotrochanteral motorneuron (TTMn - red) meets the GF axon. Elaboration of the GF dendritic field begins. The peripherally synapsing interneuron (PSI) cell bodies are visible (green).

P5(ii): The distinctive bends of the GFs are seen and appear connected to the TTMn. The PSI is visible projecting across the inframedial bridge. Elaboration of the GF dendritic field continues.

P11: The enhancer trap pattern is fully developed showing the thick GF axons and elaborate dendritic field morphology.

study of this terminal bend formation because the neurons cannot be studied by dye filling at this stage as the GFs are too small to successfully impale. When the axons are large enough to impale at 48 hours APF (P5(ii) in our study), they are already electrically coupled to the TTMn and PSI (Phelan *et al.* 1996). An alternative technique to study terminal bend formation, analysis by electronmicroscopy, is possible at the earlier P5(i) stage, but is time consuming and technically challenging, coupled to the fact that the results already obtained revealed the developmental time window of neuron contact in the P5(i) stage to be a short one. Therefore, the enhancer trap afforded a unique position to us to study these processes, as we could visualise both neurons prior to synapse formation, before they could be dye filled, and in larger number than would be possible with electronmicroscopy.

Some 274 P5(i) CNSs were dissected and stained, 97 preparations showed very clear axonal staining in T2 and of these 72 were at the midpoint of T2 with no TTMn visible (as in Figure 4.3D), or the GFs showed the characteristic bending and synaptogenesis with the TTMn seemed to be complete (Figure 4.3E). Therefore there were 25 preparations revealing intermediate stages in this process, three of which are indicated in figure 4.5 (D representing the completed process). In all 3 the neurons projecting from the periphery (left and right in these figures) can be identified as the TTMns by their projections and the location of their cell bodies.

In the first of these (Figure 4.5A), the GFs can be seen mid T2, with the 2 TTMns projecting in from the periphery (one labelled with an arrowhead). These appear to make contact with the ends of the GF at almost right angles. Also visible in this picture is the forming inframedial bridge (asterisk). The second picture (Figure 4.5B), a similar scenario is observed, although in this case one of the axons appears to have slightly overshot the position where it should meet its corresponding GF (arrowhead). Finally, in figure 4.5C, another preparation reveals that the TTMn axons can connect with the GFs not at their distal tips but at a more proximal location. In these particular examples the GF axons had projected beyond the midpoint of T2, and into T3. Taken together this data suggests that the GFs are not reaching T2 and actively bending into the periphery

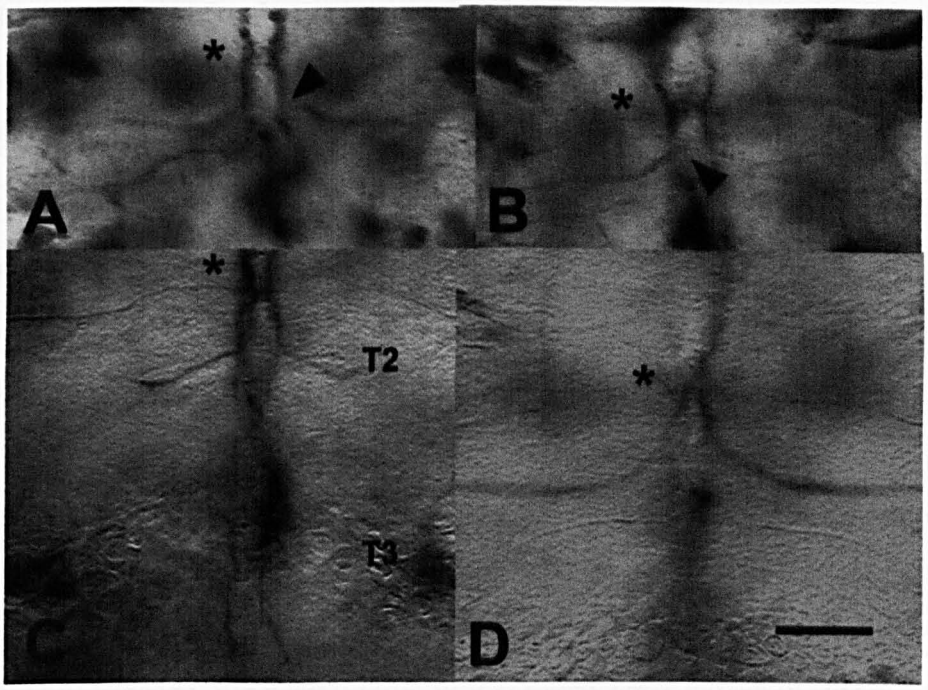

Figure 4.5: Initial stages of tergotrochanteral motorneuron / giant fibre (TTMn / GF) contact.

Dorsal views of the mesothoracic (T2) neuromere of the CNS from P5(i) stage pupae. Relatively few preparations from this stage showed this initial contact (indicating how rapidly it occurs).

A: Shows two incoming neurons contacting the distal tips of the GFs in an almost right angled fashion (one is marked with an arrowhead).

B: Similar to **A**, but it appears that one of the neurons has overshot its target (arrowhead).

C: Contact is seen between the GFs and the incoming neurons, as in **B**, except the GFs have extended into the T3 neuromere. Therefore the contact is possibly not at the distal tips of the GF axons, but in a more proximal position.

D: A slightly later staged preparation in which the distinctive bending in T2 can be seen. This presumably is the end result of the contact shown in **A** & **B**. The boundary between the GF and TTMn cannot be resolved.

In all examples the developing inframedial bridge is marked with an asterisk. Anterior is top. Scale bar = 25μm.

to contact the TTMns, but rather the TTMns are growing in from the periphery and synapsing with the GFs that have previously arrived and stalled, subsequently leading to the characteristic connection.

4.3 Discussion.

The data presented in this chapter has illustrated the usefulness of the enhancer trap line P[GAL4]307 as a tool for studying the development of the giant fibre circuit. P[GAL4]307 in combination with the immunocytochemical detection system used, has provided a detailed morphological description of circuit development and the timing of this process.

Despite the sensitivity of the immunocytochemical approach, there are factors to consider when attempting to investigate early events in circuit development. The binary detection system that "second generation" enhancer trapping represents should logically involve a lag between GAL4 activation and translation of *lacZ*. This lag may preclude expression in the GF cell bodies when they are first born. In combination with the fact that there must be a threshold of detection, below which levels of β-galactosidase cannot be detected (i.e. just after onset of expression in the GFs), we cannot state the GFs are not present prior to our earliest visualisation of them. Additional complications are provided by the difficulty in dissection of earlier larval stage CNSs and the high levels of background staining.

Third instar larval (L3) CNSs have been shown to have the giant fibre axons projecting into the prothoracic neuromere, whilst by the later P2 stage (WPP) the axons are visible in the mesothoracic neuromere. No growth rate has been assigned to the axons as we do not see the initiation of axonogenesis or the outgrowth prior to L3, nor can the distal most tip of the axon be unequivocally identified to compare distances between this and the P2. The majority of axon outgrowth has occurred in late larvae and the remaining distance the axons have to grow is comparatively small. No clearly identifiable growth cone has been visualised either, although this may be accounted for by two facts. Firstly, axons projecting along previously pioneered pathways do not tend to have large splayed

growth cones (Harris *et al.* 1997, Kaethner & Stuermer 1994, Sretavan & Reichardt 1993). Secondly, in our preparations the distal tip of the axon we see tends to be more strongly staining than the middle, suggesting we may be visualising a small growth cone of the sort mentioned in the first point. Due to the large number of CNS preparations, showing invariant axon projection, we are confident that the distal tip of the staining represents the tip of the growing axon.

The model of giant fibre terminal synapse development has been made possible by the large number of CNSs studied and the level of resolution achievable, factors that are clear advantages of the technique used here. However, when interpreting this data due consideration has to be given to the fact that we are studying CNSs at a single point in time rather than actually studying the dynamic processes of axonogenesis and synaptogenesis (a point which is equally valid for the rest of this data as features of neuron development such as axon extension followed by retraction cannot be assessed). A model of actual bend formation (as opposed to connection of the two neurons) is discussed in section 8.1.

The question of unequivocal identification of the GF cell bodies in late larval and early pupal life is also pertinent given the lack of monitoring of dynamic growth. This essentially means that whilst we have reconstructed development from serially arranged CNSs, we cannot totally exclude the possibility that the cell bodies and projections we see are different cells coincidentally found in very similar locations and with similar projections. Until stage P5(i) the identification is based upon the position of the cell body combined with the projection of the axon. As described in this chapter, these neurons appear to develop into the GFs through the stages of pupation, until they are absolutely identified after stage P5(i). The development of the the GFs has now been published twice based on the enhancer trap P[GAL4]307 and in both cases the same cell bodies have been identified as the GFs (Phelan *et al.* 1996 and Allen, Drummond & Moffat 1998). In both cases the identification has been based on sequentially arranging CNSs from different pupal stages and inferring the development of the GFs. The enhancer trap reflects the expression of an endogenous enhancer expressed in a subset of cells in the CNS and although there

appears to be consistent expression in the same cells throughout pupal development, to unequivocally follow development a technique involving lineage tracing would be required (such as DiI injection - for example Bossing & Technau 1994).

4.4 Conclusions.

As previously demonstrated (see chapter 3), the enhancer trap line P[GAL4]307 has an expression pattern in the CNS that includes the major components of the giant fibre circuit and represents an excellent marker of this circuit. P[GAL4]307 has been utilised here as a convenient tool for studying development of the GF circuit and as such has facilitated elucidation of accurate temporal and morphological details of this process. This data has allowed the proposition of a new model for the formation of the terminal bend of the giant fibre.

5. Birthdating the giant fibre interneurons.

Part of this work was done in collaboration with Dr M.J.Allen.

5.1 Introduction.

5.1.1 Previous estimates of the giant fibre birthdate based on indirect evidence.

White and Kankel (1978) investigated neural proliferation spatio-temporally, revealing that adult neurons born early lie in more medial positions than their later counterparts. Based on this data, it has been previously postulated that the birthdate of the giant fibre neurons (GFs) occurs during postembryonic neuroblast proliferation (Koto *et al.* 1981, Phelan *et al.* 1996) due to the GFs peripheral position in the CNS.

5.1.2 A combination of techniques for directly investigating the birthdate of the GFs.

A range of potential birthdates were investigated to test the postulate of postembryonic GF birthdate, using P[GAL4]307. Birthdating combines two techniques: firstly, the use of the enhancer trap line P[GAL4]307 to label the relevant neurons (chapters 3 & 4), and secondly, the monitoring of cell proliferation in the CNS during development.

Traditionally, the study of cell proliferation used [^{3}H] thymidine to allow the monitoring of DNA synthesis in individual cells (Taylor *et al.* 1957). This required detection by autoradiography. More recently the use of a non-autoradiographic technique has become more commonplace, using a thymidine analogue 5-bromo-2-deoxyuridine (BrdU) - (Gratzner *et al.* 1975, Gratzner 1982).

5.1.2.1 Monitoring cell proliferation using BrdU.

BrdU was incorporated into replicating DNA and subsequently localised using a specific monoclonal antibody (Gratzner *et al.* 1975, Gratzner 1982). The BrdU incorporation was improved by simultaneous

incubation with 5-flouro-2-deoxyuridine, an inhibitor of thymidylate synthetase (Ellwart & Dormer 1985), thereby lowering competition by endogenous thymidine. Cell proliferation was monitored immunocytochemically using a monoclonal anti-BrdU antibody to detect the BrdU incorporated into cellular DNA, this followed acid treatment to denature the DNA (to allow the antibody access to the BrdU).

The BrdU was administered in timed pulses to aged embryos and larvae to allow identification of the approximate birth time.

5.1.2.2 Using P[GAL4]307 to detect the GFs.

The enhancer trap pattern was detected using X-gal staining to adult or late pupal CNSs, as it was easiest to determine the GF cell bodies unambiguously. Staining at this time also allowed the possibility of birthdating other neurons involved in the GF circuit.

5.1.2.3 Co-localisation of BrdU and P[GAL4]307 had the potential to reveal the birthdate of the GFs.

The co-localisation of the two labels would show that the cells of interest have been dividing within the period of time the BrdU pulse was given and identifies them as cells marked by the enhancer trap (including the GFs and associated neurons). The BrdU would label the proliferating cells, being diluted in later divisions. Therefore the strongest signal would be in cells that had just undergone their last division. The last time point of co-localisation would be determined as being the neuron birthdate and it should have had the strongest labelling for BrdU.

5.1.2.4 Treatment of P[GAL4]307 larvae with BrdU.

Since the GF cell bodies are first distinguishable at L3 we chose the larvae as the starting point for the birthdating process. The method for larval BrdU treatment was adapted from Truman and Bate (1988) - (see method 2.1.6.1.1). Larvae were aged on grape juice agar plates and then transferred to media containing BrdU. Following an 8 hour feeding period the larvae were transferred to normal fly media (Sussex fly food). On developing to an

appropriate stage, dissection of the CNS ensued, followed by detection of the enhancer trap pattern with X-gal, and detection of the BrdU by antibodies (monoclonal primary and tetramethylrhodamine isothiocyanate (TRITC) conjugated secondary) - see 2.1.6.2.2.

5.1.2.5 Treatment of P[GAL4]307 embryos with BrdU.

To investigate potential early lineages, or early parts of a longer lineage, embryonic treatment with BrdU was carried out. Treatment of embryos required a bathing technique, and was carried out essentially as described by Limbourg & Zalokar (1973) and Bodmer *et al.* (1989) - see method 2.1.6.1.2. Embryos were collected and aged appropriately, dechorionated and their vitelline membrane perforated to allow the BrdU access to the developing cells and tissues. After treatment they were allowed to develop to first instar larvae (L1) under halocarbon oil. These L1s were then transferred to normal fly food media in vials to develop into adults/late pupae before having their CNSs removed and treated to detect the enhancer trap pattern and BrdU labelling (see 2.1.6.2.2).

5.2 Results I.

5.2.1 P[GAL4]307 larvae treated with BrdU.

The immunohistochemical data suggested that the GF cells were present in the late larval stages and therefore the possibility existed that the final division producing them occurred earlier in larval life. When this was tested by feeding with BrdU laced food for allotted times throughout larval life (Table 5.1), removing their CNSs in adult life and staining them, we obtained no co-localisation of the GFs marker and the BrdU antibody (for example Figure 5.1A-I). We studied over 550 CNSs that were double labelled to reveal larval proliferation, in this manner. There were a number of co-localising cells in each of the CNSs (Figure 5.1J), but never the GF cell bodies. The pattern of proliferation was constant within each time point indicating that the labelling was working and revealing proliferative changes within the CNS (figure 5.1A & B).

Figure 5.1 Adult CNSs double stained to detect P[GAL4]307 and BrdU localisation.

All times given are in hours After Egg Laying (AEL).
For methods see sections 2.1.6.1.1 & 2.1.6.2.2.

A&B: Adult CNSs from flies fed BrdU for 8 hours (40-48 hours) during larval development. These CNSs illustrate the consistency of BrdU staining pattern in the adult CNS following BrdU treatment for a given period of larval development. The cells derived from those dividing and incorporating BrdU between 40 and 48 hours AEL are detected by immunocytochemistry (patch of brightly fluorescing cells (mushroom body cells) indicated by the green arrowheads). These cells are not the giant fibre cell bodies (GFCBs) as shown by a lack of co-localisation with the X-gal staining that reveals the enhancer trap pattern of P[GAL4]307 (the GF cell bodies - white arrowheads).

C-I: The brain regions of adult CNSs, representing BrdU labelling at different treatment times throughout larval development (24 hours to 112 hours AEL). The bright orange fluorescence of the BrdU detection and dark X-gal detection of the enhancer trap line (GF cell bodies labelled with white arrowheads) are visible. In no case are the two types of staining found to co-localise indicating the GFs are probably not produced during larval development and neither is any part of the GF lineage.
C = 24-40 hours, **D** = 40-48 hours, **E** = 48-64 hours, **F** = 64-72 hours,
G = 72-88 hours, **H** = 88-96 hours and **I** = 96-112 hours AEL.
The patch of cells (labelled in A - green arrowheads) are dividing throughout larval life and are in the correct position to be cells of the mushroom bodies.

J: Examples of BrdU and X-gal co-localisation in the brain of a fly that was fed BrdU between 24 and 40 hours AEL. Unidentified cells labelled by the enhancer trap can be seen to clearly co-localise with BrdU (red arrowheads).

Scale bar = 400μm in **A**, 200μm in **C-D** and 100μm in **J**. Anterior is top, view from dorsal.

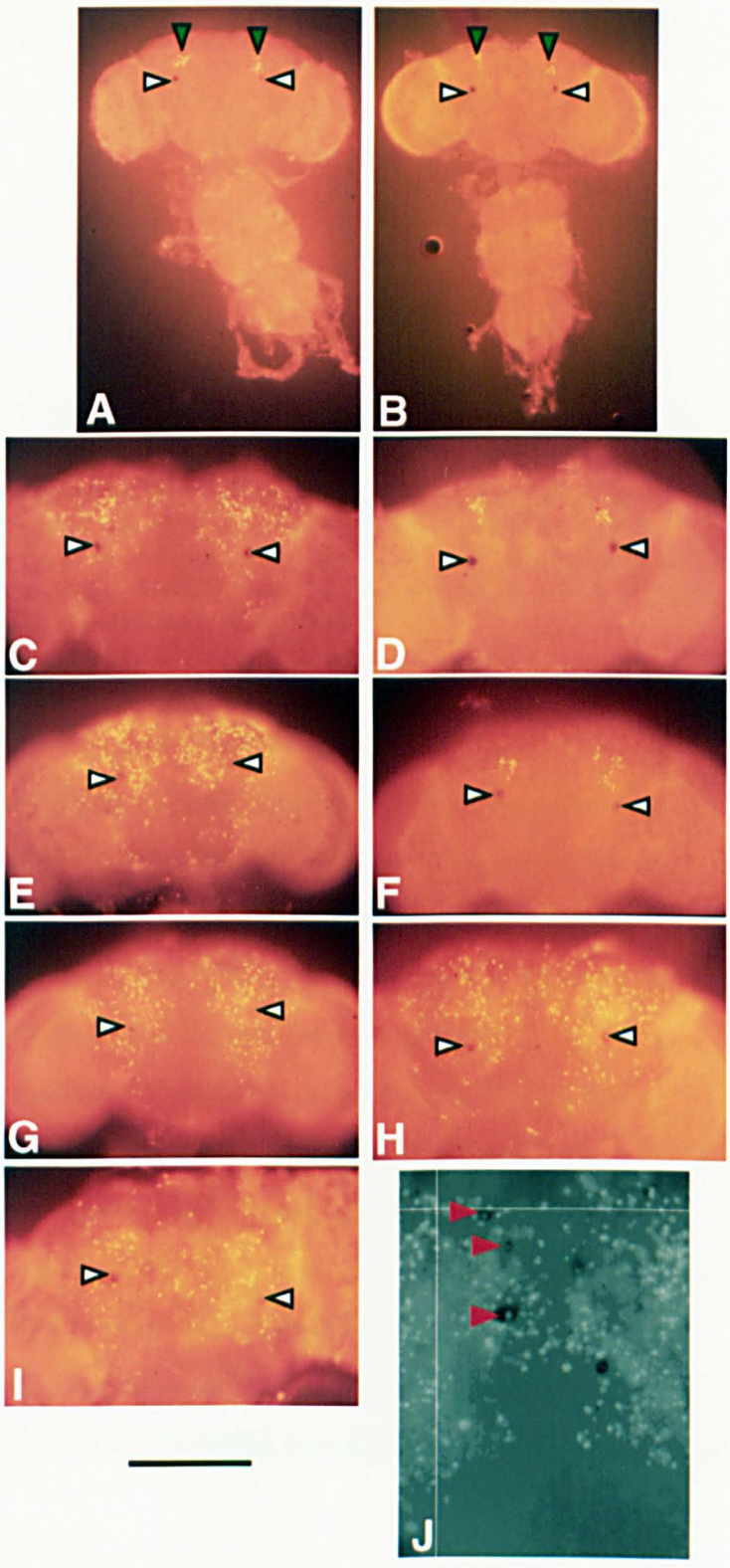
A
B
C
D
E
F
G
H
I
J

Age (+ treatment time).	Number of CNSs dissected and treated.	Number with both BrdU and X-gal staining in the CNS.
0 - 16	31	29
16 - 24	17	17
24 - 40	41	40
40 - 48	65	62
48 - 64	135	123
64 - 72	73	66
72 - 88	62	52
88 - 96	39	36
96 - 112	34	33
112 - 120	22	22
120 - 136	27	27
136 - 144	7	7
Total	553	514

Table 5.1 Larval treatment with BrdU and subsequent detection in the CNSs.
This table shows the range of ages of larvae treated with BrdU (including treatment time). The number of CNSs of each stage subsequently dissected and stained to detect BrdU and the enhancer trap pattern of P[GAL4]307 are presented. The numbers of CNSs in which both detection systems had worked are also shown.
BrdU = 5-bromo-2-deoxyuridine.

To control for the possible effects of reduced fluorescent signal from the BrdU TRITC secondary antibody upon co-localisation with X-gal staining, we chose a different second generation enhancer trap line that expresses strongly in the mushroom bodies (Smith *et al.* 1996). We then fed the larvae the same timed doses of BrdU in phases revealed to label the proliferating mushroom bodies (our data and Ito & Hotta 1992). This revealed that there was not a significant quenching effect upon the fluorescence when co-localisation occurred (data not shown). In combination with the detection of co-localisation in unidentified cells labelled by P[GAL4]307 (figure 5.1J), these data suggest that had any co-localisation occurred within the GFs it would have been detected.

Therefore, the conclusion of this work is that the final division to produce the GF neurons was not during larval life and neither was any part of the GF lineage.

5.2.2 P[GAL4]307 embryos treated with BrdU.

To follow this investigation further we moved the study into embryonic development using essentially the same techniques, with a

modification to the delivery of the BrdU. We gave the embryos timed doses of BrdU covering all the hours of embryogenesis. The level of BrdU incorporation into the embryos was initially checked by staining for BrdU shortly after the incubation (see figure 5.2). Once again we failed to reveal the birthdate of the GFs as shown by a lack of co-localisation, despite the fact both sets of labelling appeared to be working and that we had studied over 350 CNSs (see table 5.2). One possible cause of this lack of co-localisation, was the high level of mortality of early embryos due to the treatment. Two major factors have to be considered here, the first being the BrdU itself causing lethality due to the level of incorporation into so many cells (early lineages of most tissues), and the second may be simple mechanical damage of perforation and handling in early embryos (Limbourg & Zalokar 1973). Between them these problems gave us only a few early embryos (0-6 hours) that developed to adulthood to dissect the CNSs from (see table 5.2). Most that survived possibly did so because they received very small doses BrdU due a low level of perforation, as seen by the lack of anti-BrdU staining in these stages (see figure 5.3). Unfortunately this was the period during which the neuroectoderm forms and the waves of neuroblast delamination occur and was therefore essentially the best time to have labelled all neuroblasts and their progeny.

5.3 Discussion 1.

5.3.1 Calculating the possibility of an early embryonic GF birthdate.

5.3.1.1 Neuroblast delamination.

The data from larval BrdU treatment lead us to consider that the GFs were born very early and by few cell divisions. To investigate this, data from previous studies had to be used to extrapolate whether or not this was a realistic proposal. In the stage 9 embryo, at around 3 hours 40 minutes after egg laying (AEL) the first neuroblasts (NBs) delaminate from the neuroectoderm (Hartenstein & Campos-Ortega 1984). Immediately after segregating from the surrounding cells, the neuroblasts become rounded and

Figure 5.2: The labelling efficiency of BrdU in dividing cells of embryos at various stages of development.

A-N: Embryos of various ages from 1-16 hours. These have been treated and immediately had the BrdU incorporation detected by immunocytochemistry (see sections 2.1.6.1.2 & 2.1.6.2.1).

A+B: Mixed stage embryos showing the variation of incorporation of BrdU depending on age (and consequently the number of cells dividing). Most embryos are labelled and have therefore been sufficiently permeabilised to allow BrdU access to the dividing cells.

C-N: Individual embryos of various ages, labelled with BrdU and revealing the patterns of cell proliferation at each stage. Staging according to Campos-Ortega & Hartenstein (1985). Ages are given in hours as After Egg Laying (AEL). Anterior is left.

C: Stage 2 embryo (precellular embryo with dividing nuclei), 0.25-1.05 hours AEL. Lateral view.

D+E: Stage late 4-early stage 5 (blastoderm cell formation is occurring), 1.50-2.10 hours AEL. Lateral view.

F: Stage 5/6 (early gastrula stage), 2.10-3 hours AEL. Lateral view.

G: Stage 8 (germ band elongated), 3.10-3.40 hours AEL. Lateral view.

H: Stage 11 (germ band starts to retract and segmentally repeated swellings mark the appearance of neuronal precursors), 5.20-7.20 hours AEL. Dorsal view.

I,J+K: Stage 12 (germ band retracting), 7.20-9.20 hours AEL. **I+J**=Lateral view (J more medially focussed), **K**=Ventral view.

L,M+N: Stage 13 (germ band shortening and nervous system condensation), 9.20-10.20 hours AEL. **L**=Ventral view, **M**=Dorsal view, **N**=Lateral view.

From stage 11 (**H**), most of the BrdU seems to be incorporated into the developing nervous system which indicates how proliferative it is within this period of embryonic development.

Scale bar = 500μm in **A+B**, 250μm in **C-N**.

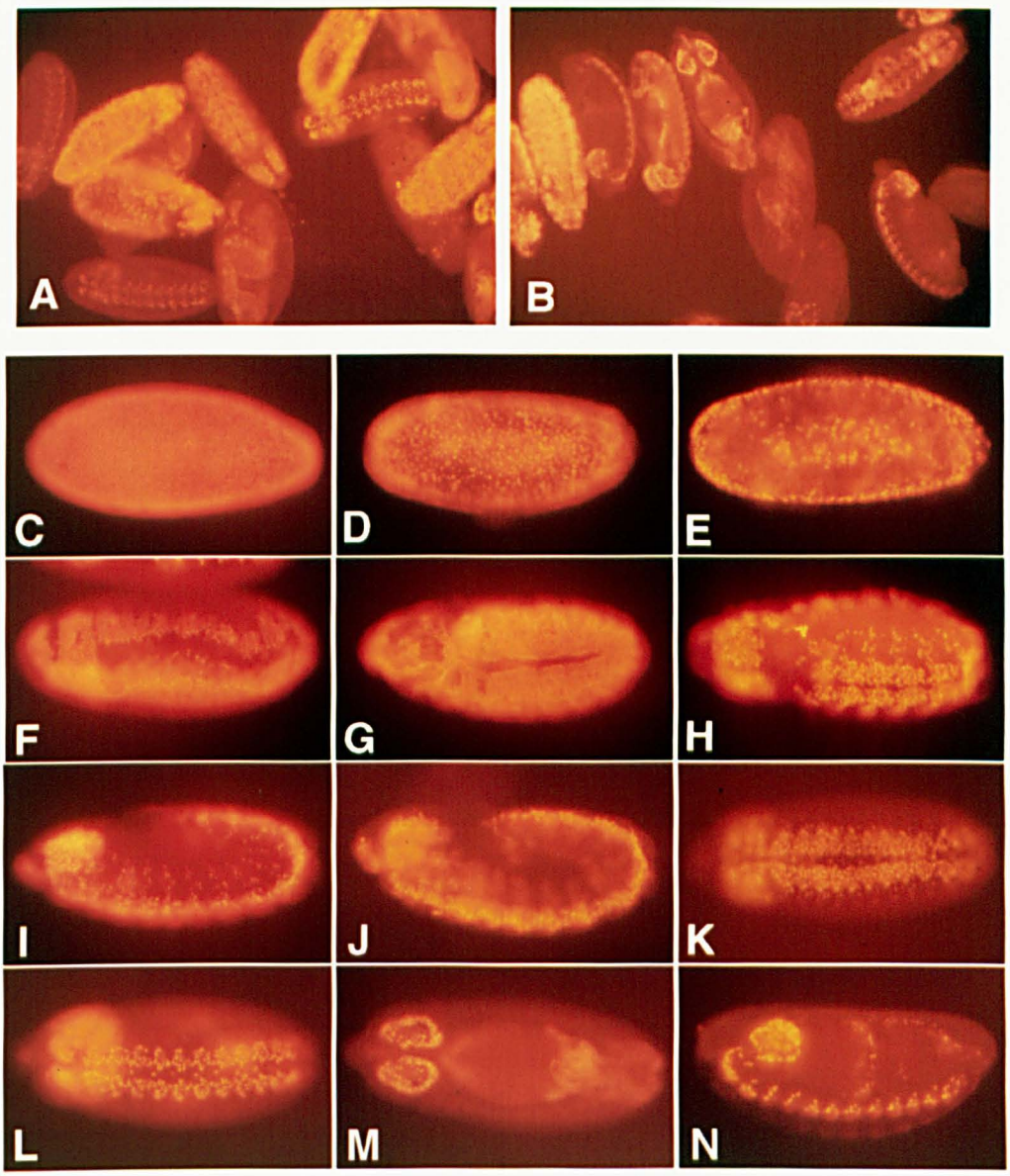
A
B
C
D
E
F
G
H
I
J
K
L
M
N

Age (hours AEL)	BrdU treatment time (hours)	Number of embryos treated	Number of adults eclosing	Number of CNSs dissected from adults	Number of CNSs stained with both BrdU & X-gal
0 - 1	1	300	0	0	
1 - 2	1	150+	2	2	
2 - 3	1	150+	38	38	
2 - 3	0.5	500	0	0	
2.5 - 3.5	0.5	300	1	1	
3 - 4	1	300+	17	17	3
3 - 4	0.5	200	0	0	
3.5 - 4.5	0.5	300	1	1	1
4 - 5	1	400	51	51	3
4 - 5	0.5	400	1	1	
4.5 - 5.5	0.5	200	1	1	
5 - 6	1	150+	10	10	1
6 - 7	1	600+	22	22	5
7 - 8	1	400	11	11	2
8 - 9	1	2100	13	13	10
9 -10	1	2050	34	34	13
10 - 11	1	1100	24	24	22
10 - 11	0.5	200	17	17	1
11 - 12	1	1750	116	31	24
12 -13	1	1450	38	26	14
13 -14	1	1350	38	36	9
14 - 15	1	500	8	8	1
15 - 16	1	200	4	4	
16 - 17	1	750	246	48	6
17 - 18	1	400	34	34	
18 - 19	1	400	6	6	
19 - 20	1				
20 - 21	1	300	4	4	
21 - 22	1	300	0	0	
22 - 23	1	150	15	15	2
23 - 24	1	200	17	17	
Totals		17550	639	390	117

Table 5.2 showing the treatment regime of embryos with BrdU, subsequent numbers surviving, being dissected and staining for BrdU and P[GAL4]307.

Embryogenesis was divided into hour intervals. Embryos were collected and aged until they reached the required time point that was to be studied (time given in hours After Egg Laying - AEL). From this point they were treated with BrdU for 1 hour or half an hour. Half hour treatments were applied when mortality following BrdU treatment appeared a problem and few embryos were reaching adulthood. Approximately 17500 embryos were treated with BrdU, 639 developed to adulthood, 390 of these were dissected and subsequently 117 of these had both staining for BrdU (cell divsion) and the enhancer trap pattern of P[GAL4]307 (marker of the giant fibre circuit). The + symbols after the number of embryos treated (in 5 of the time points) indicate that not all of the embryos treated were recorded and that the data for these time points are incomplete. Further detailed subdivision of the staining is presented in figure 5.3. For full data see appendix 10.3.

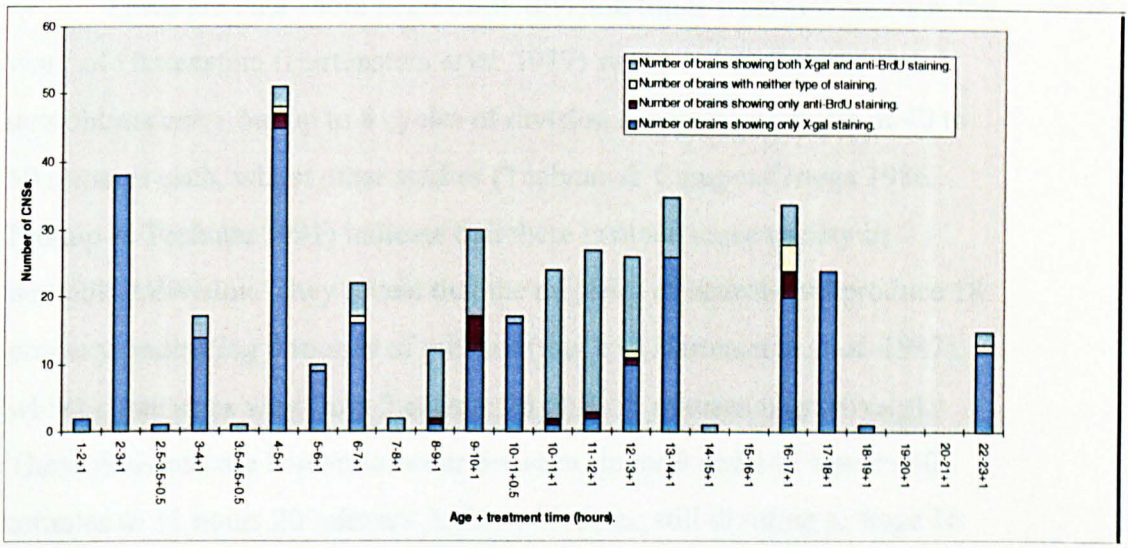

Figure 5.3: Staining within adult brains, revealed by detection for both BrdU and the enhancer trap pattern.

This graph shows the distribution of staining revealed by scoring 390 adult brains. Each bar represents the number of brains that have been dissected from adult *Drosophila*. The bars are subdivided according to the number of CNSs within which BrdU alone can be detected, the enhancer trap pattern alone can be detected (with X-gal staining) and both or neither BrdU and the enhancer trap pattern are detectable. Only brains within which both detection systems had worked could possibly reveal the giant fibre (GF) birthdate or any part of the lineage that produced the GFs. Times on the x-axis are given in hours After Egg Laying (AEL). From this graph it is clear that there was little chance of birthdating the GFs in both early (1-6 hours AEL) and late embryogenesis (17-22 hours AEL) because the detection of both BrdU and the enhancer trap pattern occurred very infrequently (in 7 cases pre 7 hours AEL and 2 cases post 17 hours). Between 6 hours and 17 hours AEL the chances of birthdating the GFs was much improved with 108 cases of double labelling. The majority of the embryos treated between 1-7 hours showed only X-gal staining, indicating they may have survived due to not incorporating any BrdU.

start dividing (within 10 - 20 minutes) - (Hartenstein *et al.* 1987).

5.3.1.2 Neuroblast division times.

There are data about neuroblast division times from two sources; the work of Hartenstein (Hartenstein *et al.* 1987) suggested that most neuroblasts carry out up to 8 cycles of division at regular intervals of 40 to 50 minutes each, whilst other studies (Technau & Campos-Ortega 1986, Prokop & Technau 1991) indicate that there is much more variety in neuroblast division. They reveal that the majority of neuroblasts produce 18 progeny, indicating 9 rounds of mitoses (much as Hartenstein *et al.* 1987), whilst clone sizes vary from 2 cells to 26 (1 & 11 mitoses respectively). These divisions are known to occur between stages 9 and 14 (3 hours 40 minutes to 11 hours 20 minutes AEL), with some still dividing at stage 16 (up to 16 hours AEL) - (Prokop & Technau 1991).

5.3.1.3 Ganglion mother cell division times.

Ganglion mother cells (GMCs) are the direct progeny of neuroblast asymmetric division, and they divide symmetrically to produce 2 neurons. In the *Drosophila* embryo the duration of the GMC cycle is approximately 100 minutes (Hartenstein *et al.* 1987).

5.3.1.4 The total division time to produce a neuron from a neuroblast make an early birthdate a possibility.

If the giant fibre neurons were produced by the divisions of a neuroblast formed immediately at the first wave of neuroblast delamination then assuming all the times listed previously (10-20 minutes for rounding up, 40 to 50 minutes for division time of the NB to produce the GMC and 100 minutes for the GMC to produce 2 neurons) then the production of the giant fibre neurons could all occur by stage 11 (6 hours 10 minutes).

This is assuming an average lineage, whilst the divisions may actually be faster if the neuroblast producing the giant fibres underwent a short lineage producing only 2 neurons (within the range of progeny sizes mentioned above). Lineages of this sort have been shown for both

unidentified neuroblasts (Technau & Campos-Ortega 1986) and identified ones (the MP1 and MP2 lineages - Doe *et al.* 1988). In these cases the GMCs are not produced and the neurons form by division of the neuroblast directly. In either eventuality, this period is not covered by the BrdU labelling data. It therefore remained a possibility the giant fibres are born early and we could not address this using the BrdU labelling technique.

5.3.1.5 Potential problems of calculations based on ventral nerve cord division times.

A *caveat* to these calculations is that whilst information is available about the neuroblast delamination and their lineages, it is largely for the ventral nerve cord of the CNS and not the brain region, simply due to the accessible nature of this developing region. Important differences include: continuous segregation of neuroblasts, rather than the waves seen in ventral nerve cord development; some procephalic lobe neuroblasts produce GMCs prior to segregation from the ectodermal layer (indicating the neurons could be born even earlier than 6 hours 10 minutes); and the spatial pattern of neuroblasts is not as regular as that seen in the ventral nerve cord (Hartenstein & Campos-Ortega 1984).

Furthermore, in addition to the asymmetric division seen in the ventral nerve cord, within the procephalic lobes, neuroblasts also divide symmetrically to produce a pair of neuroblasts which in addition to delamination increases neuroblast number (from 45 at stage 9 to 140 in total by both processes throughout embryonic development) - (Hartenstein & Campos-Ortega 1984).

This series of points infers that the timings proposed for the early giant fibre development may be incorrect, not for any direct reasons but since there are many other differences, between the brain and ventral nerve cord. In fact, data about procephalic neuroblast division, whilst scarce, has been studied (Younossi-Hartenstein *et al.* 1996). Of the procephalic neuroblasts studied, the cell cycle time appears to be approximately 45-60 minutes (similar to the ventral nerve cord neuroblasts). Futhermore the

number of ganglion mother cells produced by these neuroblasts between stages 9-11 can be 2-3. This therefore supports my estimates of division and timing.

5.3.2 The possibility of a late embryonic/early larval birthdate.

An alternative possiblity arises from the examination of the BrdU labelling data (table 5.2). Little data concerning the labelling with BrdU of late stage embryos (17 to 23 hours) was produced, although there were plenty of treated embryos surviving to be dissected, it appears that they were not incorporating BrdU into their cells (as shown by a lack of anti-BrdU staining - figure 5.3). This may be indicative of the perforation of the embryos failing to effect the cuticle which has formed by this stage, thereby effectively preventing any BrdU labelling.

Alternatively, the cells may not have been dividing within this period. A potential technique for investigating this is injection of BrdU into late embryos (Prokop & Technau 1994). This period (from 16 hours to the end of embryogenesis) has been previously studied (Prokop & Technau 1991, Truman & Bate 1988). It was demonstrated that most neuroblasts stop dividing just prior to this time and did not resume division until the second larval instar (true of all the neuroblasts in the ventral nerve cord). Five exceptions to this were demonstrated, all from the brain region: 4 mushroom body neuroblasts and one lateral neuroblast. However, the mushroom body neuroblasts are unusual in their proliferation, as they proliferate continuously from embryonic stages through to late pupal stages (Prokop & Technau 1991, Ito & Hotta 1992) - (see figure 5.1A-I in this chapter which, in agreement with these other studies, reveals their proliferation continues throughout larval life). Taken together this makes a late embryonic birthdate unlikely. For this reason we decided to investigate the early birthdate.

5.4 A second technique to investigate a potential early embryonic birthdate of the GFs.

Due to the high levels of mortality involved with BrdU labelling of early embryos a dye injection technique was applied to cover a potential early embryonic birthdate. This involved injecting high molecular weight dye into precellular (syncytial blastoderm stage) embryos and letting them develop, so the dye was incorporated into all the embryo's cells, viewed later to see if it was visible in the GFs (as seen by morphology and enhancer trap detection). If the neuron was produced early, with few cell divisions, the dye would not be diluted much by cell division and so the cell would be clearly labelled when viewed in pupal stages. This technique had been used previously (Tix *et al.* 1989) with horseradish peroxidase (HRP), but was modified here to use Biotin Dextran Amine (BDA) (Williams & Shepherd pers. comm.) - see method 2.1.7. Detection of the dye was via a standard HRP colour reaction (see method 2.1.7.2).

5.5 Results II.

5.5.1 Using the dye injection technique to study an early embryonic birthdate.

In order to test the idea of an early embryonic birthdate the dye injection method was used as a lineage tracer. Approximately 600 precellular embryos were injected with BDA, of which nearly 100 survived to pupation (appendix 10.4), when they were dissected and the dye visualised. Cells previously identified as being produced by relatively few cell divisions were noted and acted as internal controls to the experiment (see below), complemented by some uninjected controls (figure 5.4B & E). The staining was at variable levels due to small differences in the amount of dye injected into the embryos (delivery was via a controlled delivery system, but will vary with the level of embryo hydration) - for example compare figures 5.5A & B.

Figure 5.4: Biotin labelled Dextran Amine (BDA) labelled cells in pupal CNSs.

For the method see section 2.1.7.

A&C: Brain region of a CNS from a pupa (stage P3, 2 to 7 hours After Puparium Formation - APF). This illustrates the high level of proliferation in the optic lobes which is reflected in the high level of dilution of the BDA. The optic inputs that are heavily stained are the optic lobe pioneers (within dashed box - shown at a higher magnification in **C**). The 3 cell bodies from which the axons project are clearly visible in **C**.

B: Brain from an uninjected control of the same pupal stage as that in **A**. Clearly there is no background staining.

D&F: CNS from a stage P5/6 pupa (14-48 hours APF). The optic lobe pioneers are visible (in dashed box) and are shown at a higher magnification in **F**. Apparent in **D** is the effect of dilution of the BDA by cell divisions. The optic lobes which proliferate most have the lowest levels of BDA and conversely the abdominal neuromere which has the least cell division has the highest levels of BDA staining.

E: Brain from an uninjected control of a similar pupal stage as that in **F**. There is no background staining.

Anterior is top, viewed from dorsal. Scale bar = 100μm in **A** & **B**, 50μm in **C** & **F**, 120μm in **D** & **E**. All the images are montages.

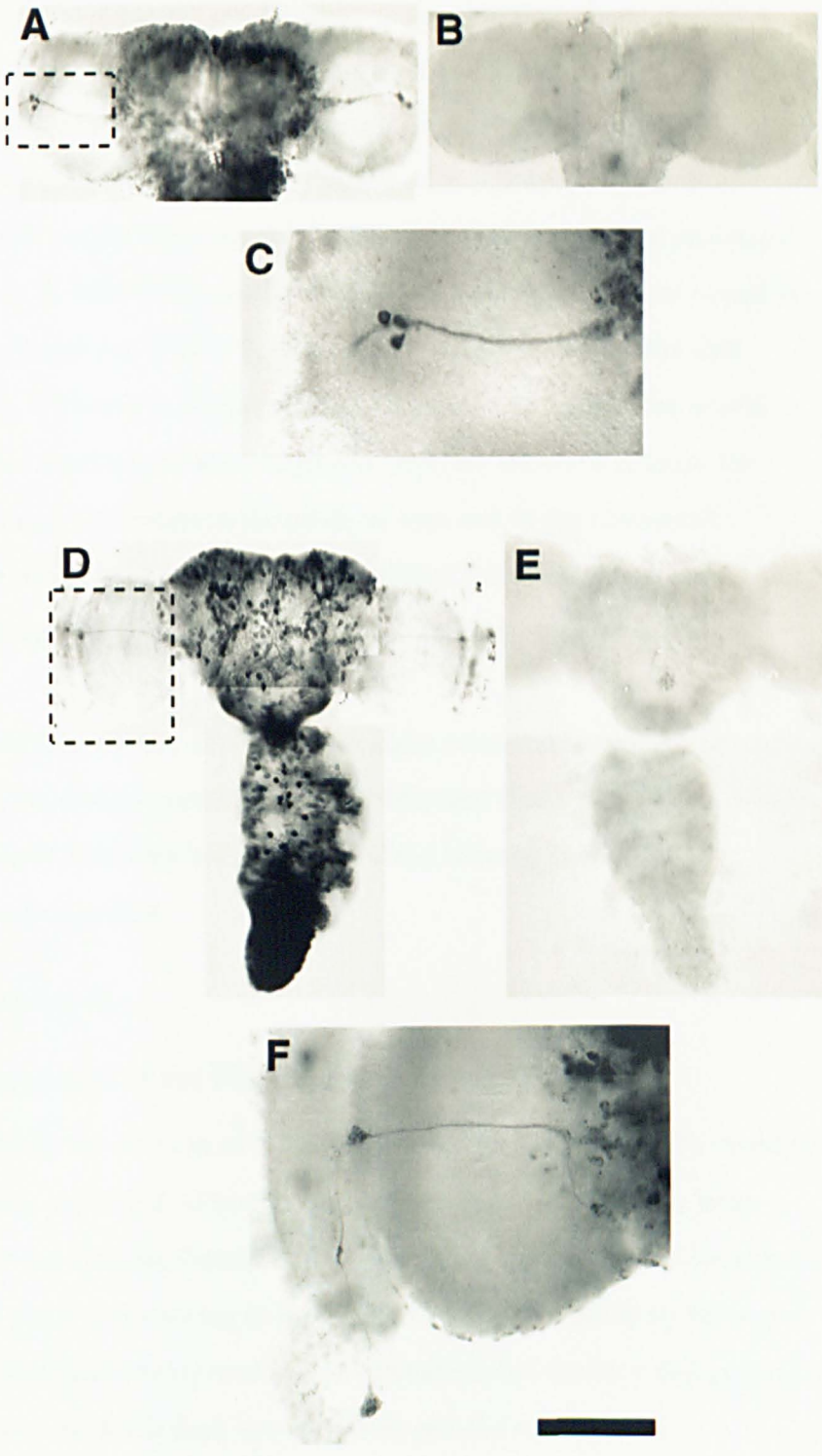
A
B
C
D
E
F

5.5.2 Identified neurons labelled by BDA injection.

The optic lobes are produced by a huge number of cell divisions during larval and pupal life and this leads to an absence of dye in the optic lobes except for the projections of a group of 3 previously identified neurons (the Optic lobe Pioneers - Tix *et al.* 1989) - see figure 5.4A,C,D & F. Likewise, the ventral nerve cord is highly proliferative in larval and pupal life (Truman & Bate 1988), and all but the abdominal neuromere revealed low levels of staining (figure 5.4D). This was consistent with the data obtained by Williams & Shepherd (pers. comm.) and reflects the neural proliferation requirement for a large and complex series of neurons to control the legs and wings in the adult, as opposed to the abdominal neuromere which is no longer the predominant locomotor region and therefore does not proliferate after larval life (it is in fact substantially reduced).

Most importantly for this study, there were cell bodies of the correct size and in the correct position to be the GFs (see figure 5.5A-H), however, without double labelling the identity of these neurons cannot be unequivocally ascribed.

5.6 Discussion II.

5.6.1 Drawbacks of the BDA injection technique.

Despite the success of this dye injection technique the GFs could not be absolutely identified, although good potential candidates have been revealed by the staining (based on position and size). Initially co-localisation of the dye and X-gal staining in the GF cell bodies was going to be used so all stages of pupal development could be studied, but the blue coloration (X-gal) tended to mask the dark brown (HRP) and the results were unsatisfactory. Therefore the identification of the GFs had to be attempted using just the dye labelling. To ease this identification the CNSs were taken from stage P4-P8 pupae when the cell bodies were large and their position

Figure 5.5: Biotin labelled Dextran Amine (BDA) labelled cells in pupal CNSs may include the giant fibres (GFs).

Staging based on Bainbridge & Bownes (1981). Hours of development are given After Puparium Formation (APF).
The dye injection method is in section 2.1.7.

A-H: Brain regions of pupal CNSs with BDA labelled cells the correct size and in an appropriate position to be the GFs (labelled with black arrowheads).
A&C, B&D, G and **H**: Brain regions of P5/6 pupae (14-48 hours APF). The regions surrounded by dashed lines in **A** and **B** are shown at a higher magnification in **C** and **D** respectively.
E&F: Two different CNSs from stage P3 pupae (2-7 hours APF). In both cases only one potential GF cell body can be seen.
I: A region of ventral nerve cord from a P5/6 pupal CNS, illustrating the effectiveness of BDA injection for labelling cells differentially depending upon the length of cell lineage. The darker cell bodies are those that have divided few times and are clearly distinguishable from those lightly staining, that have divided more times. The more cell division the greater the dilution of the BDA.
J: An area of ventral nerve cord from a P5/6 pupal CNS, illustrating the possible effect of cell size (cytoplasmic volume) upon dilution of the dye (arrowhead).

The variability in levels of dye between CNSs (compare **B** & **H**) is due to slight variations in the amount of dye injected into the embryos (which in turn was due to varying levels of dehydration). This has allowed potential GF cell bodies to be seen as they seem to be masked by highly staining small cell bodies when there is a high level of BDA in the CNS (as in **D**). Combined with an apparent dilution effect with increasing cytoplasmic volume (see **J**), this made the GF cell bodies hard to identify unless a smaller quantity of BDA was injected. In **C,G** and **H**, the cell bodies tentatively identified as the GFs (black arrowheads) are clear because less BDA was injected, and appear to be the product of a very short lineage (as they are the most intensely staining cell bodies apparent - despite the cell volume is so large).

Scale bar = 130μm in **A,B** and **E-H**, 70μm in **C&D**, **I&J**. Anterior is top. View from dorsal.

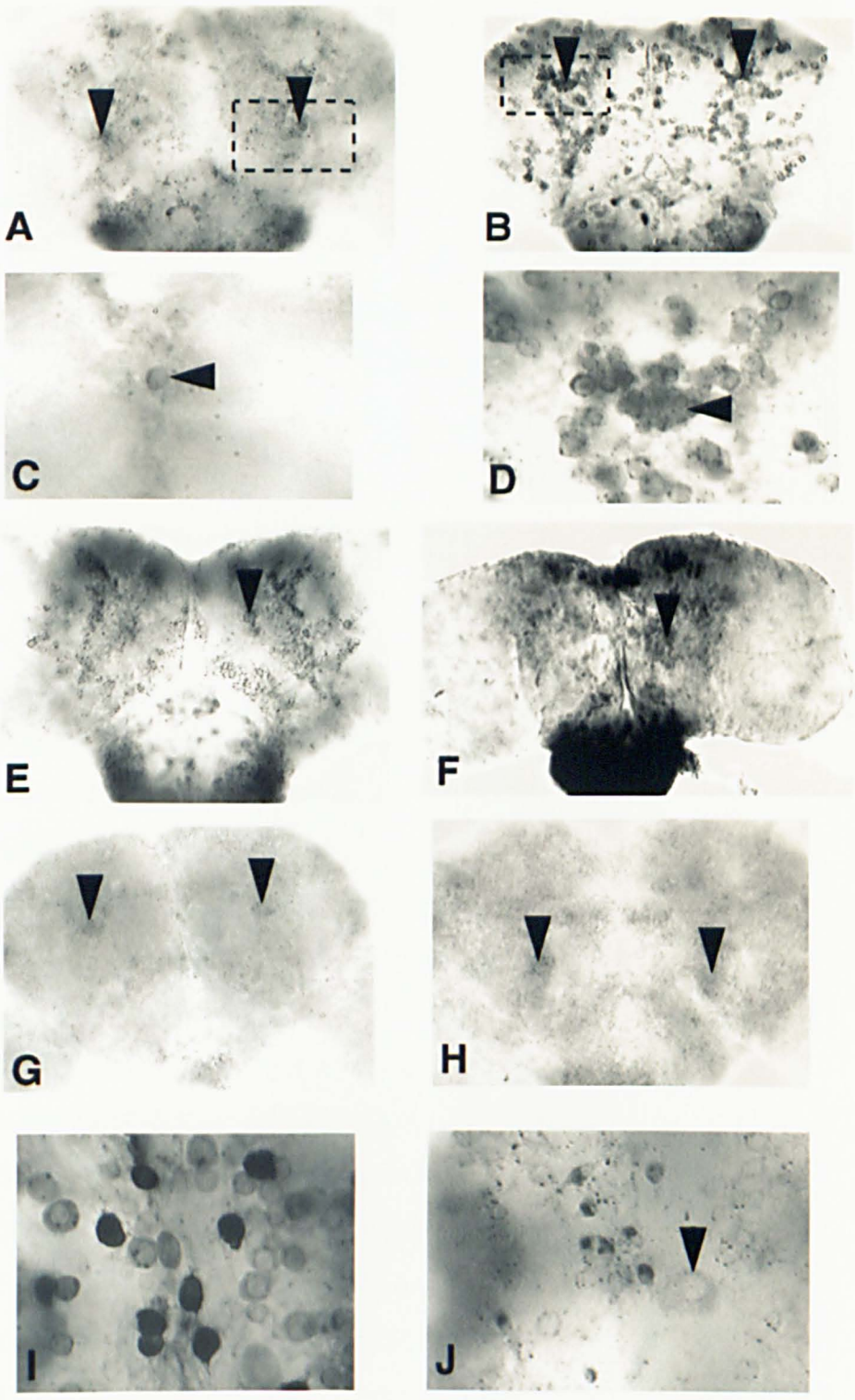
A
B
C
D
E
F
G
H
I
J

characteristic. This may have had the unfortunate effect of leading to the dilution of the dye throughout the cytoplasm and down the large axons, hence preventing easy detection in the GF cell bodies. This dilution effect can be seen in other large neurons (see figure 5.5J).

Therefore this series of experiments has provided evidence that the GFs may be born early in embryogenesis.

5.6.2 Implications of these data.

The implication of these data is that the GF cells, although born early, remain more peripheral in the ganglion during development contrary to expectations (see 5.1.1 - Koto *et al.* 1981, Phelan *et al.* 1996, White & Kankel 1978). The cells may achieve this by migration, which although common in mammalian nervous systems has been rarely reported in invertebrates (Cantera *et al.* 1995). The peripheral position of the GFs may also be explained by a combination of the large size of the cell bodies and the small number of divisions, implied by the data in this chapter, in the production of the GFs from neuroblasts. Neurons produced by few cell divisions tend to be larger (as they are a larger fraction of the size of the NB), and the fewer cell divisions the more peripheral the neuron may be, due to less displacement medially by subsequent NB progeny. The large size of the GF may place it at the periphery of the neuromere and spanning the same depth as several neuron cell bodies with smaller cell diameters. In this manner the GF cell could have been produced at the same time as the neuron that is 2 or 3 cells deep in the neuromere and still appear peripheral, due to its size and lesser degree of medial displacement.

Work from larger insects, such as *Manduca sexta* (Levine & Truman 1985) has provided much data on the changes to the nervous system of insects during metamorphosis. This work has revealed most neurons of the adult nervous system are born postembryonically from quiescent neuroblasts, or are remodelled from larval motorneurons (for example the MN5 giant motorneuron - Truman *et al.* 1993). It has been estimated that larval neurons constitute up to 10% of adult neurons, and that the larval

motor neurons are mainly embryonic in origin (Truman *et al.* 1993). Further there is evidence from ablation studies in *Manduca* that many of the pre-motor interneurons may also have embryonic origins (Truman and Booker 1986). Thus the proposal that the GF of *Drosophila* may also have an embryonic origin is not without precedent.

If the GF is a remodelled larval cell we would expect to see evidence of function such as larval dendrites. This was not apparent and suggests a novel mode of neural development in which a neuron is born embryonically, develops during late larval and pupal life and has no function until after eclosion. A restriction imposed by using an enhancer trap line as a marker was that larval dendrites may have been present and we may have been unable to visualise them due to a lack of sensitivity of the detection system. The GFs may also have larval targets that were not marked in the enhancer trap line.

5.7 Conclusions.

The use of BrdU labelling in conjunction with P[GAL4]307 has allowed the tentative exclusion of a larval and mid-embryonic birthdate of the giant fibre neurons. Having ascertained this, a BDA injection technique was used and has revealed a potential early embryonic birthdate for the giant fibre neurons.

6. Cloning and analysis of *diomedes*.

6.1 Introduction.

Approximately 25 Kb of flanking genomic DNA was plasmid rescued and isolated from around the P[GAL4]307 insertion site and mapped by *in situ* to polytene chromosomes to the 50C region on the right arm of chromosome 2. Reverse northern analysis identified 2 potential transcriptional units, one either side of the P-element insertion site. Fragments of the surrounding genomic region were subcloned into Bluescript KS+ (pBSK+). This work was carried out by Dr K.G.Moffat and Dr M.J.Allen.

A *Hin*dIII fragment sits within a 10Kb plasmid rescue clone pKpnI that stretches from the P-element polylinker to the *Kpn*I site at the end of the walk. This *Hin*dIII fragment was subcloned into pGEM-7Zf (+) (Promega) - designated pGH4.2. pGH4.2 was used as template for a probe that identified one of the potential transcriptional units from the region around the P-element insert. My work has been studying this initially identified putative gene, and then further investigating the rest of the walk on the same side of the insertion. The side of the walk studied encompasses the region from the *Kpn*I site (at the extreme left of the walk in figure 6.1) to the P-element insert. The rescued genomic region has subsequently been restriction mapped and the *Hin*dIII fragment's position placed on the walk by PCR analysis (see figure 6.1).

6.2 Library screening.

In order to isolate cDNAs from this region, library screening was undertaken. A commercially available embryonic *Drosophila* cDNA λgt11 library was used (Clontech, 5'-STRETCH cDNA library, cat. no. IL1010b). The pGH4.2 insert was isolated from the vector using *Hin*dIII digestion, yielding a 4.2Kb fragment. This band was gel purified (2.2.9) and used as a template to produce a P^{32} radiolabelled probe (2.2.5.1.1). One million plaques

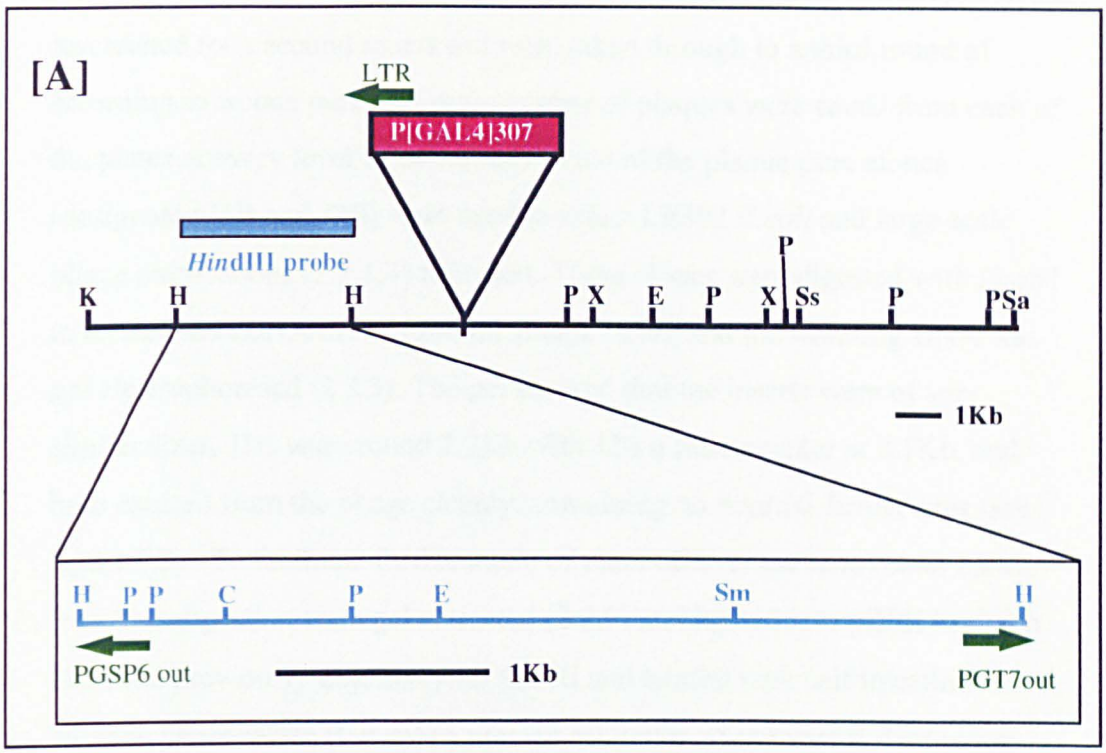

Figure 6.1: Map of the genomic region surrounding P[GAL4]307.

[**A**]: map of the region surrounding the P-element insertion as determined by restriction digestion of the plamid rescued DNA. An expanded view of the *Hin*dIII region is shown. K=*Kpn*I, H=*Hin*dIII, P=*Pst*I, X=*Xho*I, E=*Eco*RI, Ss=*Sst*I, Sa=*Sal*I, C=*Cla*I, Sm=*Sma*I.

[**B**]: The location of the *Hin*dIII fragment (c.3Kb from the insert) was determined by PCR using a primer from the end of the fragment and the end of the P-element (green arrows). The gel of the PCR is shown below, the primer combinations were: lane **1** = PGSP6out primer only, lane **2** = PGSP6out + LTR primer, lane **3** = PGT7out primer only, lane **4** = PGT7out + LTR primer, lane **5** = LTR primer only, lane **6** = no primers, lane **7** = PGT7out + LTR (no template).
This PCR confirmed that the *Hin*dIII fragment is 3Kb from the P-element insert and that the fragment is orientated with the PGT7out primer facing the P-element insert. The PGT7out and PGSP6out primers were designed to the sequenced ends of the subcloned *Hin*dIII fragment whilst the LTR primer was designed to the long terminal repeats of the P-element (section 2.2.11.1). The PCR was carried out under standard conditions (2.2.11.2).

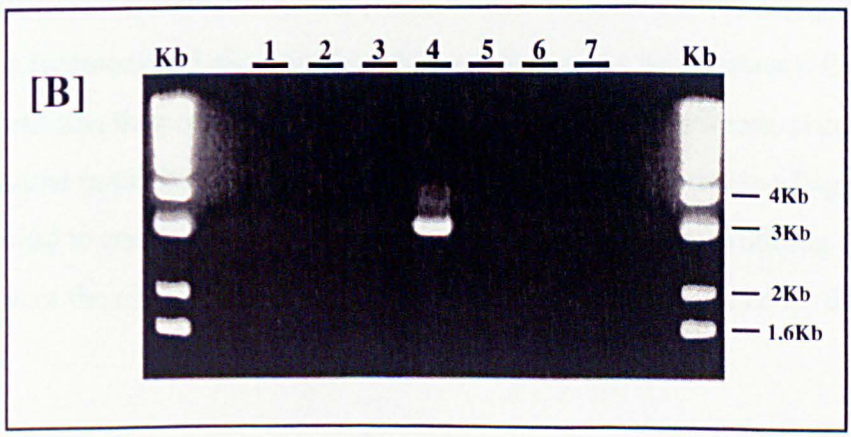

were screened (2.2.12) producing 200 positives, four of these were replated and rescreened for a second round and were taken through to a third round of screening to isolate pure clones (a number of plaques were saved from each of the plates at every level of screening). Two of the plaque pure clones (designated J1B and J2B) were used to infect LE392 *E.coli* and large scale phage preparations (2.2.1.4) followed. These clones were digested with *Eco*RI to release the cDNA insert from the phage DNA, and the resulting DNA was gel electrophoresed (2.2.3). The gel showed that the inserts were of very similar sizes, J1B was around 2.2Kb with J2B a little smaller at 2.1Kb, and both excised from the phage cleanly, containing no internal *Eco*RI sites (see figure 6.2). To facilitate further study of these cDNAs the non-vector bands from this digestion were gel extracted (2.2.9) and ligated into pBSK+, which had been previously digested with *Eco*RI and treated with calf intestinal alkaline phosphatase (Gibco) to prevent religation of the vector. Following transformation (2.2.10.3) the colonies were recovered and analysed to determine which contained the phage inserts (figure 6.3). These clones were then prepared on a large scale (2.2.1.3) ready for further analysis.

6.3 cDNAs identified by library screening.

6.3.1 cDNA J1B.

cDNA J1B was digested with a variety of restriction enzymes in order to produce a map of the clone (figure 6.4). The restriction digestion of J1B was also used to produce a number of fragments that were gel electrophoresed, gel extracted and subcloned into pBSK+ (digested in a manner complementary to each fragment and alkaline phosphatased to prevent self ligation). Each fragment was then sequenced (2.2.13.2) using T3 and T7 primers, priming at sites found in pBSK+ adjacent to the polylinker. These sequenced fragments were used to construct a number of contiguous fragments constituting 4 large regions of the cDNA. One large contiguous fragment was formed by designing

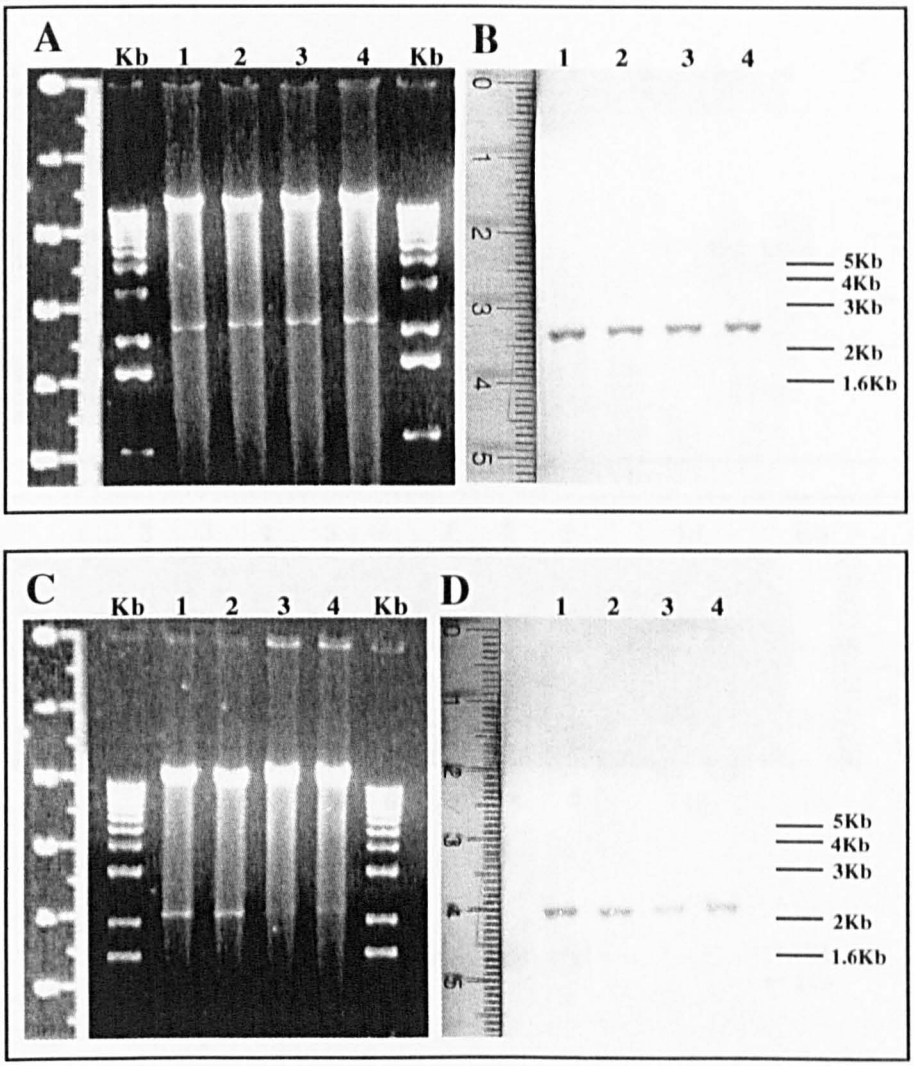

Figure 6.2: cDNAs J1B and J2B were excised whole from phage by *Eco*R1 digestion.

A&C: *Eco*RI restriction digests (see section 2.2.2) of phage maxi-preps (2.2.1.4) of positive phage plaques J1B (**A**) and J2B (**C**). The preps were split into 4 for centrifugation steps (lanes 1-4). The maxi-preps followed 3 rounds of library screening to get the phage to plaque purity (2.2.12).
In the case of J1B *Eco*RI digestion released a 2.2Kb cDNA insert, whilst a slightly smaller insert of about 2.1Kb was excised in the case of J2B.
Both cDNA inserts were intact, indicating no internal *Eco*RI sites.

B&D: Confirmation of the inserts being cDNAs that hybridise with the genomic *Hin*dIII probe (used to probe the library), by Southern blotting (2.2.5) of the gels in **A** and **C**.
The Southerns (J1B in **B**, J2B in **D**) were probed with a Dig labelled *Hin*dIII DNA probe.

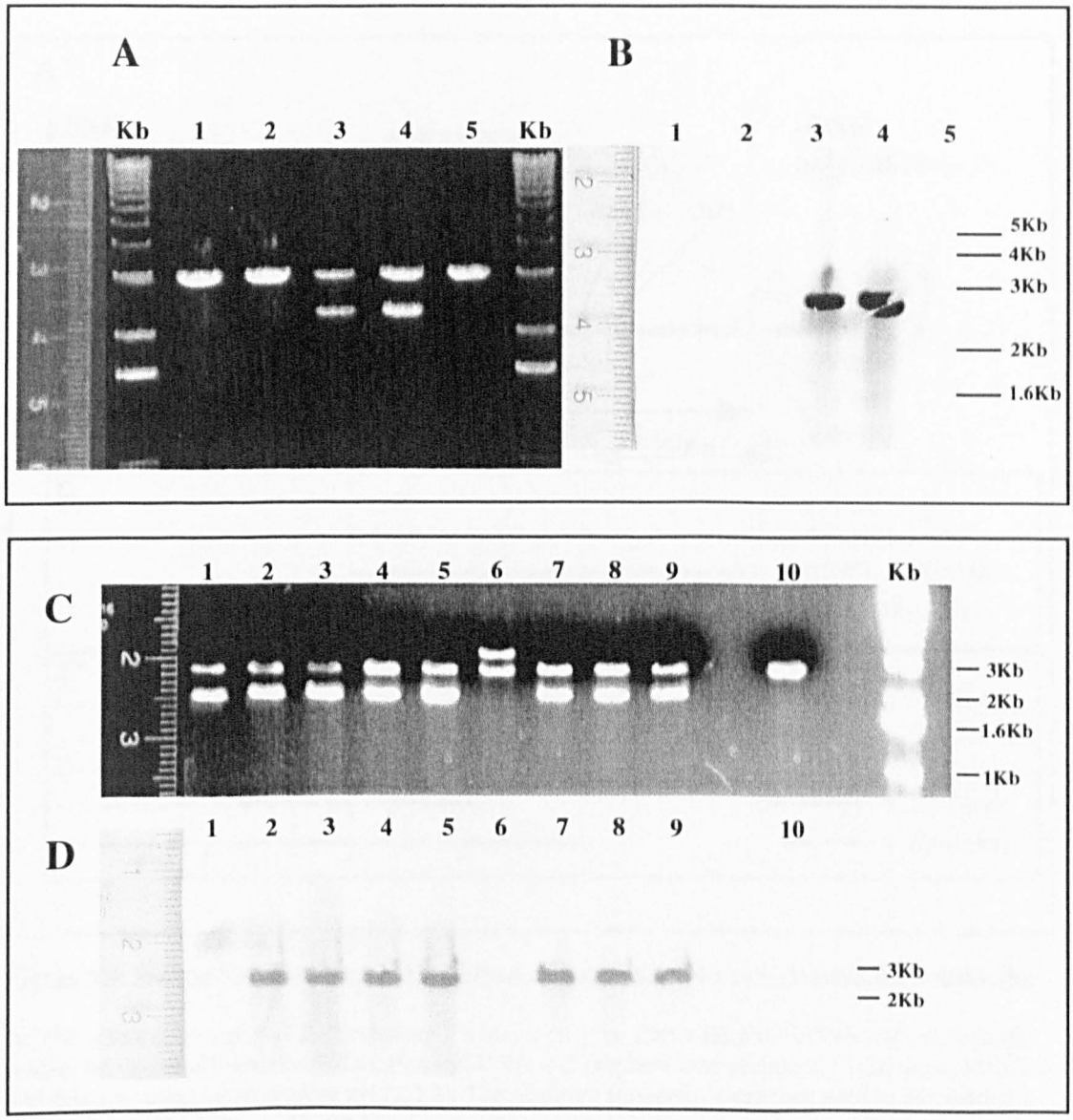

Figure 6.3: *Eco*RI restriction digests and Southern blots of mini-preps, indicate J1B and J2B have successfully been subcloned into pBluescript.

A&C: J1B & J2B cloned into pBluescriptSK+ and transformed into bacteria (section 2.2.10), mini-prepped (2.2.1.2), digested (2.2.2) with *Eco*RI and run on agarose gels (2.2.3).
A: Of the 5 colonies picked for plasmid DNA preparation (lanes 1-5), 2 appeared to contain a 2.2Kb insert that may be J1B (lanes 3 & 4).
C: Reveals that of the 9 colonies picked for plasmid DNA preparation (lanes 1-9), 8 appeared to contain a 2.1Kb insert that may have been J2B (all lanes except lane 6). Lane 10 in gel **C** was a plasmid only control.

B&D: The identity of the inserts as the cDNAs isolated in the library screen was confirmed by the probing of Southern blots (2.2.5) of gels **A** and **C** with the genomic *Hin*dIII fragment used to probe the library. This identified the 2 inserts in lanes 3 and 4 as J1B cDNA that had been successfully subcloned into pBluescript (**B**) - the disruption in lane 4 was due to the gel being damaged prior to blotting. The probed blot shown in **D** confirmed that all the colonies with a 2.1Kb insert were indeed J2B with the exception of lane 1.

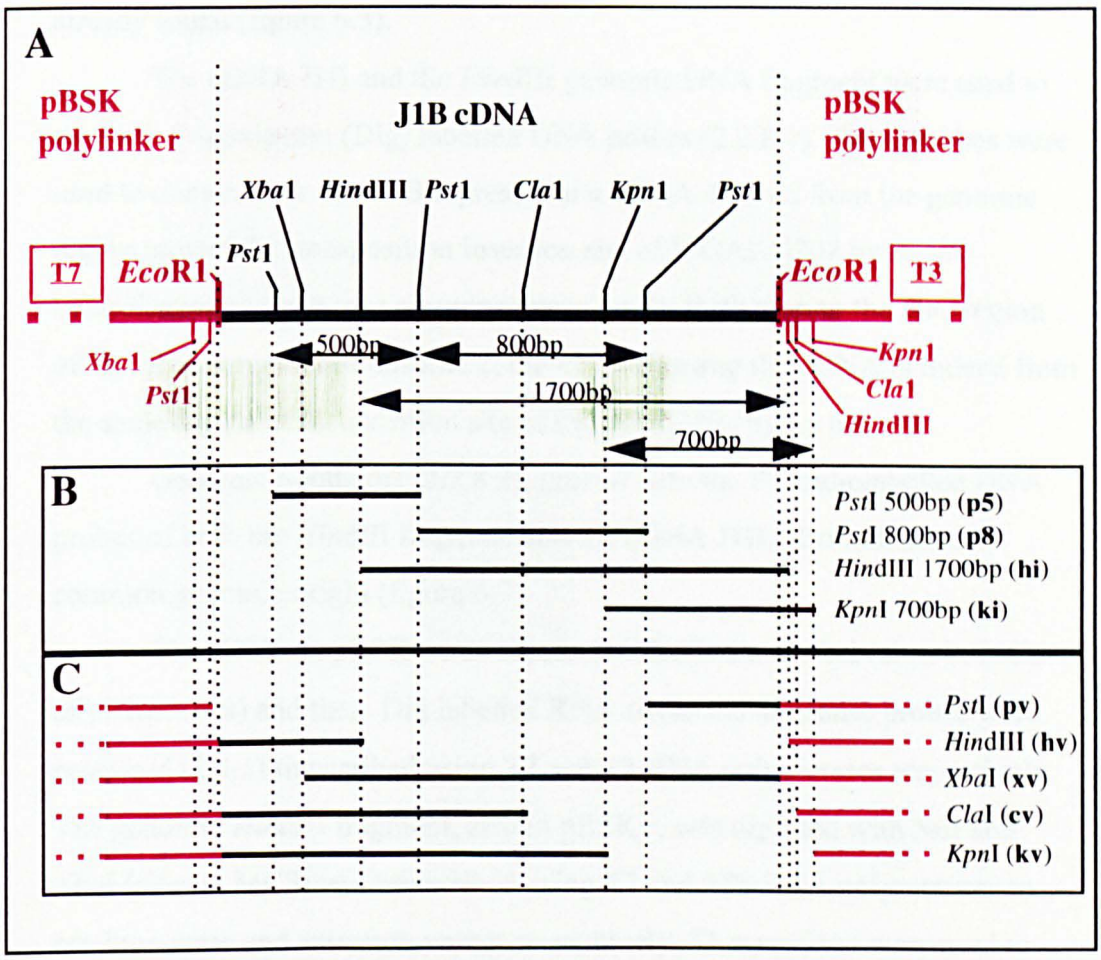

Figure 6.4: Restriction mapping of J1B allowed a fragment subcloning strategy for sequencing.

A: The restriction map of J1B, illustrating the major enzyme sites within the cDNA and orientation within the vector pBluescript (SK+). Plasmid DNA was prepared (see section 2.2.1.3), digested (2.2.2) and size separated on an agarose gel (2.2.3). The resulting fragments were then used to reconstruct a map of the cDNA J1B.

B: Fragments digested from the cDNA and subsequently cloned into pBluescript (2.2.10). These were then sequenced using T3 and/or T7primers.

C: Fragments of cDNA still attached to vector after digestion with different enzymes were religated and sequenced using T3 and/or T7 primers.

Vector sequences are highlighted in red and cDNA insert is in black. The names of the constructs in **B** & **C** are shown in brackets (bold text - e.g. **hv**). These constructs were used to produce a sequence framework subsequently completed by designing primers to fill any gaps (see figure 6.5).

primers (2.2.11.1) that spanned the gaps between the 4 regions of sequence already found (figure 6.5).

The cDNA J1B and the *Hin*dIII genomic DNA fragment were used to produce Digoxigenin (Dig) labelled DNA probes (2.2.8.1). These probes were used to demonstrate that J1B represented a cDNA derived from the genomic region around the transposition insertion site of P[GAL4]307 by *in situ* hybridisations to polytene chromosomes (2.4.2). Both map to the 50C region of the right arm on chromosome 2, thereby indicating the cDNA is indeed from the same region as the insertion site of P[GAL4]307 (figure 6.6).

Genomic Southerns (2.2.8.2), probed with the P^{32} radiolabelled DNA probes of both the *Hin*dIII fragment and the cDNA J1B, also indicated a common genomic origin (figure 6.7).

The cDNA in pBSK+ was digested with *Xho*I and *Not*I (sites in MCS of pBluescript) and then Dig labelled RNA sense and antisense probes were produced (2.4.1) transcribed using T7 and T3 RNA polymerases respectively. The genomic *Hin*dIII fragment, also in pBSK+, was digested with *Sst*I and *Xba*I (sites in MCS) and transcribed using T7 and SP6 RNA polymerases to produce sense and antisense probes respectively. These probes were used to perform *in situs* to embryos ranging in age from 1 to 16 hours revealing the expression pattern is the same with both probes (figure 6.8). This pattern is neural.

6.3.2 cDNA J2B.

cDNA J2B was digested with a variety of restriction enzymes in order to produce a map of the clone (figure 6.9). The ends of the cDNA were then automatically sequenced priming from the T3 and T7 primer sites in the pBSK+ polylinker. Both these analyses revealed that J2B is a shorter length of the same cDNA as J1B (figure 6.9). As this was not a novel clone there was no subsequent analysis of J2B.

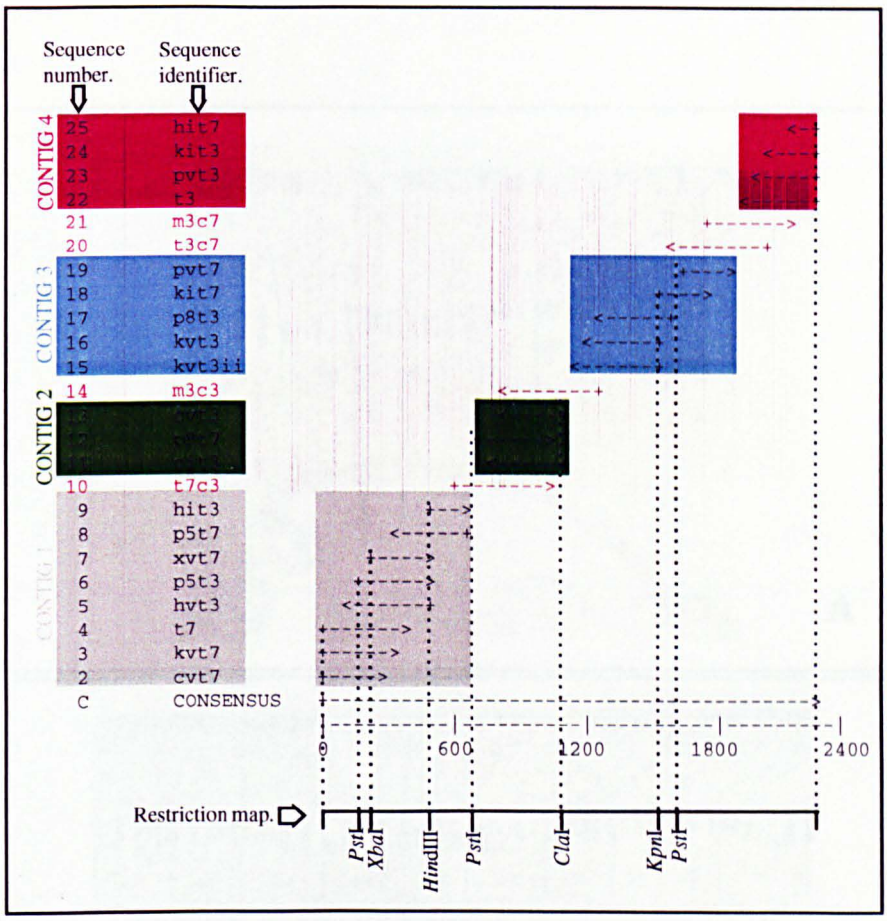

Figure 6.5: The sequencing scheme for cDNA J1B.

The fragments sequenced were produced as described (figure 6.4) and sequenced (as described in section 2.2.13.2) using T3 &/or T7 primers (found either side of the multiple cloning site of pBluescript SK+). Four contiguous fragments were assembled from this sequencing (Contigs 1-4). The component sequences are shown, boxed (grey for contig 1, green for contig 2, blue for contig 3 and red for contig 4). Directions of individual sequences and their extent of overlap are discernable by examining the arrows in the row corresponding to the identifier. Gaps between the four contigs were sequenced by designing primers to the sequenced ends of the contigs and using these to prime from the full length J1B (resulting sequence is shown in red, as are the identifiers and numbers). This lead to the production of single stranded sequence along whole length of the cDNA. Sequences were all aligned using the WISCONSIN PACKAGE (Version 8.1-UNIX, August 1995) from the Genetics Computer Group, Inc., using the Gelstart, Gelenter, Gelmerge, and Gelassemble programs with default settings.

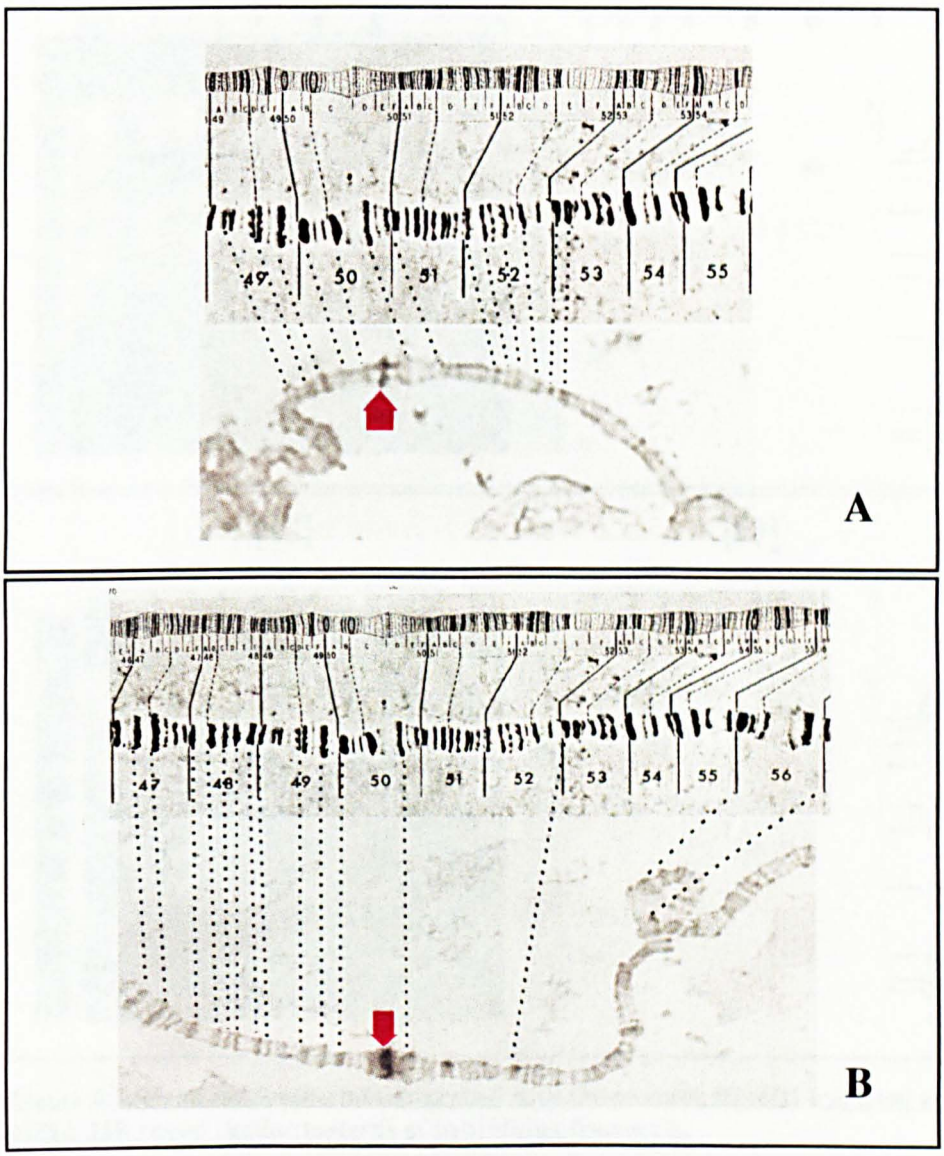

Figure 6.6: Mapping of the cDNA J1B to polytene chromosomes by *in situ*.

A: A polytene chromosome probed with a Dig labelled J1B DNA probe (for method see section 2.4.2). The location of hybridisation was revealed by the signal at a single genomic location at 50C on the right arm of the second chromosome.

B: A polytene chromosome probed with a Dig labelled *Hin*dIII DNA probe (probe made from plasmid rescued DNA). The signal was also only at 50C on the right arm of the second chromosome. The P-element had previously been mapped to this location (see section 6.1).

Therefore the cDNA J1B maps to the same genomic location as the P-element insertion. The lower image in both **A** & **B** is the preparation probed with a Dig probe, whilst the map above is a composite image used for mapping (Linsley & Zimm, 1992). Arrows indicate the signal from the Dig probes.

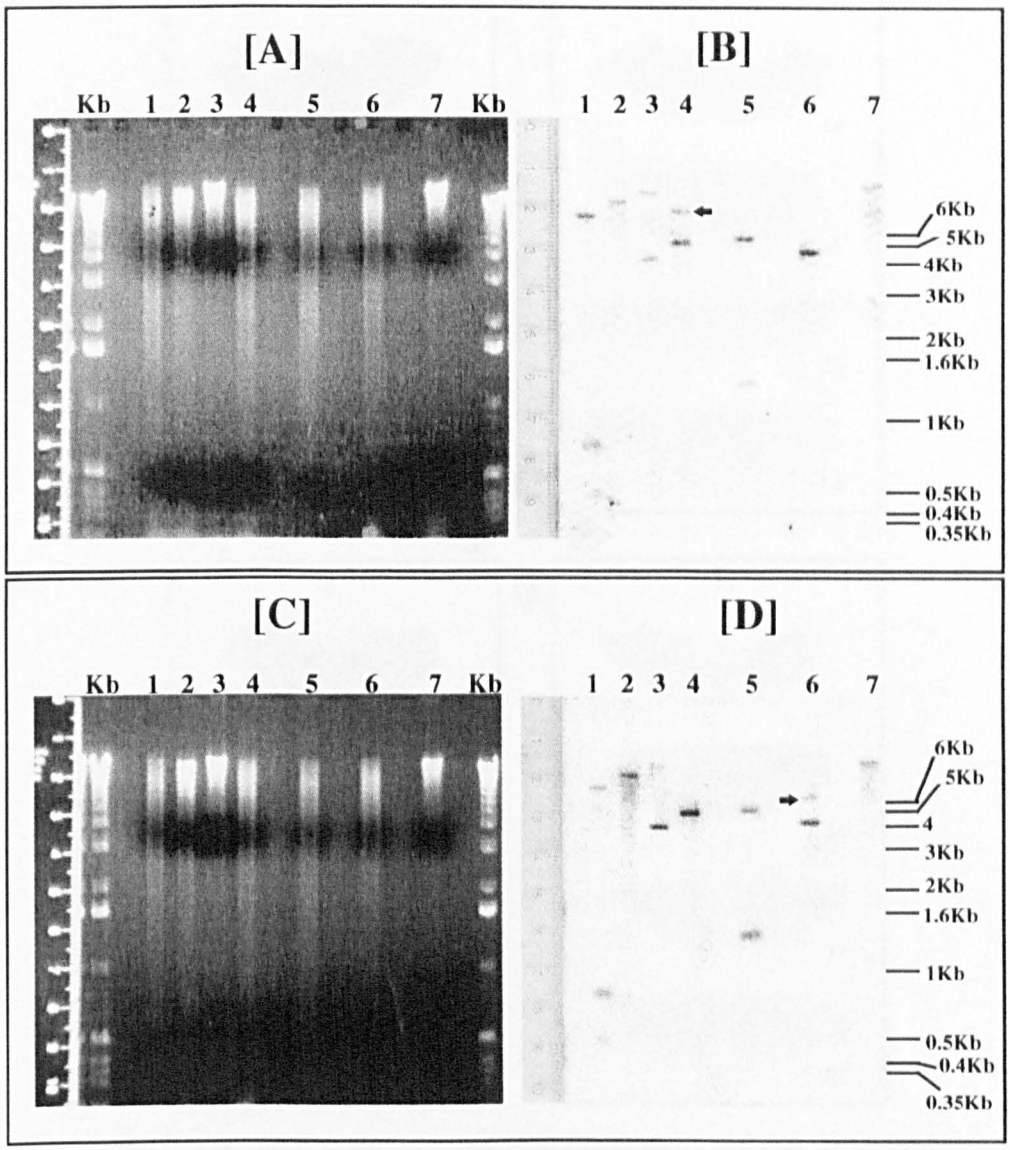

Figure 6.7: Genomic Southern blots probed with the genomic *Hin*dIII fragment and cDNA J1B reveal similar patterns of hybridising fragments.

[A] & **[C]**: Agarose gels of genomic DNA digested with restriction enzymes.
Genomic DNA was extracted (see section 2.2.1.1),digested (2.2.2) and size fractionated on an agarose gel (2.2.3). The restriction enzymes used were:
Lane 1 = *Pst*I, 2 = *Xho*I, 3 = *Kpn*I, 4 = *Eco*RI, 5 = *Cla*I, 6 = *Hin*dIII and 7 = *Sma*I.
Kb = kilobase ladder. The even smear indicates a full digestion.

[B] & **[D]**: Southern blots of the agarose gels **[A]** & **[C]** hybridised with radioactive probes.
The DNA from the agarose gels was transferred to nylon membrane (2.2.4), hybridised with a radiolabelled probe (produced as described in 2.2.5.1.1) and detected (2.2.6). The blot **[B]** was hybridised with a probe produced from the genomic *Hin*dIII fragment, whilst **[D]** was hybridised with J1B cDNA probe. Approximate sizes of the fragments are indicated by the ladder (on right of the blot).
Both probes hybridised to genomic DNA fragments of the same sizes (exceptions indicated by black arrows). This suggests a common genomic origin for both fragments used as probes.

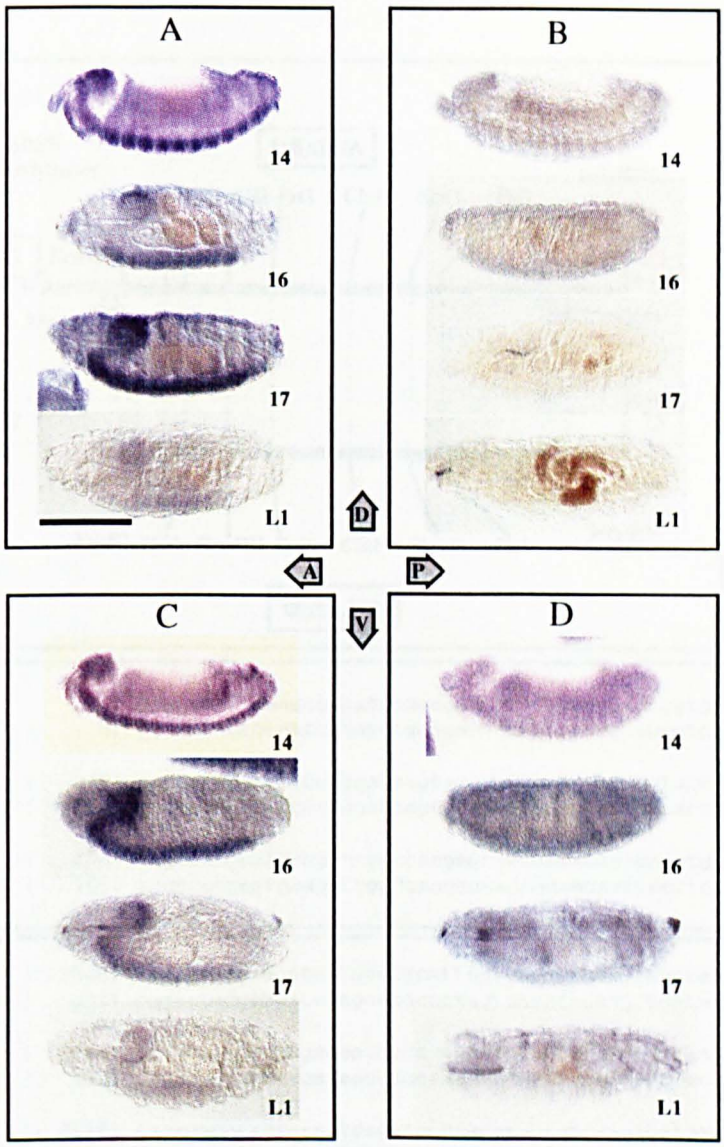

Figure 6.8: *In situs* to embryos reveal both the genomic and J1B cDNA probe hybridise within the nervous system.

*Hind*III genomic fragment (**A** & **B**) and the cDNA J1B (**C** & **D**) derived probes were produced specifically in the manner described in section 6.3.1 using the method described in 2.4.1. The *in situs* were carried out as described in section 2.4.3 using essentially wild type flies (White Canton Specials).
A & **C**: Embryos incubated with antisense Dig labelled RNA probes.
B & **D**: Embryos incubated with sense Dig labelled RNA probes.

The sense strand probes indicate non-specific probe hybridisation, whilst the antisense probes hybridise specifically in regions where a transcript related to the probe is expressed. The expression pattern revealed by these *in situs*, is the same for both genomic and cDNA probes. Expression is pan-neural, first distinguishable at stage 14, peaking at stage 16 and decreasing into first instar larvae. The coincidence of both expression patterns was more evidence that the cDNA was derived from the genomic fragment and that only one gene is contained in this region (or more than one but with coincident neural expression).

The anterior, posterior, dorsal and ventral are labelled in the centre of the page (see grey arrows labelled with A,P,D,V). Scale bar = 200µm. Lateral view of embryos.

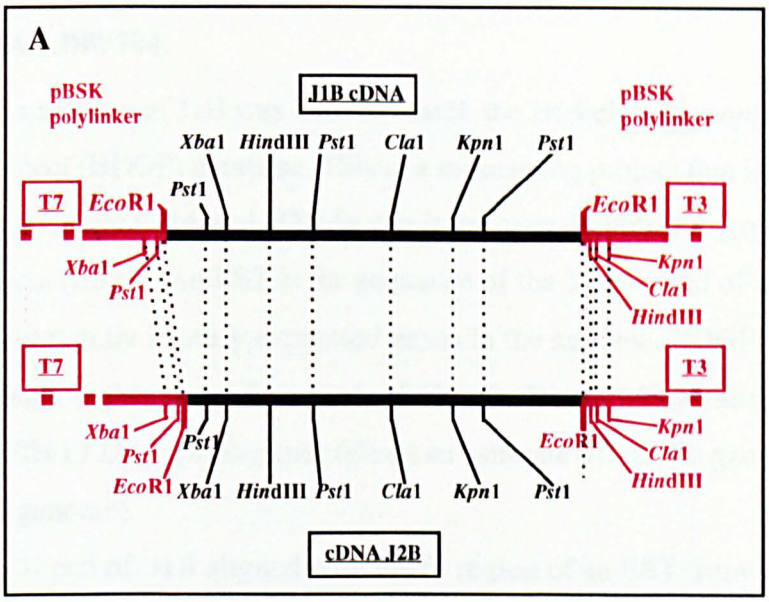

B

```
J1B     (   96) gcaatcattcccactgcagctggagaacggacagaccgtatggtgcaccg
J2B 5'  (    5) gcaatcattcccactgcagctggagaacggacagaccgtanagtgcaccg

J1B     (  146) tggccaagtacttcctggacaagtaccgcatgaagttgcgctacccgcac
J2B 5'  (   55) tggccaagtacttcctggacaagtaccgcatgaagttgcgctacccgcac

J1B     (  196) ttgccctgcctgcaggttggccaagagcacaagcacacttacctgcctct
J2B 5'  (  105) ttgccctgcctgcaggttggccaagagcacaagcacacttacctgcctct
```

C

```
J1B     ( 2048) cagaatacgaagatcttgcatgcattagttacgtacacgtacatatatag
J2B 3'  (  191) cagaatacgaagatcttgcatgcattagttacgtacacgtacatatatag

J1B     ( 2098) taagcagagtaatgaaaatcccacaaaaaccatccacacactcantcatc
J2B 3'  (  141) taagcagagtaatgaaaatcccacaaacaccatccacacactcactcatc

J1B     ( 2148) cacacacacaca--aatcagatagccacacagtgagaaatgataactaat
J2B 3'  (   91) cacacacacacacaaatcagatagccacacagtgagaaatgataactaat

J1B     ( 2196) cgaatgtcaggcacaagtttgcgaaatcaaagaaatgtgag
J2B 3'  (   41) cgaatgtcaggcacaagtttacgaaatcaaagaaatgtgag
```

Figure 6.9: Alignment of the restriction map and sequenced ends of cDNA J2B reveal it to be a short version of J1B.

A: The alignment of the restriction maps of cDNAs J1B and J2B. The cDNAs were prepared (as described in section 2.2.1.3), digested with restriction enzymes (2.2.2) and size separated on an agarose gel (2.2.3). The pattern of sites of restriction enzyme action were then ascertained and used to make maps of the cDNAs. These suggest both cDNAs are the same, J2B appears to be shorter than J1B.

B: 5' alignment of the sequence of J1B and the sequenced 5'end of J2B show that the two cDNAs align. J1B extends further 5' than J2B. The sequenced 5' end of J2B constitutes 450bp of sequence, all of which aligns with J1B.

C: 3' alignment of the sequence of J1B and the sequenced 3'end of J2B show that the two cDNAs align and extend the same length. The sequenced 3' end of J2B amounts to around 400bp of sequence, all of which aligns with J1B.

6.3.3 cDNA LD09704.

The sequence of J1B was used to search the Berkeley *Drosophila* Genome Project (BDGP) database. This is a sequencing project that is sequencing genomic DNA and cDNAs. On it are over 40,000 end sequence tagged cDNAs (ESTs). An EST is the sequence of the 5' or 3' end of a cDNA that is used to rapidly identify expressed genes in the genome. BDGP estimate that obtaining a sequence tag from each of 40,000 cDNAs will identify cDNAs from over 70% of *Drosophila* genes (given an estimate of 12,000 genes in the *Drosophila* genome).

The 3' end of J1B aligned with the 5' region of an EST from BDGP, designated LD09704. The LD library was derived from embryonic tissue (0-22 hours of age) with the RNA polyA selected twice. The cDNA was synthesised using oligo(dT) primers with *Xho*I site at end of the primer and an *Eco*RI adapter on the 5' ends of clones. The cDNAs were then size fractionated and directionally cloned into *Eco*RI/*Xho*I-digested Stratagene Uni-Zap XR vector, which allowed excision and recircularisation of pBSK- plasmid containing the cDNA clone (more details are available through their web site http://www.fruitfly.org/). The cDNA was ordered through a distribution company Genome Systems Incorporated (details found at the web site - http://www.genomesystems.com/gpages/flycdna.html). The clone was supplied in a bacterial stab which was isolated by streaking onto LB agar plate containing ampicillin (2.2.10.3). The colonies subsequently growing were grown up and large scale plasmid DNA preparation ensued (2.2.1.3).

LD09704 was restriction digested and the fragments were size fractionated by electrophoresis on a gel. The gel showed 3 fragments were present that did not correspond to vector, these were 1.1Kb, 900 bp and 600bp, giving the length of the cDNA as 2.6Kb. The gel was then Southern blotted and probed with a Dig labelled DNA probe of the genomic *Hin*dIII fragment.

A replicate blot was probed with a Dig labelled DNA probe made from J1B. Hybridisation with these probes revealed that the cDNA was from the genomic region within the *Hin*dIII fragment and overlapped with J1B (figure 6.10).

Having ascertained LD09704 did indeed originate from the genomic region around the P[GAL4]307 insert, the cDNA was sequenced using a mixture of new primers and those used to sequence the 3' end of J1B. This sequencing produced 2.6Kb of contiguous sequence running to a polyA tail at the 3' and appears to largely consist of untranslated region (UTR) - figure 6.11.

6.4 LD09704 & J1B constitute a single contig.

Aligning J1B and LD09704 creates a contig of 3.6 Kb (figure 6.12). A northern blot using embryonic total RNA (2.3) and probed with a radiolabelled *Hin*dIII fragment, indicates the gene has at least 3 different transcripts of more than 5Kb (approximately 5Kb, 6Kb and >9.5Kb - see figure 6.13). The 5' end of the gene has not yet been cloned, nor has a full-length cDNA.

PCR screening of other positives from the initial library screen has been undertaken. This was achieved by designing primers to the phage λgt11 arms (gt11F and gt11R) and to the most 5' end of the cDNA currently isolated (PKout1). As the orientation of the insert in the phage arms was not known both sets of phage primers had to be used individually with the 5' primer. Of the 42 phage plaques stored in the fridge in SM from all three rounds of library screening only 2, using primers gt11F and PKout1 for PCR, gave products of a size indicating more 5' sequence (figure 6.14). The larger of these was then gel extracted, subcloned into pGEM-T vector (Promega), transformed and small scale plasmid preparations followed. Automatic sequencing yielded new sequence which was then aligned with the rest of the 3.6Kb contig, producing a new contig of approximately 4Kb in length (figure 6.15).

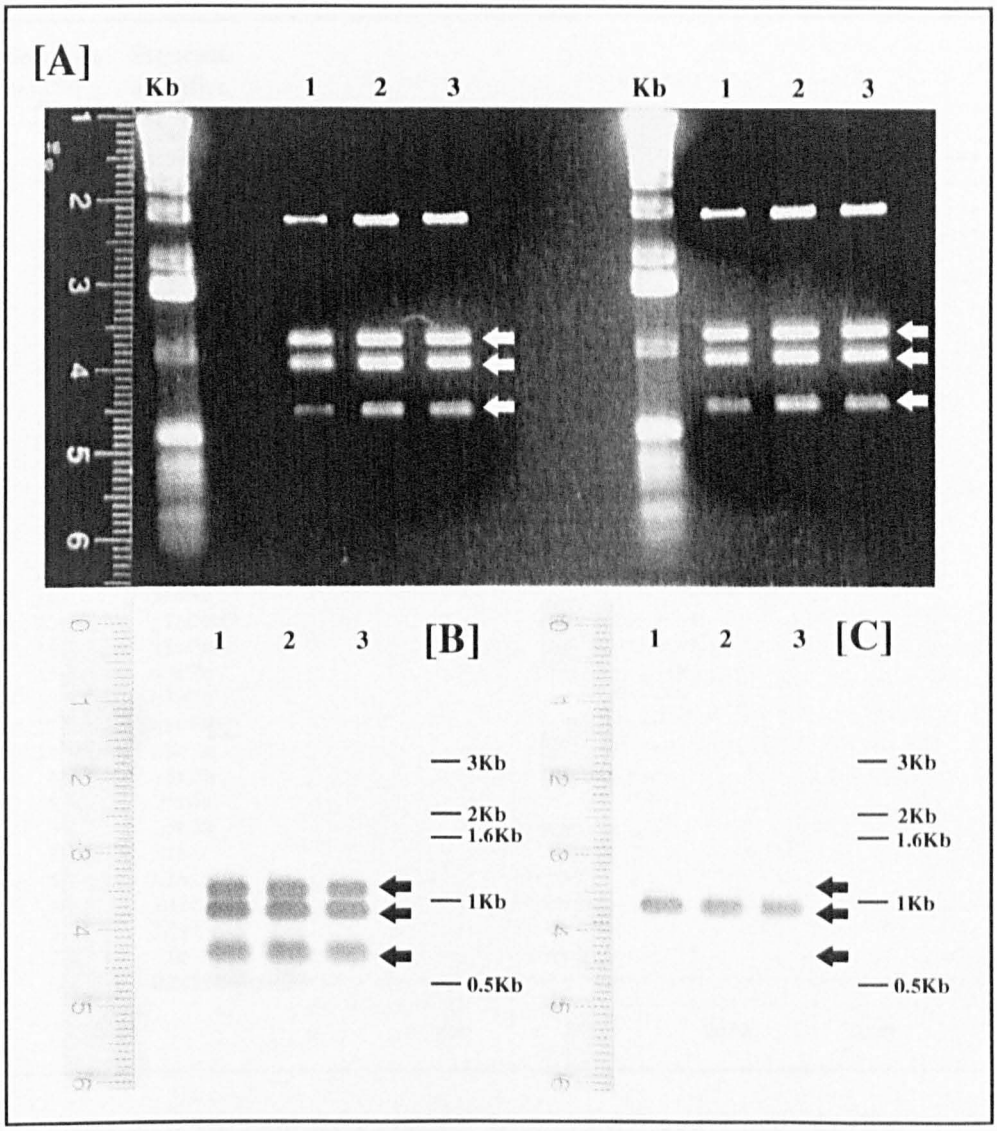

Figure 6.10: Restriction digestion of cDNA LD09704 with *Eco*R1 and *Xho*I yields 3 insert fragments which map to the region around P[GAL4]307.

[A]: A restriction digest (see method 2.2.2) of the cDNA clone LD09704 size separated on an agarose gel (2.2.3). All 3 lanes are the cDNA cut with *Eco*RI and *Xho*I, all were mini-prepped (2.2.1.2.2) from independent colonies. The cDNA insert was digested into 3 fragments (white arrows) of 1.1Kb, 900bp and 600bp, totalling 2.6Kb.

[B] & **[C]**: Southern blots of gel **[A]** (2.2.4).
[B] was hybridised with a radiolabelled DNA probe (2.2.5.1.1) produced from the genomic *Hin*dIII fragment. All the insert fragments hybridised to the probe indicating that LD09704 is located within the *Hin*dIII genomic region.
[C] was hybridised with a radiolabelled probe made from the cDNA J1B. The hybridisation is limited to the 900bp fragment indicating that there is a region of overlap between the cDNAs J1B and LD09704.

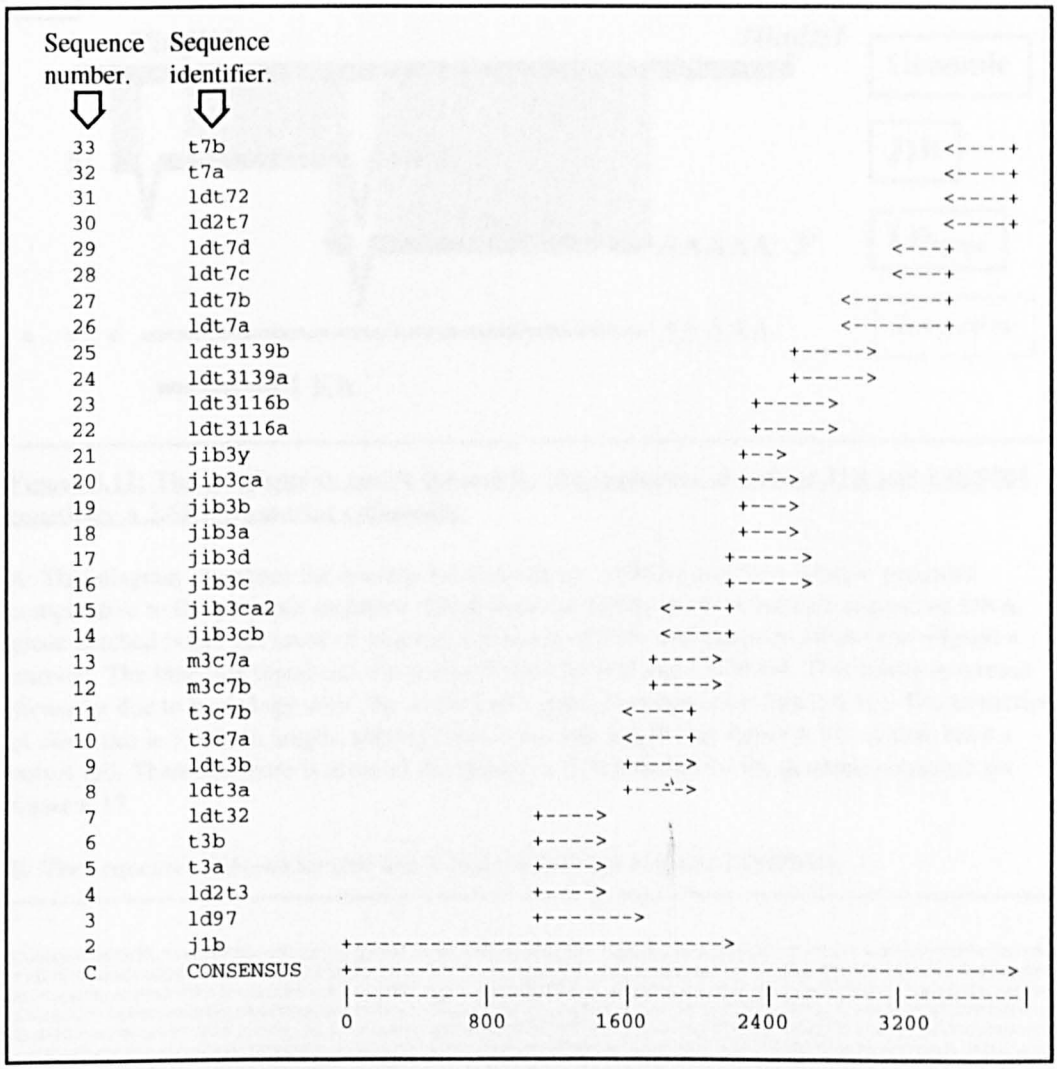

Figure 6.11: The contiguous sequence formed by cDNAs J1B and LD09704.

For details of J1B sequencing see figures 6.4 and 6.5.
Automatic sequencing (as described in section 2.2.13.2) of LD09704 using primers designed sequentially to the newly sequenced ends of fragments obtained from the previous set of primers (see appendix 10.5 for details). This sequencing was initiated using T3 and T7 primers (as the clone is in pBSK). Sequences were obtained and confirmed by using the same primer more than once (see sequence identifiers suffixed with a or b). The exceptions to this are J1B sequence (see above), and the sequence identified as LD97 which is the EST sequence of cDNA LD 09704 from the Berkeley *Drosophila* Genome Project (the source of the clone).
The component sequences are shown with directions of individual sequences and their extent of overlap discernable by examining the arrows in the row corresponding to the identifier.
Sequences were all aligned using the WISCONSIN PACKAGE (Version 8.1-UNIX, August 1995) from the Genetics Computer Group, Inc., using the Gelstart, Gelenter, Gelmerge, and Gelassemble programs with default settings. The length of sequence entered into these packages was discerned by aligning multiple sequences obtained from a single primer, using the Align Plus programme (Scientific and Educational software, Version 3). This lead to the production of single stranded sequence along whole length of the cDNA.

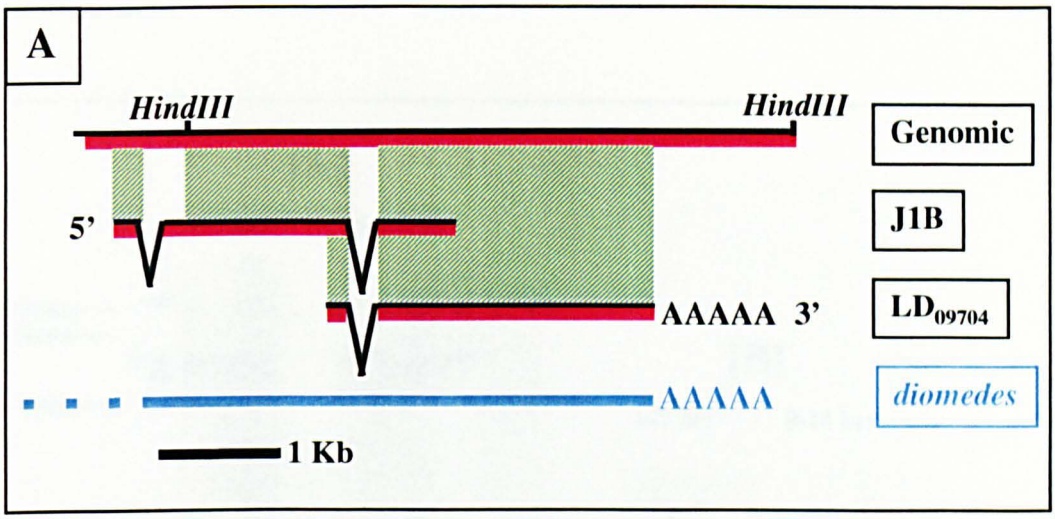

Figure 6.12: The overlapping contig formed by the sequences of cDNAs J1B and LD09704 constitute a 3.6Kb transcript - *diomedes*.

A: This diagram illustrates the overlap between the two cDNAs and their relative positions comparative to the genomic sequence. Black lines are DNA, red bars indicate sequenced DNA, green hatched boxes are areas of alignment between cDNAs and genomic DNA (non aligned = introns). The blue line represents the contig formed by J1B and LD09704. This contig is termed *diomedes* due to homology with the *Arabidopsis* gene *argonaute* (see figure 6.16). The transcript of *diomedes* is 3.6Kb in length, although this is not full length (see figure 6.13), it does have a polyA tail. Therefore there is more of the transcript 5'.For details of the genomic sequence see figure 6.17.

B: The sequence of *diomedes* (red text = overlap between J1B and LD09704).

CCGGAGATCAAGGGTCTCAAGATCGAGATCACCCACTGCGGCCAGATGCGTCGCAAGTATCGTGTGTGCAACGTCACTCGCCGCCCCGCTCAGATGCAATCATTCCCACT
GCAGCTGGAGAACGGACAGACCGTATGGTGCACCGTGGCCAAGTACTTCCTGGACAAGTACCGCATGAAGTTGCGCTACCCGCACTTGCCCTGCCTGCAGGTTGGCCAAG
AGCACAAGCACACTTACCTGCCTCTAGAGGTGTGCAACATTGTGGCCGGACAGCGGTGCATTAAAAAGCTGACCGATATGCAGACGTCNACCATGATCAAGGCCACAGCT
CGTTCAGCTCCGGATCGTGAGCGTGAGATTAACAATTTGGTAAAGCGCGCCGACTTCAACAACGATTCTTATGTGCAAGAGTTTGGCCTGACCATCTCCAATTCGATGAT
GGAGGTACGAGGACGCGTCTTGCCTCCTCCCAAGCTTCAGTATGGGGGAGGTGTGTCTACCGGCCTCACCGGCCAGCAGCTGTTCCCGCCACAGAACAAGGTGAGCTTGG
CCTCGCCCAACCAGGGTGTTTGGGATATGCGCGGCAAGCAGTTCTTCACTGGCGTCGAGATCCGCATCTGGGCCATCGCCTGTTTTGCCCCACAGCGCACGGTGCGCGAG
GATGCGCTGCGTAATTTCACCCAGCAGCTGCAGAAGATCTCAAACGATGCAGGCATGCCGATAATTGGACAGCCGTGCTTCTGTAAGTACGCCACCGGGCCGGATCAAGT
GGAACCCATGTTCCGTTACNTGAAGATCACNTTCCCCGGCCTGCAGNTNGTCGTGGTTGTGCTGCCCGGCAAGACTCCAGTGTACGCCGAGGTGAAGCGTGTAGGTGACA
CCGTTCTGGGTATGGCCACACAGTGTGTACAGGCCAAGAACGTGAACAAGACATCGCCACAGACGCTCTCTAATCTGTGTCTGAAGATCAACGTCAAGTTGGGCGGCATC
AATTCAATTCTGGTCCCCTCCATTCGGCCAAAGGTCTTCAATGAGCCGGTCATCTTTTTGGGTGCCGATGTGACACACCCACCAGCTGGCGACAACAAGAAACCATCGAT
TGCCGCCGTCGTGGGCTCCATGGATGCCCATCCATCGCGGTATGCCGCCACCGTTCGCGTACAGCAGCACCGACAGGAGATCATCCAGGAGCTGAGCAGCATGGTGCGCG
AGCTGTTGATCATGTTCTACAAGTCGACGGGCGGCTACAAGCCCCACCGCATCATACTCTATCGTGACGGAGTCTCCGAGGGACAATTCCCACATGTCCTGCAACACGAA
TTGACCGCCATTCGCGAGGCCTGCATTAAGCTAAAACCANAGTATCGGNCGGGCATCACATTCATTGTGGTGCAGAAGCGCCATCACACTCGACTCTTCTGCGCGGANAA
NAAGGAGCAGAACGGCAAATCGGGCAATATTCCCNCNGGCNCCACCGTCCGATGTTGGCATCNCCCATCCCCCGAATTTGATTTCTATCTNTGCAGCCATCAGGGCATCC
AGGGNACCAGTCGCCCCTCGCACTACCACGTTCTGTGGGACGACAATCACTTTGACTCGGACGAGCTGCAGTGCCTCACGTATCAGCTATGNCATACGTACGTGCGCTGN
ACCCGATCCGTCAGTATACCGGCGCCAGCCTACTACGCCCATTTAGTGGCCTTCCGTGCCAGATATCATCTGGTGGAGAAGGAGCACGATTCGGGCGAGGGTTCGCACCA
GAGCGGCTGCTCAGAGGATCGTACGCCAGGTGCCATGGCCAGGGCCATCACTGTGCACGCGGATACCAAGAAGGTCATGTACTTTGCCTAAAAAGTATCGCCCCTCCCCA
ATACCAACACCAAAAAGCTAAAGAATACAAAATCAGTTTCGAATTTCGATTCGAATAAGCAACTCCCCACTTCCTTCCCTCAAATCAGAAAGCGGAAAGCGGATGAAAGC
CAAGCATAGAAGTTTAGAATTAAGTTACGTTTTACGTTGAGAGAGCGCGGATGGGTGGAAAAACCAATCAGAATACGAAGATCTTGCATGCATTAGTTACGTACACGTAC
ATATATAGTAAGCAGAGTAATGAAAATCCCACAAACACCATCCACACACTCACTCATCCACACACACAAATCAGATAGCCACACAGTGAGAAATGATAACTAATCGAA
TGTCAGGCACAAGTTTGCGAATTCAAAGAATGTGAGANTTCTCAAAAACAAGCGTAGCAAACAAATTGAAAGCAAATAGGAAATCAACTANAGGGAACAAAAACTACGAC
AGCAACACCAACCAACACCAGAAAAACAAAACAAATTAAAACATAACCAAAATGGAAGTGAAATTACGTGAAAAGCGAGCGTCATCAGCACGAGAGAGAGAGACAAGTTT
TGTAATANAAATTACGATTAAATTGTACAATATATTTTTTACACGATACGAAATGAAGACATGATGAATGATAATGAATGCATACNACCNAAGGTTTTTTAGTATACN
AAATGAATACGTTGCTGATCGACTCACACAGCAAACACCACATGAACACCAACCACTCGGATTCTCTGTACTGTGAACGAAGACCACCACCCNAATATAAACCAAAACCA
CAAGCGACATTAAAGCGACAAGCATTGAAAGAGTGTGTTAGACACAACTTAGCATGTNCTAATGAATTACTTCAATACTTCAACTAGGGCGCTGACAAAACCAAGCNAGA
ACATTTAATAGTTTGTAAGTTGGGCTCTACCAAAAACCGAACNCCNNATGAGAGAGAGAGAGAGAGAAAAATGCCCGCCNGGCCNGATNAGTTAAGTGGGCAATGAAT
AACGAGAACTGCCATTTCAACAAGGGACAAACTTTTGGTCAAAACAATAGCTANACTTATAGNGCAGNCCCTAANATANACANACATAATTNGAATTCTAAAANTAAAAA
TTTAAAGTTTTTTACGGAAANGATAACCCAGNGGGAGGGGCTGTNGTAAACAAGGTGGATAAATTAAAATTCAAAGGGGCAAATAACACGGNAGCAGAACACGTAAACGTG
GGCNGGGCGGANATTAAANGTTANNCGTNAGNAAACCTTTTNTNNGGGCACCACACCACCACACAATCNGATTCCGAATTTCTTCAACCTTCCTGGAGTCCAAGGCATAT
CANTCAATGTCTTCTTATTAAGGAACCTCCAACAATAAGCCTTATGATATATTTAGTGGTACCTTATATATATATATATATTTTTTAAAACGAATGCCTAACGAAATT
TGTTGATTTCTTCATGTTGATGCTTCGAATTGGCTTCTTCGCTGCTTTTCGTTGTAATAATTTCGTATTAATTAACTTTAGATCAAAGTGGTGTACGGGTAATAATAAAC
AAGGTAATTGTTCTCCACCGTCNNCCGGAGGGAGGTGGCAACAACATTTCAATATTTAACAAAGTAGTTTTAGTTTCGCCAAAATCAACAAGCAAACAAACAATATCAAT
ATCAATATGAAACGTATGCTTAGTAATTGTACTATATNGAGGACACAGTTCAAGTTAACATTATAATGAGTTGTTATTTATGCGGCGCGGGCGACGACGTTNTATCCACT
CGGAATCGCCCGGGCCAAACCTAATTTATAATTGTATACATCCTTNTTCACAGAACCTTTAATTTAGATTTAGTTTCCAAGTTTGCAAGCTGTTTTGCCAATCGTACATT
ATGTGAGCATTATAAAATACATAATATATATAAATTTAAAAAAAAAAAAAAAAAA

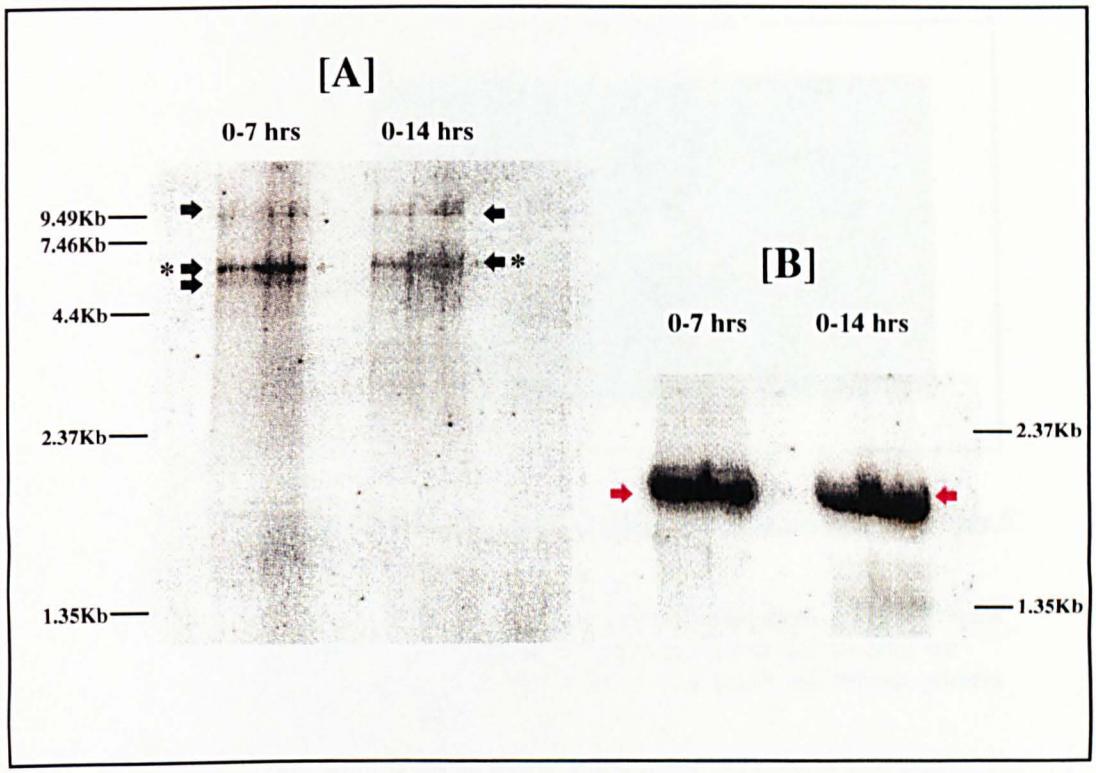

Figure 6.13: A northern blot probed with the *Hin*dIII fragment reveals 3 transcripts.

[A] & **[B]** are northern blots of total RNA samples extracted from embryonic samples (0-7hours and 0-14 hours old).

[A]: After extraction (see section 2.3.1.1), the RNA was size fractionated on a gel (2.3.2), transferred to a nylon membrane (2.3.3) and a *Hin*dIII genomic probe (produced as described in 2.3.3.2) was hybridised to the membrane (2.3.4). The resultant hybridisation reveals there are 3 transcripts detectable in the 0-7 hour old embryo sample, whilst only 2 are clearly visible in the 0-14 hour old sample (black arrows). The major transcript (the strongest signal from hybridisation) is the middle one (marked on the blot by an arrowhead with an asterisk next to it). The size of the fragments detected was ascertained by a marker lane run on the gel, blotted and subsequently stained (2.3.3.1). The size of the fragments, based on the markers are approximately 5Kb, 6Kb and >9.5Kb. The major transcript appears to be 6Kb.

[B]: The initial probe was stripped from the blot (2.3.5), before a new control probe was made (2.3.3.2). The control probe was used to ascertain the equality of loading between lanes of the gel. In this case the probe was to the housekeeping gene *EF1-α*. This has a 2Kb transcript which is clearly visible (labelled with arrows) in both samples. The loading is roughly equal with a slightly higher amount visible in the 0-7 hour sample. This may explain the inability to detect the smallest transcript in the 0-14 hour sample probed with *Hin*dIII. Alternatively the 5Kb transcript could be regulated developmentally, being less abundant in older embryos.

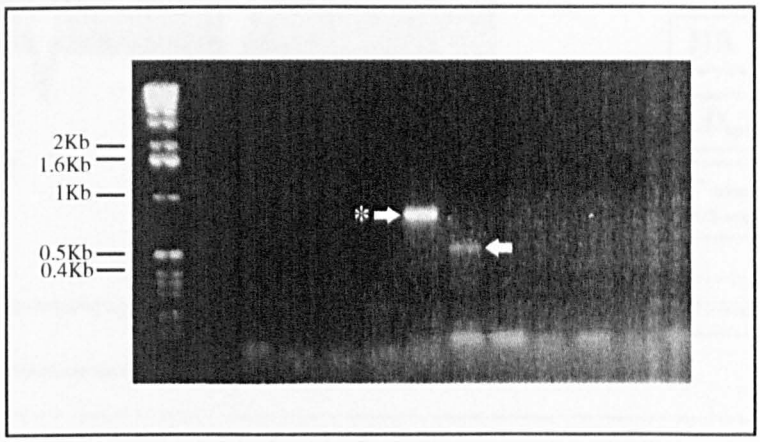

Figure 6.14: PCR screening of positive library plaques for longer 5' extensions.

A PCR approach was used (see section 6.4) to screen positive plaques from the library screen (see section 6.2). Primers and methods are described in section 2.2.11.4 and 2.2.11.5. gt11R and PKout1 primers gave the result above.

Two of the 42 plaques screened in this manner revealed more 5' sequence than had previously been identified in J1B (white arrows). The larger of these was subsequently subcloned into pGEM-T and then sequenced (arrow with asterix next to it). The 800 base pair insert corresponded to approximately 600 base pairs of novel 5' cDNA sequence (see figure 6.15).

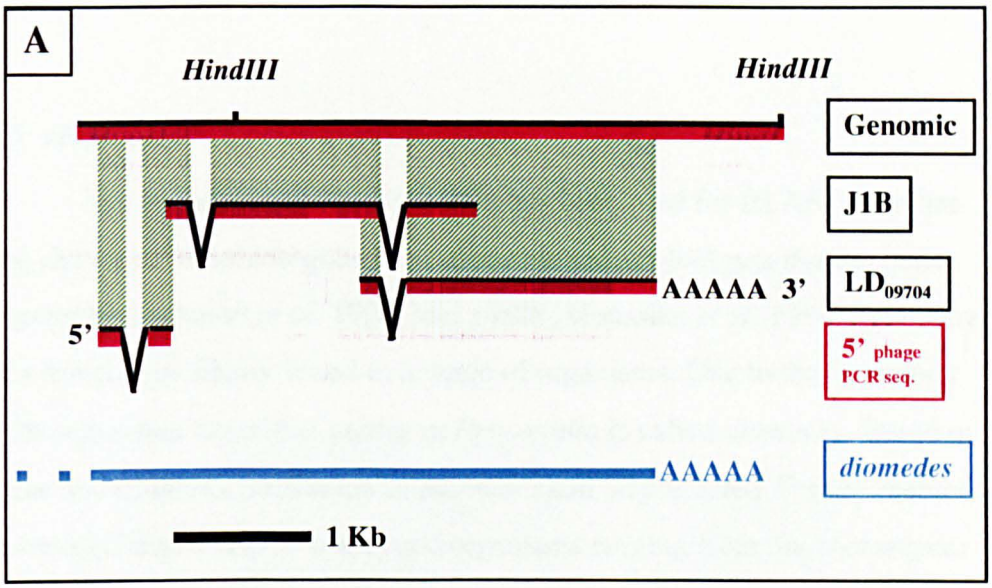

Figure 6.15: *diomedes* can be assigned more 5' cDNA sequence following PCR screening of positive library plaques.

See figure 6.14 and section 6.4 for a description of the library screen using PCR. A PCR approach was used to determine if any of the other positive phage clones from the library screening (see section 6.2) contained cDNAs that were longer 5'. The larger of the positives was subcloned into pGEM-T and sequenced.

A: The 400 base pairs of new sequence from the sequenced cDNA resulted in the transcript called *diomedes* (in blue) now totalling more than 4Kb in length. The sequence also revealed a third intron, when the cDNA was compared to the genomic (see figure 6.17 for details of the genomic sequencing). The cDNA is still incomplete 5' by more than 2Kb (for the most abundant transcript - see figure 6.13).

B: The 5' extension of the new cDNA sequence as it relates to the genomic sequence (non aligned = intron).

B

```
Genomic (   205) gagctggaggttactctacccggcgagggcaaagatcgaatctttcgcgt
PCR 5'  (     1) gagctggaggttactctacccggcgagggcaaggatcgaatgtttcgcgt

Genomic (   255) gacgatcaagtggcaggctcaggtctcgctcttcaatttggaggaagctc
PCR 5'  (    51) gacgatcaagtggcaggctcaagtctcgctcttcaatttggaggaagctc

Genomic (   305) tcgaaggccgcacgcggcagataccctatgatgccatttttggcgctcgat
PCR 5'  (   101) tcgaaggccgcacgcggcagataccctatgatgccatttttggcgctcgat

Genomic (   355) gtggtcatgcgccatctgcccagcatgacgtacacgccagtgggacgtag
PCR 5'  (   151) gtggtcatgcgccatctgcccagcatgacgtacacgccagtgggacgtag

Genomic (   405) cttcttcagttccccggagggttactaccatcccctgggtggtggacgcg
PCR 5'  (   201) cttcttcagttccccggagggttactaccatcccctgggtggtggacgcg

Genomic (   455) aggtttggttcggtttccatcagagcgtaaggccctcgcagtggaagatg
PCR 5'  (   251) aggtttggttcggtttccatcagagcgtaaggccctcgcagtggaagatg

Genomic (   505) atgctcaatatcgatggtgagttcgcaatgctctgtattatctatttgcc
PCR 5'  (   301) atgctcaatatcgatg---------------------------------

Genomic (   555) caactaatgattacaaaatcctcagtctcggccaccgctttctacaaggc
PCR 5'  (   317) -------------------------tctcggccaccgctttctacaaggc

Genomic (   605) tcaaccagtcattgacttcatgtg-cgrggtkctggacattcgcgacatc
PCR 5'  (   342) tcaaccagtcattgacttcatgtgtcgaggtgctggacattcgcgacatc

Genomic (   654) aacgagcagcgcaaaccgctcac
PCR 5'  (   392) aacgagcagcgcaaaccgctcac
```

6.5 Homology to known genes/proteins.

The sequence of this 4Kb contig has been used for BLAST searches and shown to be homologous to recently cloned *Arabidopsis thalina* genes *argonaute* (Bohmert *et al.* 1998) and *zwille* (Moussian *et al.* 1998), members of a novel gene family found in a range of organisms. Due to the homology with *argonaute* the cDNA contig in *Drosophila* is called *diomedes*. Based on these homologies a translation of *diomedes* can be predicted. Family members have only been found in eukaryotic organisms ranging from *Saccharomyces pombe* to humans. The homology between the proteins coded for by these genes is shown in the pileup in figure 6.16 (region of highest homology shown). Potential protein motifs have been screened for using MotifFinder (http://www.motif.genome.ad.jp/) on the internet, with no major motifs being detected to help categorise the protein, Diomedes.

One of the interesting alignments shown in the pileup (figure 6.16), is with the rabbit eIF2C protein (also known as Co-eIF-2A). This has been shown to play a role in the eukaryotic peptide chain initiation process (Zou *et al.* 1998). Within eukaryotes the proteins involved in this function are highly conserved, and they differ significantly from those in prokaryotes. This may explain the high degree of conservation between the peptide sequences in the pileup from single celled *S.pombe* to humans, whilst no prokaryotic peptides align.

6.6 The intron/exon structure of the genomic fragment coding for diomedes.

Sequencing of the genomic DNA has provided details of the intron exon structure of *diomedes*. Three small 60bp introns were identified when the cDNA and genomic sequences were compared (figure 6.17).

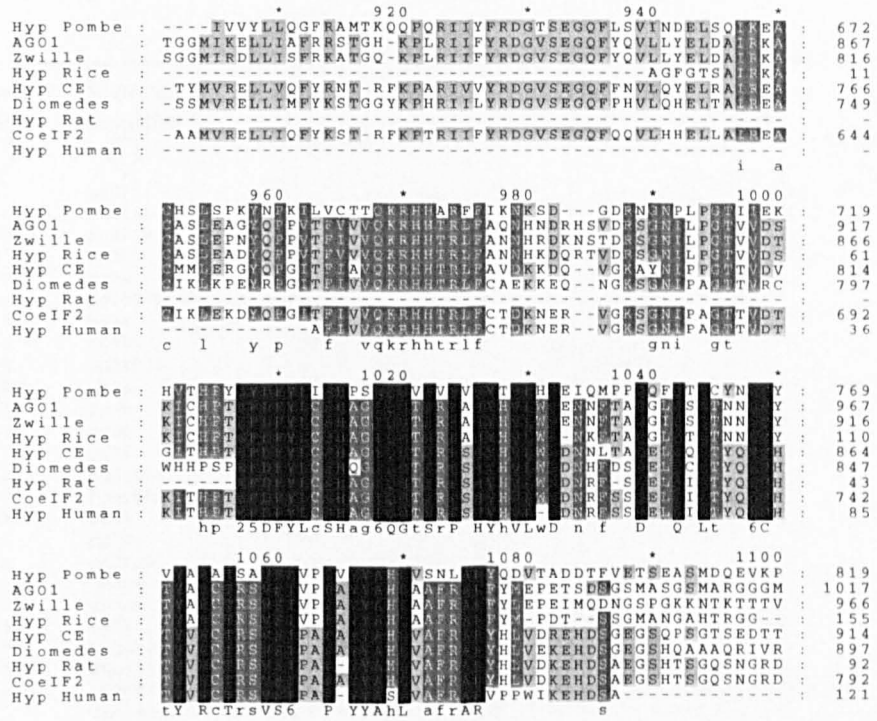

Figure 6.16: Alignment of Diomedes with amino acid sequences of proteins from a range of eukaryotic organisms.

The region shown is selected from a longer alignment (see appendix 10.6 for full alignment), and was chosen to illustrate the level of identity in a region where there is sequence for all the peptides compared.

This alignment was done on the WISCONSIN PACKAGE (Version 8.1-UNIX, August 1995) from the Genetics Computer Group, Inc., using the PileUp program with default settings. PileUp creates a multiple sequence alignment from a group of related sequences using progressive, pairwise alignments. The sequences aligned were retrieved from internet databases using a Basic Local Alignment Search Tool (BLAST). BLAST is a sequence similarity search served by GenomeNet. A BLASTP (amino acid sequence) search of SwissProt, SwissProt-upd, PIR, PRF, nr-aa and GENES databases was carried out, using default settings.

Of the sequences retrieved those above were chosen for an alignment to illustrate the conservation in amino acid sequence in eukaryotes from *Saccharomyces pombe* to humans. These sequences are:

Hyp Pombe = *S. pombe* protein, a hypothetical translational product of a cDNA from the *S.pombe* genome sequencing project. DDBJ/EMBL/GenBank accession number SPCC736.11.

AGO1 = The protein product of the *Arabidopsis thalina* gene *argonaute*.DDBJ/EMBL/GenBank accession number U91995.

Zwille = The translational product of the *zwille* gene of *Arabidopsis*.DDBJ/EMBL/GenBank accession number AJ223508.

Hyp Rice = Hypothetical protein product of a cDNA (EST) found in *Oryza sativa*.DDBJ/EMBL/GenBank accession number 2798235.

Hyp CE = Hypothetical translation of cDNA identified by the *Caenorhabditis elegans* sequencing project. DDBJ/EMBL/GenBank accession number CEF48F7.1.

Diomedes = Hypothetical translational product of the region of *diomedes* currently cloned.

Hyp Rat = Hypothetical translation of cDNA found in rat (EST).DDBJ/EMBL/GenBank accession number 977110.

CoeIF2 = Amino acid sequence of a translation initiation co-factor (CO-eIF-2A) identified in rabbit (also known as eIF2C). DDBJ/EMBL/GenBank accession number AF005355.

Hyp Human = Hypothetical translation of a cDNA found in human (EST).DDBJ/EMBL/GenBank accession number 868384.

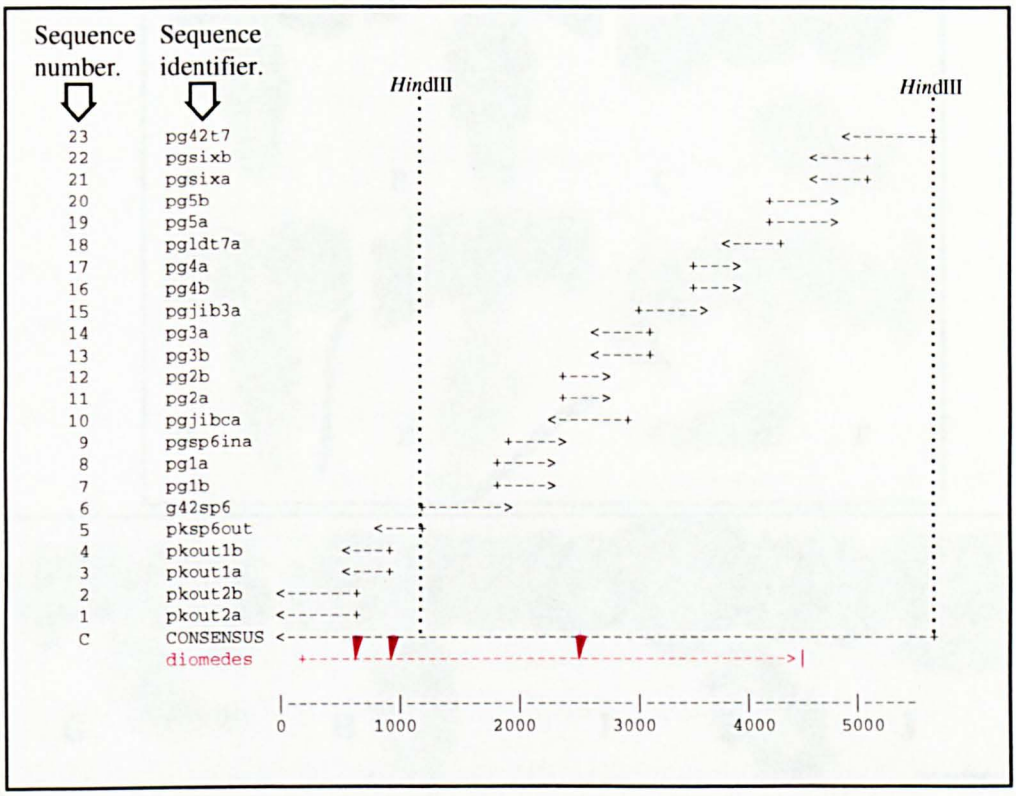

Figure 6.17: The genomic sequence of plasmid rescued DNA from around the P[GAL4]307 insert aligns with the *diomedes* transcript, revealing three introns.

The *Hin*dIII genomic fragment subcloned into pGEM-7Zf (+) (pGH4.2) was sequenced using primers. Automatic sequencing (as described in section 2.2.13.2) of pGH4.2 was carried out using primers designed sequentially to the newly sequenced ends of fragments obtained from the previous set of primers (see appendix 10.7 for details). This sequencing was initiated using SP6 and T7 primers (as the clone is in pGEM-7Zf). The sequence identifiers g42sp6, pg42t7, pgjib3a, pgjibca & pgsp6ina are contigs formed from the sequence obtained by priming using the following primers:
g42sp6 was primed with PGM3C3, PGT7C3 & SP6.
pg42t7 with PGT7IN & T7.
pgjib3a with PGLDT313, PGLDT31169 & PGJIB3.
pgjibca with PGLDT3, PGT3C7 & PGJIBC.
pgsp6ina with PGSP6IN & PGTOSP6.
The other sequences were produced by priming with primers that have the same designation as the sequence identifier (for example pg1a was primed with PGONE). For sequence falling outside of pGH4.2, the *Kpn*I plasmid rescue clone was sequenced using primers designed to sequence further 5' (pksp6out, pkout1a & b, pkout2a & b). Sequences were obtained and confirmed by using the same primer more than once (see sequence identifiers suffixed with a or b). The component sequences are shown with directions of individual sequences and their extent of overlap are discernable by examining the arrows in the row corresponding to the identifier. This lead to the production of single stranded sequence along the length of the genomic region depicted above.
Alignment of the genomic sequence with *diomedes* (composed of J1B, LD09704 and 5' sequence from positive phage clones) reveals 3 introns (red arrows), of around 60 base pairs.

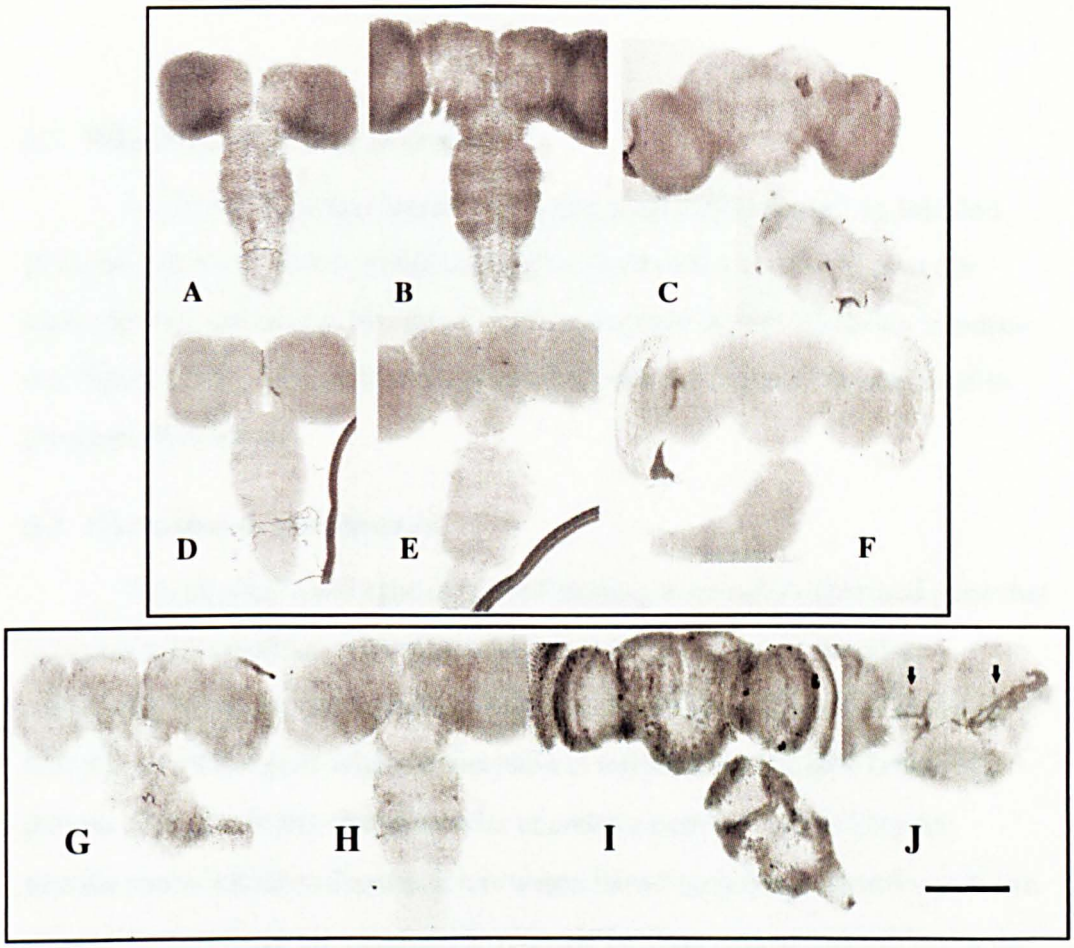

Figure 6.18: *In situs* to pupal CNSs reveal the widespread expression of *diomedes* within the CNS throughout development.

Dig labelled RNA probes were produced and hybridised to wholemount CNS tissue (for method see sections 2.4.1and 2.4.4).
A-C: CNSs probed with Dig labelled antisense RNA produced using J1B as a template
D-F: CNSs probed with Dig labelled sense RNA produced using J1B as a template.
G-J: CNSs probed with Dig labelled antisense RNA produced using *shaking-B* inverse PCR product 8 (SIPC8; a gift from Jane Davies, University of Sussex). This acts as a control probe as the pupal pattern has been published (Crompton *et al.* 1995).
A, D & G: CNSs from WPP/P3 stage pupae (for staging see section 2.11.3).
B, E & H: CNSs from P4/5 stage pupae.
C, F & I: CNSs from P7/8 stage pupae.
J: CNS from an adult.
Scale bar (in **J**) = 200µm, for all images. Images C,H & I are composites, montaged on GraphicConverter and Canvas (see section 2.1.9). Anterior is top, view from dorsal.

The sense strand probes indicate non-specific probe hybridisation, whilst the antisense probe hybridises specifically in regions where a transcript related to the probe (*diomedes*) is expressed. Expression is throughout the CNS (**A** & **B**) until the late stages of pupation (**C**) when it declines. No expression was detectable in the adult CNS (not shown). This was in contrast to the expression of *shaking-B*, which was found at low levels in the CNS in a restricted subset of cells until P5 (**G** & **H**). Later expression was in a large number of cells until some time after stage P8 (**I**). In the adult CNS, expression seemed to become restricted to the giant fibre cell bodies (arrows in **J** - the other staining is background tracheal staining).
This pattern indicated that *diomedes* was not the transcript whose expression was reflected by P[GAL4]307, as the expression was not restricted to the giant fibre circuit and a small number of other cells (as the enhancer trap pattern is in these stages - see chapter 4).

6.7 Wholemount in situs to brains.

In situs to dissected larval, pupal and adult CNSs using Dig labelled RNA probes (J1B cDNA, produced as described in 6.3.1) have shown the transcript is expressed at low levels in larvae and in increasing levels in pupae (see figure 6.18). The pattern of expression does not seem to be restricted to the giant fibre circuit.

6.8 Discussion & conclusions.

This chapter covers the details of cloning a neurally expressed gene that is novel in *Drosophila*, belonging to a larger family of genes found in eukaryotic organisms from yeast to humans. *In situs* to CNSs have revealed that this is not the gene whose expression is mirrored by the enhancer trap pattern. The possibility that *diomedes* encodes a peptide with eukaryotic peptide chain initiation functions has arisen based on peptide homology. It is a possibility that there are other eukaryotic eIF2C homologues, identified in the pileup, that have yet to be assigned this function. The more general expression pattern of *diomedes* (rather than tight localisation of the transcript to the giant fibres) is not a surprise if it has a much more general function, as suggested by its similarity with eIF2C. Moreover the unusual feature seems to be the localisation of the transcript to a single tissue (neural only in embryos). This may be due to levels of the transcript being detected by the *in situ* protocol, or different forms (at least 3 are detected in the embryo - see northern in figure 6.13) being differentially expressed in tissues. The possibility of Diomedes being an eIF2C in *Drosophila* is disscussed in section 8.4.

7. Chapter 7: Analysis of cDNA LD07701.

7.1 Introduction.

The previous chapter described the cloning and analysis of a gene that was identified near the P[GAL4]307 P-element insert. The study of this gene revealed it not to be the gene whose expression was mirrored by the enhancer trap. There was still a 3Kb stretch of genomic DNA, between the 3' end of the *Hin*dIII fragment and the P-element insert, that had not been studied. This region now became of interest, because of the possibility there was another gene lying closer to the P-element, with an expression pattern in the giant fibre circuit in pupae and adults.

The genomic sequence between the P-element insert and the *Hin*dIII fragment (shown in chapter 6 to be a distance of 3 Kb - figure 6.1) was subject to sequencing. This was initiated by sequencing out from the P-element and the *Hin*dIII fragment using primers designed to the known sequence at the end of both, using plasmid rescue clone pKpn as template. A long terminal repeat (LTR) primer was used to sequence out of the P-element, whilst the primer PGT7out primed from the known end of the *Hin*dIII fragment (see appendix 10.7 for primers).

75 base pairs from the *Hin*dIII site, a fragment of sequence aligned with an EST using the Basic Local Alignment Search Tool (BLAST) - see figure 7.1. This EST was from the Berkeley *Drosophila* Genome Project (BDGP) and corresponded to a cDNA that was isolated from an embryonic library (the LD library). This EST, designated LD07701, was obtained from Genome Systems Inc. (for more details of BDGP, the LD library and Genome Systems Inc., see section 6.3.3).

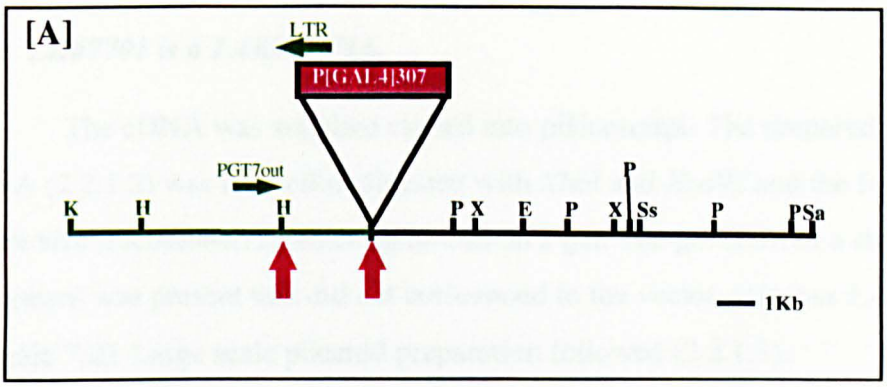

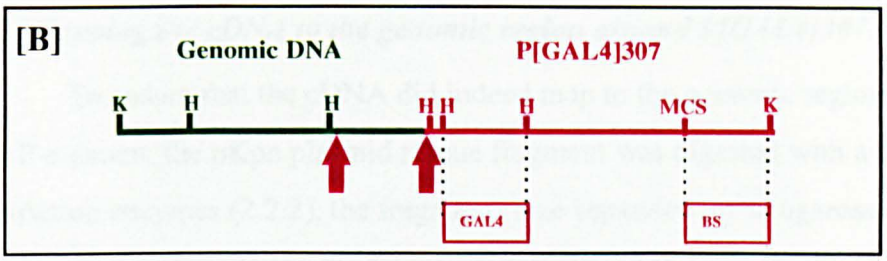

[C]

```
PGT7out        (  75) ttaacttactcgcaagatgaatgaagcggaaatatcgttgggaaaaccct
LD07701 EST    (   1) ttaacttactcgcaagatgaatgaagcggaaatatcggtgggaaaaccct

PGT7out        ( 125) tatcactaatgaaaatgccaataacaagctgctatctcctcccatccaan
LD07701 EST    (  51) tatcactaatgaaaatgccaataacaagctgctatctcctcccatccaag

PGT7out        ( 175) aaaaatgggctgtnacagttgtccctatatacacgcgtaaaacttataca
LD07701 EST    ( 101) aaaaatgggctgtaacagttgtccctatatacacgcgtaaaacttataca

PGT7out        ( 225) tatatagtanagctggataactccgattttcccaagaactcaagaaaact
LD07701 EST    ( 151) tatatagtaaagctggataactccgattttcccaagaactcaagaaaact
```

Figure 7.1: Map of the genomic region surrounding P[GAL4]307, and the identification of LD07701.

[A]: map of the region surrounding the P-element insertion as determined by restriction digestion of the plasmid rescued DNA.
Primers PGT7out and LTR are shown; from which the sequencing was initiated.
K=*Kpn*I, H=*Hin*dIII, P=*Pst*I, X=*Xho*I, E=*Eco*RI, Ss=*Sst*I, Sa=*Sal*I, C=*Cla*I, Sm=*Sma*I.

[B]: map of the pKpn plasmid rescue clone which encompasses the P-element (in red, which contains GAL4 coding region and Bluescript sequences (BS) in red boxes) and a region of genomic DNA extending to the *Kpn*I site shown at the far left of the figure (see also [A]). MCS = multiple cloning site of Bluescript.

[A] & **[B]**: Region between the red arrows indicates the new area of study in this chapter.

[C]: The sequence of the genomic region adjacent to the *Hin*dIII fragment aligns with the cDNA LD07701 from BDGP. This sequence was produced by priming with PGT7out using pKpn as template.

7.2 LD07701 is a 1.4Kb cDNA.

The cDNA was supplied cloned into pBluescript. The prepared plasmid DNA (2.2.1.2) was restriction digested with *Xho*I and *Eco*RI and the fragments were size fractionated by electrophoresis on a gel. The gel showed a single fragment was present that did not correspond to the vector, this was 1.4Kb (figure 7.2). Large scale plasmid preparation followed (2.2.1.3).

7.3 Mapping the cDNA to the genomic region around P[GAL4]307.

To ensure that the cDNA did indeed map to the genomic region around the P-element, the pKpn plasmid rescue fragment was digested with a series of restriction enzymes (2.2.2), the fragments size separated on an agarose gel by electrophoresis (2.2.3) and the fragments transferred to a membrane (2.2.4). LD07701 cut from the vector (using *Eco*RI and *Xho*I) was used as template for a radiolabelled probe (2.2.5.1.1). This probe was then hybridised to the membrane (2.2.6). The hybridisation of the probe to the filter indicated that the cDNA LD07701 was indeed from the genomic region on the pKpn side of the P-element insert (figure 7.3). This was further confirmed by the probing of a genomic Southern, which produced a pattern of hybridisation that was consistent with that seen when genomic Southerns were probed with J1B, LD09704 or pGH4.2 (figure 7.4).

7.4 LD07701 is a full length cDNA.

Having ascertained that LD07701 was from the region of interest, it was used as a template for the production of a radiolabelled probe to probe a northern blot. The RNA for the blot was extracted from embryos (0-16 hours old), larvae (all 3 instars), adult males and adult females (2.3.1.1), 5μg of each total RNA sample was size fractionated on a gel (2.3.2) and the fragments were transferred to a membrane (2.3.3). The radiolabelled LD07701 probe (2.3.3.2) was hybridised to the membrane (2.3.4) and the signal detected. This revealed

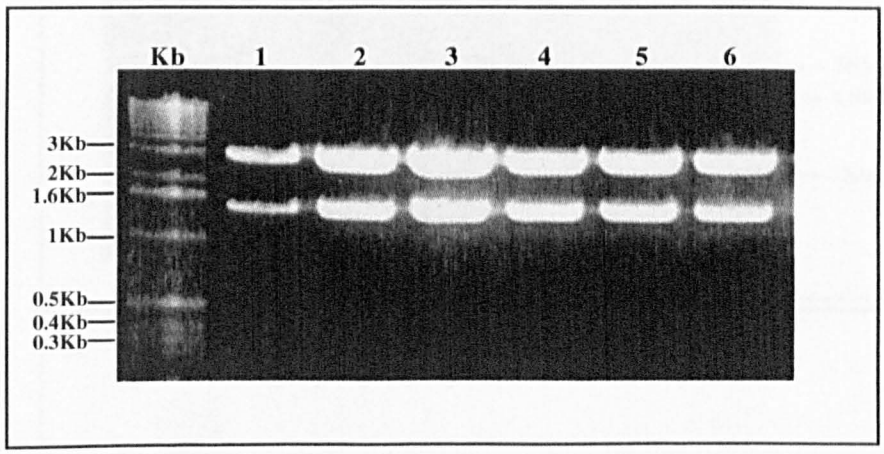

Figure 7.2: LD07701 is a 1.4Kb cDNA.

Restriction digestion (2.2.2) of the mini-prepped (2.2.1.2) clone containing LD07701 with the enzymes *Xho*I and *Eco*RI produces two fragments, a vector band (at 3Kb) and an insert of 1.4Kb. The insert corresponds to the cDNA. The fragments are visualised on an agarose gel (2.2.3). Lanes 1-6 are digestions of different small scale plasmid preparations from individual colonies of the plated bacterial stab (see section 7.2).

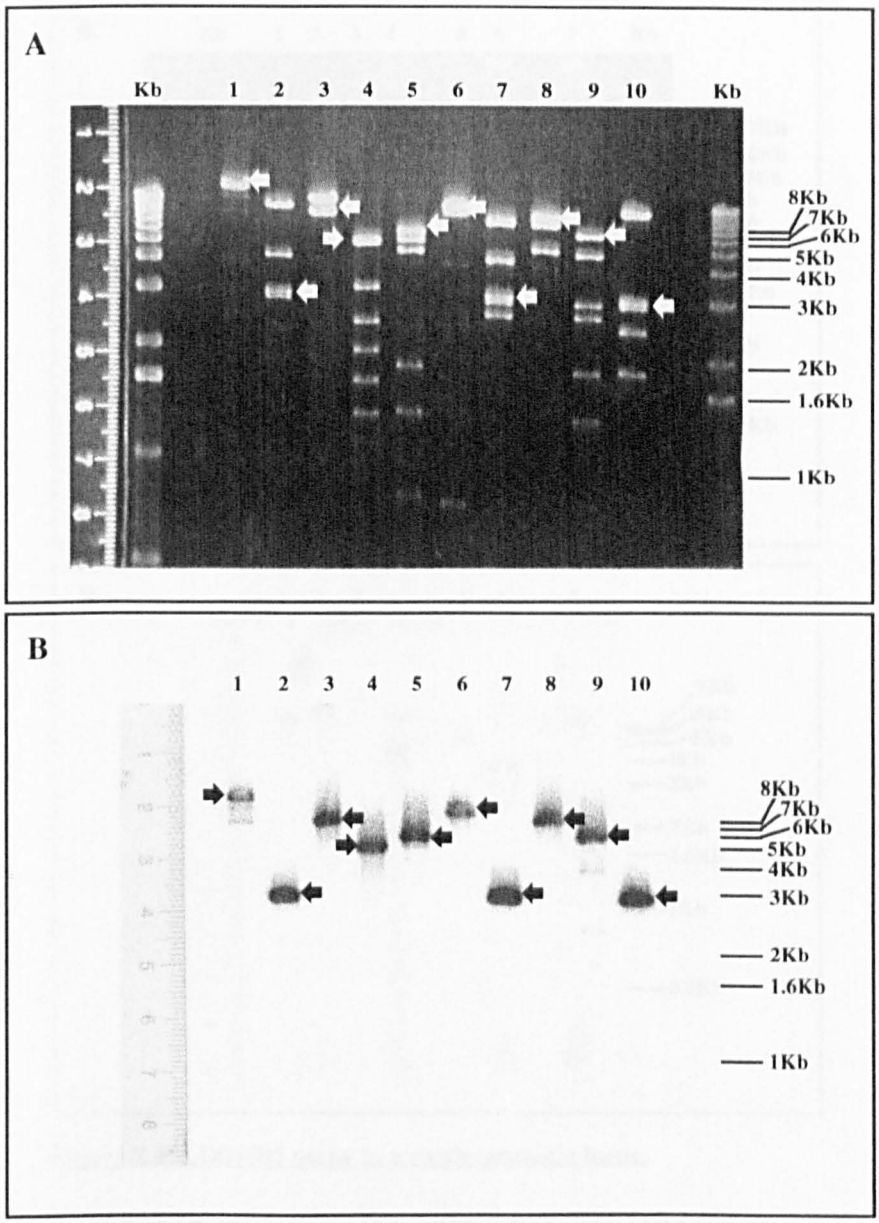

Figure 7.3: The cDNA LD07701 maps to the pKpn plasmid rescue fragment.

A: A preparation of pKpn plasmid DNA (see section 2.2.1.3) was digested with a series of restriction enzymes (2.2.2) and size separated on an agarose gel (2.2.3). Restriction enzymes used are: lane **1**=*Kpn*I, lane **2**=*Hin*dIII, lane **3**=*Eco*RI, lane **4**=*Cla*I, lane **5**=*Pst*I, lane **6**=*Xba*I, lane **7**=*Kpn*I & *Hin*dIII, lane **8**=*Kpn*I & *Eco*RI, lane **9**=*Kpn*I & *Pst*I, lane **10**=*Hin*dIII & *Eco*RI. Kb = kilobase ladder.

B: Southern blot (2.2.4) of gel **A**, probed with a radiolabelled (2.2.5.1) LD07701 1.4Kb insert (released by *Xho*I and *Eco*RI digestion) and detected (2.2.6). The black arrows indicate the hybridising fragments (these correspond to the white arrows in A to reveal which fragments are hybridising with the probe).

This data indicates that the cDNA LD07701 maps to the genomic region adjacent to the P-element P[GAL4]307. Approximate sizes are indicated on the right of figures.

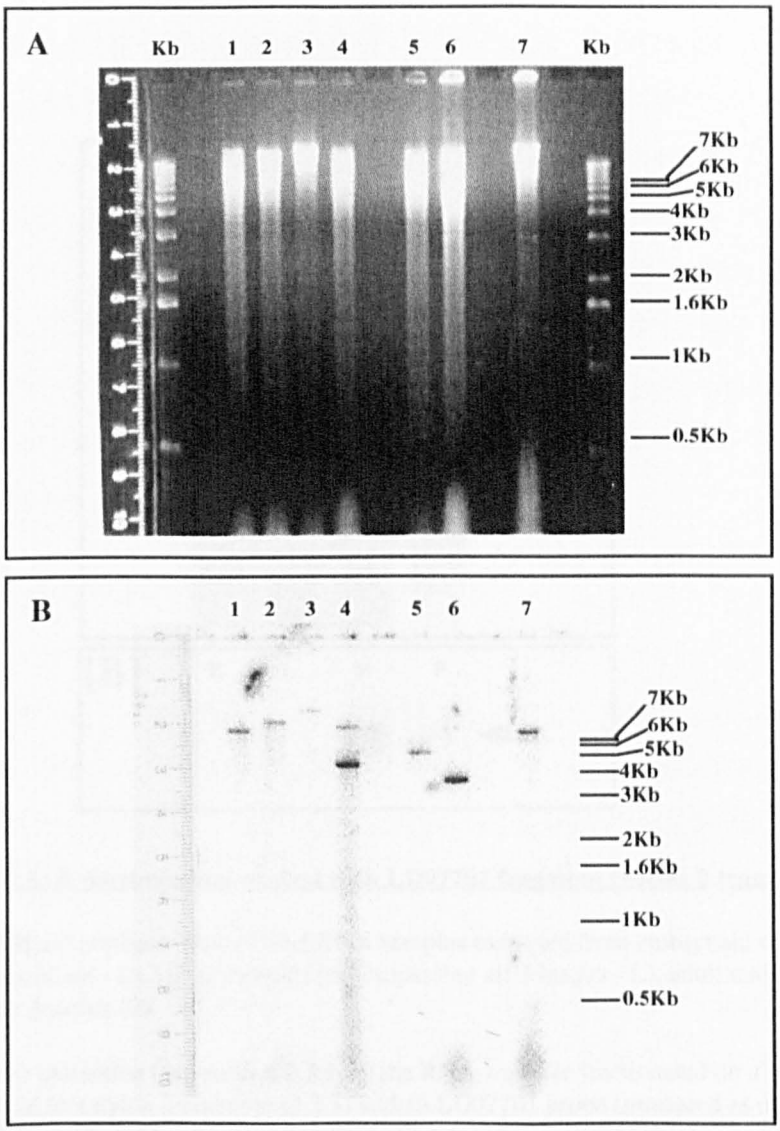

Figure 7.4: LD07701 maps to a single genomic locus.

A: Agarose gel of genomic DNA digested with restriction enzymes. Genomic DNA was extracted (see section 2.2.1.1),digested (2.2.2) and size fractionated on an agarose gel (2.2.3). The restriction enzymes used were: Lane 1 = *Pst*I, 2 = *Xho*I, 3 = *Kpn*I, 4 = *Eco*RI, 5 = *Cla*I, 6 = *Hin*dIII and 7 = *Sma*I. Kb = kilobase ladder. The even smear indicates a full digestion.

B : Southern blots of the agarose gel **A** hybridised with an radioactive probe made from the 1.4Kb LD07701 insert. The DNA from the agarose gels was transferred to nylon membrane (2.2.4), hybridised with the radiolabelled probe (produced as described in 2.2.5.1.1 and figure 7.3) and detected (2.2.6). Approximate sizes of the fragments are indicated by the ladder (on right of the blot).

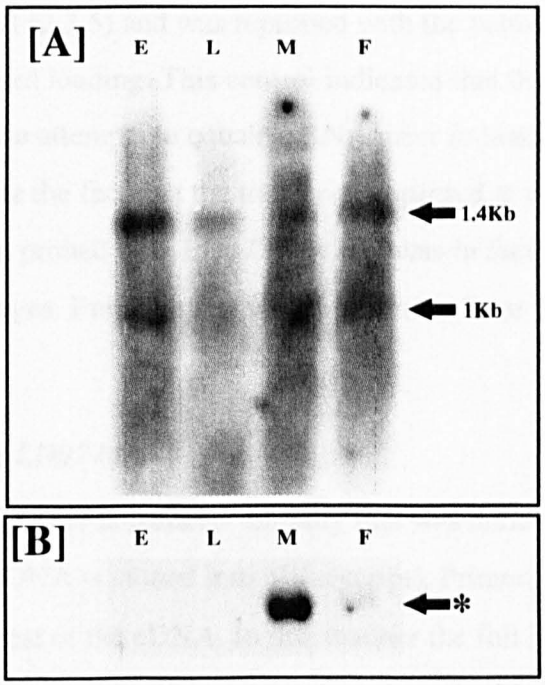

Figure 7.5: A northern blot probed with LD07701 fragment reveals 2 transcripts.

[A] & **[B]** are northern blots of total RNA samples extracted from embryonic samples (0-16 hours old - E), larval samples (encompassing all 3 instars - L), adult males (M) and adult females (F).

[A]: After extraction (see section 2.3.1.1), the RNA was size fractionated on a gel (2.3.2), transferred to a nylon membrane (2.3.3) and an LD07701 probe (produced as described in 2.3.3.2) was hybridised to the membrane (2.3.4). The resultant hybridisation reveals there are 2 transcripts detectable in all the samples.
The size of the fragments detected was ascertained by a marker lane run on the gel, blotted and subsequently stained (2.3.3.1). The size of the fragments, based on the markers are approximately 1Kb and 1.4Kb.

[B]: The initial probe was stripped from the blot (2.3.5), before a new control probe was made (2.3.3.2). The control probe was used to ascertain the equality of loading between lanes of the gel. In this case the probe was to the housekeeping gene *EF1-α*.. This has a 2Kb transcript which is clearly visible (labelled with arrow and asterisk) in the adult samples. The loading appears very unequal despite attempts to load 5µg of total RNA into each well. Accordingly, the embryo has very high levels of LD07701 transcript compared to the adult samples.The female adults appear to have higher levels of the transcript than the males.

that there are 2 transcripts of approximately 1Kb and 1.4Kb (figure 7.5). Therefore the LD07701 was a full length cDNA. The membrane then had the probe stripped off (2.3.5) and was reprobed with the control probe *EF1-α*, to check for equalised loading. This control indicated that the loading was very uneven despite the attempts to equalise RNA prior to loading. In turn this meant that despite the fact that the transcript appeared at equal levels between all samples when probed with LD07701, there was in fact much less in adults than the other stages. Embryos and larvae appear to have the highest levels of both transcripts.

7.5 Sequencing LD07701.

The cDNA was sequenced. Initially this was done using T3 and T7 primers (as the cDNA is cloned into pBluescript). Primers were then designed to sequence the rest of the cDNA. In this manner the full length of the cDNA was sequenced (figure 7.6). This sequence was used with BLAST to identify any potential homologies. The search produced nothing significant (anything with high A or T content). Next the translation of the sequence was attempted on the computer using Align (Version 3, Scientific & Educational Software) and on the Wisconsin Package (Version 8.1-UNIX, August 1995) from the Genetics Computer Group Inc., using TestCode and Frames with default settings and CodonPreference with *Drosophila*_high.cod (a *Drosophila* codon preference setting). This was attempted to see if the amino acid sequence produced any significant homologies with molecules in the databases. However, the cDNA does not appear to have a long open reading frame, or good predicted codon usage in *Drosophila* - figure 7.7.

7.6 Expression pattern of LD07701 throughout development.

To discover whether or not LD07701 was a real cDNA rather than a genomic fragment accidently cloned by BDGP, the expression of LD07701

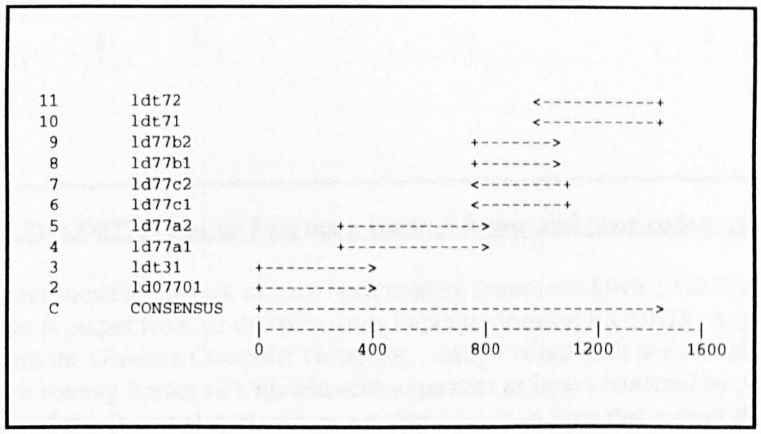

Figure 7.6: The sequencing of LD07701.

Sequencing (as described in section 2.2.13.2) of LD07701 using primers designed sequentially to the newly sequenced ends of fragments obtained from the previous set of primers (see appendix 10.8 for details). This sequencing was initiated using T3 and T7 primers (ldt31 and ldt71 & 2 respectively, as the clone is in pBSK). Sequences were obtained and confirmed by using the same primer more than once (see sequence identifiers suffixed with 1 or 2). The exception to this is ld07701 sequence (see above) which is the EST sequence of cDNA LD07701 from the BDGP (the source of the clone).
The component sequences are shown with directions of individual sequences and their extent of overlap are discernable by examining the arrows in the row corresponding to the identifier. This lead to the production of single stranded sequence along whole length of the cDNA (1.4Kb).
Sequences were all aligned using the WISCONSIN PACKAGE (Version 8.1-UNIX, August 1995) from the Genetics Computer Group, Inc., using the Gelstart, Gelenter, Gelmerge, and Gelassemble programs with default settings. The length of sequence entered into these packages was discerned by aligning multiple sequences obtained from a single primer, using the Align Plus programme (Scientific and Educational software, Version 3).

A

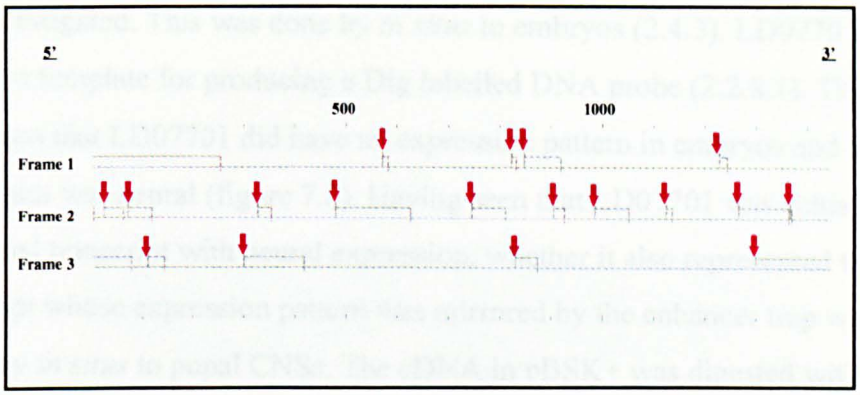

Figure 7.7: LD07701 has no long open reading frame and poor codon usage.

A: Diagram showing the lack of long open reading frames in cDNA LD07701.
The figure is output from on the Wisconsin Package (Version 8.1-UNIX, August 1995) from the Genetics Computer Group Inc., using Frames with default settings. Frames plots open reading frames of a nucleic acid sequences as boxes bordered by potential start and stop codons. Potential start codons are shown as short lines that extend above the box (red arrows) and potential stop codons are shown as short lines that extend below the box. By default, only the start and stop codons at the ends of open reading frames are shown in the frame display; if a stop codon has been passed, no stops are shown again until a start codon is passed; if a start codon is passed, no start codons are shown again until a stop codon is passed. Frames examines all six translation frames of a sequence. Pictured here are the frames that are in the correct orientation for the expression demonstrated by *in situs* (see figure 7.9).

B: Graph illustrating the poor codon usage of cDNA LD07701.
The figure is output from on the Wisconsin Package (Version 8.1-UNIX, August 1995) from the Genetics Computer Group Inc., using TestCode with default settings. TestCode helps identify translated regions in a fragment of DNA. TestCode plots a measure of the period three constraint of each region of a DNA molecule using a statistic developed by Fickett (1982). The statistic is independent of the reading frame and is based on measurements of the period three compositional constraints in the entire database for regions thought to be coding and non-coding. The plot is divided into three regions for which the statistic makes prediction. For windows larger than 200 nucleotides, the top region is supposed to predict coding regions to a 95% level of confidence. The bottom region is supposed to predict non-coding regions to the same confidence level. The middle region is the window of vulnerability for the method where the statistic can make no significant prediction. In the plot, there are markings above the curve that identify the potential start codons (ATG) and stop codons for each reading frame.

B

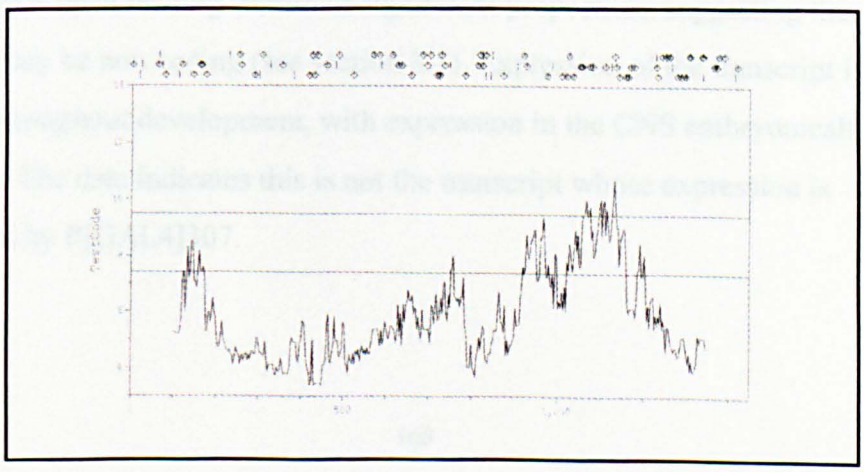

was investigated. This was done by *in situs* to embryos (2.4.3). LD07701 was used as a template for producing a Dig labelled DNA probe (2.2.8.1). The result was that LD07701 did have an expression pattern in embryos and that the pattern was neural (figure 7.8). Having seen that LD07701 was actually an expressed transcript with neural expression, whether it also represented the transcript whose expression pattern was mirrored by the enhancer trap was tested by *in situs* to pupal CNSs. The cDNA in pBSK+ was digested with *Kpn*I and *Pst*I and then Dig labelled RNA sense and antisense probes were produced (2.4.1) transcribed using T3 and T7 RNA polymerases respectively. These were used to probe pupal CNSs (2.4.4). The expression of a transcript(s) corresponding to cDNA LD07701 was detected in early and mid pupal stages (WPP to P5) but it dropped in late pupal stages (P6 on) and was absent in adults (figure 7.9). More importantly the pattern of expression did not correspond to the enhancer trap pattern seen in P[GAL4]307. The expression seen in these adult *in situs* is very low or not present, whereas the northern blot expression data suggests that the cDNA is expressed in adult tissue. The transcript must therefore be expressed in tissue other than the CNS in adults.

7.7 Discussion and conclusions.

The investigation of a second cDNA from the region of genomic DNA between the P-element insert and the end of the pKpn plasmid rescue clone has been described in this chapter. This cDNA lies between the insert and the first *Hin*dIII site on the genomic walk. The full length cDNA has been sequenced and reveals no homologies within the databases searched by BLAST. There are no obvious open reading frames of significant proportions suggesting the cDNA may be non coding (see section 8.5). Expression of the transcript is found throughout development, with expression in the CNS embryonically and pupally. The data indicates this is not the transcript whose expression is reflected by P[GAL4]307.

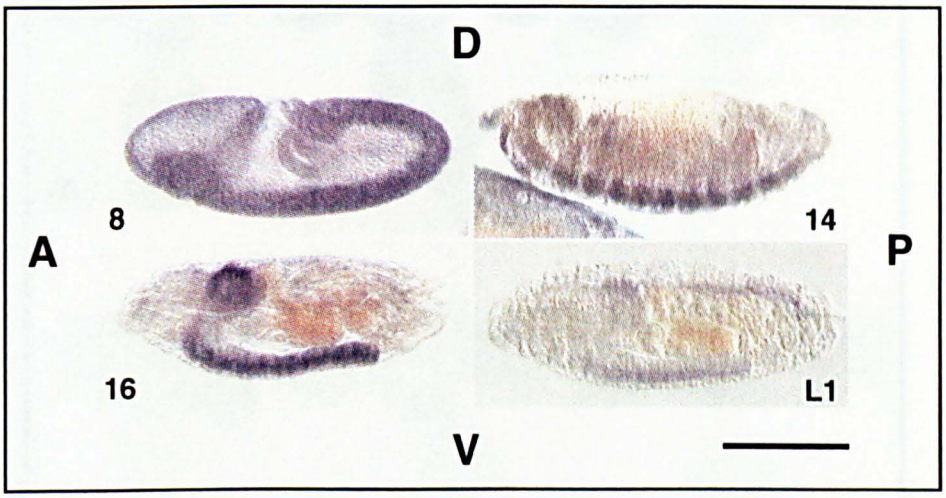

Figure 7.8 : *In situs* to embryos reveal that the LD07701 cDNA probe hybridises within the nervous system.

The embryos were incubated with a Dig labelled DNA probe, produced using LD07701 as a template. The probes were produced using the method described in 2.4.1.
The *in situs* were carried out as described in section 2.4.3 using essentially wild type flies (White Canton Specials).

Expression is first distinguishable at stage 8 through out the mesoderm and ectoderm, by stage 14 the expression seems to have become pan neurally localised, with neural expression peaking at stage 16 and decreasing into first instar larvae.

The anterior, posterior, dorsal and ventral are labelled (see A,P,D,V).
Scale bar = 200µm. Lateral view of the embryos.

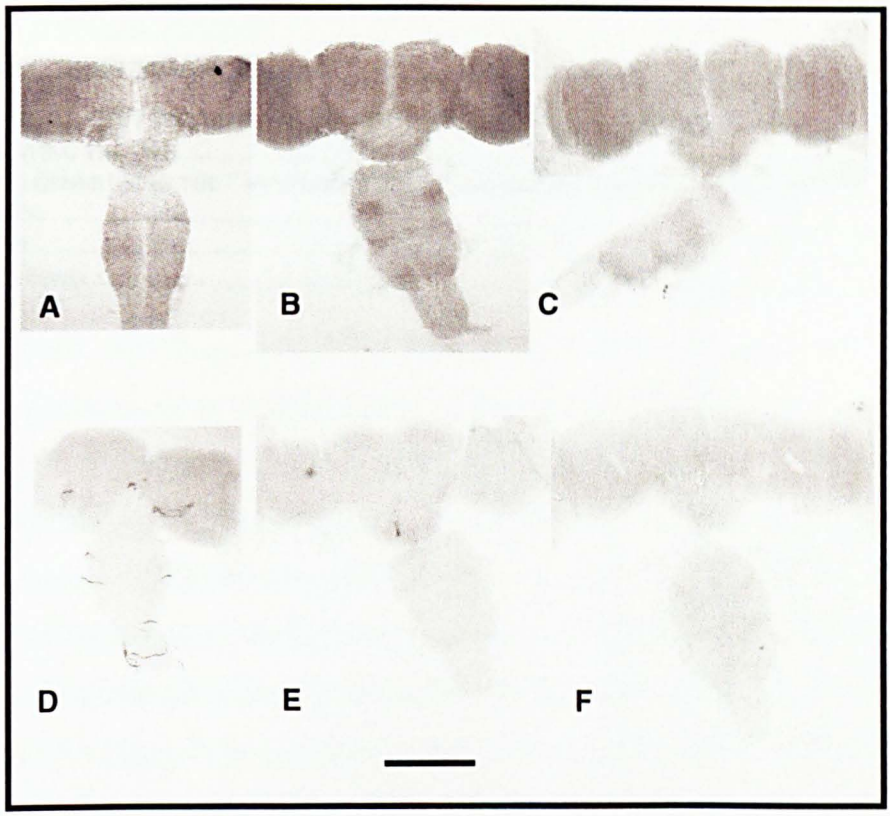

Figure 7.9: *In situs* to pupal CNSs reveal the widespread expression of LD07701 within the CNS throughout development.

Dig labelled RNA probes were produced and hybridised to wholemount CNS tissue (for method see sections 2.4.1and 2.4.4).

A-C: CNSs probed with Dig labelled antisense RNA produced using LD07701 as a template
D-F: CNSs probed with Dig labelled sense RNA produced using LD07701 as a template.
CNSs probed with Dig labelled antisense RNA produced using *shaking-B* inverse PCR product 8 (SIPC8; a gift from Jane Davies, University of Sussex) can be seen in figure 6.18 (**G-J**). This acts as a control probe as the pupal pattern has been published (Crompton *et al.* 1995). Both sets of *in situs* (this figure and 6.18) were done at the same time.
A & D: CNSs from WPP/P3 stage pupae (for staging see section 2.11.3).
B & E: CNSs from P4/5 stage pupae.
C & F: CNSs from P7/8 stage pupae.

Scale bar = 200µm, for all images. Images C,E & F are composites, montaged on GraphicConverter and Canvas (see section 2.1.9). Anterior is top, view from dorsal.

The sense strand probes indicate non-specific probe hybridisation, whilst the antisense probe hybridises specifically in regions where a transcript related to the probe (LD07701) is expressed. Expression is throughout the CNS (**A & B**) until the late stages of pupation (**C**) when it declines. No expression was detectable in the adult CNS (not shown).
This pattern indicates that LD07701 is not the transcript whose expression is reflected by P[GAL4]307, as the expression is not restricted to the giant fibre circuit and a small number of other cells (as the enhancer trap pattern is in these stages - see chapter 4).

8. General discussion.

8.1 Using P[GAL4]307 to study the GF circuit in adults and developing pupae.

This thesis has been based on the study of an enhancer trap line P[GAL4]307. Once the enhancer trap line had been established as a clear marker of the giant fibres, using an immunocytochemical detection technique that was both easy to use and provided very detailed staining of the intricacies of the circuit (chapter 3), it was utilised to study the development of the giant fibre circuit (chapter 4). The immunocytochemical approach has demonstrated very sensitive detection in the adult, almost on a par with that shown by dye filling of neurons (for a very good recent example see Phelan *et al.* 1996). This study has provided a timing of developmental events in the establishment of the giant fibre circuit, based on the morphology revealed by the enhancer trap.

The timing of developmental events described is not entirely in agreement with that of another study (Phelan *et al.* 1996), also using P[GAL4]307, although the timing of development of the GF circuit was not the main aim of the paper. The reasons for the slight differences in the timings could be due to factors separating the techniques used to study the same enhancer trap line. The first of these is our use of an antibody to assay for the presence of β-galactosidase instead of the chromogenic substrate X-gal. The antibody approach appears be more sensitive in detection of the β-galactosidase and this may be because the threshold of detection is lower. In the adult this seems to be the case, with a high level of detail discernible using antibodies to β-galactosidase (compare figures in chapter 3 of this thesis and those in Phelan *et al.* (1996), although once again these have only been included to illustrate the enhancer trap line P[GAL4]307 marks the GFs throughout development and not to illustrate the detail of the marker). Consequently, the GFs were detected earlier in this study (at L3) than they were in Phelan *et al.* (1996), when they were first detected at 6 hours APF. This may be a result of the secondary antibody being labelled with an avidin-biotin complex after binding to the primary antibody, greatly enhancing

the signal. This also, seems to be borne out by the level of detail distinguishable in this work when compared to that of Phelan *et al.* (1996). Additionally, the activity of the β-galactosidase is not an important factor for antibody binding, so a long period of fixing can be done prior to antibody treatment. Activity is essential for the X-gal colour reaction, when fixing can only be done briefly prior to the reaction with further fixing after colour reaction with X-gal, leading to a decrease in the CNS integrity.

However, this said, the two studies are largely comparable in timing, barring the prepupal GF development. Any slight differences in timing of later pupal development, could be due to the actual method employed for assessing the stage at which the CNSs were removed. Traditionally this has been carried out using simple timing of development (expressed as hours APF) and this is indeed the method used in Phelan et al. (1996). We opted for a slightly different approach, using markers of development visible through the pupal case (based on Bainbridge & Bownes 1981). This reduces the discrepancies in developmental timing caused by different microclimates within a single bottle or tube and the different time periods that different stocks take to develop.

Two important features of the developmental profile are the early descent of the GF axons to their terminal position and the proposed model of terminal bending at the GF/TTMn synapse. Analysis of the enhancer trap shows the GF cells to be labelled continuously from late larval life to adulthood. As stated in the discussion in chapter 4 the identity of the GF cell bodies and axons is believed to be correct based on position and morphology. The early staining perikaryon project neurites that are traceable back to the cell body. Changes in the ganglion shape (Truman *et al.* 1993) seem to be responsible for the alterations in the projection pattern of the neurite from an anterodorsal projection initially, to a more medial position in early pupal stages and finally a more ventral position. The visualisation of the GFs before L3 has not been possible using the enhancer trap line, and this has precluded the observation of the earliest projection of the GF axons. By L3 when the axon is first visible it has already projected into the future T1 neuromere. By P4(ii) the GF axons have reached their final destination in T2, and they appear to stall until connection with the TTMns in P5(i). This

seems to be an unusual feature in axon development, as does the slow growth of the axons from T1-T2 which appears to take about 13 hours.

Phelan *et al.* (1996), show that the GF/TTMn electrical contact is present by 48 hours APF, consistent with the data presented here (chapter 4), showing contact is made in P5(i) - 12.5-48 hours APF. The model of TTMn/GF contact shown in chapter 4 is very different to the idea of the GF bending and contacting the TTMn, suggested by Thomas and Wyman (1984). The model is based on the TTMn being the "active partner" in the synapse formation, where the TTMn approaches and synapses with the stalled GF. The detailed analysis of the events occurring during meeting of the GF/TTMn presented here suggests the bending occurs after the formation of the synapse. Bending could be a result of fasciculation of the GF along the TTMn, or alternatively shortening of both neurons post synapsing could produce a bend. However a third possibility for the production of the bend is favoured here. When the axons meet the ganglion is relatively flat. During pupal stage P5 the thoracic ganglia undergo rapid expansion (Truman *et al.* 1993). The bending could therefore be a consequence of morphological movement of the CNS during pupation. Movements of this sort have previously been reported to be responsible for the adult projection patterns of neurons in the ventral nerve cord (Shepherd & Smith 1996). The effects of morphogenetic movements of the ganglion on a linked GF and TTMn might be expected to result in the observed adult projection pattern, diving ventrally and bending laterally.

Evidence for this model of synaptogenesis and morphological movement producing bending comes from several sources. Firstly, over 800 CNSs were examined and in none were the characteristic terminal bends seen when the GF was not connected to the TTMn. Secondly, if the GF was actively bending to seek the more peripherally located TTMn then we would expect to see some evidence of this in the study of development we carried out at P5(i). In fact, we see what appears to be the TTMn projecting in from the periphery and meet the GF at almost right angles with no GF bending seen; indeed the TTMn seems to deflect anteriorly to meet the GF target. Thirdly, the cases of aberrant development support this model. In the preparation with only 1 GF the single

axon appears to make 2 bends in the T2 region. The belief is that the right hand bend to be the extended neurite of the right hand TTMn, as it is the same diameter and continuous with this unpartnered neuron. Bending has presumably occurred because it is physically linked to the other GF, possibly through an inframedial bridge neurite. If the GF normally bends towards the TTMns, then in this case we would expect to see only one bend, as the single GF would head to the TTMn on the same side, or two bends of the one GF, both of which would presumably be the same diameter, in response to a signal from the unpartnered TTMn. The fact that extension of the GFs into T3 often occurs suggests that there is no signal to bend *per se* but bending occurs when connected to the TTMns. hence both correct bending in T2 and extension of the T3 can be seen.

Overall therefore, the final model sees the GF neuron extend from the cell bodies down into the thoracic ganglia during larval and early pupal development. By 14 hours APF it has reached the mesothoracic neuromere where it makes contact with the TTMn. The GF appears to wait for the incoming TTMns which contact the GFs during P5(i), becoming active by 48 hours APF. The bending occurs during P5 after the connection between the GFs and TTMn has been made, due to changing morphology of the ganglion. Presumably the GF subsequently grows along the TTMn and thickens, giving the adult morphology.

Previous studies of bendless mutations (Muralidhar & Thomas, 1993, Oh *et al.* 1994), have attempted to infer development of the GF circuit by studying wild type versus mutant axon development. The data presented here suggests that the bendless phenotype may be due to incorrect synaptogenesis of the TTMn with the GFs and not due to a failure of the GF to bend out towards the TTMN, as previously believed. How a UBC may have this role is not clear. It is apparent that the role of the UBC is required in the GF and not the TTMn, as mosaic analysis has revealed the genotype of the GF as important in failure of the establishment of the terminal bend. The data presented here suggests that the failure of the terminal bend formation may be due to the failure of the TTMn to recognise the GF. This may be due to the alteration of receptor function or signalling, as proposed by Oh *et al.* (1994). This may lead to a lack of recognition in a *ben*^{1} background or that the connection forms but is not stable

and consequently becomes disrupted by subsequent morphological movements. This could be tested by crossing P[GAL4]307 into a *ben*^{1} background and monitoring development, in a similar manner to this study.

8.2 Birthdating the GFs.

Having established a timing of axonogenesis and connection of major components of the circuit, a potential birthdate was investigated and assigned to the giant fibre neurons (chapter 5). Based on the available data it appears that the GF neurons have an early embryonic birthdate (after delamination in stage 9 at 3 hours 40 minutes AEL and by stage 11 at 6 hours 10 minutes). The GF neurons are protocerebral and as such are likely to be derived from a protocerebral subset of the 75-80 neuroblasts that segregate from the procephalic neuroectoderm between stages 9-11. Of these NBs, the groups Pc1-4 delaminate from the central domain of the protocerebral neuroectoderm during stage 9 (Younossi-Hartenstein et al. 1996). These neuroblast groups have formed one to two GMCs during late stage 10, these could then produce neurons within the remaining time before stage 11 (up to an hour and a half later). Of these groups of neuroblasts Pc1-4, Pc-1 alone has only one neuroblast in its group. Pc-1 is also particularly interesting because on following its position during subsequent development to stage 16, the cell body Pc-1 appears to achieve a position that is very much where the GF cell bodies are located when we detect them in later life (Younossi-Hartenstein et al. 1996). Consequently Pc-1 is an interesting potential candidate for the NB that produces the GF neurons (see figure 8.1).

The data suggests the idea of a novel phenomenon in insect development, in which some cells are born embryonically and yet have no neurites until late larval stages. This is not directly ascertainable however, as the enhancer trap pattern may not reveal an earlier series of projections that regress prior to formation of the GF circuit. The possibility of an adult specific circuit being produced from cell bodies produced embryonically and quiescent until late larval life is an interesting one, which could potentially be studied more directly by labelling the Pc-1 neuroblast early in development and seeing if its progeny do indeed become the GF neurons.

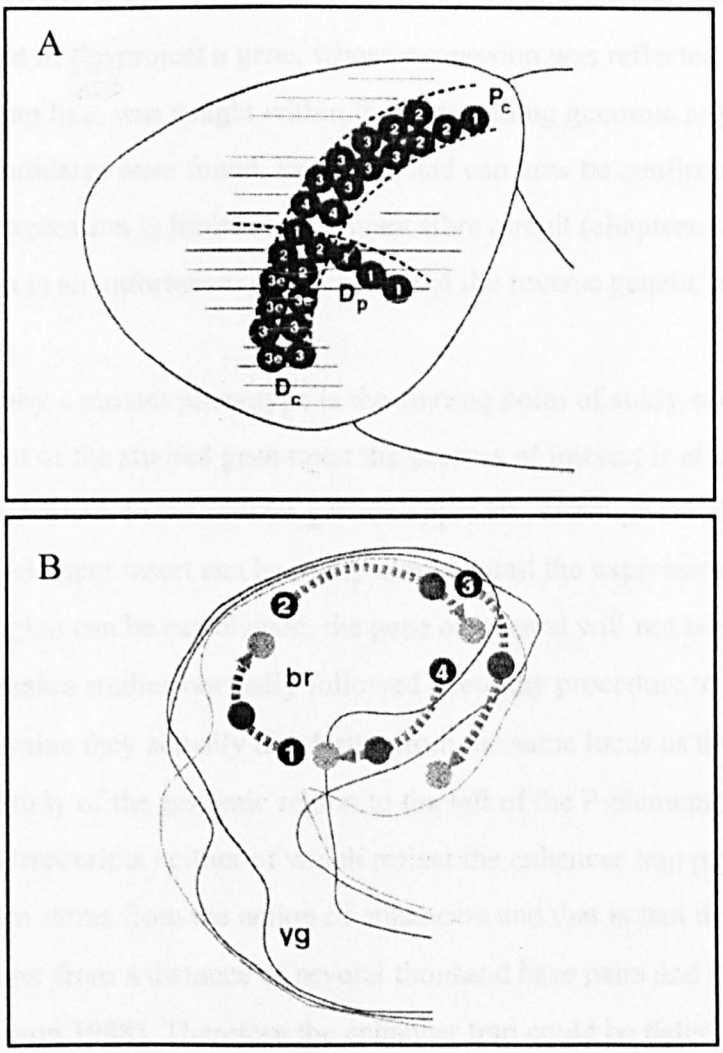

Figure 8.1: The position of neuroblast Pc1.

A: The position of Pc1 after delamination at stage 9. The diagram is a schematic lateral view of the head of a stage 9 embryo. Pc1 is in the first wave of neuroblasts to delaminate. **Pc** = central protocerebrum, **Dp** = posterior deuterocerebrum and **Dc** = central deuterocerebrum. Stage 9 is the predicted birthdate of the giant fibre progenitor cell based on the work in this thesis (see chapter 5).

B: The position of Pc1 after dorso-posterior bending of the neuraxis during late embryogenesis. This diagram shows the outline of the brain (**br**) and the anterior ventral nerve cord (**vg**), as well as the location of 4 neuroblasts at 3 different stages (dark shading : stage 12, intermediate shading : stage 13, light shading : stage 16). Broken arrows delineate shift of neuroblasts. Deuterocerebral neuroblasts (Dc3, represented by **1**) move anterior-dorsally; anterior protocerebral neuroblasts (Pc3, **2**) shift posteriorly; posterior protocerebral neuroblasts (Pc1: **3** and Pp3: **4**) move ventrally and anteriorly. Pc1 (**3**) is therefore, left in a position that is consistent with that of the giant fibre cell body.

Pc1 is therefore born at a time and is left in a position that make it a good potential giant fibre neuron progenitor.
Both figures are from Younossi-Hartenstein *et al.* (1996).

8.3 Cloning genes using the " reverse genetic", enhancer trapping approach.

For the rest of the project a gene, whose expression was reflected by that of the enhancer trap line, was sought within the surrounding genomic region. Two potential candidates were found, examined and can now be confirmed not to be genes whose expression is limited to the giant fibre circuit (chapters 6 & 7). In some respects this is an unfortunate disadvantage of the reverse genetic approach used here.

Traditionally a mutant phenotype is the starting point of study and therefore the effect of the studied gene upon the process of interest is already, to some degree, ascertained. In the reverse genetic approach, although the flanking DNA around a P-element insert can be easily cloned, until the expression pattern of genes in the region can be established, the gene of interest will not be known. In this case expression studies normally followed a lengthy procedure to isolate cDNAs and determine they actually did derive from the same locus as the insertion event. Study of the genomic region to the left of the P-element insertion has revealed two transcripts neither of which reflect the enhancer trap pattern. An additional problem stems from the action of enhancers and that is that they can act upon a promoter from a distance of several thousand base pairs and in either orientation (Atchison 1988). Therefore the enhancer trap could be detecting the action of an enhancer that is acting on a native gene some distance away in either direction.

Enhancer trapping, therefore, is most invaluable when a traditional mutagenesis is not possible, for example, to isolate genes that may have both early and late phases of expression, and those with redundant or pleiotropic effects. For a standard method of gene isolation it can be a slow process of cloning and testing lots of genes found by genomic walk from the plasmid rescued region. Despite this the reverse genetic approach has been successfully demonstrated by many groups (for example Wilson *et al.* 1989, Bier *et al.* 1989, Bellen *et al.* 1990).

This study has therefore provided two novel genes, which despite not being the genes I was originally looking for, are of some interest. Both genes are expressed neurally, transiently, in embryos, larvae and pupae, providing the

possibility that they may be involved in some aspect of neural development.

8.4 diomedes.

The first of the genes cloned, *diomedes*, is not a full length clone and appears to be missing at least 1.5Kb 5'. Given more time, the next step would be to find the 5' end by sequencing more of the pKpn plasmid rescue clone and finding ESTs that align with the new sequence. Assuming no major introns this strategy could yield most or all of the missing sequence. The ESTs from BDGP should all terminate in a polyA tail, and so alignment with the most 5' sequence should produce a full length clone. This could then be sequenced on both strands to produce high quality full length sequence. Despite the lack of 5' sequence, the data gained from alignments with known molecules has provided some insights into the possible nature of *diomedes*. Further work to produce mutants or to undertake over-expression work would possibly reveal the nature of *diomedes* function.

diomedes, is part of a family of genes that are highly conserved between eukaryotes (*S.pombe* to humans). Of these genes, three have had data published on them; *argonaute*, *zwille* from *A.thalina* and *eIF2C* from rabbit.

Both *zwille* and *argonaute* have roles that are demonstrated by their mutant alleles, and perhaps surprisingly, both genes are very different with respect to their roles in development and expression. *zwille* is expressed in provascular cells early in development and in the shoot apex in later embryogenesis, exerting an effect on shoot meristem genes (Moussian *et al.* 1998). *argonaute* has no restriction in its expression pattern, being found in all tissues and apparently at consistent levels throughout development (Bohmert *et al.* 1998). Alignment of the two gene products shows that the amino acids sequences are 75% identical at the C-terminus and that they differ most over the first 123 N-terminal residues, where they do not align. This suggests that this 5' difference is sufficient to produce the differences between the function of the two proteins. Alignment with amino acid sequences of proteins from a range of eukaryotes (as shown in figure 6.16) reveal that the region of highest conservation is the C-terminus suggesting it plays an important functional role.

This also suggests a common functional domain for all the proteins with specificity of this function being attributed by the divergent N-terminus. *diomedes*, *zwille* and *argonaute* have all been assessed for hydrophobicity, and all appear highly hydrophilic, suggesting they are soluble in the cytosol (no signal cleavage or membrane spanning domains are uncovered).

Direct evidence for a function is provided by the role of one of the amino acids that is shown in the pileup (chapter 6) - that is *eIF2C*. This has been recently cloned, sequenced and characterised (Zou *et al.* 1998). Rabbit eIF2C (protein originally isolated by Chakravarty 1985) has been shown to play two important roles in the eukaryotic peptide chain initiation process. The first step in protein synthesis initiation in eukaryotes involves the formation of a ternary complex among eukaryotic initiation factor 2 (eIF2), Met-tRNA$_i$ and GTP. The second step is the transfer of Met-tRNA$_i$ to the 40S ribosomal subunit, and the Met-tRNA$_i$ 40S mRNA complex is formed. These steps have been indicated to be regulated by auxiliary factors, including eIF2C. eIF2C plays two important roles in protein synthesis initiation. The first is the stimulation of ternary complex formation and the second is the stabilisation of ternary complex and the Met-tRNA$_i$ 40S mRNA complex in the presence of mRNAs. The exact working mechanism is not known. This would suggest that the role of this family of eukaryotically conserved proteins may well be to act as protein co-factors in peptide chain initiation. The data (Zou *et al.* 1998) does not suggest the region of the protein that has the co-factor activity, and so this assumption may be wrong. However, the conservation of the C-terminal region is a characteristic of this newly identified family and is found from *S.pombe* to humans. Elongation factor conservation amongst eukaryotes is so high it has been used as a basis for establishing phylogenetic trees (Baldauf *et al.* 1996). It therefore seems likely the co-factors would be highly conserved. Divergent N-terminal regions may play a role in tissue specificity.

eIF2C activity has been found in divergent eukaryotic organisms including mouse (Dasgupta *et al.* 1978), wheat germ (Seal *et al.* 1983), brine shrimp (Woodley *et al.* 1981) and yeast (Ahmad *et al.* 1985). To date the sequences of these proteins has not been submitted to any database or published,

raising the possibility that the family of proteins that includes *diomedes* may have more, as yet not cloned, members.

The active eIF2 is composed of three non-identical subunits, α, β and γ. In *Drosophila* the eIF2α subunit has been cloned (Qu & Cavener, 1994). This raises the possibility of testing my putative eIF2C (diomedes protein) for interactions with eIF2α (although the interaction may be with the uncloned δ or γ subunits – which subunits interact with the co-factor is currently unknown). The interaction with the whole complex could also be tested as this has been purified previously (Mateu & Sierra, 1987a,b).

8.5 LD07701.

The number of homologous sequences aligning with *diomedes* is somewhat starkly contrasted by the lack of sequence homology between LD07701 and anything else in the database. Open reading frame analysis and codon useage suggested that LD07701 may be non-coding. Other non-coding RNAs have been identified in *Drosophila*, including two from the bithorax complex (Martin *et al.* 1995), *infra-abdominal-4* (*iab-4*) and *bithoraxoid* (*bxd*). To compare LD07701 to another non-coding RNA, the sequence of *bxd* was taken from the database (accession number U31961), and used in the 2 prediction packages used to analyse LD07701: Frames and TestCode from the Wisconsin Package (Genetics Computer Group Inc.). Both LD07701 and *bxd* show a lack of long open reading frames and exhibit poor codon useage (see figures 7.7 and 8.2 for LD07701 and *bxd* respectively). It therefore seems likely LD07701 truely is a non-coding RNA.

The roles of *bxd* and *iab-4* have not yet been fully elucidated, although studies of *bxd* have proposed different functions; including short peptide coding or interaction with pre-mRNAs or mRNAs of other genes to regulate processing or translation respectively (Lipshitz *et al.* 1987). This study also suggested the possibility that *bxd* may be a functionless by-product of tissue-specific activation of a locus. It has also been suggested that *bxd* transcripts may serve as structural RNAs that facilitate the association of cis-regulatory regions (Mathog 1990).

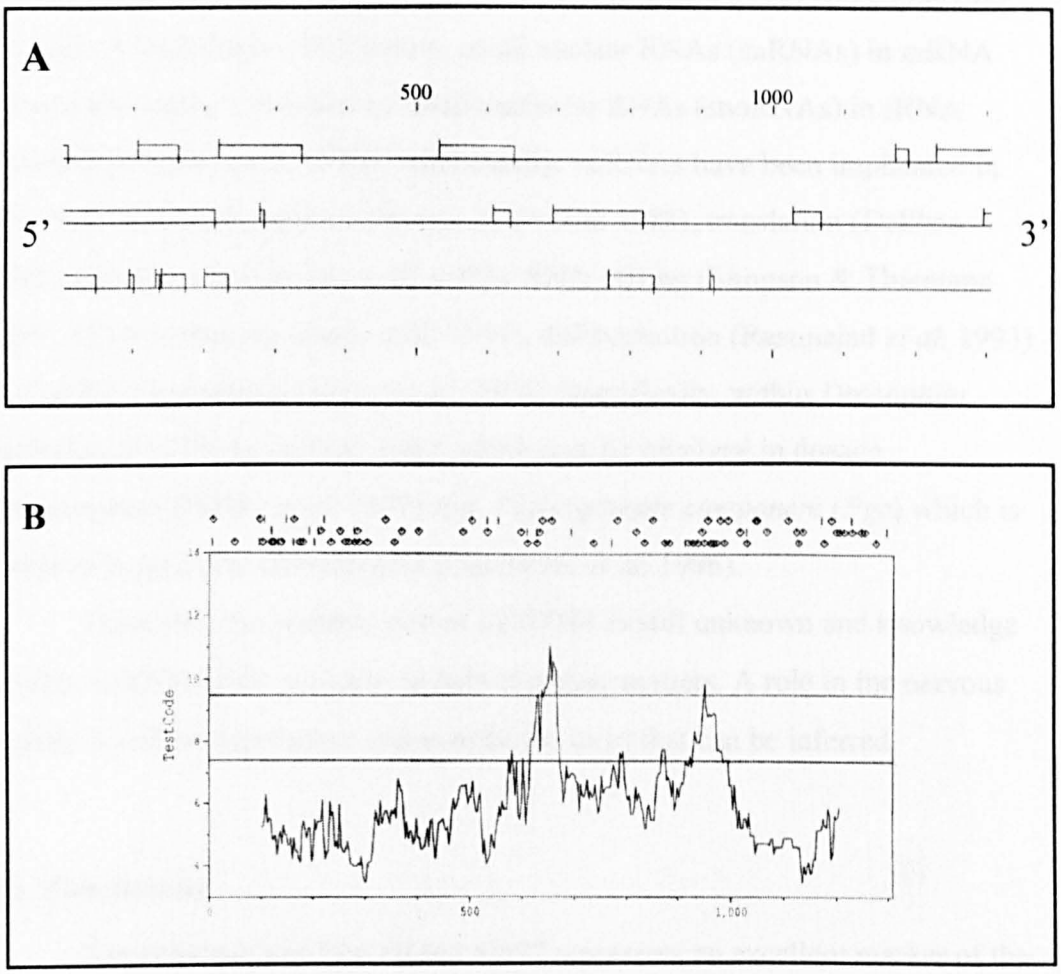

Figure 8.2 *bithoraxoid* (*bxd*) has no long open reading frame and poor codon useage.

A: Potential open reading frames in *bxd* are short.
The figure is output from on the Wisconsin Package (Version 8.1-UNIX, August 1995) from the Genetics Computer Group Inc., using Frames with default settings. Pictured here are the frames that are in the correct orientation.

B: Graph illustrating the poor codon useage of *bxd*.
The figure is output from on the Wisconsin Package (Version 8.1-UNIX, August 1995) from the Genetics Computer Group Inc., using TestCode with default settings.

When compared with figure 7.7, these figures illustrate the similarities in lack of predicted long open reading frames and poor codon useage for a known non-coding RNA *bxd* and for the novel cDNA LD07701.
For details of the programmes used here see figure 7.7.

It has been reported by Olivas *et al.* (1997) that non-coding RNAs (ncRNAs), are diverse and found in all cell types. In a variety of organisms functions include roles of ncRNAs in RNaseP (Kirsebom 1995) and telomerase (Prescott & Blackburn 1997) action, small nuclear RNAs (snRNAs) in mRNA splicing (Newman 1994) and of small nucleolar RNAs (snoRNAs) in rRNA maturation (Kiss-Laszlo 1996). Additionally, ncRNAs have been implicated in the processes of transcription (Inouye & Delihas 1988), translation (Delihas 1995), transport (Kickhoefer *et al.* 1993), RNA editing (Simpson & Thiemann 1995), mRNA stability (Geck *et al.* 1994), differentiation (Rastinejad *et al.* 1993) and protein degredation (Keiler *et al.* 1996). Specifically, within *Drosophila* examples of ncRNAs include: *roX1* which may be involved in dosage compensation (Meller *et al.* 1997) and *Polar granule component* (*Pgc*) which is involved in germline development (Nakamura *et al.* 1996).

Therefore, the possible role of LD07701 is still unknown and knowledge of other ncRNAs does not seem to help elucidate matters. A role in the nervous system, based on expression, seems to be the most that can be inferred.

8.6 Conclusions.

The enhancer trap line P[GAL4]307 represents an excellent marker of the giant fibre circuit in adults and throughout pupal development. Used as a marker it has also allowed a potential birthdate to be assigned to the giant fibre neurons, and a possible candidate progenitor neuroblast to be identified. Two neurally expressed genes have been cloned, although neither appears to be expressed in a pattern that is restricted to the giant fibre circuit.

9. References.

Allen, M. J., Drummond, J. A. & Moffat, K. G. (1998). Development of the Giant Fibre neuron of *Drosophila melanogaster*. *The Journal of Comparative Neurology* **397**, 519-531.

Ahmad, M.F., Nasrin, N., Banerjee, A.C. & Gupta, N.K. (1985). Purification and Properties of Eukaryotic Initiation Factor 2 and its Ancillary Protein Factor (Co-eIF-2A) from Yeast *Saccharomyces cerevisiae*. *Journal of Biological Chemistry* **260**, 6955-6959.

Artavanistsakonas, S., Matsuno, K. & Fortini, M. E. (1995). Notch Signaling. *Science* **268**, 225-232.

Atchison, M. L. (1988). Enhancers - Mechanisms of Action and Cell Specificity. *Annual Review of Cell Biology* **4**, 127-153.

Bacon, J. P. & Strausfeld, N. J. (1986). The Dipteran Giant Fiber Pathway - Neurons and Signals. *Journal Of Comparative Physiology a-Sensory Neural and Behavioral Physiology* **158**, 529-548.

Bailey, A. M. & Posakony, J. W. (1995). Suppressor of Hairless Directly Activates Transcription of *Enhancer of Split Complex* Genes in Response to Notch Receptor Activity. *Genes & Development* **9**, 2609-2622.

Bainbridge, S. P. & Bownes, M. (1981). Staging the Metamorphosis Of *Drosophila melanogaster*. *Journal Of Embryology and Experimental Morphology* **66**, 57-80.

Baird, D. H., Schalet, A. P. & Wyman, R. J. (1990). The *Passover* Locus in *Drosophila melanogaster* - Complex Complementation and Different Effects On the Giant Fiber Neural Pathway. *Genetics* **126**, 1045-1059.

Baird, D. H., Koto, M. & Wyman, R. J. (1993). Dendritic Reduction In *Passover*, a *Drosophila* Mutant With a Defective Giant Fiber Neuronal Pathway. *Journal Of Neurobiology* **24**, 971-984.

Baldauf, S.L., Palmer, J.D. & Doolittle, W.F. (1996). The Root of the Universal Tree and the Origin of Eukaryotes Based on Elongation Factor Phylogeny. *Proceedings of the National Academy of Sciences U.S.A.* **93**,7749-7754.

Barnes, T. M. (1994). OPUS - a Growing Family of Gap Junction Proteins. *Trends in Genetics* **10**, 303-305.

Bastiani, M. J., Harrelson, A. L., Snow, P. M. & Goodman, C. S. (1987). Expression of Fasciclin-I and Fasciclin-II Glycoproteins On Subsets of Axon Pathways During Neuronal Development in the Grasshopper. *Cell* **48**, 745-755.

Bellen, H. J., Okane, C. J., Wilson, C., Grossniklaus, U., Pearson, R. K. & Gehring, W. J. (1989). P-Element Mediated Enhancer Detection - a Versatile Method to Study Development In *Drosophila*. *Genes & Development* **3**, 1288-1300.

Bellen, H. J., Wilson, C. & Gehring, W. J. (1990). Dissecting the Complexity Of the Nervous System By Enhancer Detection. *Bioessays* **12**, 199-204.

Bellen, H. J., Develyn, D., Harvey, M. & Elledge, S. J. (1992). Isolation of Temperature-Sensitive Diphtheria Toxins in Yeast and Their Effects On *Drosophila* Cells. *Development* **114**, 787-796.

Bentley, D. & O'Connor, T. P. (1994). Cytoskeletal events in growth cone steering. *Current Opinion in Neurobiology* **4**, 43-48.

Berg, C. A. & Spradling, A. C. (1991). Studies On the Rate and Site-Specificity of P-Element Transposition. *Genetics* **127**, 515-524.

Bier, E., Vaessin, H., Shepherd, S., Lee, K., McCall, K., Barbel, S., Ackerman, L., Carretto, R., Uemura, T., Grell, E., Jan, L. Y. & Jan, Y. N. (1989). Searching For Pattern and Mutation In the *Drosophila* Genome With a P-LacZ Vector. *Genes & Development* **3**, 1273-1287.

Bingham, P. M., Kidwell, M. G. & Rubin, G. M. (1982). The Molecular Basis of P-M Hybrid Dysgenesis - the Role of the P-Element, a P-Strain-Specific Transposon Family. *Cell* **29**, 995-1004.

Bixby, J. L. & Harris, W. A. (1991). Molecular Mechanisms of Axon Growth and Guidance. *Annual Review of Cell Biology* **7**, 117-159.

Blaumueller, C. M., Qi, H. L., Zagouras, P. & ArtavanisTsakonas, S. (1997). Intracellular Cleavage of Notch leads to a Heterodimeric Receptor on the Plasma Membrane. *Cell* **90**, 281-291.

Bodmer, R., Carretto, R. & Jan, Y. N. (1989). Neurogenesis Of the Peripheral Nervous System In *Drosophila* Embryos - DNA Replication Patterns and Cell Lineages. *Neuron* **3**, 21-32.

Bohmert, K., Camus, I., Bellini, C., Bouchez, D., Caboche, M. & Benning, C. (1998). *AGO1* Defines a Novel Locus of Arabidopsis Controlling Leaf Development. *The EMBO Journal* **17**, 170-180.

Bossing, T. & Technau, G. M. (1994). The Fate of the CNS Midline Progenitors in *Drosophila* As Revealed By a New Method For Single-Cell Labeling. *Development* **120**, 1895-1906.

Bossing, T., Udolph, G., Doe, C. Q. & Technau, G. M. (1996). The Embryonic Central Nervous System Lineages of *Drosophila melanogaster* .1. Neuroblast Lineages Derived from the Ventral Half of the Neuroectoderm. *Developmental Biology* **179**, 41-64.

Bownes, M. (1975). A photographic study of development in the living embryo of *Drosophila melanogaster*. *Journal of Embryology and Experimental Morphology* **33**, 789-801.

Bownes, M. (1982). Embryogenesis. In *Handbook of Drosophila development*, pp. 66-94. Edited by Ransom. Amsterdam: Elsevier.

Brand, A. H. & Perrimon, N. (1993). Targeted Gene-Expression As a Means of Altering Cell Fates and Generating Dominant Phenotypes. *Development* **118**, 401-415.

Brand, A. (1995). GFP in *Drosophila*. *Trends in Genetics* **11**, 324-325.

Brand, A. H. & Dormand, E. L. (1995). The GAL4 System As a Tool For Unraveling the Mysteries of the *Drosophila* Nervous System. *Current Opinion in Neurobiology* **5**, 572-578.

Broadie, K. (1998). Forward and Reverse Genetic Approaches to Synaptogenesis. *Current Opinion in Neurobiology* **8**, 128-138.

Budnik, V., Koh, Y. H., Guan, B., Hartmann, B., Hough, C., Woods, D. & Gorczyca, M. (1996). Regulation of Synapse Structure and Function by the *Drosophila* Tumor Suppressor Gene *dlg*. *Neuron* **17**, 627-640.

Callahan, C. A. & Thomas, J. B. (1994). Tau-Beta-Galactosidase, an Axon-Targeted Fusion Protein. *Proceedings Of the National Academy Of Sciences Of the United States Of America* **91**, 5972-5976.

Callahan, C. A., Muralidhar, M. G., Lundgren, S. E., Scully, A. L. & Thomas, J. B. (1995). Control of Neuronal Pathway Selection By a *Drosophila* Receptor Protein-Tyrosine Kinase Family Member. *Nature* **376**, 171-174.

Callahan, C.A., Yoshikawa, S. & Thomas, J.B. (1998). Tracing Axons. *Current Opinion in Neurobiology* **8**, 582-586.

Campos-Ortega, J. A. & Hartenstein, V. (1985). *The embryonic development of Drosophila melanogaster.*: Springer-Verlag.

Campuzano, S. & Modolell, J. (1992). Patterning of the *Drosophila* Nervous System - the *Achaete-Scute* Gene Complex. *Trends in Genetics* **8**, 202-208.

Cantera, R., Thompson, K. S. J., Hallberg, E., Nassel, D. R. & Bacon, J. P. (1995). Migration Of Neurons Between Ganglia In the Metamorphosing Insect Nervous-System. *Rouxs Archives Of Developmental Biology* **205**, 10-20.

Chakravarty, I., Bagchi, M.K., Roy, R., Banerjee, A.C. & Gupta, N.K. (1985). Protein Synthesis in Rabbit Reticulocytes. *Journal of Biological Chemistry* **260**, 6945-6949.

Chalfie, M., Tu, Y., Euskirchen, G., Ward, W. W. & Prasher, D. C. (1994). Green Fluorescent Protein As a Marker For Gene-Expression. *Science* **263**, 802-805.

Challacombe, J. F., Snow, D. M. & Letourneau, P. C. (1996). Role Of the Cytoskeleton In Growth Cone Motility and Axonal Elongation. *Seminars In the Neurosciences* **8**, 67-80.

Challacombe, J. F., Snow, D. M. & Letourneau, P. C. (1996). Actin Filament Bundles Are Required For Microtubule Reorientation During Growth Cone Turning to Avoid an Inhibitory Guidance Cue. *Journal Of Cell Science* **109**, 2031-2040.

Chan, S. S. Y., Zheng, H., Su, M. W., Wilk, R., Killeen, M. T., Hedgecock, E. M. & Culotti, J. G. (1996). *UNC-40*, a *C.elegans* Homolog of *DCC* (*Deleted in Colorectal Cancer*), is Required in Motile Cells Responding to UNC-6 Netrin Cues. *Cell* **87**, 187-195.

Chen, H., He, Z. G. & TessierLavigne, M. (1998). Axon Guidance Mechanisms: Semaphorins as Simultaneous Repellents and Anti-Repellents. *Nature Neuroscience* **1**, 436-439.

Chiba, A., Snow, P., Keshishian, H. & Hotta, Y. (1995). Fasciclin-III As a Synaptic Target Recognition Molecule in *Drosophila*. *Nature* **374**, 166-168.

Chien, C. B. (1996). Py In the Fly: Receptor-Like Tyrosine Phosphatases In Axonal Pathfinding. *Neuron* **16**, 1065-1068.

Cline, H. (1996). Can There Be Growth Without Growth Cones. *Seminars In the Neurosciences* **8**, 89-95.

Cohen, J., Nurcombe, V., Jeffrey, P. & Edgar, D. (1989). Developmental Loss of Functional Laminin Receptors On Retinal Ganglion Cells Is Regulated By Their Target Tissue, the Optic Tectum. *Development* **107**, 381-387.

Coles, J. A. & Abbott, N. J. (1996). Signaling From Neurons to Glial Cells In Invertebrates. *Trends In Neurosciences* **19**, 358-362.

Cook, G., Tannahill, D. & Keynes, R. (1998). Axon Guidance to and from Choice Points. *Current Opinion in Neurobiology* **8**, 64-72.

Cooley, L., Kelley, R. & Spradling, A. (1988). Insertional Mutagenesis of the *Drosophila* Genome With Single P-Elements. *Science* **239**, 1121-1128.

Coy, D. L. & Howard, J. (1994). Organelle Transport and Sorting in Axons. *Current Opinion in Neurobiology* **4**, 662-667.

Crompton, D., Todman, M., Wilkin, M., Ji, S. Q. & Davies, J. (1995). Essential and Neural Transcripts From the *Drosophila Shaking-B* Locus Are Differentially Expressed In the Embryonic Mesoderm and Pupal Nervous System. *Developmental Biology* **170**, 142-158.

Culotti, J. G. & Kolodkin, A. L. (1996). Functions Of Netrins and Semaphorins In Axon Guidance. *Current Opinion In Neurobiology* **6**, 81-88.

Cunningham, B. A., Hemperly, J. J., Murray, B. A., Prediger, E. A., Brackenbury, R. & Edelman, G. M. (1987). Neural Cell Adhesion Molecule - Structure, Immunoglobulin-Like Domains, Cell-Surface Modulation, and Alternative RNA Splicing. *Science* **236**, 799-806.

Dai, Z. S. & Peng, H. B. (1996). From Neurite to Nerve Terminal - Induction Of Presynaptic Differentiation By Target-Derived Signals. *Seminars In the Neurosciences* **8**, 97-106.

Dasgupta, A., Das, A., Roy, R., Ralston, R., Majumdar, A. & Gupta, N.K. (1978). Protein Synthesis in Rabbit Reticulocytes. *Journal of Biological Chemistry* **253**, 6054-6059.

Davenport, R. W. & Kater, S. B. (1992). Local Increases In Intracellular Calcium Elicit Local Filopodial Responses In *Helisoma* Neuronal Growth Cones. *Neuron* **9**, 405-416.

Davenport, R. W., Dou, P., Rehder, V. & Kater, S. B. (1993). A Sensory Role For Neuronal Growth Cone Filopodia. *Nature* **361**, 721-724.

Davenport, R. W., Dou, P., Mills, L. R. & Kater, S. B. (1996). Distinct Calcium Signaling Within Neuronal Growth Cones and Filopodia. *Journal Of Neurobiology* **31**, 1-15.

Davis, L., Ping, D., Dewit, M. & Kater, S. B. (1992). Protein Synthesis Within Neuronal Growth Cones. *Journal Of Neuroscience* **12**, 4867-4877.

Delihas, N. (1995). Regulation of Gene Expression by Trans-encoded Antisense RNAs. *Molecular Microbiology* **15**, 411-414.

Desai, C. J., Gindhart, J. G., Goldstein, L. S. B. & Zinn, K. (1996). Receptor Tyrosine Phosphatases are Required for Motor Axon Guidance in the *Drosophila* Embryo. *Cell* **84**, 599-609.

Desai, C. J., Sun, Q. & Zinn, K. (1997). Tyrosine Phosphorylation and Axon Guidance: Of Mice and Flies. *Current Opinion in Neurobiology* **7**, 70-74.

Dodd, J., Morton, S. B., Karagogeos, D., Yamamoto, M. & Jessell, T. M. (1988). Spatial Regulation of Axonal Glycoprotein Expression On Subsets of Embryonic Spinal Neurons. *Neuron* **1**, 105-116.

Doe, C.Q. & Goodman, C.S. (1985). Early Events in Insect Neurogenesis.I. Development and Segmental Differences in the Pattern of Neuronal Precursor Cells. *Developmental Biology* **111**, 193-205.

Doe, C.Q, Hiromi, Y., Gehring, W.J. & Goodman, C.S. (1988). Expression and Function of the Segmentation Gene *fushi-tarazu* during *Drosophila* Neurogenesis. *Science* **239**, 170-175.

Dodd, J. & Schuchardt, A. (1995). Axon Guidance - a Compelling Case For Repelling Growth. *Cell* **81**, 471-474.

Doe, C. Q., Chulagraff, Q., Wright, D. M. & Scott, M. P. (1991). The *Prospero* Gene Specifies Cell Fates in the *Drosophila* Central Nervous System. *Cell* **65**, 451-464.

Doe, C. Q. (1992). Molecular Markers For Identified Neuroblasts and Ganglion Mother Cells In the *Drosophila* Central Nervous System. *Development* **116**, 855.

Doe, C. Q. & Skeath, J. B. (1996). Neurogenesis In the Insect Central Nervous System. *Current Opinion In Neurobiology* **6**, 18-24.

Doherty, P. & Walsh, F. S. (1992). Cell Adhesion Molecules, Second Messengers and Axonal Growth. *Current Opinion in Neurobiology* **2**, 595-601.

Doherty, P. & Walsh, F. S. (1994). Signal Transduction Events Underlying Neurite Outgrowth Stimulated by Cell Adhesion Molecules. *Current Opinions in Neurobiology* **4**, 49-55.

Drescher, U., Kremoser, C., Handwerker, C., Loschinger, J., Noda, M. & Bonhoeffer, F. (1995). *In Vitro* Guidance of Retinal Ganglion Cell Axons By Rags, a 25 Kda Tectal Protein Related to Ligands For Eph Receptor Tyrosine Kinases. *Cell* **82**, 359-370.

Drummond, J. A., Allen, M. J. & Moffat, K. G. (1997). P[GAL4]307 Enhancer Trap Pattern. *Flybrain on-line: [http://www.flybrain.org]* , Accession number: AA00098.

Eaton, R. C., Hofve, J. C. & Fetcho, J. R. (1995). Beating the Competition - the Reliability Hypothesis For Mauthner Axon Size. *Brain Behavior and Evolution* **45**, 183-194.

Ebens, A. J., Garren, H., Cheyette, B. N. R. & Zipursky, S. L. (1993). The *Drosophila* Anachronism Locus - a Glycoprotein Secreted By Glia Inhibits Neuroblast Proliferation. *Cell* **74**, 15-27.

Edgecomb, R. S., Ghetti, C. & Schneiderman, A. M. (1993). *Bendless* Alters Thoracic Musculature In Drosophila. *Journal Of Neurogenetics* **8**, 201-219.

Eggleston, W. B. (1990). P-Element Transposition and Excision in *Drosophila*: Interactions Between Elements. In *Genetics*: University of Wisconsin.

Ellwart, J. & Dormer, P. (1985). Effect Of 5-Fluoro-2'-Deoxyuridine (FdUrd) On 5-Bromo-2'-Deoxyuridine (BrdUrd) Incorporation Into DNA Measured With a Monoclonal BrdUrd Antibody and By the BrdUrd Hoechst Quenching Effect. *Cytometry* **6**, 513-520.

Emson, P. C. (1993). *In situ* Hybridization As a Methodological Tool For the Neuroscientist. *Trends In Neurosciences* **16**, 9-16.

Engel, J. E. & Wu, C. F. (1996). Altered Habituation of an Identified Escape Circuit in *Drosophila* Memory Mutants. *Journal of Neuroscience* **16**, 3486-3499.

Engel, J. E. & Wu, C. F. (1998). Genetic Dissection of Functional Contributions of Specific Potassium Channel Subunits in Habituation of an Escape Circuit in *Drosophila*. *Journal of Neuroscience* **18**, 2254-2267.

Engels, W. R., Johnsonschlitz, D. M., Eggleston, W. B. & Sved, J. (1990). High-Frequency P-Element Loss in *Drosophila* Is Homolog Dependent. *Cell* **62**, 515-525.

Engels, W. R. (1992). The Origin of P-Elements in *Drosophila melanogaster*. *Bioessays* **14**, 681-686.

Fambrough, D. & Goodman, C. S. (1996). The *Drosophila* Beaten Path Gene Encodes a Novel Secreted Protein that Regulates Defasciculation at Motor Axon Choice Points. *Cell* **87**, 1049-1058.

Fan, J. H. & Raper, J. A. (1995). Localized Collapsing Cues Can Steer Growth Cones Without Inducing Their Full Collapse. *Neuron* **14**, 263-274.

Fawcett, J. W. (1993). Growth Cone Collapse - Too Much Of a Good Thing. *Trends In Neurosciences* **16**, 165-167.

Fehon, R. G., Kooh, P. J., Rebay, I., Regan, C. L., Xu, T., Muskavitch, M. A. T. & Artavanistsakonas, S. (1990). Molecular-Interactions Between the Protein Products of the Neurogenic Loci *Notch* and *Delta*, 2 *Egf* Homologous Genes in *Drosophila*. *Cell* **61**, 523-534.

Feinburg, A. P. & Vogelstein, B. (1983). A Technique for Radioactive DNA Restriction Endonuclease Fragments to High Specific Activity. *Analytical Biochemistry* **132**, 6-13.

Fernandes, J. & Vijayraghavan, K. (1993). The Development Of Indirect Flight Muscle Innervation In *Drosophila melanogaster*. *Development* **118**, 215-227.

Fickett, J. (1982). *Nucleic Acids Research*. **10**(17); 5303-5318

Fischer, J. A., Giniger, E., Maniatis, T. & Ptashne, M. (1988). Gal4 Activates Transcription In *Drosophila*. *Nature* **332**, 853-856.

Flanagan, J. G. & VanVactor, D. (1998). Through the Looking Glass: Axon Guidance at the Midline Choice Point. *Cell* **92**, 429-432.

Fortini, M. E. & Artavanistsakonas, S. (1994). The Suppressor of Hairless Protein Participates in Notch Receptor Signaling. *Cell* **79**, 273-282.

Francois, V., Solloway, M., O'Neill, J. W., Emery, J. & Bier, E. (1994). Dorsal-Ventral Patterning of the *Drosophila* Embryo Depends On a Putative Negative Growth Factor Encoded By the *Short Gastrulation* Gene. *Genes & Development* **8**, 2602-2616.

Gao, P. P., Zhang, J. H., Yokoyama, M., Racey, B., Dreyfus, C. F., Black, I. B. & Zhou, R. (1996). Regulation of Topographic Projection in the Brain: *Elf-1* in the Hippocamposeptal System. *Proceedings of the National Academy of Sciences of the United States of America* **93**, 11161-11166.

Garrity, P. A. & Zipursky, S. L. (1995). Neuronal Target Recognition. *Cell* **83**, 177-185.

Garrity, P. A., Rao, Y., Salecker, I., McGlade, J., Pawson, T. & Zipursky, S. L. (1996). *Drosophila* Photoreceptor Axon Guidance and Targeting Requires the Dreadlocks SH2/SH3 Adapter Protein. *Cell* **85**, 639-650.

Geck, P., Medveczky, M.M., Chou, C.S., Brown, A., Cus, J. & Medveczky, P.G. (1994). *Herpesvirus saimiri* Small RNA and Interleukin-4 mRNA AUUUA Repeats Compete for Sequence Specific Factors Including a Novel 70K Protein. *Journal of General Virology* **75**, 2293-2301.

Ghysen, A. & O'Kane, C. (1989). Neural Enhancer-Like Elements As Specific Cell Markers in *Drosophila*. *Development* **105**, 35-52.

Giniger, E., Varnum, S. M. & Ptashne, M. (1985). Specific DNA Binding of Gal4, a Positive Regulatory Protein of Yeast. *Cell* **40**, 767-774.

Golic, K. G. (1994). Local Transposition Of P-Elements In *Drosophila melanogaster* and Recombination Between Duplicated Elements Using a Site-Specific Recombinase. *Genetics* **137**, 551-563.

Goodman, C. S. & Shatz, C. J. (1993). Developmental Mechanisms That Generate Precise Patterns Of Neuronal Connectivity. *Cell* **72**, 77-98.

Goodman, C. S. (1994). The Likeness Of Being - Phylogenetically Conserved Molecular Mechanisms Of Growth Cone Guidance. *Cell* **78**, 353-356.

Goodman, C. S. (1996). Mechanisms and Molecules That Control Growth Cone Guidance. *Annual Review Of Neuroscience* **19**, 341-377.

Gratzner, H. G., Leif, R. C., Ingram, D. J. & Castro, A. (1975). The Use of Antibody Specific for Bromodeoxyuridine for the Immunoflourescent Determination of DNA Replication in Single Cells and Chromosomes. *Experimental Cell Research* **95**, 88-94.

Gratzner, H. G. (1982). Monoclonal Antibody to 5-Bromodeoxyuridine and 5-Iododeoxyuridine - a New Reagent For Detection Of DNA Replication. *Science* **218**, 474-475.

Grenningloh, G., Rehm, E. J. & Goodman, C. S. (1991). Genetic Analysis Of Growth Cone Guidance In *Drosophila* - Fasciclin-II Functions As a Neuronal Recognition Molecule. *Cell* **67**, 45-57.

Gu, Y., Hukriede, N. A. & Fleming, R. J. (1995). *Serrate* Expression Can Functionally Replace Delta Activity During Neuroblast Segregation In the *Drosophila* Embryo. *Development* **121**, 855-865.

Guan, B., Hartmann, B., Kho, Y. H., Gorczyca, M. & Budnik, V. (1996). The *Drosophila* Tumor Suppressor Gene, *dlg*, is Involved in Structural Plasticity at a Glutamatergic Synapse. *Current Biology* **6**, 695-706.

Guo, M., Jan, L. Y. & Jan, Y. N. (1996). Control of Daughter Cell Fates During Asymmetric Division: Interaction of Numb and Notch. *Neuron* **17**, 27-41.

Halder, G., Callaerts, P. & Gehring, W. J. (1995). Induction Of Ectopic Eyes By Targeted Expression Of the *Eyeless* Gene In *Drosophila*. *Science* **267**, 1788-1792.

Hall, D. E., Neugebauer, K. M. & Reichardt, L. F. (1987). Embryonic Neural Retinal Cell Response to Extracellular Matrix Proteins - Developmental Changes and Effects of the Cell Substratum Attachment Antibody (CSAT). *Journal of Cell Biology* **104**, 623-634.

Hamelin, M., Zhou, Y. W., Su, M. W., Scott, I. M. & Culotti, J. G. (1993). Expression of the UNC-5 Guidance Receptor in the Touch Neurons of *C.Elegans* Steers Their Axons Dorsally. *Nature* **364**, 327-330.

Harrelson, A. L. & Goodman, C. S. (1988). Growth Cone Guidance In Insects - Fasciclin-II Is a Member Of the Immunoglobulin Superfamily. *Science* **242**, 700-708.

Harris, W. A., Holt, C. E. & Bonhoeffer, F. (1987). Retinal Axons With and Without their Somata, Growing to and Arborising in the Tectum of *Xenopus* Embryos: a Time-Lapse Video Study of Single Fibres *In vivo*. *Development* **101**, 123-133.

Harris, R., Sabatelli, L. M. & Seeger, M. A. (1996). Guidance Cues At the *Drosophila* CNS Midline - Identification and Characterization Of 2 *Drosophila Netrin/Unc-6* Homologs. *Neuron* **17**, 217-228.

Harrison, D. A. & Perrimon, N. (1993). Simple and Efficient Generation Of Marked Clones In *Drosophila*. *Current Biology* **3**, 424-433.

Hartenstein, V. (1993). *Atlas of Drosophila development*: Cold Spring Harbour Laboratory Press.

Hartenstein, V. & Campos-Ortega, J.A. (1984). Early Neurogenesis in Wildtype *Drosophila melanogaster*. *Roux's Archives of Developmental Biology* **193**, 308-325.

Hartenstein, V. & Campos-Ortega, J.A. (1987). The Pattern of Proliferation of the Neuroblasts in the Wildtype Embryo of *Drosophila melanogaster*. *Roux's Archives of Developmental Biology* **196**, 473-485.

Hatten, M. E. (1993). The Role of Migration in Central Nervous System Neuronal Development. *Current Opinion in Neurobiology* **3**, 38-44.

Haydon, P. G. (1996). Introduction - From Growth Cone to Synapse. *Seminars In the Neurosciences* **8**, 65-65.

Hedgecock, E. M., Culotti, J. G. & Hall, D. H. (1990). The *UNC-5*, *UNC-6*, and *UNC-40* Genes Guide Circumferential Migrations of Pioneer Axons and Mesodermal Cells On the Epidermis in *C.Elegans*. *Neuron* **4**, 61-85.

Hirata, J., Nakagoshi, H., Nabeshima, Y. & Matsuzaki, F. (1995). Asymmetric Segregation of the Homeodomain Protein Prospero During *Drosophila* Development. *Nature* **377**, 627-630.

Holley, S. A., Jackson, P. D., Sasai, Y., Lu, B., Derobertis, E. M., Hoffmann, F. M. & Ferguson, E. L. (1995). A Conserved System For Dorsal-Ventral Patterning in Insects and Vertebrates Involving *Sog* and *Chordin*. *Nature* **376**, 249-253.

Hosoya, T., Takizawa, K., Nitta, K. & Hotta, Y. (1995). *Glial Cells Missing* - a Binary Switch Between Neuronal and Glial Determination In *Drosophila*. *Cell* **82**, 1025-1036.

Howe, A., Aplin, A. E., Alahari, S. K. & Juliano, R. L. (1998). Integrin Signaling and Cell Growth Control. *Current Opinion in Cell Biology* **10**, 220-231.

Hummon, M. R. & Costello, W. J. (1987). Induced Disruption In the Connectivity Of an Identified Neuron In the *Drosophila* Ts Mutant *Shibire*. *Journal Of Neuroscience* **7**, 3633-3638.

Hynes, R. O. & Lander, A. D. (1992). Contact and Adhesive Specificities In the Associations, Migrations, and Targeting Of Cells and Axons. *Cell* **68**, 303-322.

Innis,M.A., Gelfand, D.H., Sninsky, J..J. & White, T.J. (1990). PCR Protocols: A Guide to Methods and Applications. Academic Press, Inc.

Inouye, M. & Delihas, N. (1988). Small RNAs in the Prokaryotes: a Growing List of Diverse Roles. *Cell* **53**, 5-7.

Irish, V. F. & Gelbart, W. M. (1987). The *Decapentaplegic* Gene Is Required For Dorsal Ventral Patterning of the *Drosophila* Embryo. *Genes & Development* **1**, 868-879.

Ito, K. & Hotta, Y. (1992). Proliferation Pattern Of Postembryonic Neuroblasts In the Brain Of *Drosophila melanogaster*. *Developmental Biology* **149**, 134-148.

Ito, K., Urban, J. & Technau, G. M. (1995). Distribution, Classification, and Development Of *Drosophila* Glial Cells In the Late Embryonic and Early Larval Ventral Nerve Cord. *Rouxs Archives Of Developmental Biology* **204**, 284-307.

Ito, K., Sass, H., Urban, J., Hofbauer, A. & Schneuwly, S. (1997) GAL4-responsive UAS-*tau* as a Tool for Studying the Anatomy and Development of the *Drosophila* Central Nervous System. *Cell and Tissue Research* **290**:1-10

Jacobs, J., Hiromi, Y., Patel, N. & Goodman, C. (1989). Lineage, Migration and Morphogenesis of Longitudinal Glia in the *Drosophila* CNS as Revealed by a Molecular Lineage Marker. *Neuron* **2**, 1625-1631.

Jan, Y. N. & Jan, L. Y. (1994). Neuronal Cell Fate Specification in *Drosophila*. *Current Opinion in Neurobiology* **4**, 8-13.

Jarman, A. P., Grau, Y., Jan, L. Y. & Jan, Y. N. (1993). *Atonal* Is a Proneural Gene That Directs Chordotonal Organ Formation In the *Drosophila* Peripheral Nervous System. *Cell* **73**, 1307-1321.

Jarriault, S., Brou, C., Logeat, F., Schroeter, E. H., Kopan, R. & Israel, A. (1995). Signaling Downstream of Activated Mammalian Notch. *Nature* **377**, 355-358.

Jones, B. W., Fetter, R. D., Tear, G. & Goodman, C. S. (1995). *Glial Cells Missing* - a Genetic Switch That Controls Glial Versus Neuronal Fate. *Cell* **82**, 1013-1023.

Kaethner, R. J. & Stuermer, C. A. O. (1994). Growth Behaviour of Retinotectal Axons in Live Zebrafish Embryos Under TTX-Induced Neuronal Blockade. *Journal of Neurobiology* **25**, 781-796.

Kaiser, K. (1993). Transgenic *Drosophila* - 2nd Generation Enhancer Traps. *Current Biology* **3**, 560-562.

Kater, S. B. & Guthrie, P. B. (1990). Neuronal Growth Cone As an Integrator Of Complex Environmental Information. *Cold Spring Harbor Symposia On Quantitative Biology* **55**, 359-370.

Kater, S. B. & Mills, L. R. (1991). Regulation Of Growth Cone Behavior By Calcium. *Journal Of Neuroscience* **11**, 891-899.

Kater, S. B. & Shibata, A. (1994). The Unique and Shared Properties Of Neuronal Growth Cones That Enable Navigation and Specific Pathfinding. *Journal Of Physiology-Paris* **88**, 155-163.

Kater, S. B., Davenport, R. W. & Guthrie, P. B. (1994). Filopodia As Detectors Of Environmental Cues - Signal Integration Through Changes In Growth Cone Calcium Levels. *Progress In Brain Research* **102**, 49-60.

Kater, S. B. & Rehder, V. (1995). The Sensory-Motor Role of Growth Cone Filopodia. *Current Opinion in Neurobiology* **5**, 68-74.

Kaufman, P. D., Doll, R. F. & Rio, D. C. (1989). *Drosophila* P-Element Transposase Recognizes Internal P-Element DNA Sequences. *Cell* **59**, 359-371.

Kaufman, P. D. & Rio, D. C. (1992). P-Element Transposition *In vitro* Proceeds By a Cut-and-Paste Mechanism and Uses GTP As a Co-factor. *Cell* **69**, 27-39.

Keegan, L., Gill, G. & Ptashne, M. (1986). Separation of DNA Binding From the Transcription Activating Function of a Eukaryotic Regulatory Protein. *Science* **231**, 699-704.

Keiler, K.C., Waller, P.R.H. & Sauer, R.T. (1996). Role of a Peptide Tagging System in Degredation of Proteins Synthesised from Damaged mRNA. *Science* **271**, 990-993.

KeinoMasu, K., Masu, M., Hinck, L., Leonardo, E. D., Chan, S. S. Y., Culotti, J. G. & TessierLavigne, M. (1996). *Deleted in Colorectal Cancer* (*DCC*) Encodes a Netrin Receptor. *Cell* **87**, 175-185.

Kelley, M. R., Kidd, S., Berg, R. L. & Young, M. W. (1987). Restriction of P-Element Insertions At the *Notch* Locus of *Drosophila melanogaster*. *Molecular and Cellular Biology* **7**, 1545-1548.

Kennedy, T. E. & Tessier-Lavigne, M. (1995). Guidance and Induction of Branch Formation in Developing Axons by Target Derived Diffusible Factors. *Current Opinion in Neurobiology* **5**, 83-90.

Keynes, R. J. & Cook, G. M. W. (1995). Repulsive and Inhibitory Signals. *Current Opinion in Neurobiology* **5**, 75-82.

Keynes, R. & Cook, G. M. W. (1995). Axon Guidance Molecules. *Cell* **83**, 161-169.

Kickhoefer, V.A., Searles, R.P., Kedersha, N.L., Garber, M.E., Johnson, D.L. & Rome, L.H. (1993). Vault Ribonucleoprotein Particles from Rat and Bullfrog

Contain a related Small RNA that is Transcribed by RNA polymerase III. *Journal of Biological Chemistry* **268**, 7868-7873.

Kidd, T., Russell, C., Goodman, C. S. & Tear, G. (1998 A). Dosage Sensitive and Complementary Functions of *Roundabout* and *Commissureless* Control Axon Crossing of the CNS Midline. *Neuron* **20**, 25-33.

Kidd, T., Brose, K., Mitchell, K. J., Fetter, R. D., TessierLavigne, M., Goodman, C. S. & Tear, G. (1998 B). *Roundabout* Controls Axon Crossing of the CNS Midline and Defines a Novel Subfamily of Evolutionarily Conserved Guidance Receptors. *Cell* **92**, 205-215.

Kidwell, M. G., Kidwell, J. F. & Sved, J. A. (1977). Hybrid Dysgenesis in *Drosophila melanogaster*: a Syndrome of Aberrant Traits Including Mutation, Sterility, and Male Recombination. *Genetics* **86**, 813-833.

Kidwell, M. G. (1979). Hybrid Dysgenesis in *Drosophila melanogaster*. The Relationship Between the P-M and the I-R Interaction Systems. *Genet. Res. Camb.* **33**, 105-117.

Kidwell, M. G. (1983). Evolution of Hybrid Dysgenesis Determinants in *Drosophila melanogaster*. *Proceedings of the National Academy of Sciences of the United States of America-Biological Sciences* **80**, 1655-1659.

Kimura, K. & Truman, J. W. (1990). Postmetamorphic Cell Death In the Nervous and Muscular Systems Of *Drosophila melanogaster*. *Journal Of Neuroscience* **10**, 403-411.

King, D. G. & Wyman, R. J. (1980). Anatomy of the Giant Fiber Pathway in *Drosophila* .1. 3 Thoracic Components of the Pathway. *Journal of Neurocytology* **9**, 753-770.

Kirsebom, L.A. (1995). RNase P - A "Scarlet Pimpernel". *Molecular Microbiology* **17**, 411-420.

Kiss-Laslo, Z., Henry, Y., Bachellene, J.P., Caizergues-Ferrer, M. & Kiss, T. (1996). Site-specific Ribose Methylation of Preribosomal RNA: a Novel Function for Small Nucleolar RNAs. *Cell* **85**, 1077-1088.

Klaes, A., Menne, T., Stollewerk, A., Scholz, H. & Klambt, C. (1994). The ETS Transcription Factors Encoded By the *Drosophila* Gene *Pointed* Direct Glial-Cell Differentiation In the Embryonic CNS. *Cell* **78**, 149-160.

Klambt, C., Jacobs, J. R. & Goodman, C. S. (1991). The Midline Of the *Drosophila* Central Nervous System - a Model For the Genetic Analysis Of Cell Fate, Cell-Migration, and Growth Cone Guidance. *Cell* **64**, 801-815.

Knoblich, J. A., Jan, L. Y. & Jan, Y. N. (1995). Asymmetric Segregation of Numb and Prospero During Cell Division. *Nature* **377**, 624-627.

Kooh, P. J., Fehon, R. G. & Muskavitch, M. A. T. (1993). Implications Of Dynamic Patterns Of *Delta* and *Notch* Expression For Cellular Interactions During *Drosophila* Development. *Development* **117**, 493-507.

Kopan, R., Schroeter, E. H., Weintraub, H. & Nye, J. S. (1996). Signal Transduction by Activated mNotch: Importance of Proteolytic Processing and its Regulation by the Extracellular Domain. *Proceedings of the National Academy of Sciences of the United States of America* **93**, 1683-1688.

Korn, H. & Faber, D. S. (1996). Escape Behavior - Brainstem and Spinal Cord Circuitry and Function. *Current Opinion in Neurobiology* **6**, 826-832.

Koto, M., Tanouye, M. A., Ferrus, A., Thomas, J. B. & Wyman, R. J. (1981). The Morphology Of the Cervical Giant Fiber Neuron Of *Drosophila*. *Brain Research* **221**, 213-217.

Krasne, F. B. & Teshiba, T. M. (1995). Habituation of an Invertebrate Escape Reflex Due to Modulation By Higher Centers Rather Than Local Events. *Proceedings of the National Academy of Sciences of the United States of America* **92**, 3362-3366.

Kraut, R. & CamposOrtega, J. A. (1996). *Inscuteable*, a Neural Precursor Gene of *Drosophila*, Encodes a Candidate for a Cytoskeleton Adaptor Protein. *Developmental Biology* **174**, 65-81.

Krishnan, S. N., Frei, E., Swain, G. P. & Wyman, R. J. (1993). *Passover* - a Gene Required For Synaptic Connectivity In the Giant Fiber System Of *Drosophila*. *Cell* **73**, 967-977.

Krishnan, S. N., Frei, E., Schalet, A. P. & Wyman, R. J. (1995). Molecular Basis of Intracistronic Complementation in the *Passover* Locus of *Drosophila*. *Proceedings of the National Academy of Sciences of the United States of America* **92**, 2021-2025.

Kuhn, T. B., Schmidt, M. F. & Kater, S. B. (1995). Laminin and Fibronectin Guideposts Signal Sustained But Opposite Effects to Passing Growth Cones. *Neuron* **14**, 275-285.

Laski, F. A., Rio, D. C. & Rubin, G. M. (1986). The Tissue Specificity of *Drosophila* P-Element Transposition Is Regulated At the Level of Messenger-RNA Splicing. *Journal of Cellular Biochemistry* , 86.

Lecourtois, M. & Schweisguth, F. (1995). The Neurogenic Suppressor of Hairless DNA-Binding Protein Mediates the Transcriptional Activation of the *Enhancer of Split Complex* Genes Triggered By Notch Signaling. *Genes & Development* **9**, 2598-2608.

Lecourtois, M. & Schweisguth, F. (1998). Indirect Evidence for Delta Dependent Intracellular Processing of Notch in *Drosophila* embryos. *Current Biology* **8**, 771-774.

Leptin, M. (1991). *Twist* and *Snail* As Positive and Negative Regulators During *Drosophila* Mesoderm Development. *Genes & Development* **5**, 1568-1576.

Letourneau, P. C., Condic, M. L. & Snow, D. M. (1994). Interactions Of Developing Neurons With the Extracellular Matrix. *Journal Of Neuroscience* **14**, 915-928.

Levi, R. & Camhi, J. M. (1995). Distributing Coordinated Motor Outputs to Several Body Segments - Escape Movements in the Cockroach. *Journal of Comparative Physiology a-Sensory Neural and Behavioral Physiology* **177**, 427-437.

Levine, R. B. & Truman, J. W. (1982). Metamorphosis of the Insect Nervous System: Changes in the Morphology and Synaptic Interactions of Identified Cells. *Nature* **294**, 250-252.

Levine, R. B., Morton, D. B. & Restifo, L. L. (1995). Remodeling of the Insect Nervous System. *Current Opinion in Neurobiology* **5**, 28-35.

Lewis, E.B., Knafels, J.D., Mathog, D.R. & Celniker, S.E. (1995). Sequence Analysis of the Cis-Regulatory Regions of the Bithorax Complex of *Drosophila*. *Proceedings of the National Academy of Sciences U.S.A.* **92**, 8403-8407.

Lieber, T., Kidd, S., Alcamo, E., Corbin, V. & Young, M. W. (1993). Antineurogenic Phenotypes Induced By Truncated Notch Proteins Indicate a Role in Signal Transduction and May Point to a Novel Function For Notch in Nuclei. *Genes & Development* **7**, 1949-1965.

Limbourg, B. & Zalokar, M. (1973). Permeabilization of *Drosophila* Eggs. *Developmental Biology* **35**, 382-387.

Lin, D. M., Fetter, R. D., Kopczynski, C., Grenningloh, G. & Goodman, C. S. (1994). Genetic-Analysis Of Fasciclin-II In *Drosophila* - Defasciculation, Refasciculation, and Altered Fasciculation. *Neuron* **13**, 1055-1069.

Lin, C. H., Thompson, C. A. & Forscher, P. (1994). Cytoskeletal Reorganisation Underlying Growth Cone Motility. *Current Opinions in Neurobiology* **4**, 640-647.

Lin, D. M. & Goodman, C. S. (1994). Ectopic and Increased Expression Of Fasciclin-II Alters Motoneuron Growth Cone Guidance. *Neuron* **13**, 507-523.

Lin, C. H. & Forscher, P. (1995). Growth Cone Advance Is Inversely Proportional to Retrograde F-Actin Flow. *Neuron* **14**, 763-771.

Lin, M. Q. & Nash, H. A. (1996). Influence of General Anesthetics on a Specific Neural Pathway in *Drosophila melanogaster*. *Proceedings of the National Academy of Sciences of the United States of America* **93**, 10446-10451.

Lin, H. & Schagat, T. (1997). Neuroblasts: A model for the Asymmetric division of stem cells. *Trends in Genetics* **13**, 33-39.

Lindsley, D.L. & Zimm,G.G. (1992). The Genome of Drosophila melanogaster. Academic Press, Inc. San Diego.

Lipshitz, H.D., Peattie, D.A. & Hogness, D.S. (1987). Novel Transcripts from the *Ultrabithorax* Domain of the Bithorax Complex. *Genes & Development* **1**, 307-322.

Luo, Y. L., Raible, D. & Raper, J. A. (1993). Collapsin - a Protein in Brain That Induces the Collapse and Paralysis of Neuronal Growth Cones. *Cell* **75**, 217-227.

Luo, Y. & Raper, J. A. (1994). Inhibitory Factors Controlling Growth Cone Motility and Guidance. *Current Opinions in Neurobiology* **4**, 648-654.

Luo, L. Q., Liao, Y. J., Jan, L. Y. & Jan, Y. N. (1994). Distinct Morphogenetic Functions Of Similar Small GTPases - *Drosophila* Drac1 Is Involved In Axonal Outgrowth and Myoblast Fusion. *Genes & Development* **8**, 1787-1802.

Mackay, D. J. G., Nobes, C. D. & Hall, A. (1995). The Rho Progress - a Potential Role During Neuritogenesis For the Rho Family Of GTPases. *Trends In Neurosciences* **18**, 496-501.

Marmorstein, R., Carey, M., Ptashne, M. & Harrison, S. C. (1992). DNA Recognition By Gal4 - Structure of a Protein DNA Complex. *Nature* **356**, 408-414.

Martin, C.H., Mayeda, C.A., Davis, C.A., Ericsson, C.L., Knafels, J.D., Mathog, D.R., Celniker, S.E., Lewis, E.B. & Palazzolo, M.J. (1995). Complete Sequence of the Bithorax Complex of *Drosophila*. *Proceedings of the National Academy of Sciences U.S.A.* **92**, 8398-8402.

Mateu, M.G. & Sierra, J.M. (1987a). Protein Synthesis in *Drosophila melanogaster* embryos. Purification and Characterisation of Polypeptide Chain Initiation factor 2. *European Journal of Biochemistry* **162**, 221-229.

Mateu, M.G. & Sierra, J.M. (1987b). Protein Synthesis in *Drosophila melanogaster* embryos. Two Mechanisms for Guanine Nucleotide Exchange on Eukaryotic Initiation factor 2. *European Journal of Biochemistry* **165**, 507-513.

Mathog, D. (1990). Transvection in the Ultrabithorax domain of the Bithorax Complex of *Drosophila melanogaster*. *Genetics* **125**, 371-382.

Matthes, D. J., Sink, H., Kolodkin, A. L. & Goodman, C. S. (1995). Semaphorin-II Can Function As a Selective Inhibitor of Specific Synaptic Arborizations. *Cell* **81**, 631-639.

Meller, V.H., Wu, K.H., Roman, G., Kuroda, M.I. & Davis, R.L. (1997). roX1 RNA Paints the X-chromosome of Male *Drosophila* and is Regulated by the Dosage Compensation System. *Cell* **88**, 445-457.

Messersmith, E. K., Leonardo, E. D., Shatz, C. J., Tessierlavigne, M., Goodman, C. S. & Kolodkin, A. L. (1995). Semaphorin-III Can Function As a Selective Chemorepellent to Pattern Sensory Projections in the Spinal-Cord. *Neuron* **14**, 949-959.

Missler, M. & Sudhof, T. C. (1998). *Neurexins*: Three Genes and 1001 Products. *Trends in Genetics* **14**, 20-26.

Mitchell, K. J., Doyle, J. L., Serafini, T., Kennedy, T. E., Tessierlavigne, M., Goodman, C. S. & Dickson, B. J. (1996). Genetic Analysis Of *Netrin* Genes In *Drosophila* - Netrins Guide CNS Commissural Axons and Peripheral Motor Axons. *Neuron* **17**, 203-215.

Moffat, K. G., Gould, J. H., Smith, H. K. & O'Kane, C. J. (1992). Inducible Cell Ablation In *Drosophila* By Cold-Sensitive Ricin-A Chain. *Development* **114**, 681.

Moussian, B., Schoof, H., Haecker, A., Jurgens, G. & Laux, T. (1998). Role of the *ZWILLE* gene in the Regulation of Central Shoot Meristem Cell Fate during Embryogenesis. *The EMBO Journal* **17**, 1799-1809.

Muller, U. & Kypta, R. (1995). Molecular Genetics of Neuronal Adhesion. *Current Opinion in Neurobiology* **5**, 36-41.

Muller, B. K., Bonhoeffer, F. & Drescher, U. (1996). Novel Gene Families Involved In Neural Pathfinding. *Current Opinion In Genetics & Development* **6**, 469-474.

Muralidhar, M. G. & Thomas, J. B. (1993). The *Drosophila bendless* Gene Encodes a Neural Protein Related to Ubiquitin-Conjugating Enzymes. *Neuron* **11**, 253-266.

Myers, P. Z. & Bastiani, M. J. (1993). Growth Cone Dynamics During the Migration Of an Identified Commissural Growth Cone. *Journal Of Neuroscience* **13**, 127-143.

Nakamura, A., Amikura, R., Mukai, M. Kobayashi, S. & Lasko, P.F. (1996). Requirement for a Noncoding RNA in *Drosophila* Polar Granules for Germ Cell Establishment. *Science* **274**, 2075-2079.

Newmann, A. (1994). Small Nuclear RNAs and pre-mRNA Splicing. *Current Opinion in Cell Biology* **6**, 360-367.

Nissanov, J., Eaton, R. C. & Didomenico, R. (1990). The Motor Output of the Mauthner Cell, a Reticulospinal Command Neuron. *Brain Research* **517**, 88-98.

Nose, A., Takeichi, M. & Goodman, C. S. (1994). Ectopic Expression of Connectin Reveals a Repulsive Function During Growth Cone Guidance and Synapse Formation. *Neuron* **13**, 525-539.

O'Brochta, D. A., Gomez, S. P. & Handler, A. M. (1991). P-Element Excision In *Drosophila melanogaster* and Related Drosophilids. *Molecular & General Genetics* **225**, 387-394.

O'Connor, T. P., Duerr, J. S. & Bentley, D. (1990). Pioneer Growth Cone Steering Decisions Mediated By Single Filopodial Contacts *In situ*. *Journal Of Neuroscience* **10**, 3935-3946.

Oh, C. E., McMahon, R., Benzer, S. & Tanouye, M. A. (1994). *bendless*, a *Drosophila* Gene Affecting Neuronal Connectivity, Encodes a Ubiquitin-Conjugating Enzyme Homolog. *Journal Of Neuroscience* **14**, 3166-3179.

O'Hare, K. & Rubin, G. M. (1983). Structures of P-Transposable Elements and Their Sites of Insertion and Excision in the *Drosophila melanogaster* Genome. *Cell* **34**, 25-35.

O'Hare, K., Driver, A., McGrath, S. & Johnsonschiltz, D. M. (1992). Distribution and Structure of Cloned P-Elements From the *Drosophila melanogaster* P-Strain Pi. *Genetical Research* **60**, 33-41.

O'Kane, C. J. & Gehring, W. J. (1987). Detection *In situ* Of Genomic Regulatory Elements In *Drosophila. Proceedings Of the National Academy Of Sciences Of the United States Of America* **84**, 9123-9127.

Olivas, W.M., Muhlrad, D. & Parker, R. (1997). Analysis of the Yeast Genome: Identification of New Noncoding and Small ORF Containing RNAs. *Oxford University Press* **25**, 4619-4625.

Pan, D. J. & Rubin, G. M. (1997). Kuzbanian Controls Proteolytic Processing of Notch and Mediates Lateral Inhibition During *Drosophila* and Vertebrate Neurogenesis. *Cell* **90**, 271-280.

Pardue, M. L. (1986). *In situ* Hybridisation to DNA of Chromosomes and Nuclei. In *Drosophila a practical approach.*, pp. 111-136. Edited by D. B. Roberts. Oxford: IRL Press.

Pavlidis, P. & Tanouye, M. A. (1995). Seizures and Failures In the Giant Fiber Pathway Of *Drosophila* Bang- Sensitive Paralytic Mutants. *Journal Of Neuroscience* **15**, 5810-5819.

Peles, E., Nativ, M., Campbell, P. L., Sakurai, T., Martinez, R., Lev, S., Clary, D. O., Schilling, J., Barnea, G., Plowman, G. D., Grumet, M. & Schlessinger, J. (1995). The Carbonic-Anhydrase Domain of Receptor Tyrosine Phosphatase-Beta Is a Functional Ligand For the Axonal Cell Recognition Molecule Contactin. *Cell* **82**, 251-260.

Phelan, P., Nakagawa, M., Wilkin, M. B., Moffat, K. G., O'Kane, C. J., Davies, J. A. & Bacon, J. P. (1996). Mutations In *Shaking-B* Prevent Electrical Synapse Formation In the *Drosophila* Giant Fiber System. *Journal Of Neuroscience* **16**, 1101-1113.

Phelan, P., Stebbings, L. A., Baines, R. A., Bacon, J. P., Davies, J. A. & Ford, C. (1998). *Drosophila* Shaking-B protein forms gap junctions in paired *Xenopus* oocytes. *Nature* **391**, 181-184.

Phillis, R. W., Bramlage, A. T., Wotus, C., Whittaker, A., Gramates, L. S., Seppala, D., Farahanchi, F., Caruccio, P. & Murphey, R. K. (1993). Isolation of Mutations Affecting Neural Circuitry Required For Grooming Behavior in *Drosophila melanogaster. Genetics* **133**, 581-592.

Phillis, R., Statton, D., Caruccio, P. & Murphey, R. K. (1996). Mutations in the 8 kDa Dynein Light Chain Gene Disrupt Sensory Axon Projections in the *Drosophila* Imaginal CNS. *Development* **122**, 2955-2963.

Power, M. E. (1948). The Thoracio-Abdominal Nervous System of an Adult Insect, *Drosophila melanogaster*. *Journal of Comparative Neurology* **88**, 347-409.

Prescott, J. & Blackburn, E.H. (1997). Telomerase RNA Mutations in *S.cerevisiae* Alter Telomerase Action and Reveal Nonprocessivity *in vivo* and *in vitro*. *Genes & Development* **11**, 528-540.

Preston, C. R., Sved, J. A. & Engels, W. R. (1996). Flanking Duplications and Deletions Associated with P-induced Male Recombination in *Drosophila*. *Genetics* **144**, 1623-1638.

Prokop, A. & Technau, G. M. (1991). The Origin of Postembryonic Neuroblasts in the Ventral Nerve Cord of *Drosophila melanogaster*. *Development* **111**, 79-88.

Prokop, A. & Technau, G. M. (1994). Normal Function Of the *Mushroom Body Defect* Gene Of *Drosophila* Is Required For the Regulation Of the Number and Proliferation Of Neuroblasts. *Developmental Biology* **161**, 321-337.

Prokop, A., Landgraf, M., Rushton, E., Broadie, K. & Bate, M. (1996). Presynaptic Development at the *Drosophila* Neuromuscular Junction: Assembly and Localization of Presynaptic Active Zones. *Neuron* **17**, 617-626.

Qu, S. & Cavener, D.R. (1994). Isolation and Characterisation of the *Drosophila melanogaster eIF2-α* gene Encoding the Alpha Subunit of Translation Initiation Factor eIF-2. *Gene* **140**, 239-242.

Raghavan, S. & White, R. A. H. (1997). Connectin Mediates Adhesion in *Drosophila*. *Neuron* **18**, 873-880.

Rajan, I. & Denburg, J. L. (1996). Error-Correction During Guidance Of Pioneer Axons In the Leg Of the Cockroach Embryo. *Rouxs Archives Of Developmental Biology* **205**, 476-485.

Rakic, P., Cameron, R. S. & Komuro, H. (1994). Recognition, Adhesion, Transmembrane Signaling and Cell Motility in Guided Neuronal Migration. *Current Opinion in Neurobiology* **4**, 63-69.

Ramon y Cahal, S. (1892). *La Cellule* **9**, 119.

Rastinejad, F., Conboy, M.J., Rando, T.A. & Blau, H.M. (1993). Tumor Supression by RNA from the 3' Untranslated region of Alpha-tropomyosin. *Cell* **75**, 1107-1117.

Rehder, V. & Kater, S. B. (1992). Regulation Of Neuronal Growth Cone Filopodia By Intracellular Calcium. *Journal Of Neuroscience* **12**, 3175-3186.

Rehder, V. & Kater, S. B. (1996). Filopodia On Neuronal Growth Cones - Multifunctional Structures With Sensory and Motor Capabilities. *Seminars In the Neurosciences* **8**, 81-88.

Rhyu, M. S., Jan, L. Y. & Jan, Y. N. (1994). Asymmetric Distribution of Numb Protein During Division of the Sensory Organ Precursor Cell Confers Distinct Fates to Daughter Cells. *Cell* **76**, 477-491.

Rio, D. C. & Rubin, G. M. (1988). Identification and Purification of a *Drosophila* Protein That Binds to the Terminal 31-Base-Pair Inverted Repeats of the P Transposable Element. *Proceedings of the National Academy of Sciences of the United States of America* **85**, 8929-8933.

Rio, D. C. (1990). Molecular Mechanisms Regulating *Drosophila* P-Element Transposition. *Annual Review of Genetics* **24**, 543-578.

Robertson, H. M., Preston, C. R., Phillis, R. W., Johnsonschlitz, D. M., Benz, W. K. & Engels, W. R. (1988). A Stable Genomic Source of P-Element Transposase in *Drosophila melanogaster*. *Genetics* **118**, 461-470.

Rooke, J., Pan, D., Xu, T. & Rubin, G. M. (1996). KUZ, a Conserved Metalloprotease-Disintegrin Protein with Two Roles in *Drosophila* Neurogenesis. *Science* **273**, 1227-1231.

Rooke, J. E. & Xu, T. (1998). Positive and Negative Signals Between Interacting Cells for Establishing Neural Fate. *Bioessays* **20**, 209-214.

Rubin, G. M., Kidwell, M. G. & Bingham, P. M. (1982). The Molecular Basis of P-M Hybrid Dysgenesis - the Nature of Induced Mutations. *Cell* **29**, 987-994.

Sambrook, J., Fritsch, E. F. & Maniatis, T. (1989). *Molecular Cloning, A laboratory approach.*: Cold Spring Harbor Laboratory Press.

Schmidt, H., Rickert, C., Bossing, T., Vef, O., Urban, J. & Technau, G. M. (1997). The Embryonic Central Nervous System Lineages of *Drosophila melanogaster* .2. Neuroblast Lineages Derived from the Dorsal Part of the Neuroectoderm. *Developmental Biology* **189**, 186-204.

Schneiderman, A. M., Tao, M. L. & Wyman, R. J. (1993). Duplication Of the Escape Response Neural Pathway By Mutation Of the *Bithorax-Complex*. *Developmental Biology* **157**, 455-473.

Schroeter, E. H., Kisslinger, J. A. & Kopan, R. (1998). Notch-1 Signalling Requires Ligand Induced Proteolytic Release of Intracellular Domain. *Nature* **393**, 382-386.

Schrons, H., Knust, E. & Camposortega, J. A. (1992). The *Enhancer-of-Split Complex* and Adjacent Genes in the 96f Region of *Drosophila melanogaster* Are Required For Segregation of Neural and Epidermal Progenitor Cells. *Genetics* **132**, 481-503.

Schuch, U., Lohse, M. J. & Schachner, M. (1989). Neural Cell Adhesion Molecules Influence 2nd Messenger Systems. *Neuron* **3**, 13-20.

Seal, S.N., Schmidt, A. & Marcus, A. (1983). Wheat Germ eIF2 and Co-eIF2. *Journal of Biological Chemistry* **258**, 10573-10576.

Searles, L. L., Jokerst, R. S., Bingham, P. M., Voelker, R. A. & Greenleaf, A. L. (1982). Molecular Cloning of Sequences From a *Drosophila* RNA Polymerase-II Locus By P-Element Transposon Tagging. *Cell* **31**, 585-592.

Seeger, M. A. (1994). Genetic and Molecular Dissection of Axon Pathfinding in the *Drosophila* Nervous System. *Current Opinions in Neurobiology* **4**, 56-62.

Serafini, T., Kennedy, T. E., Galko, M. J., Mirzayan, C., Jessell, T. M. & Tessierlavigne, M. (1994). The Netrins Define a Family of Axon Outgrowth-Promoting Proteins Homologous to *C.Elegans UNC-6*. *Cell* **78**, 409-424.

Serano, T. L., Cheung, H. K., Frank, L. H. & Cohen, R. S. (1994). P-Element Transformation Vectors For Studying *Drosophila melanogaster* Oogenesis and Early Embryogenesis. *Gene* **138**, 181-186.

Shepherd, D. & Smith, S. A. (1996). Central Projections Of Persistent Larval Sensory Neurons Prefigure Adult Sensory Pathways In the CNS Of *Drosophila*. *Development* **122**, 2375-2384.

Shirasaki, R., Tamada, A., Katsumata, R. & Murakami, F. (1995). Guidance of Cerebellofugal Axons in the Rat Embryo - Directed Growth Toward the Floor Plate and Subsequent Elongation Along the Longitudinal Axis. *Neuron* **14**, 961-972.

Simpson, L. & Thiemann, O.H. (1995). Sense from Nonsense: RNA editing in Mitochondria of Kinetoplastid Protozoa and Slime molds. *Cell* **81**, 837-840.

Skeath, J. B., Panganiban, G., Selegue, J. & Carroll, S. B. (1992). Gene-Regulation in 2 Dimensions - the Proneural *Achaete* and *Scute* Genes Are Controlled By Combinations of Axis-Patterning Genes Through a Common Intergenic Control Region. *Genes & Development* **6**, 2606-2619.

Smith, S. A. & Shepherd, D. (1996). Central Afferent Projections of Proprioceptive Sensory Neurons in *Drosophila* Revealed with the Enhancer-trap Technique. *Journal of Comparative Neurology* **364**, 311-323.

Smith, H. K., Roberts, I. J. H., Allen, M. J., Connoly, J. B., Moffat, K. G. & O'Kane, C. J. (1996). Inducible Ternary Control of Transgene Expression and Cell Ablation in *Drosophila*. *Development, Genes and Evolution* **206**, 14-24.

Spana, E. P. & Doe, C. Q. (1995). The Prospero Transcription Factor Is Asymmetrically Localized to the Cell Cortex During Neuroblast Mitosis In *Drosophila*. *Development* **121**, 3187-3195.

Spana, E. P., Kopczynski, C., Goodman, C. S. & Doe, C. Q. (1995). Asymmetric Localization of Numb Autonomously Determines Sibling Neuron Identity in the *Drosophila* CNS. *Development* **121**, 3489-3494.

Spana, E. P. & Doe, C. Q. (1996). Numb Antagonizes Notch Signaling to Specify Sibling Neuron Cell Fates. *Neuron* **17**, 21-26.

Sretavan, D. W. & Reichardt, L. F. (1993). Time-lapse Video Analysis of Retinal Ganglion Cell Axon Pathfinding at the Mammalian Optic Chiasm: Growth Cone Guidance Using Intrinsic Chiasm Cues. *Neuron* **10**, 761-777.

Stoeckli, E. T., Sonderegger, P., Pollerberg, G. E. & Landmesser, L. T. (1997). Interference with Axonin-1 and NrCAM Interactions Unmasks a Floor-plate Activity Inhibitory for Commissural Axons. *Neuron* **18**, 209-221.

Stoeckli, E. T. & Landmesser, L. T. (1998). Axon Guidance at Choice Points. *Current Opinion in Neurobiology* **8**, 73-79.

Stoker, A. W. (1996). Axon Guidance - Motor-Way Madness. *Current Biology* **6**, 794-797.

Stoker, A. & Dutta, P. (1998). Protein Tyrosine Phosphatases and Neural Development. *Bioessays* **20**, 463-472.

Sun, Y. A. & Wyman, R. J. (1996). *Passover* Eliminates Gap Junctional Communication Between Neurons of the Giant Fiber System in *Drosophila*. *Journal of Neurobiology* **30**, 340-348.

Suter, D. M. & Forscher, P. (1998). An Emerging Link Between Cytoskeletal Dynamics and Cell Adhesion Molecules in Growth Cone Guidance. *Current Opinion in Neurobiology* **8**, 106-116.

Sweeney, S. T., Broadie, K., Keane, J., Niemann, H. & O'Kane, C. J. (1995). Targeted Expression Of Tetanus Toxin Light-Chain In *Drosophila* Specifically Eliminates Synaptic Transmission and Causes Behavioral Defects. *Neuron* **14**, 341-351.

Sydor, A. M., Su, A. L., Wang, F. S., Xu, A. & Jay, D. G. (1996). Talin and Vinculin Play Distinct Roles in Filopodial Motility in the Neuronal Growth Cone. *Journal of Cell Biology* **134**, 1197-1207.

Tanaka, E. & Sabry, J. (1995). Making the Connection - Cytoskeletal Rearrangements During Growth Cone Guidance. *Cell* **83**, 171-176.

Tanouye, M. A. & Wyman, R. J. (1980). Motor Outputs of Giant Nerve Fibre in *Drosophila*. *Journal of Neurophysiology* **44**, 405-421.

Tautz, D. & Pfeifle, C. (1989). A Non-Radioactive *in situ* Hybridisation Method For the Localisation of Specific RNAs in *Drosophila* Embryos Reveals Translation Control of the Segmentation gene *hunchback*. *Chromosoma* **98**, 81-85.

Taylor, J.H., Woods, P. & Hughes, W. (1957). Detection of Replicating Cells using [^{3}H] Thymidine. *Proceedings of the National Academy of Sciences U.S.A* **43**, 122.

Tear, G., Harris, R., Sutaria, S., Kilomanski, K., Goodman, C. S. & Seeger, M. A. (1996). *commissureless* Controls Growth Cone Guidance Across the CNS Midline in *Drosophila* and Encodes a Novel Membrane Protein. *Neuron* **16**, 501-514.

Technau, G.M. & Campos-Ortega, J.A. (1986). Lineage Analysis of Transplanted Individual Cells in the Embryos of *Drosophila melanogaster*. II Commitment and Proliferative Capabilities of Neural and Epidermal Cell Progenitors. *Roux's Archives of Developmental Biology* **195**, 445-454.

Tejedor, F., Zhu, X. R., Kaltenbach, E., Ackermann, A., Baumann, A., Canal, I., Heisenberg, M., Fischbach, K. F. & Pongs, O. (1995). Minibrain - a New Protein Kinase Family Involved In Postembryonic Neurogenesis In *Drosophila*. *Neuron* **14**, 287-301.

TessierLavigne, M. & Goodman, C. S. (1996). The Molecular Biology of Axon Guidance. *Science* **274**, 1123-1133.

TessierLavigne, M. & Zipursky, S. L. (1998). Overview. *Current Opinion in Neurobiology* **8**, 13-17.

Thomas, J. B. & Wyman, R. J. (1982). A Mutation In *Drosophila* Alters Normal Connectivity Between 2 Identified Neurons. *Nature* **298**, 650-651.

Thomas, J. B. & Wyman, R. J. (1983). Normal and Mutant Connectivity Between Identified Neurons In *Drosophila*. *Trends In Neurosciences* **6**, 214-219.

Thomas, J. B. & Wyman, R. J. (1984). Mutations Altering Synaptic Connectivity Between Identified Neurons In *Drosophila*. *Journal Of Neuroscience* **4**, 530-538.

Thomas, J. B. (1998). Axon Guidance: Crossing the Midline. *Current Biology* **8**, R102-R104.

Tix, S., Minden, J. S. & Technau, G. M. (1989). Pre-Existing Neuronal Pathways in the Developing Optic Lobes of *Drosophila*. *Development* **105**, 739-746.

Tower, J. & Kurapati, R. (1994). Preferential Transposition Of a *Drosophila* P-Element to the Corresponding Region Of the Homologous Chromosome. *Molecular & General Genetics* **244**, 484-490.

Trimarchi, J. R. & Schneiderman, A. M. (1993). Giant Fiber Activation Of an Intrinsic Muscle In the Mesothoracic Leg Of *Drosophila melanogaster*. *Journal Of Experimental Biology* **177**, 149-167.

Trimarchi, J. R. & Schneiderman, A. M. (1994). The Motor-Neurons Innervating the Direct Flight Muscles Of *Drosophila melanogaster* Are Morphologically Specialized. *Journal Of Comparative Neurology* **340**, 427-443.

Trimarchi, J. R. & Schneiderman, A. M. (1995 A). Initiation Of Flight In the Unrestrained Fly, *Drosophila melanogaster*. *Journal Of Zoology* **235**, 211-222.

Trimarchi, J. R. & Schneiderman, A. M. (1995 B). Flight Initiations in *Drosophila melanogaster* Are Mediated By Several Distinct Motor Patterns. *Journal of Comparative Physiology a-Sensory Neural and Behavioral Physiology* **176**, 355-364.

Trimarchi, J. R. & Schneiderman, A. M. (1995 C). Different Neural Pathways Coordinate *Drosophila* Flight Initiations Evoked By Visual and Olfactory Stimuli. *Journal of Experimental Biology* **198**, 1099-1104.

Truman, J. W. & Booker, R. (1986). Adult Specific Neurons in the Nervous System of the Moth, *Manduca sexta*: Selective Chemical Ablation using Hydroxyurea. *Journal of Neurobiology* **17**, 613-625.

Truman, J. W. & Bate, M. (1988). Spatial and Temporal Patterns Of Neurogenesis In the Central Nervous System Of *Drosophila melanogaster. Developmental Biology* **125**, 145-157.

Truman, J. W. (1990). Metamorphosis Of the Central Nervous System Of *Drosophila. Journal Of Neurobiology* **21**, 1072-1084.

Truman, J. W., Taylor, B. & Awad, T. A. (1993). Formation of the Adult Nervous System. In *The development of Drosophila melanogaster.*, pp. 1245-1275. Edited by M. Bate & A. Martinez-Arias: Cold Spring Harbor Press.

Udolph, G., Prokop, A., Bossing, T. & Technau, G. M. (1993). A Common Precursor For Glia and Neurons in the Embryonic CNS of *Drosophila* Gives Rise to Segment-Specific Lineage Variants. *Development* **118**, 765-775.

Uemura, T. (1998). The Cadherin Superfamily at the Synapse: More Members, More Missions. *Cell* **93**, 1095-1098.

Vaessin, H., Grell, E., Wolff, E., Bier, E., Jan, L. Y. & Jan, Y. N. (1991). *Prospero* Is Expressed in Neuronal Precursors and Encodes a Nuclear Protein That Is Involved in the Control of Axonal Outgrowth in *Drosophila. Cell* **67**, 941-953.

VanVactor, D. (1998 A). Adhesion and Signaling in Axonal Fasciculation. *Current Opinion in Neurobiology* **8**, 80-86.

VanVactor, D. (1998 B). Protein Tyrosine Phosphatases in the Developing Nervous System. *Current Opinion in Cell Biology* **10**, 174-181.

VarelaEchavarria, A. & Guthrie, S. (1997). Molecules Making Waves in Axon Guidance. *Genes & Development* **11**, 545-557.

Vaughn, D. E. & Bjorkman, P. J. (1996). The (Greek) Key to Structures Of Neural Adhesion Molecules. *Neuron* **16**, 261-273.

Voelker, R. A., Greenleaf, A. L., Gyurkovics, H., Wisely, G. B., Huang, S. M. & Searles, L. L. (1984). Frequent Imprecise Excision Among Reversions of a P-Element Caused Lethal Mutation in *Drosophila. Genetics* **107**, 279-294.

Weichaus, E. & Nusslein-Volhard, C. (1986). Looking at Embryos. In *Drosophila a practical approach.*, pp. 199-226. Edited by D. B. Roberts. Oxford: IRL Press.

Weinmaster, G. (1998). Notch Signaling: Direct or What? *Current Opinion in Genetics & Development* **8**, 436-442.

White, K. & Kankel, D. R. (1978). Patterns of Cell Division and Cell Movement in the Formation of the Imaginal Nervous System in *Drosophila melanogaster*. *Developmental Biology* **65**, 296-321.

Wilson, C., Pearson, R. K., Bellen, H. J., O'Kane, C. J., Grossniklaus, U. & Gehring, W. J. (1989). P-Element Mediated Enhancer Detection - an Efficient Method For Isolating and Characterizing Developmentally Regulated Genes in *Drosophila*. *Genes & Development* **3**, 1301-1313.

Winberg, M. L., Mitchell, K. J. & Goodman, G. S. (1998). Genetic Analysis of the Mechanisms Controlling Target Selection: Complementary and Combinatorial Functions of Netrins, Semaphorins, and IgCAMs. *Cell* **93**, 581-591.

Winslow, J. W., Moran, P., Valverde, J., Shih, A., Yuan, J. Q., Wong, S. C., Tsai, S. P., Goddard, A., Henzel, W. J., Hefti, F., Beck, K. D. & Caras, I. W. (1995). Cloning of *Al-1*, a Ligand For an Eph-Related Tyrosine Kinase Receptor Involved in Axon Bundle Formation. *Neuron* **14**, 973-981.

Woodley, C.L., Roychowdhury, M., Macrae, T.H., Olsen, K.W. & Wahba, A.J. (1981). Protein Synthesis in Brine Shrimp Embryos. *European Journal of Biochemistry* **117**, 543-551.

Xiong, W. C. & Montell, C. (1995). Defective Glia Induce Neuronal Apoptosis in the *Repo* Visual System of *Drosophila*. *Neuron* **14**, 581-590.

Yang, M. Y., Armstrong, J. D., Vilinsky, I., Strausfeld, N. J. & Kaiser, K. (1995). Subdivision Of the *Drosophila* Mushroom Bodies By Enhancer-Trap Expression Patterns. *Neuron* **15**, 45-54.

Yeh, E., Gustafson, K. & Boulianne, G. L. (1995). Green Fluorescent Protein As a Vital Marker and Reporter Of Gene- Expression In *Drosophila*. *Proceedings Of the National Academy Of Sciences Of the United States Of America* **92**, 7036-7040.

Yeh, S. R., Fricke, R. A. & Edwards, D. H. (1996). The Effect of Social Experience on Serotonergic Modulation of the Escape Circuit of Crayfish. *Science* **271**, 366-369.

YounossiHartenstein, A., Nassif, C., Green, P. & Hartenstein, V. (1996). Early Neurogenesis of the *Drosophila* Brain. *Journal of Comparative Neurology* **370**, 313-329.

YounossiHartenstein, A., Green, P., Liaw, G. J., Rudolph, K., Lengyel, J. & Hartenstein, V. (1997). Control of Early Neurogenesis of the *Drosophila* Brain by the Head Gap Genes *tll*, *otd*, *ems*, and *btd*. *Developmental Biology* **182**, 270-283.

Zhang, P. & Spradling, A. C. (1993). Efficient and Dispersed Local P-Element Transposition From *Drosophila* Females. *Genetics* **133**, 361-373.

Zhang, J. H., Cerretti, D. P., Yu, T., Flanagan, J. G. & Zhou, R. P. (1996). Detection of Ligands in Regions Anatomically Connected to Neurons Expressing the Eph Receptor Bsk: Potential Roles in Neuron-Target Interaction. *Journal of Neuroscience* **16**, 7182-7192.

Zou, C., Zhang, Z., Wu, S. & Osterman, J.C. (1998). Molecular Cloning and Characterisation of a Rabbit eIF2C Protein. *Gene* **211**,187-194.

Appendix 10.1.

Drummond,J.A., Allen,M.J. & Moffat,K.G. (1997). P[GAL4]307 Enhancer trap pattern. *Flybrain on-line: [http://www.flybrain.org]* , Acession number: AA00098.

The *Drosophila Giant Fibre System*

J.A. Drummond, M.J. Allen and K.G. Moffat

Dept. Biological Sciences, University of Warwick, Coventry, CV4 7AL, U.K.

Introduction

The giant fiber circuit mediates the light-off escape response by relaying excitation from the eyes to the muscles of the thorax.

The giant fibers are a pair of large bilaterally symetrical interneurons (2) with cell bodies about 20mm in diameter. The cell bodies are located close to the posterior border of the brain, adjacent to the neuropile of the protocerebrum, about 30mm dorsal to the oesophageal canal. The main process of the neuron is connected to the cell body via a neurite, some 60mm long. The dendritic field, composed of dorsomedial, ventrolateral and posterolateral processes, branch from this point, as does the axon. The axon projects dorsally and posteriomedially towards the ventral midline, before ascending past the oesophageal canal and through the dorsal region of the cervical connective to the mesothoracic neuromere (3).

Each giant fiber axon has a lateral bend in the mesothoracic neuromere.

Just before the lateral bend each giant fiber electrically synapses, near the inframedial bridge at a tuft of collaterals, with the peripherally synapsing interneuron (PSI). The PSI projects across the ganglion and chemically synapses onto the five motorneurons (DLMNs) of the contralateral dorsal longitudinal flight muscles (dlms), fibrillar indirect flight muscles (4). At the end of the lateral bend the giant fiber synapses again, this time with the large tergotrochanteral motorneuron (TTMN) - innervating the tergotrochanteral muscle (also known as the jump muscle or flight starter muscle) (5). The ttm is the largest tubular muscle in the thorax, spanning the thorax dorsoventrally. It originates on the scutum and inserts on an apodeme in the proximal femur of the mesothoracic leg. This muscle acts as a leg extensor during escape take off. In addition to this there is good

evidence that the GFs also activate other neurons during the escape behaviour. These include the motorneurons for the bilateral anterior pleural number 3 muscles, controlling abduction of the wings to their flight position; the tibial levator motorneuron (TLMN), responsible for femur-tibia joint extension; and the dorsal ventral muscle motorneurons, innervating the antagonistic muscles to the DLMs to generate wing movements necessary for initiation and maintenance of flight during escape behaviour (6)

P[GAL4]A307, picked out in an enhancer trap screen, marks the giant fibers throughout their development (7) and also appears to mark other neurons of the circuit, including the PSI and the TTMN.

P[GAL4]-307 enhancer trap pattern.

P[GAL4] enhancer trap line A307 crossed to UAS-lacZ (a cytoplasmic LacZ provided by Andrea Brand) on the X chromosome. Beta-galactosidase was detected as described, with the exception of a biotinylated anti-rabbit IgG secondary and visualised using Vector labs Elite ABC kit (PK-6101). A number of distinctive cell bodies can be discriminated, including the GFs, the TTMN and the PSI. Other cells are also marked but have not been identified

The pattern reveals the characteristic morphology of the giant fiber projections, the cell bodies (gfcb), present just below the dorsal protocerebrum. These project a neurite posteriorly and ventrally to the dendritic field and the axons. The axons project ventrally and posteriorly towards the ventral midline subsequently projecting dorsally to the connective (Conn). The axons extend unbranched into the ventral nerve cord (VNC) as far as the mesothoracic neuromere (T2), where they project ventrally and bend laterally (arrowhead). An anterior dorsal cell body (ADCB) is also a characteristic feature of the pattern, with an axon projecting medially toward the deuterocerebrum, ending in a mesh of fine projections.

This image gives an overview of the pattern using a Zeiss axioskop with attached JVC TK-1280E colour video camera . Images were processed on a PowerMac. Greater detail is achieved using higher magnifications and heavier staining (prolonging the colour reaction, using higher concentrations of antibodies and growing the developing flies at 29 C all contribute). Adult CNS, dorsal view. Scale bar is 100μm.

The following images present the data in greater detail.

Giant fibre dendritic field.

The accompanying series of images more clearly illustrate divisions and extent of the dendritic field in the brain. From the giant fiber cell body (GFCB) a neurite projects ventrally and posteriorly, to the site of the dendritic arborisations. These are the dorsomedial dendrites (DMD), ventrolateral dendrites (VLD) and the posterolateral dendrites (PLD). Two large cell bodies in the posterior suboesphageal ganglion can also be seen sending axons dorsally towards the foramen.

Adult CNS of which the brain is shown here. View from dorsal. Focused dorsal to ventral, A - D. Scale bar is 50μm

Giant intercommisure.

On further staining, processes from the giant intercommisure neurons can be seen crossing the giant intercommisure (GIC). Although these neurons are known to dye couple they have not been shown to participate in the functioning of the GF pathway. At a medial level (compared with the GFs at a dorsal level) are neurons, labelled with red arrowheads, also seen in accompanying images of the connective. Their cell bodies have not been identified

Adult CNS showing brain region . Dorsal to ventral A - D. Scale bar is 50μm

Cervical connective.

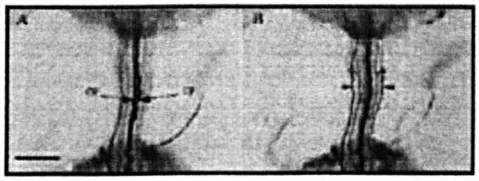

The connective between brain and vnc show gfs and two other pairs of axons. As the giant fiber is at the dorsal edge of the connective it is amongst many descending neurons (8). It is difficult to ascertain whether the other neurons are ascending or descending as they are located medially (red and green arrowheads).

Adult CNS, connective visible here. Scale bar is 50μm

Ventral Nerve Cord

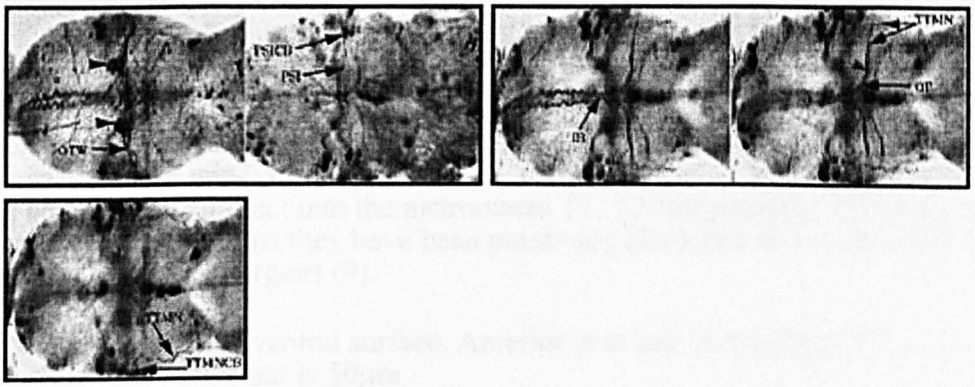

The GFs enter the vnc, passing through T1 into T2 bending and electrically synapsing with the TTMN (synapse shown by red arrowhead). The cell body marked (PSICB) has a position and projection (PSI) consistent with it being the peripharally synapsing interneuron. This feeds into the bundle of afferent projections, passing by two large cell bodies (black arrowheads, A). The inframedial bridge (IB) is also visible (C).

Adult CNS of which vnc, largely T1 and T2, are visible. Anterior is left. Dorsal to ventral A - E. Scale bar is 50μm

Giant fibre - TTMN synapse.

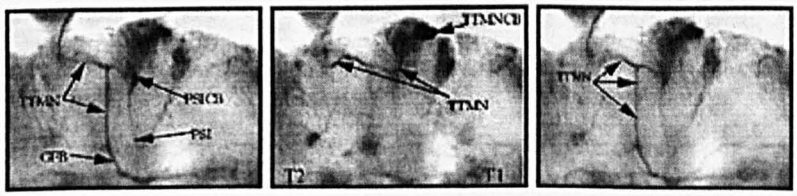

Other neurons (arrowheads) enter the neuromeres via nerve roots at the ventral surface of the vnc (ventral prothoracic nerves and mesothoracic accessory nerves). These neurons project into the neuromeres T1, T2 and possibly T3. Based upon previous descriptions they have been putatively identified as a subset of projections from chordotonal organs (9).

Dorsal view of the ventral surface. Anterior is to left. Adult CNS, T1 and T2 visible here. Scale bar is 50µm

Chordatonal neurons.

Other neurons (arrowheads) enter the neuromeres via nerve roots at the ventral surface of the vnc (ventral prothoracic nerves and mesothoracic accessory nerves). These neurons project into the neuromeres T1, T2 and possibly T3. Based upon previous descriptions they have been putatively identified as a subset of projections from chordotonal organs (9).

Dorsal view of the ventral surface. Anterior is to left. Adult CNS, T1 and T2 visible here. Scale bar is 50µm

References

1. Koto,M. et .al. Brain Res. 221:213-217 (1981)
2. Power,M.E. J.Comp.Neurol. 88: 347-409 (1948)
3. Bacon,J.P. & Strausfeld,N.J. J.Comp.Physiol. A 158: 529-548 (1986)
4. Tanouye, M.A. & Wyman,R.J. J.Neurophysiol. 44: 405-421 (1980)
5. Thomas,J.B. & Wyman,R.J. Nature 298: 12 (1982)
6. Trimarchi,J.R. and A.M. Schneiderman J. Exp. Biol. 177: 149-167 (1993)
7. Phelan,P. et .al. J.Neuroscience 116: 1101-1113 (1996)
8. Strausfeld,N.J. Atlas of an Insect Brain (1976) Springer-Verlag
9. Phillis,R. et al Development 122 (10): 2955-2963 (1996)

Return to Flybrain

Appendix 10.2.

Allen,M.J., Drummond,J.A. & Moffat,K.G. (1998). Development of the Giant Fibre Neuron of *Drosophila melanogaster*. *Journal of Comparative Neurology* **397**:519-531.

THE JOURNAL OF COMPARATIVE NEUROLOGY 397:519–531 (1998)

Development of the Giant Fiber Neuron of *Drosophila melanogaster*

MARCUS J. ALLEN, JAMES A. DRUMMOND, AND KEVIN G. MOFFAT*
Department of Biological Sciences, University of Warwick,
Coventry CV4 7AL, United Kingdom

ABSTRACT

The giant fiber system (GFS) of *Drosophila melanogaster* provides a convenient system in which to study neural development. It mediates escape behaviour through a small number of neurons, including the giant fibers (GFs), to innervate the tergotrochantral jump muscle (TTM) and the dorsal longitudinal flight muscles.

The GFS has been intensively studied physiologically in both wild-type and mutant flies, and is often used as a system to study the effects of neural mutations on the physiology of the adult nervous system. Recently, much information has been gleaned as to how and when synaptogenesis, with its major target neurons, is achieved. However, little is known of the earlier development of this neuron. Here we have used an enhancer-trap, marking parts of the GFS, in conjunction with BrdU labelling, to attempt to follow the birth, axonogenesis, and the early morphological meeting of the GFs with their target neurons. From these anatomical observations we propose that the GF cell is not born during the larval or pupal stages and, therefore, appears to be a persistent embryonic cell. The axons of the GFs develop during the third instar. During the early pupal stages the GFs contact other identified neurons of the GFS. In addition, we see some aberrant development of the network, with some flies carrying only one GF, and yet others with extended axons.

We present a model for the initial joining of the GFs and tergotrochanteral motorneurons (TTMns). J. Comp. Neurol. 397:519–531, 1998.

Indexing terms: insect; neural; axon; development; enhancer-trap; GAL4

The establishment of the correct connections between identified neurons is a major focus of research in both vertebrates and invertebrates, where, in both, many of the same molecular families are involved (Goodman and Shatz, 1993; Tessier-Lavigne and Goodman, 1996). In *Drosophila melanogaster*, much effort has lead to the identification of mutants with defects in neural trajectory and pathfinding in the developing embryonic nervous system (Seeger et al., 1993; Van Vactor et al., 1993). However, less is known about the mechanisms underlying neural connections formed through larval and pupal central nervous system (CNS) development where the landscape for the developing neurons is very different from that found in the embryo. It is now possible, with new genetic markers (Brand and Dormand, 1995), to follow the early development of specific cells that are known to be part of identified adult circuits or structures. For example, Smith and Shepherd (1996) have recently described the development of sensory neurons, and their central projections, during metamorphosis in *Drosophila*. The GFS of *Drosophila* is an adult circuit comprising a small number of neurons (see Fig. 1), known to be involved in certain escape behaviors (Thomas and Wyman, 1982; Trimarchi and Schneiderman, 1995a,b), whose development should also be suitable for such analysis.

The aptly named giant fibers (GFs) of *Drosophila* were first described by Power (1948), and are a pair of large bilaterally symmetrical interneurons approximately 8 mm in diameter. The study of Koto et al. (1981) presented the first morphological description of the GF neuron by using intracellular injection of Lucifer yellow. This study, and more recent descriptions (Phelan et al., 1996; Sun and Wyman, 1996), show that the distinctive cell body of each neuron is located near the posterior border of the brain, adjacent to the neuropil of the protocerebrum, approximately 30 μm dorsal to the oesophageal canal. A thin neurite, 60 μm long, extends from the cell body ventrally and posteriorly. The dendritic field, composed of dorsome-

Grant sponsor: Wellcome Trust; Grant number 041999/Z/94/Z.

*Correspondence to: Kevin G. Moffat, Department of Biological Sciences, University of Warwick, Coventry CV4 7AL, United Kingdom.
E-mail km@dna.bio.warwick.ac.uk

Received February 26 1998; Revised March 24 1998; Accepted March 31 1998

dial, ventrolateral and posterolateral processes, branch from the end of the neurite at the point where the giant axon initiates. The axon projects dorsally and posteriomedially towards the ventral midline, before ascending past the oesophageal canal and through the dorsal region of the cervical connective to the mesothoracic neuromere (T2). Here the neuron makes two identified electrical synaptic connections. The first, near the inframedial bridge at a tuft of collaterals, is with the peripherally synapsing interneuron (PSI; Tanouye and Wyman, 1980). The second, after a lateral bend, is with the large tergotrochanteral motorneuron (TTMn; Thomas and Wyman, 1982). The PSI projects across the ganglion and chemically synapses onto the five dorsal longitudinal motorneurons (DLMns) of the contralateral dorsal longitudinal flight muscles (DLMs), which are fibrillar indirect flight muscles (Tanouye and Wyman, 1980). The TTMn innervates the ipsilateral tergotrochanteral muscle (TTM), also known as the jump muscle or flight starter muscle. In addition, there is good evidence that the GFs also activate other neurons during escape behaviour. These include the motorneurons for the bilateral anterior pleural number 3 muscles, controlling abduction of the wings to their flight position; the tibial levator motorneuron, responsible for femur-tibia joint extension; and the dorsal ventral muscle motorneurons, innervating the antagonistic muscles to the DLMs to generate wing movements necessary for initiation and maintenance of flight during escape behaviour (Trimarchi and Schneiderman, 1993).

The giant fiber system has provided a neural circuit in which to combine genetic, molecular, electrophysiological and behavioral analyses on a group of identified neurons. It has been used as a model system to study the affects of gene mutations on the functioning of an adult neural circuit in vivo. For example Pavlidis and Tanouye (1995) analyzed the effects of bang-sensitive behavioral phenotypes on various electrophysiological aspects of the GF pathway.

Behavioral screens, based upon the stereotypic activation of the escape response, were used to isolate two mutant genes, *bendless* and an allele of the *shaking-B* locus (Thomas and Wyman, 1984). bendless flies fail to show the terminal bend of the GF and do not subsequently form direct synapses with the TTMns. The *bendless* gene has subsequently been cloned (Muralidhar and Thomas, 1993; Oh et al., 1994) and shown to be a ubiquitin-conjugating enzyme with a suggested role in controlling growth cone movements. Flies carrying certain alleles of *shaking B* are also known to be deficient in escape behavior. Thomas and Wyman (1984) showed that such mutations disrupt transmission at the GF-TTMn synapse and probably the GF-PSI synapse. This has been demonstrated to be directly due to the prevention of electrical synapse formation or maintenance (Phelan et al., 1996; Sun and Wyman, 1996). The GFS has therefore become an important invertebrate model to study neural development and connectivity (Krishnan et al., 1993; Phelan et al., 1996; Sun and Wyman, 1996).

Enhancer trapping has provided a means of marking neuronal cells during development (Ghysen and O'Kane, 1989). Recently P[GAL4] enhancer trapping (Brand and Perrimon, 1993) has been used for a range of investigations into the nervous system (see Brand and Dormand, 1995 for review). P[GAL4] enhancer-traps can be used as a powerful means of revealing axon trajectory (Phillis et al., 1996) and neuronal complexity (Smith and Shepherd, 1996; Yang et al., 1995). The simplicity of the technique allows a large number of preparations to be analyzed and can, therefore, be applied to studies which would be too laborious with more traditional methods. Given the large number of enhancer-trap lines that are now available, this approach can applied to many different neurobiological problems.

This account proposes an early, prelarval origin of the GFs by using an enhancer-trap and BrdU labeling. We have used an enhancer-trap to the GFS to follow early axonogenesis of the GF and found this to occur during the larval stages. We examined neurogenesis in the larval central nervous system (CNS) by detecting the incorporation of 5-bromo-2'-deoxyuridine (BrdU) into the DNA of replicating cells and report no colocalization of BrdU and the enhancer-trap marker in the GFs. This indicates that the final division producing the GF cell pre-dates the larval period. In addition, we have used the enhancer-trap to observe the early development of the major neurons of the GFS and their assembly to form this neural circuit.

MATERIALS AND METHODS

Drosophila stocks and culture

Drosophila melanogaster (Canton S) were raised at 25°C by using standard procedures (Ashburner, 1989). The line P[GAL4]A307 was originally isolated in this laboratory and has previously been described (Drummond et al., 1997; Phelan et al., 1996; Sun and Wyman, 1996; Smith et al., 1996). The UAS-*lacZ* reporter line was a gift from A. Brand (University of Cambridge, UK). Metamorphosis was staged by careful inspection of morphology exactly as described by Bainbridge and Bownes (1981). We found this more accurate than simple timing as developmental rates can vary between batches and individuals.

Treatment with BrdU

BrdU labeling was performed to identify timing of neuron differentiation.

Reagents for BrdU labeling were obtained from a cell proliferation kit (Amersham, Buckinghamshire, UK).

Overnight (16 hours) and daytime (8 hours) collections of embryos were aged for the appropriate amount of time, and the larvae were transferred to small Petri dishes containing labeling media (0.2% glucose, 3% agar, and 1 mg BrdU/ml). After feeding, larvae were transferred to vials containing standard media and allowed to complete development.

Nervous system dissection

Dissection of adult and pupal nervous systems was performed in PBS (0.1M $NaPO_4$, pH 7.3, 0.1M NaCl). Permeabilization was then achieved by bathing in PBS-Tx (0.1M $NaPO_4$, pH 7.3, 0.1M NaCl, 0.1% Triton X-100) for approximately 15 minutes. Alternatively, dissection was performed in PBS-Tx, thereby negating the extra bathing step. This is a modified procedure of that described by Armstrong et al. (1995)

Immunocytochemistry

Method adapted from Armstrong et al. (1995). Nervous systems dissected as described above were washed in PBS

and fixed for 30 minutes at room temperature in 4% paraformaldehyde. After blocking for 2 hours in PAT (0.1 M $NaPO_4$, pH 7.3, 0.1 M NaCl, 1% BSA w/v, and 0.1% Triton X-100), the preparations were incubated overnight in a 1:4,000 dilution of a rabbit anti-β-galactosidase polyclonal antibody (Cappel, Tunhout, Belgium). After at least 3× 1 hour washes in PAT, a biotinylated goat anti-rabbit secondary (Vector Laboratories, Burlingame, CA) was applied at a 1:100 dilution and incubated overnight at room temperature. After further washing, detection was then achieved using a Vectastain ABC kit (Vector Laboratories, Burlingame, CA) and staining with diaminobenzidine (DAB) in 0.1 M Tris.HCl (pH 6.8) and 0.1% H_2O_2. Following dehydration in alcohol, preparations were cleared in Xylene and mounted in DePeX (BDH, Ltd., Poole, Dorset, UK).

Staining for β-galactosidase (LacZ) and BrdU detection

Nervous systems dissected as described above were washed in PBS and fixed for 5 minutes at room temperature in 4% paraformaldehyde. The fixative was washed out with two rinses in PBS, replaced with staining solution (0.1 M $NaPO_4$, pH 7.3, 0.15 M NaCl, 5 mM $Fe[III]K_3(CN)_6$, 5 mM $Fe[II]K_4(CN)_6$, and 0.2% X-gal; Sigma, Poole, Dorset, UK) and incubated only until the GF cell bodies were visible. After a further wash in PBS, the preparations were treated with 2 N HCl in PBS-Tx for 30 minutes to denature the DNA and expose the incorporated BrdU. Reagents for BrdU detection were obtained from a cell proliferation kit (Amersham), briefly, after washing in PBS-Tx and then blocking for 2 hours in PAT, the preparations were incubated overnight in a 1:100 dilution of a mouse anti-BrdU monoclonal antibody (Amersham). After at least 3× 1 hour washes in PAT, a goat anti-mouse secondary antibody conjugated to crystalline tetramethylrhodamine isothiocyanate (TRITC; Vector Laboratories) was applied at a 1:40 dilution and incubated overnight in the dark at room temperature.

Microscopy

DAB-stained preparations were examined with a Zeiss Axioskop FS. Fluorescence and double-labeled preparations were viewed on a Nikon Optiphot by using a UV source and a DM580 Rodamine filter.

Image capture and processing

Images were captured from the Zeiss Axioskop FS by using a JVC TK-1280E video camera directly linked to an Apple MacIntosh 7100 80/AV. The images were processed on both Apple MacIntosh and PC's using Powerpoint (Microsoft Corp., Redmond, WA) and Canvas (Deneba, South Miami, Florida) software packages.

RESULTS

Enhancer trapping the GFS

Enhancer trapping has provided a wealth of information on the development of the embryonic nervous system of *Drosophila* (Ghysen and O'Kane, 1989). P[GAL4] enhancer trapping (Brand and Perrimon, 1993) has allowed not only the cell bodies of neurons to be studied but also by expressing cytoplasmic markers has allowed the visualization of axonal and dendritic processes (Smith and Sheperd, 1996). The P[GAL4] line described here, A307, was isolated in a screen for adult CNS expression patterns (K.G.M and C.J. O'Kane, unpublished results). The results presented describe the development of the enhancer-trap pattern with reference to the GFS. A previous description of the development of the GF pattern of A307 after staining with X-gal has been reported by one of us (KGM, Phelan et al., 1996); however the use of antibodies, to detect LacZ protein, reveals much higher resolution of the pattern. We dissected the CNS from 113 adult progeny (Table 1.) from a cross between A307 and a UAS-*lacZ* "reporter" line and immunohistochemically stained for LacZ protein. The final adult pattern has been previously reported (Drummond et al. 1997). The most striking element of the adult A307 pattern is the LacZ expression in a pair of large descending neurons in the CNS (Figs. 1B, 2B). The cell body is located just below the dorsal protocerebral surface. A thin neurite extends ventrally before enlarging to form the dendritic arborizations. The major dendritic arborization projects posterolaterally and ventrally, arborizing in the deutocerebrum. Minor dendrites project ventrolaterally and dorsomedially (Fig. 2B). The latter follow the path of the giant commissure interneurons which are also marked with A307 (Fig. 2C). The axon runs posteriorly towards the ventral midline, and projects dorsally, exiting the brain along the dorsal midline of the cervical connective. It projects unbranched through the prothoracic neuromere (T1), until reaching the mesothoracic neuromere (T2) where it turns ventrally and laterally towards the edge of the ganglion (Fig. 2D). The position and size of the cell body, the trajectory of the axon, and the characteristic terminal bend, distinguish this cell as the GF described previously by others in *Drosophila* (Koto et al., 1981) and in larger flies (Bacon and Strausfeld, 1986). The *Drosophila* giant fiber is slightly different to that found in *Calliphora* and *Musca*, as it does not reach the edge of the ganglion. A variety of other cells in the thoracic and abdominal neuromeres are also clearly marked in A307, amongst them, cells that have locations that are equivalent to those occupied by the PSI and TTMn (Fig. 2D) as identified by intracellular dye fills (Baird et al., 1993; Koto et al., 1981; Phelan et al., 1996). Other stained neurons in the brain are not so easily identified.

TABLE 1. Developmental Stages of the CNSs, Dissected and Stained for LacZ Expression[1]

Stages from Bainbridge and Bownes	Approximate timing APF (hours)	CNSs dissected
(L3)	—	393
P1(WPP)	0–1	77
P2–3	1–7	17
P4(i)–5(i)	7–13.5	7.5
P5(i)	12.5–48	274
P5(i)–6	14–48	35.5
P7–9	34–78	18.5
P10–12(i)	72.5–97	16.5
P12(i)–15(i)	75–105	16
Adults	—	113
Total		968

[1]WPP, white prepupae; APF, after puparium formation.

A307 marks the GF cells from the 3rd larval instar to adulthood

To determine whether A307 highlighted the GFs during development, 855 UAS-*lacZ*;A307 larval and pupal nervous systems were dissected (Table 1) and LacZ detected

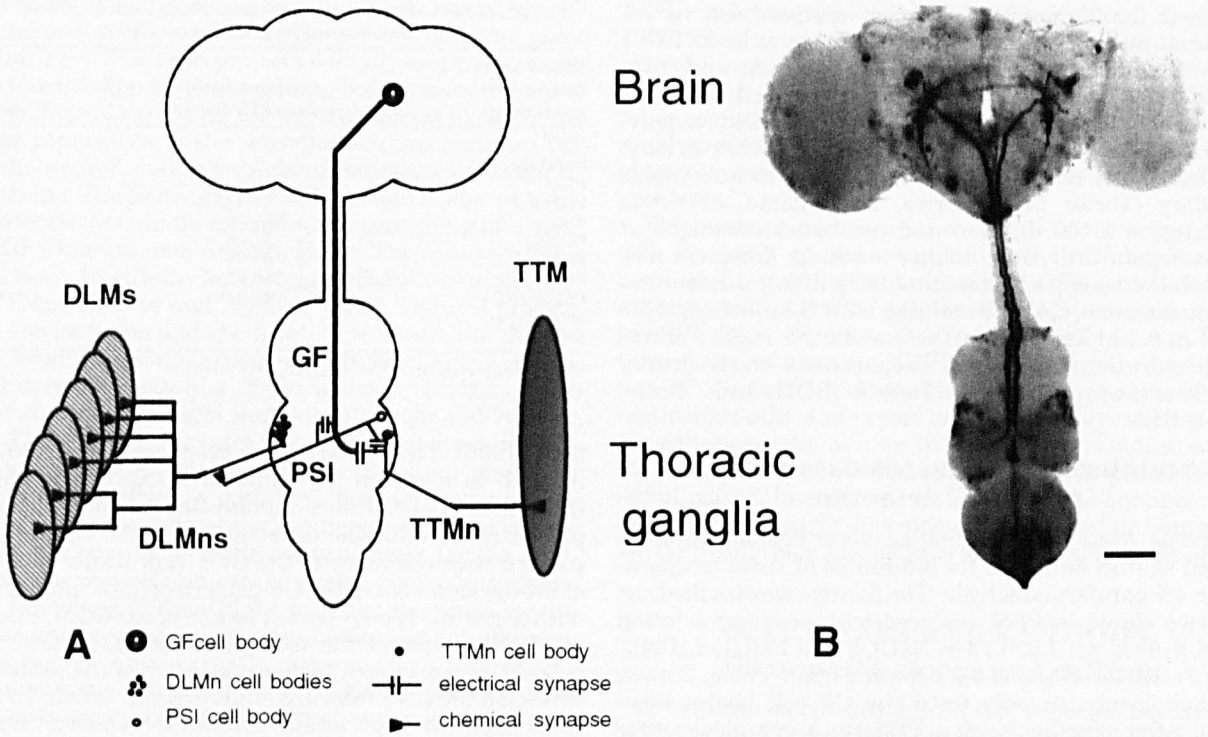

Fig. 1. The giant fiber system (GFS) of *Drosophila*. **A:** Schematic diagram of the identified neurons and muscles of the GFS. Only one half of the bilateral circuit is shown. The giant fiber (GF) interneuron relays information from the brain to the second thoracic neuromere. Here it electrically synapses with the peripherally synapsing interneuron (PSI) and the tergotrochanteral motorneuron (TTMn). The PSI makes chemical synapses with the dorsal longitudinal motorneurons (DLMns) that drive the six wing depressor muscles (the dorsal longitudinal muscles or DLMs). The TTMn drives the jump muscle (the tergotrochanteral muscle or TTM). Adapted in part from King and Wyman (1980) and Sun and Wyman (1996). **B:** Adult expression pattern of A307. The CNS has been stained for LacZ protein by immunocytochemistry. Expression is clearly seen in the GF cells and in other unidentified cells in the brain and thoracic ganglia. This is a montage image processed on Canvas software. Anterior is top. Scale bar = 100 μm.

immunologically. Two large bilaterally symmetrical perikaryon were seen near the dorsal surface of the protocerebrum throughout development (Fig. 3A–H). These are in the correct position and are of the appropriate size to be the GF cell bodies (Phelan et al., 1996). These cell bodies have a very characteristic pear-shape during early development (Fig. 3A–C). From the P5(ii) pupal stage onwards these same dorsal cells (Fig. 3D–H) can be identified as the GF cell bodies by the connection of their neurite to the giant axons, although these connections are out of focus in Figure 3 (see Fig. 6B). We are confident that the large perikaryon seen at earlier stages are indeed the GF cells. Preparations covering all developmental stages were analysed and these perikaryon were seen continuously. Thus, the possibility that the enhancer-trap marks different cells, in two very close developmental time windows, is unlikely; in addition we neither observed the absence of GF-like cell staining nor the presence of more than two GF-like cells.

We reasoned that following the very early development of the neuron would be difficult with the enhancer-trap as, logically, there would be a lag between the activation of GAL4 and the expression and translation of *lacZ* in the binary system. Such a lag would mean that LacZ may not be expressed in the GF cell body when the cell was first born. Also, preparing whole mount CNS of early larval stages is technically difficult, due to their small size, and we observed background staining with little definition (data not shown).

Larval CNS neurogenesis (BrdU/LacZ colocalization)

The immunohistochemical data suggested that the GF cells were present in the late larval stages and therefore the final division producing them occurred earlier in larval life. To determine when the GFs are born, staged larvae of genotype UAS-*lacZ*; A307 were fed BrdU in different eight hour windows covering the three larval instars (Fig. 4C). After feeding they were allowed to continue development on standard food. Adult flies emerging after such treatment (553) were then dissected and the GF cell bodies identified in the CNS. LacZ was detected enzymatically using X-gal as the substrate. BrdU incorporation, by those cells dividing during feeding, was detected with a TRITC conjugated antibody. Adult flies hatching from larvae fed for 8 hours 24–40 hours after egg laying (AEL) clearly showed no colocalization of BrdU and LacZ in the GF cell bodies (Fig. 4A). In preparations from flies fed at 48–64 hours AEL no colocalization was seen in the GF cell bodies but colocalization of BrdU was observed in other cells in the brain that expressed LacZ (Fig. 4B). The CNS preparations of adult flies, hatching from larvae fed for all the allotted time points throughout larval life (Table 2), also showed some colocalization in LacZ positive cells, in the brain and thoracic ganglion, but never in the giant fiber cell bodies (data not shown). As a control we incorporated BrdU into early first instar larval progeny of a cross between the UAS-*lacZ* reporter line and another P[GAL4]

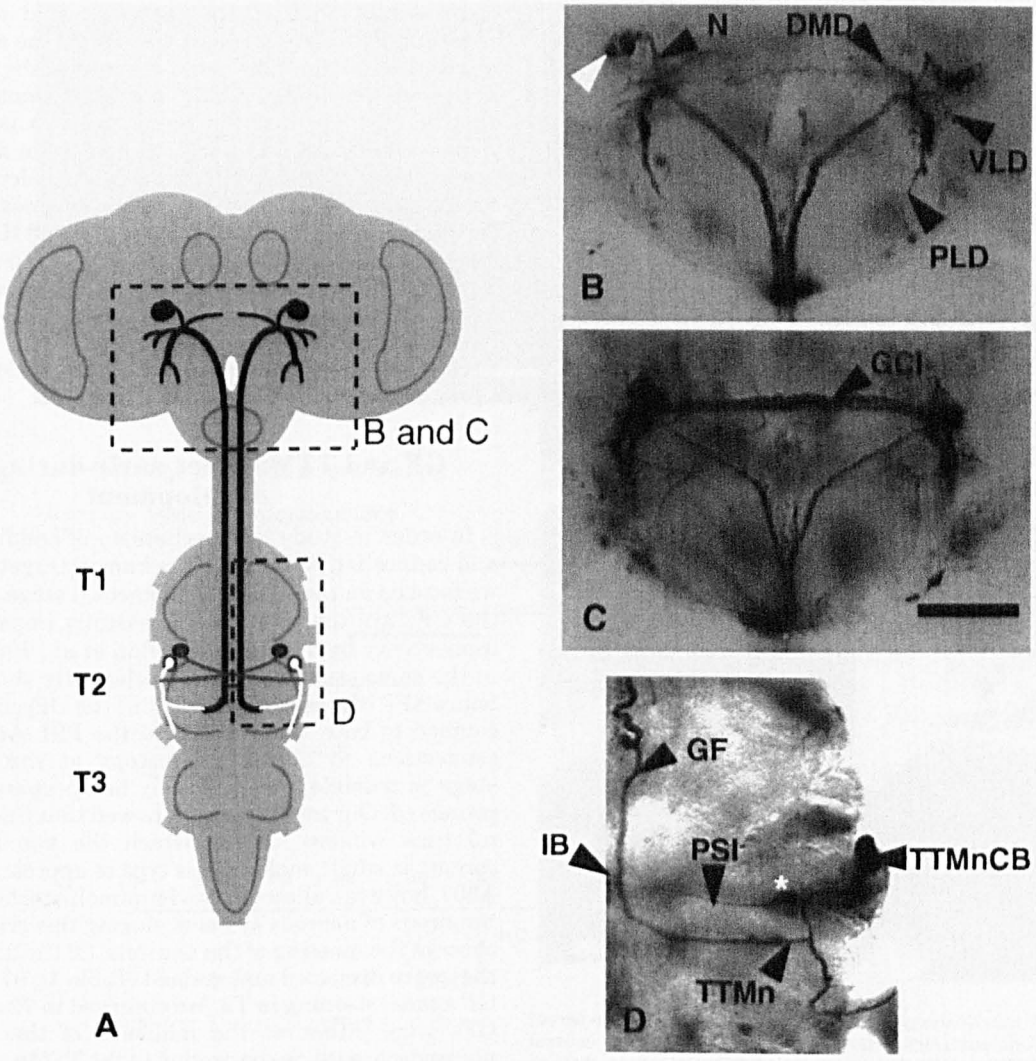

Fig. 2. Expression pattern of enhancer-trap line A307 reveals the giant fiber system (GFS). **A:** Schematic diagram of the central nervous system (CNS) indicating the regions of the brain or thoracic ganglia shown in B-D. T1 (Prothoracic neuromere),T2 (Mesothoracic neuromere), and T3 (Metathoracic neuromere). **B:** A montage of serial focal planes of the supraoesophogeal ganglion showing the neurite (N) projecting from the giant fiber cell body (GFCB, white arrowhead) to the axon and characteristic GF dendritic field. This comprises the dorsal medial dendrite (DMD), the ventral lateral dendrite (VLD), and the large posterior lateral dendrite (PLD). **C:** The pattern also shows the giant commisural internerons (GCI) connecting with the GF dendritic field. **D:** A montage of serial focal planes of the thoracic ganglia from a pupal CNS clearly expose other neurons of the GFS including the peripherally synapsing interneuron (PSI) with its cell body and axon projecting medially where it synapses with the GFs at the inframedial bridge (IB). The tergotrochanteral motorneuron (TTMn) can also be seen with its cell body (B) and distinctive projections with link to the GF. Anterior is top. Scale bars = 100 μm in B,C, 50 μm in D.

line, A107. This line expresses in the mushroom bodies (Smith et al., 1996). The only neuroblasts known to be continually dividing during this early larval stage are those of the mushroom bodies (Ito and Hotta, 1992). The CNS from seven adults following this treatment were dissected and colocalization of BrdU with LacZ was seen in several of the mushroom body cells in all the preparations (data not shown).

Axonogenesis of the GF neuron

Axonogenesis of the GFs could first be detected during the late third instar larval stage. By which time the axons had extended into the prothoracic neuromere (T1; Fig. 5A,B). We frequently observed the staining of only one axon at this time, presumably this reflects accidental removal of peripheral cells during dissection, as occasionally both axons were visible, yet only one cell body. The example shown in Figure 5A also shows that the single axon visible has extended as far as the future T1. Only the distal end of the axon and cell body are in focus in Figure 5A due to the shape of the CNS at this stage. In the preparation itself the axon can be followed back to the cell body via a neurite extending anterodorsally. By the stage of white prepuparium formation (WPP) the axons are at the T1/T2 border (Fig. 5B). Careful examination of the preparation revealed that the left giant fiber had extended into T2. Although we have not been able to clearly see a splayed growth cone, we have noticed that many times

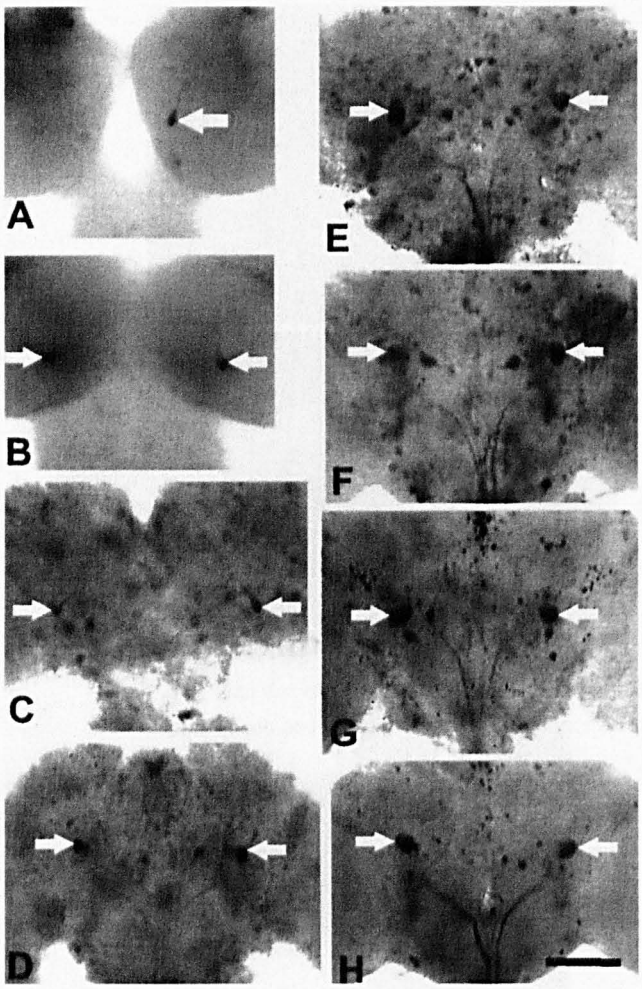

Fig. 3. A307 marks the giant fiber (GF) cells through late larval and pupal development. Dorsal views of the brain region of the central nervous system (CNS) at several stages through development, stained for LacZ protein by immunocytochemistry. Intense staining is seen in two large perikaryon (arrows, shown in focus) which can be identified as the GF cell bodies after pupal stage (P5). **A:** larval third instar (L3); **B:** white prepupal stage (WPP); **C:** P4(ii); **D:** P5(ii); **E:** P8; **F:** P11; **G:** P15(i); **H:** adult. Anterior is top. Scale bars = 50 μm in A,B, 100 μm in C-H.

staining is seen more strongly near the distal tip of the axon than in the middle.

All other pupal stages were staged from white prepupae according to Bainbridge and Bownes (1981; Table 1). By the end of stage P3 (7 hours APF) the GF axons had reached the mid point of T2. By the end of stage P4(ii) (13.5 hours APF) the axon has thickened slightly to ~2μm, and can be clearly seen (Fig. 6A,D). In several preparations the axon appeared to be in contact with another neuron, probably the TTMn, marked by A307. By stages P5(ii)-P6 each GF appeared to be linked to both its target neurons the TTMn and PSI (Fig. 6E) and had essentially reached their adult shape with characteristic bend. The axon is still however only 2–3μm thick and the boundary between the GF and TTMn is indistinguishable at this level of resolution. During this stage the enhancer-trap pattern becomes much more elaborate with many cells starting to stain. Arborization of the dendritic field also becomes apparent (Fig. 6B). During stages P7-P9 the axon thickens reaching approximately three quarters of the adult dimensions (≅6 μm). The TTMn however, remains 2–3 μm allowing the boundary between the two neurons to be visualized (Fig. 6F). Dendritic arborization also increases in complexity (Fig. 6C). The growth of the dendritic field is concomitant with the onset of synaptogenesis within the developing optic lobe (Meinhertzhagen and Hanson, 1993). The axon and dendrites can be observed also to be thickening from stage P7 onwards. The mechanism for this is unknown. The thickening of the GFs continues to eclosion, reaching their final 7–8 μm.

The observed development of the GFs, TTMn, and PSI is summarized in pictorial form in Figure 7.

GF and TTMn meet early during pupal development

In order to study the mechanism of bending of the GF and connection with one of its known targets, the TTMn, we focused on the P5(i) developmental stage. At this stage the GFs are too small to successfully impale and study connectivity by dye filling (Phelan et al., 1996). However, in the same study the authors elegantly show that by 48 hours APF (the end of stage P5[ii]) the GFs are electrically coupled to both the TTMn and the PSI. Analysis of the connections by electronmicroscopy at the earlier P5(i) stage is possible, but relatively few preparations can be processed. Our initial results showed that the developmental time window, during which the two neurons first contact is small, making this type of approach unrealistic. A307, however, allowed us to immunohistochemically stain hundreds of nervous systems, during this critical stage, to observe the meeting of the neurons. Of the 274 pupal CNS that were dissected and stained (Table 1), 97 showed clear GF axonal staining in T2. We observed in 72 cases that the GFs were either at the midpoint of the mesothoracic neuromere, with no connection to the TTMn apparent (Fig. 6D), or the GFs showed their characteristic bends and connection to the TTMn appeared complete (Fig. 6E). In 25 cases we observed what we consider to be the transitional stage. Three such examples are illustrated in Figure 8. In the first (Fig. 8A) , the GFs can be seen at the mid point of the mesothoracic neuromere. Two neurons can be seen projecting in from the periphery (one marked with arrowhead). These appear to make contact with the ends of the GFs (the marked neuron's connection is out of focus). This contact appears to be made almost at right angles to the GF. Both neurons can be followed back to cell bodies in appropriate positions to be the TTMn cell bodies. The inframedial bridge can also be seen forming between the two GFs (marked with asterisk). In the second example (Fig. 8B) a similar scenario is observed with two neurons making contact with the GFs. In this case, it appears that the one of the neurons (marked with arrowhead) has slightly overshot the position where it should meet its corresponding GF. We have observed other preparations where it appears that the two incoming neurons have connected with the GFs not at the distal tips but more proximal. This seemed to occur when the GFs had projected beyond the mid point of T2 often into T3 as in the example shown (Fig. 8C).

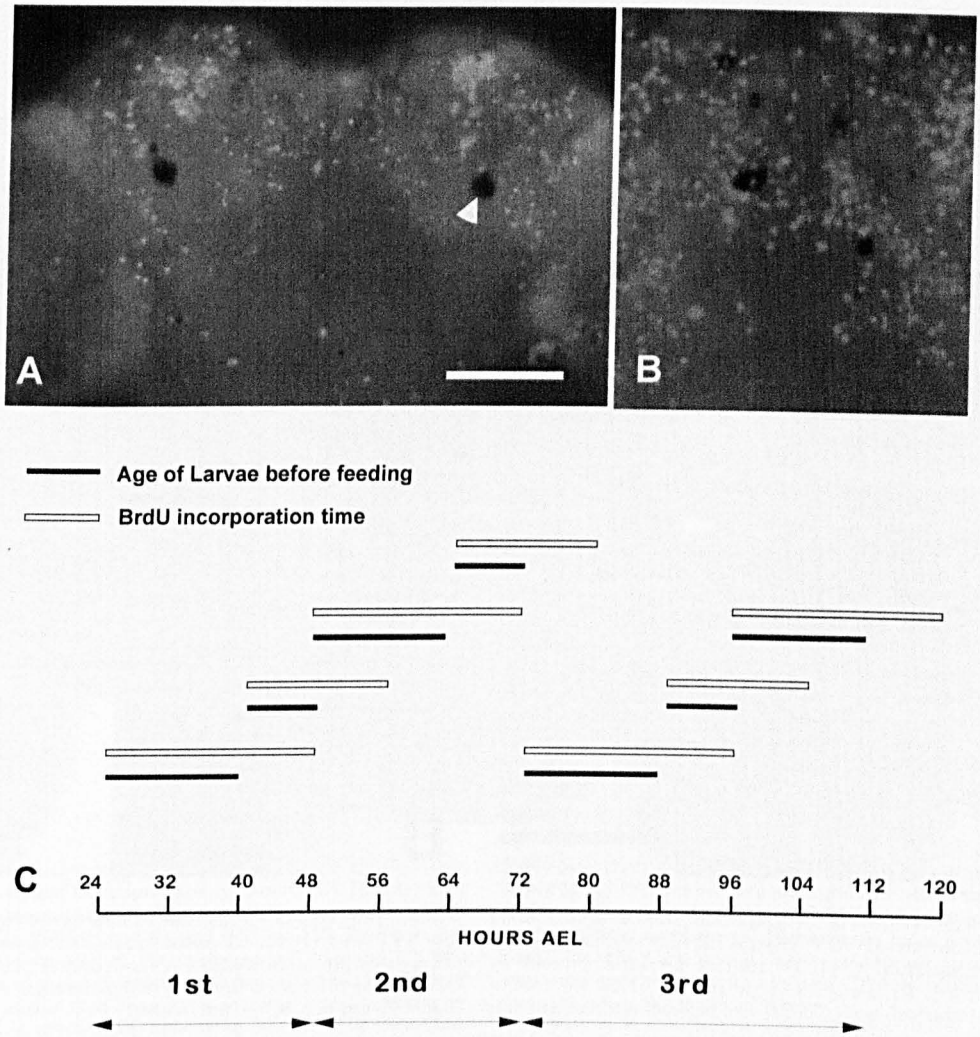

Fig. 4. BrdU fails to colocalize with the giant fibers (GFs) when administered during larval stages. **A:** Adult brain, 1–3 days post eclosion, from a UAS-*lacZ*;A307 fly fed on a diet containing BrdU 24–40 hours after egg laying (AEL) and stained for LacZ activity and BrdU incorporation. X-gal staining (dark and non-fluorescent) reveals the giant fiber cell bodies (one marked with arrowhead) and other cells in the brain. Antibody detection of incorporated BrdU molecules (fluorescent) shows many cells have persisted from larval life. No colocalization can be seen in the giant fibers. Anterior is top. **B:** High power of adult brain, 1–3 days post eclosion, from a UAS-*lacZ*;A307 fly fed on a diet containing BrdU, 48–64 hours AEL, stained for LacZ activity and BrdU incorporation. Colocalization of the two signals can be seen in several cells. Anterior is top. **C:** Pulses of BrdU during larval life. The lower bars (black) indicate the age range (AEL) of the UAS-*lacZ*;A307 larvae at the start of the 8 hour feeding. The upper bars (white) indicate the total time that dividing cells could have incorporated BrdU during each feeding. The larval instars are indicated below the timescale. Scale bar = 100 μm in A, 50 μm in B.

Aberrant development

We have previously reported the ablation of one giant fiber axon, having no affect on the growth or survival of the other (Smith et al., 1996). During the course of these experiments, we also observed two CNS preparations that clearly showed the presence of only one GF. In each case we clearly observed that only one GF cell body was present with normal dendritic and axonal morphology (Fig. 9A). Indeed only a single large axon was visible in the connective, where there should have been a pair (data not shown). This is clearly absence of a neuron as opposed to differential staining. Moreover, in T2 the single GF can be seen to make both bends to connect still with both TTMn target neurons (Fig. 9A). Closer examination of the preparation

TABLE 2. BrdU Treatment of ULZ-*lacZ;* A307 Larvae

Age before feeding (hours AEL)[1]	CNSs dissected
0–16	31
16–24	17
24–40	41
40–48	65
48–64	135
64–72	73
72–88	62
88–96	39
96–112	34
112–120	22
120–136	27
136–144	7
Total	553

[1]AEL, after egg laying.

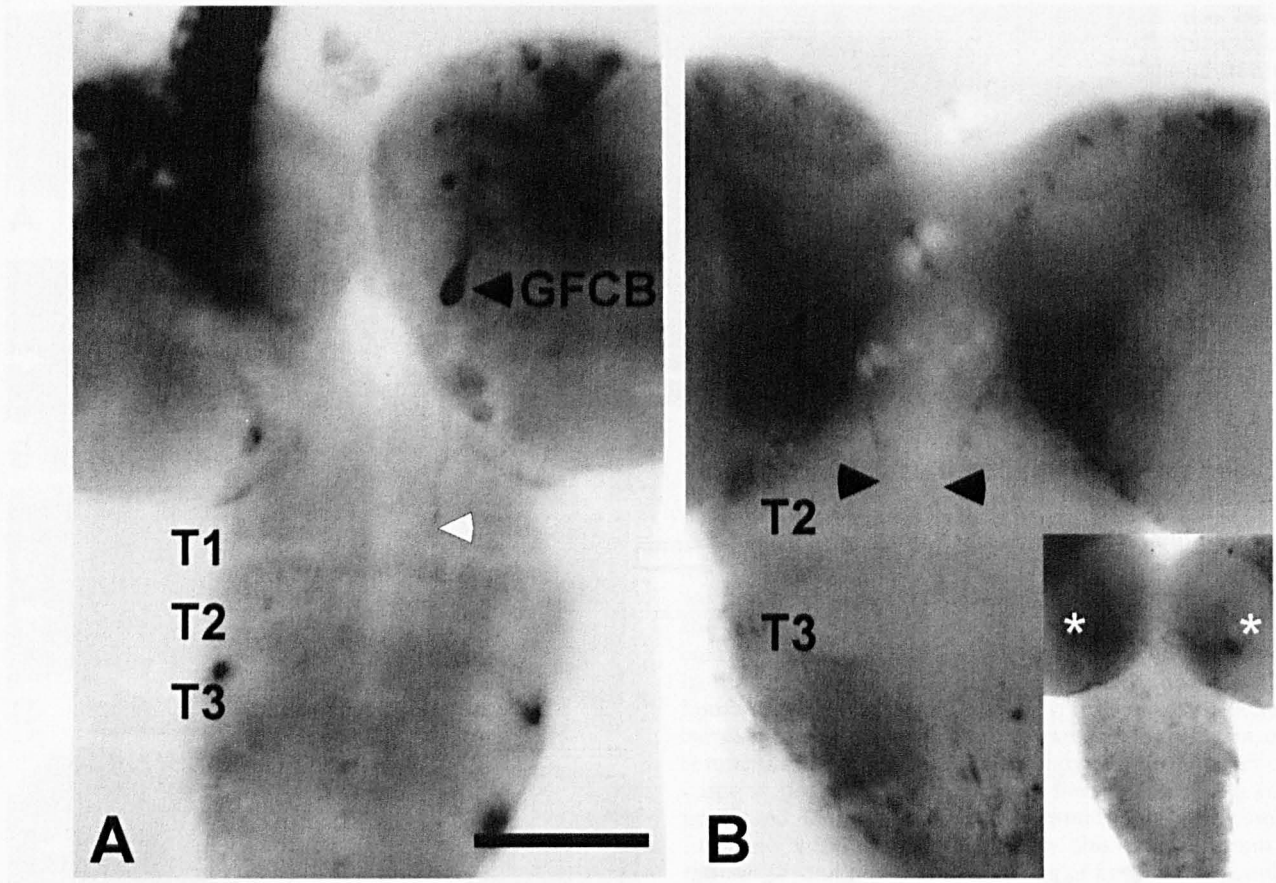

Fig. 5. Early axonogenesis of the giant fiber (GF) neuron. Dorsal views of a third instar larval (WPP) central nervous system (CNS; **A**) and a white prepuparium CNS (**B**) stained for LacZ protein by immunocytochemistry. By the third larval instar (A) the distinctive pear shaped giant fiber cell body (GFCB) can be seen and the axon has already projected down into the T1 neuromere (white arrowhead). By the WPP stage (B) the GF axons can be seen entering the presumptive T2 neuromere (arrowheads). A more dorsal plain of focus (B inset) reveals the cell bodies (marked with asterisks). Anterior is top. Scale bar = 75 μm in A,B, 150 μm in inset.

reveals that the TTMn, on the absent GF side of T2, appears to have joined with the outgrowing inframedial neurite of the remaining giant neuron.

Consistently, during development, the GF seemed to extend its axon into T3, as reported previously (Phelan et al., 1996). This was often seen to persist into adults (Fig. 9B–D), although on most occasions we assume the extensions degenerated during the remaining 50–60 hours of pupation. The nature of these extensions was variable but often involved them crossing the midline (Fig. 9B,C).

Given that we did not observe these extensions in the majority of preparations, and the variability of such extensions, persuades us that A307 is not marking other descending neurons that track down the same fascicle as the GF, emerging only after the GF has formed its lateral bend. Further, the thickness and continuity with the GF axons are consistent with them being true extensions of the GFs (Fig. 9D).

DISCUSSION

Birthdating the GF

Spatio-temporal analysis of neural proliferation has previously shown that adult neurons born early reside in more medial positions than their later counterparts (White and Kankel, 1978). From the position of the GF cells within the brain it has previously been suggested that they are born late, during postembryonic neuroblast proliferation (Koto et al., 1981; Phelan et al., 1996). We have described an enhancer-trap that clearly marks the GFS of *Drosophila*. We have performed an extensive pulse chase analysis of neurons born during larval development that persist in the adult CNS using the BrdU labeling technique (Truman and Bate, 1988). In association with the staining revealed by the enhancer-trap within the GF neuron, we have attempted to determine during which period of larval life the final cell division producing this neuron occurs. Our data suggests that the GF neuron is not born during pupal or larval development. We are confident of this result as we have analyzed over 550 preparations and, while we have seen colocalization of other cells marked by A307 and in another enhancer-trap line marking the mushroom bodies (data not shown), we have never observed colocalization in the GFs. Some quenching of the fluorescent BrdU labeling by the X-gal stain was observed in cells where the two colocalized. In such cases BrdU incorporation could still be detected but the intensity of fluorescence was less. In every preparation the GF cell bodies were identified by X-gal staining, position within the brain, size, and often by observation of

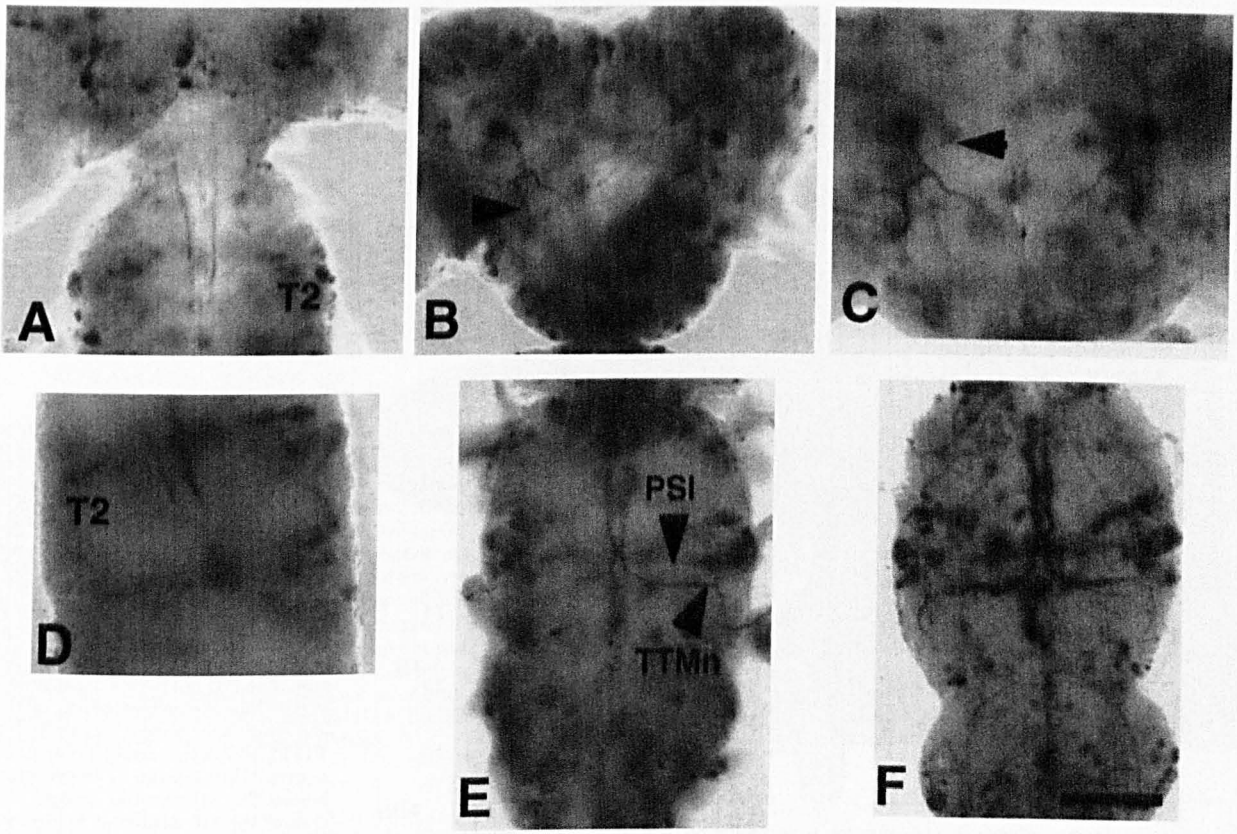

Fig. 6. **A–F:** Later development of the enhancer-trap pattern shows further elements of the giant fiber system (GFS). Dorsal views of pupal nervous systems stained for LacZ protein by immunocytochemistry: P4(ii)(A and D), P5(ii)(B and E), and P8(C and F). By P4(ii), the axons of the GFs can be seen at the midpoint of T2 (A and D). The distinctive cell bodies are clearly seen but no dendritic field has formed (A). By P5(ii) the dendritic field has started to stain, with the posterior lateral dendrite (PLD; arrowhead) appearing first (B). The GFs have made both connections with their targets, the peripherally synapsing interneuron (PSI) and tergotrochanteral motorneuron (TTMn; E). Between P7 and P9 the dendritic field increases in complexity with the ventral lateral dendrite (VLD) becoming more prominent (C, arrowhead), and the GFs thicken to approximately three quarters of the adult thickness ≅6 μm) while the TTMns remain at 2–3 μm (F). Anterior is top. Scale bar = 75 μm.

connection to the stained GF axons (although this was sometimes difficult due to non-consistent axon staining and the fact that the preparations were not cleared prior to mounting). The nucleus of the cells was easily distinguishable and we are confident that any colocalization, even with quenching, would have been detected. We cannot rule out the possibility that there is an unknown shortcoming in the BrdU technique for this particular cell lineage, although this would appear unlikely. We must therefore assume that the GF neuron has an embryonic origin. The implication of the data is that the GF cells, although born early, remain more peripheral in the ganglion during development. The mechanism for this is unclear but may require the cells to migrate.

Work from larger insects, such as the moth *Manduca sexta* (Levine and Truman, 1985) has provided much information on the changes to the nervous system of insects during metamorphosis. Most neurons of the adult nervous system are either born post embryonically from quiescent neuroblasts, or are remodeled from larval neurons, an example being the MN5 giant motor neuron (Truman et al., 1993). It has been estimated that larval neurons constitute up to 10% of adult neurons, and the larval motor neurons are mainly embryonic in origin (Truman et al., 1993). Further there is evidence from ablation studies in *Manduca* that many of the premotor interneurons may also have embryonic origins (Truman and Booker, 1986). Thus the proposal that the GF of *Drosophila* may also have an embryonic origin is not without precedent. If the GF neuron is a remodeled larval cell, we would expect to see early evidence of function such as larval dendrites. This is not apparent and suggests a novel mode of neural development in which a neuron is born embryonically, develops during late larval and pupal stages, and has no function until after eclosion. However, our analysis is restricted by the enhancer-trap used. A larval dendritic field may be present but cannot be seen at the resolution provided by A307. The GFs may also have larval targets that are not marked in the enhancer-trap line.

GF axonogenesis

Analysis of the enhancer-trap shows the GF cells to be labeled continuously through late larval and pupal development. At late pupal stages the GF cells can be positively identified by their distinctive axonal projections. The early staining perikaryon could also be seen projecting neurites. Initially these project anterodorsally, but their projections are more medial during early pupal stages, and are finally

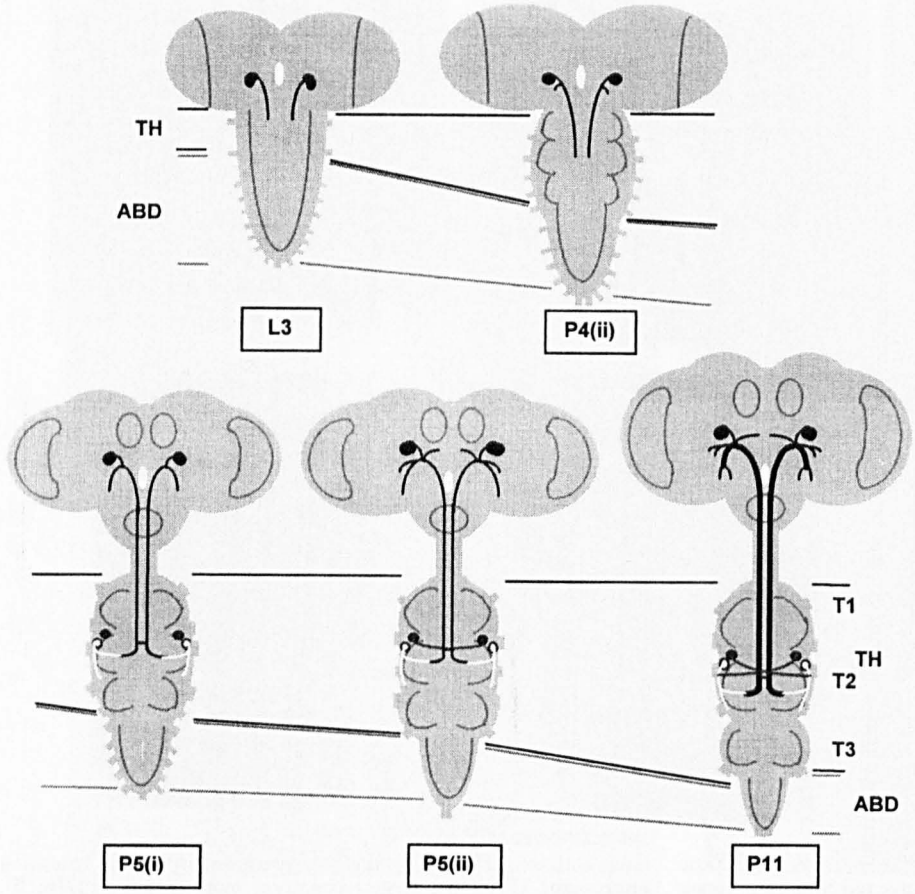

Fig. 7. Schematic of the observed development of the giant fiber system (GFS), highlighted by A307. L3: The GF cell bodies (in black) have already projected fine axons into the thoracic ventral nerve cord (future T1 region). P4(ii): The GF axons have reached their final position in the mesothoracic neuromere. P5(i): The dendrite of the tergotrochanteral motorneuron (TTMn; white) meets the GF axon. Elaboration of the GF dendritic field begins. The PSI cell bodies are visible (grey). P5(ii): The distinctive bends of the GFs are seen and appear connected to the TTMn, the peripherally synapsing interneuron (PSI) neuron is visible projecting across the inframedial bridge. Elaboration of the GF dendritic field continues. P11: The enhancer-trap pattern is fully developed showing the thick GF axons and elaborate dendritic field morphology.

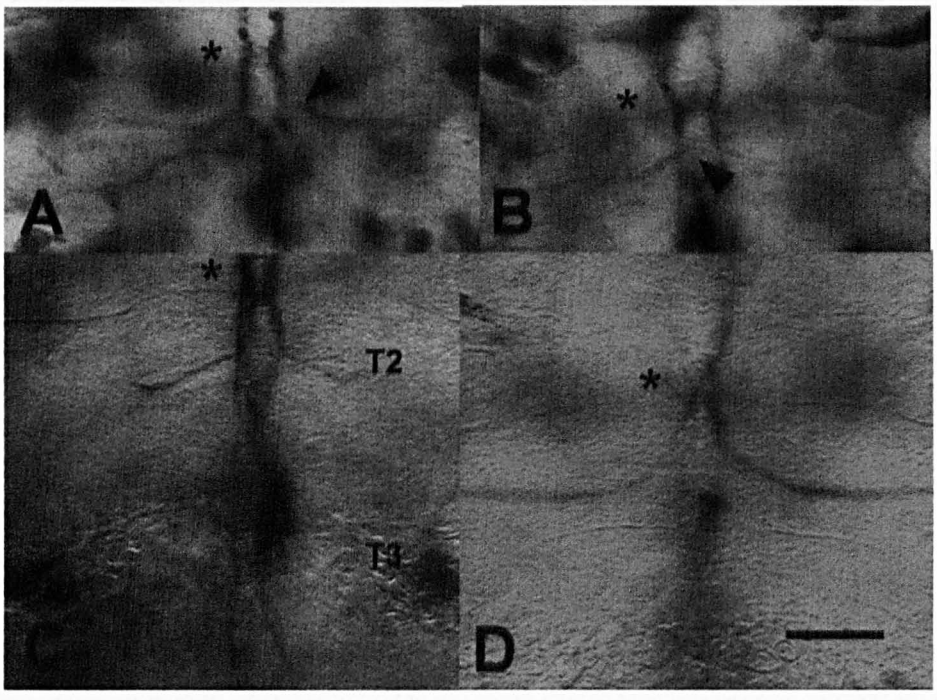

Fig. 8. Initial stages of tergotrochanteral motorneuron / giant fiber (TTMn/GF) contact. High-magnification dorsal views of the T2 neuromere of the central nervous system (CNS) from P5(i) pupae. Relatively few preparations from this stage showed this initial contact. Example **A** shows two incoming neurons contacting the distal tips of the GFs in an almost right angled fashion, one is marked with an arrowhead. Example **B** is similar, but it appears that one of the neurons has overshot its target (marked with arrowhead). Example **C** shows this same contact , but the GFs have extended into the T3 neuromere and therefore contact is not with the distal tips but more proximal. D shows a slightly later staged preparation in which the distinctive bending in T2 can be seen. This presumably is the end result of the contact shown in A and B. The boundary between the GF and TTMn cannot be resolved. In all examples the position of the developing inframedial bridge is marked with an asterisk. Anterior is top. Scale bar = 25 μm.

more ventral as the GF cells mature. We assign these alterations to the clear morphological changes in ganglion shape during these stages (Truman et al., 1993). Despite this, the observed neural projections could always be traced back to the GF cell body and therefore reflect the dynamic development of the neuron.

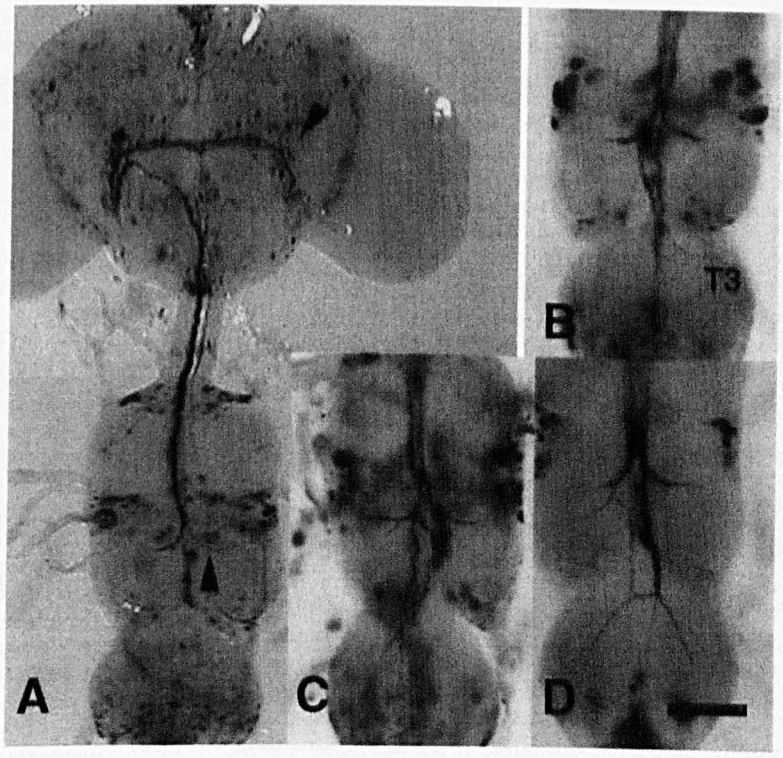

Fig. 9. Aberrations in the giant fiber system (GFS). Dorsal views of adult nervous systems 1–3 days post eclosion stained for LacZ protein by immunocytochemistry. A preparation of a central nervous system (CNS) that exhibits only one GF (**A**) clearly shows a missing GF cell body (GFCB) in the brain (upper arrowhead). At least some of the giant commisural interneurons are present and project correctly to the position of the dendritic field of the absent GF. In T2 the single GF appears to have connected with both tergotrochanteral motorneurons (TTMns). In focus (lower arrowhead in A) is the TTMn whose normal GF partner is absent. **B–D:** preparations that show GF extensions into the T3 neuromere. Anterior is top. Scale bar = 100 μm.

The ability to observe the early growth of the axon is obviously limited by technical constraints. The axons are too thin to impale and dye fill, and identification is problematic. However, the enhancer-trap approach using A307 has provided a method for observing early axonogenesis of the GFs. The major limitation of this enhancer-trap is that the resolution of the pattern within the GFs, the amount of LacZ produced and detected, is still limiting at this stage of development. The axon is first visible in L3 larvae by which time it is already present in the future T1 neuromere. During the WPP stage 30–40 minutes later, it can be seen entering T2. From these results we cannot make reasonable estimates of axonal growth rate for the GFs, as the majority of growth must occur before it is possible to detect them using this enhancer-trap. However the L3 and WPP data suggest growth between T1 and T2 is covered in 30–40 minutes. The extreme thinness of the GFs at these stages could lead to misinterpretation of the true distal tips of the axons, we do not know whether the LacZ is successfully transported to the distal end of the neuron. We did however notice, as previously described (Phelan et al., 1996) that there appears to be some differences between the growth of the two axons. It is not known whether A307 truly marks the GFs throughout their entire development. A307 does, however, show expression in cells in both the brain region and ventral nerve cord of the developing embryo (data not shown).

Connection of The TTMn to the GF

The apparent bending of the axons occurs during stage P5(i), by which time it appears, at the resolution presented, to be in contact with the TTMn. From the work of Phelan et al. (1996) we know that the electrical connections are present by 48 hours APF (end of stage P5[ii]). Our data suggests that the morphological bending occurs early in stage P5(i), and relatively quickly due to the low number of intermediate stage preparations seen.

The detailed analysis of the earliest events in the meeting of the GF and the TTMn presented here suggest that the bending of the GF occurs after the neurons have contacted, and possibly after the synapse has formed. Bending could be a result of fasciculation along the TTMn; indeed Figure 8A does show the TTMn dendrite projecting more anteriorly at its most distal tip. Alternatively, shortening of both neurons following connection could result in production of a bend. However, when these neurons meet, the thoracic ganglia are relatively flat. During pupal stage P5 the thoracic ganglia undergo a rapid expansion (Truman et al., 1993). The bending could therefore be a consequence of morphological movement of the CNS during pupation. Such movements have previously been reported to be responsible for the adult projection patterns of the proprioreceptive sensory neurons in *Drosophila* (Shepherd and Smith, 1996). More recently such tension based movements have been proposed to shape structural features in the mammalian brain and have been suggested as a mechanism to compact neural circuits (Van Essen, 1997).

While all of the above processes may play a role in determining the final projection pattern, we favor the latter model. The effects of morphogenetic movements of the ganglion on a linked GF and TTMn might be expected to result in the adult projection pattern of the giant fiber, diving ventrally and bending laterally (Truman et al., 1993).

Three pieces of evidence support a morphogenetic bending hypothesis: First, from 800+ preparations examined the characteristic bend of the giant fiber was never seen without connection to the TTMn. If the GF were to actively bend to seek its target we would have expected to see an intermediate stage in which bending had at least partially

occurred with connection to the TTMn not apparent. Secondly, we have presented what we believe to be the intermediate stage where the TTMn appears to project in from the periphery and meets its GF target neuron in a right angled fashion with no GF bending involved; indeed it appears that the TTMn diverts anteriorly from its medial projection to meet the GF target. These stages also show some developmental plasticity that involves the TTMn overshooting its target slightly or not synapsing at the tip of the GF axon. This evidence implies that it is the TTMn that seeks the GF. Thirdly, we have noted occasions of what appears to be aberrant development that support the hypothesis. In a preparation of an adult CNS that shows the development of only one GF, two bends can be seen (Fig. 9A). We believe the right hand bend to be the extended dendrite of the right hand TTMn , as it is the same diameter, and continuous with this unpartnered neuron. Bending has presumably occurred because it is physically linked with the other GF, possibly through an inframedial bridge neurite. If during normal development the GF bends towards the TTMn dendrite, then in this aberrant case we would expect to see one of two possibilities. Either, no second bend, as the single GF had already found its target, or the right hand bend would be the same diameter as the rest of the GF axon, presumably responding to a second signal from the unpartnered TTMn. The fact that extension of the GFs into T3 often occurs (Fig. 9B–D) suggests that there is no signal for the GF to bend per se but bends where it is connected to the TTMn. Hence both correct bending in T2 and extension of the GF into T3 can be seen.

Model for GF/TTMn bending

The GF neuron extends from the cell bodies down into the thoracic ganglia during larval and early pupal development. By 14 hours APF it has reached the middle of the mesothoracic neuromere where it will make contact with the TTMn. Three possibilities can be considered: the GF waits for the incoming TTMn; the growth of both the GF and the TTMn is such that they meet at the correct position or that the TTMn projects earlier and waits for the descending GF. We favour the first hypothesis because we have seen many P4(i) and (ii) stage pupal CNS preparations that show the stalled GF with no TTMn visible. Later during stage P5(i), when the TTMn becomes detectable in the enhancer-trap pattern, some variability in the TTMn/GF contact is seen. Morphological movements of the ganglia then determine the adult projection patterns. We presume that subsequently the GF grows along the TTMn and thickens to give its adult morphology.

Implications for the bendless phenotype

Previous studies analyzing bendless mutations (Muralidhar and Thomas, 1993; Oh et al., 1994) have only been able to infer the developmental events underlying the elaboration of the adult projection patterns of the wild-type and mutant axons. The data presented here suggests that the previously described bendless phenotype (Thomas and Wyman, 1984) is due to incorrect synaptogenesis of the TTMn with the GF and not due to a lack of GF bending. The *bendless* gene has been shown to encode a Ubiquitin conjugating enzyme (Muralidhar and Thomas, 1993; Oh et al., 1994). Its role in the development of the GFS is still not clear, although mosaic analysis has shown it to be required in the GFs and not the TTMn. While we do not support the hypothesis that it affects the bending of the GF per se, our work implies that it is involved in target recognition of the GF by the TTMn, possibly in the alteration of receptor function and or signaling as suggested by Oh et al. (1994). We predict that either the TTMn would not be able to recognize its target in a ben^1 background, or alternatively initial contact may occur, but that morphological movements pull the neurons apart. This is currently being tested by putting A307 and a UAS-*lacZ* reporter into a ben^1 background to allow observation of joining at the P5(i) time window.

Aberrant development?

As reported previously, we observe overgrowth of the GFs into the metathoracic neuromere (Phelan et al., 1996). Such growth seems generally to be pruned back after synapse formation (post 48 hours APF). This resembles the pruning of extraneous processes of embryonic motorneurons described for *Drosophila* and locust (Myers et al. 1990; Sink and Whitington, 1991). However, we observed a proportion of adult preparations in which T3 projections persist. This is unusual as insect nerve cells usually grow directly towards their target cells. The presence of such extensions may reflect the mechanism of target selection of the GF by the TTMn. This mechanism would involve the dendrite of the TTMn performing the pathfinding roles, while the GF axon is a more passive partner. It is, however, possible that these extensions are a dominant phenotype of the A307 insert or a consequence of *lacZ* or GAL4 expression in the neuron. A preliminary analysis of another P[GAL4] enhancer-trap line also shows similar extensions.

Future perspectives

The experiments presented here, and by others, demonstrate the usefulness of P[GAL4] enhancer-trap technology to follow either the development or remodeling of neurons (e.g., Smith and Shepherd, 1996). This applies especially to those neurons too small or inaccessible to analysis by dye filling. Our data suggests the possibility of a novel phenomenon in insect neural development, in which some cells may be born embryonically and yet have no neurites until late larval/pupal stages. In addition the GFS is unusual in that the TTMn apparently finds the GF axon via its dendrite. However, neither of these hypotheses can be unequivocally proved because of the limitations of the method. The data are reliant on reporter gene expression from an unknown genomic enhancer. Analysis is therefore restricted to those cells that show a detectable level of expression during development.

A307 provides us with the first genetic marker for several of the identified neurons of the GFS. The enhancer-trap not only shows expression in the adult neurons but also during some stages of their development. This unique staining pattern can form the basis on which to develop further screens for mutants affecting the development and/or connectivity of this simple neural circuit.

LITERATURE CITED

Armstrong, J.D., M-Y Yang, and K. Kaiser (1995) Kaiser lab P[GAL4] line methods. Flybrain on-line: [http://www.flybrain.org] Accession Number. AA00089.

Ashburner, M. (1989) *Drosophila:* A Laboratory Manual. Cold Spring Harbor, NY: Cold Spring Harbor Press.

Bacon, J.P. and N.J. Strausfeld (1986) The dipteran giant fiber pathway - neurons and signals: A sensory neural and behavioral physiology. J. Comp. Physiol. *158:*529–548.

Bainbridge, S.P. and M. Bownes (1981) Staging the metamorphosis of *Drosophila melanogaster.* J. Embryol. Exp. Morphol. *66:*57–80.

Baird, D.H., M. Koto, and R.J. Wyman (1993) Dendritic reduction in passover, a *Drosophila* mutant with a defective giant fiber neuronal pathway. J. Neurobiol. *24:*971–984.

Brand, A.H. and N. Perrimon (1993) Targeted gene expression as a means of altering cell fates and generating dominant phenotypes. Development *118:*401–415.

Brand, A.H. and E.L. Dormand (1995) The GAL4 system as a tool for unravelling the mysteries of the *Drosophila* nervous system. Curr. Op. Neurobiol. *5:*572–578.

Drummond, J.A., M.J. Allen, and K.G. Moffat (1997) P[GAL4]-307 enhancer-trap pattern. Flybrain on-line: [http://www.flybrain.org] Accession Number. AA00098.

Ghysen, A. and C.J. O'Kane (1989) Neural enhancer-like elements as specific cell markers in *Drosophila*. Development *105:*35–52.

Goodman, C.S. and C.J. Shatz (1993) Developmental mechanisms that generate precise patterns of neuronal connectivity. Cell *72:*77–98.

Ito, K. and Y. Hotta (1992) Proliferation pattern of postembryonic neuroblasts in the brain of *Drosophila melanogaster*. Dev. Biol. *149:*134–148.

Koto, M., M.A. Tanouye, A. Ferrus, J.B. Thomas, and R.J. Wyman (1981) The morphology of the cervical giant fiber neuron of *Drosophila*. Brain Res. *221:*213–217.

Krishnan, S.N., E. Frei, G.P. Swain, and R.J. Wyman (1993) passover: A gene required for synaptic connectivity in the giant fiber system of *Drosophila*. Cell *73:*967–977.

Levine, R.B. and J.W.Truman (1982) Metamorphosis of the insect nervous system: Changes in the morphology and synaptic interactions of identified cells. Nature *299:*250–252.

Meinertzhagen, I.A. and T.E. Hanson (1993) The development of the optic lobe. In M. Bate, and A. Martinez Arias (eds): The Development of *Drosophila melanogaster*. Cold Spring Harbor Press, pp. 1363–1491.

Muralidhar, M.G. and J.B. Thomas (1993) The *Drosophila bendless* gene encodes a neural protein related to ubiquitin-conjugating enzymes. Neuron *11:*253–266.

Myers, C.M., P.M. Whitington, and E.E. Ball (1990) Embryonic development of the innervation of the locust extensor tibiae muscle by identified neurons: formation and elimination of inappropriate axon branches. Dev. Biol. *137:*194– 206.

Oh, C.E., R. McMahon, S. Benzer, and M.A. Tanouye (1994) *bendless*, a *Drosophila* gene affecting neuronal connectivity, encodes a ubiquitin-conjugating enzyme homolog. J. Neurosci. *14:*3166–3179.

Pavlidis, P. and M.A. Tanouye (1995) Seizures and failures in the giant fiber pathway of *Drosophila* bang-sensitive paralytic mutants. J. Neurosci. *15:*5810–5819.

Phelan, P., M. Nakagawa, M.B. Wilkin, K.G. Moffat, C.J. O'Kane, J.A. Davies, and J.P. Bacon (1996) Mutations in *shaking-B* prevent electrical synapse formation in the *Drosophila* giant fiber system. J. Neurosci. 16:1101–1113.

Phillis, R., D. Statton, P. Caruccio, and R.K. Murphey (1996) Mutations in the 8 kDa dynein light-chain gene disrupt sensory axon projections in the *Drosophila* imaginal CNS. Development *122:*2955–2963.

Power. M.E. (1948) The thoracico-abdominal nervous system of an adult insect, *Drosophila melanogaster*. J. Comp. Neurol. *88:*347–409.

Seeger, M., G. Tear, D. Ferresmarco, and C.S. Goodman (1993) Mutations affecting growth cone guidance in *Drosophila*: Genes necessary for guidance toward or away from the midline. Neuron *10:*409–426.

Shepherd, D. and S.A. Smith (1996) Central projections of persistent larval sensory neurons prefigure adult sensory pathways in the CNS of *Drosophila*. Development *122:*2375–2384.

Sink, H. and P.M. Whitington, (1991) Pathfinding in the central nervous system and periphery by identified embryonic *Drosophilia* motor axons. Development *112:*307–316.

Smith, H.K., I.J.H. Roberts, M.J. Allen, J.B. Connolly, K.G. Moffat, and C.J. O'Kane (1996) Inducible ternary control of transgene expression and cell ablation in *Drosophila*. Dev. Gen. Evol. *206:*14–24.

Smith, S.A. and D. Shepherd (1996) Central afferent projections of proprioceptive sensory neurons in *Drosophila* revealed with the enhancer-trap technique. J. Comp. Neurol. *364:*311–323.

Sun, Y.A. and R.J. Wyman (1996) passover eliminates gap junctional communication between neurons of the giant fiber system in *Drosophila*. J. Neurobiol. *30:*340–348.

Tanouye, M.A. and R.J. Wyman (1980) Motor outputs of giant nerve fibre in *Drosophila*. J. Neurophysiol *44:*405–421.

Tessier-Lavigne, M. and C.S. Goodman (1996) The molecular biology of axon guidance. Science *274:*1123–1133.

Thomas, J.B. and R.J. Wyman (1982) A mutation in *Drosophila* alters normal connectivity between two identified neurons. Nature *298:*650–651.

Thomas, J.B. and R.J. Wyman (1984) Mutations altering synaptic connectivity between identified neurons in *Drosophila*. J. Neurosci. *4:*530–538.

Trimarchi, J.R. and A.M. Schneiderman (1993) Giant fiber activation of an intrinsic muscle in the mesothoracic leg of *Drosophila melanogaster*. J. Exp. Biol. *177:*149–167.

Trimarchi, J.R. and A.M. Schneiderman (1995a) Different neural pathways coordinate *Drosophila* flight initiations evoked by visual and olfactory stimuli. J. Exp. Biol. *198:*1099–1104.

Trimarchi, J.R. and A.M. Schneiderman (1995b) Flight initiations in *Drosophila melanogaster* are mediated by several distinct motor patterns. J. Comp. Physiol. *176:*355–364.

Truman, J.W. and R. Booker (1986) Adult-specific neurons in the nervous system of the moth, *Manduca sexta*: Selective chemical ablation using hydroxyurea. J. Neurobiol. *17:*613–625.

Truman, J.W. and M. Bate (1988) Spatial and temporal patterns of neurogenesis in the central nervous system of *Drosophila melanogaster*. Dev. Biol. *125:*145–157.

Truman, J.W., B.J. Taylor, and T.A. Awad (1993) Formation of the adult nervous system: In M. Bate, and A. Martinez Arias (eds): The Development of *Drosophila melanogaster*. Cold Spring Harbor Press, pp. 1245–1275.

Van Essen, D.C. (1997) A tension-based theory of morphogenesis and compact wiring in the central nervous system. Nature *385:*313–318.

Van Vactor, D., H. Sink, D. Fambrough, R. Tsoo, and C.S. Goodman (1993) Genes that control neuromuscular specificity in *Drosophila*. Cell *73:* 1137–1153.

White, K. and D.R. Kankel (1978) Patterns of cell division and cell movement in the formation of the imaginal nervous system in *Drosophila melanogaster*. Dev. Biol. *65:*296–321.

Yang, M.Y., J.D. Armstrong, I. Vilinsky, N.J. Strausfeld, and K. Kaiser (1995) Subdivision of the *Drosophila* mushroom bodies by enhancer-trap expression patterns. Neuron *15:*45–54.

Appendix 10.3.

Collated raw data for larval and embryonic BrdU treatments.

Table showing the results of larval feeding with BrdU. (307:ULZ larvae grown to adulthood, brains removed & stained).

Age + Treatment time	Number of brains showing only X-gal staining	Number of brains showing only anti-BrdU staining	Number of brains with neither type of staining	Number showing BOTH types of staining	**TOTAL number of brains**
0 - 16	1	1	0	29	**31**
16 - 24	0	0	0	17	**17**
24 - 40	0	1	0	40	**41**
40 - 48	0	3	0	62	**65**
48 - 64	8	3	1	123	**135**
64 - 72	0	7	0	66	**73**
72 - 88	0	10	0	52	**62**
88 - 96	0	3	0	36	**39**
96 - 112	0	1	0	33	**34**
112-120	0	0	0	22	**22**
120-136	0	0	0	27	**27**
136-144	0	0	0	7	**7**
TOTAL	**9**	**29**	**1**	**514**	**553**

Embryonic treatment regime.

Age (hr AEL)	BrdU (hr)	Number pre treatment	Number post treatment	% surviving treatment	Number hatched (larvae)	Number of adults eclosed	% surviving	Overall % surviving	**Number dissected**
0 - 1	1	300	200	67	2	0	0	0	**0**
1 - 2	1	150	50	33	3	0	0	0	**0**
2 - 3	1	150	50	33	0	0	0	0	**0**
2 - 3	0.5	500	400	80	1	0	0	0	**0**
2.5 - 3.5	0.5	300	200	67	1	1	100	0.3	**1**
3 - 4	1	300	150	50	16	9	56	3	**9**
3 - 4	0.5	200	150	75	0	0	0	0	**0**
3.5 - 4.5	0.5	300	100	33	2	1	50	0.3	**1**
4 - 5	1	400	300	75	1	0	0	0	**0**
4 - 5	0.5	400	100	25	2	1	50	0.25	**1**
4.5 - 5.5	0.5	200	50	25	1	1	100	0.5	**1**
5 - 6	1	150	40	27	0	0	0	0	**0**
6 - 7	1	600	300	50	13	6	46	1	**6**
7 - 8	1	400	100	25	22	11	50	2.75	**11**
Totals		**4350**	**2190**		**64**	**30**			**30**

Age (hr AEL)	BrdU (hr)	Number pre treatment	Number post treatment	% surviving treatment	Number hatched (larvae)	Number of adults eclosed	% surviving	Overall % surviving	**Number dissected**
8 - 9	1	2100	1230	59	19	13	68	0.6	**13**
9 - 10	1	2050	980	48	53	34	64	1.7	**34**
10 - 11	1	1100	600	55	234	19	8	1.7	**19**
10 - 11	0.5	200	120	60	20	17	85	8.5	**17**
11 - 12	1	1750	1050	60	150	116	77	6.6	**31**
12 - 13	1	1450	750	52	79	38	48	2.6	**26**
13 - 14	1	1350	710	53	158	38	24	2.8	**36**
14 -15	1	500	250	50	23	8	35	1.6	**8**
15 - 16	1	200	60	30	17	4	24	2	**4**
16 - 17	1	750	500	67	400	246	62	33	**48**
17 - 18	1	400	200	50	56	34	61	8.5	**34**
18 - 19	1	400	150	38	12	6	50	1.5	**6**
19 - 20	1								
20 - 21	1	300	100	33	5	4	80	1.3	**4**
21 - 22	1	300	100	33	0	0	0	0	**0**
22 - 23	1	150	100	67	25	15	58	10	**15**
23 - 24	1	200	120	60	20	17	85	8.5	**17**
Totals		**13200**	**7020**		**1271**	**609**			**312**
Grand Total		**17550**	**9210**		**1335**	**639**			**342**
		100%	**52%**		**7.6%**	**3.6%**			**2%**

Table showing the results of embryonic treatment with BrdU.

Age + treatment time.	Number of brains showing only X-gal staining.	Number of brains showing only anti-BrdU staining.	Number of brains with neither type of staining.	Number showing BOTH types of staining.	TOTAL number of brains.
1-2+1	2	0	0	0	2
2-3+1	38	0	0	0	38
2.5-3.5+0.5	1	0	0	0	1
3-4+1	14	0	0	3	17
3.5-4.5+0.5	0	0	0	1	1
4-5+1	45	2	1	3	51
5-6+1	9	0	0	1	10
6-7+1	16	0	1	5	22
7-8+1	0	0	0	2	2
8-9+1	1	0	0	10	12
9-10+1	12	5	0	13	30
10-11+0.5	16	0	0	1	17
10-11+1	1	1	0	22	24
11-12+1	2	1	0	24	27
12-13+1	10	1	1	14	26
13-14+1	26	0	0	9	35
14-15+1	0	0	0	1	1
16-17+1	20	4	4	6	34
17-18+1	24	0	0	0	24
18-19+1	1	0	0	0	1
22-23+1	12	0	1	2	15
TOTALS	**250**	**15**	**8**	**117**	**390**

N.B. figures do not tally with those in previous table of treatment, because additional embryos were treated to cover early and late birthdates and these were not scored for survival. These have been scored for staining.

Appendix 10.4.

Raw data for BDA treatments.

BDA injection into syncitial blastoderm embryos.

Slide number.	Number of embryos injected.	Number of first instar larvae.	% injected surviving to larval life.	Number of pupae.	% injected surviving to pupal life.
1	8	0			
2	12	6			
3	20	13			
4	6	2			
5	14	7			
6	28	6			
7	27	7			
8	16	3			
9	19	6			
10	26	3			
11	23	4			
12	24	4			
13	29	8			
14	23	5			
15	27	8			
16	30	14			
17	6	4			
18	22	9			
19	17	4			
20	38	11			
21	48	16			
22	12	1			
23	20	6			
24	21	7			
25	22	7			
26	32	11			
27	20	3			
28	26	6			
29	22	6			
Totals	638	187	29%	92	14%
C1	50	25			
C2	58	30			
Totals	108	55	51%	28	26%

C1 and C2 are uninjected controls that were dechorionated, dehydrated and left to develop under halocarbon oil. All the pupae resulting from both control and injected treatments were dissected and stained.

Appendix 10.5.

The sequence of *diomedes* (composed of 5'PCR sequence, J1B and LD09704), and the primers used in the sequencing and analysis of the gene.

diomedes (minus figures = 5′ PCR seq) showing the location of PRIMERs. Arrows (>>) indicate direction of priming. Complementary strand primers have their sequence listed above that of the cDNA. Primer identifiers are next to the primer (in some cases where primers overlap symbols (|) denote the extent of the primer.

```
-437                    GAGCTGG AGGTTACTCT ACCCGGCGAG GGCAAGGATC

-401  GAATCTTTCG CGTGACGATC AAGTGGCAGG CTCAAGTCTC GCTCTTCAAT

-351  TTGGAGGAAG CTCTCGAAGG CCGCACGCGG CAGATACCCT ATGATGCCAT

-301  TTTGGCGCTC GATGTGGTCA TGCGCCATCT GCCCAGCATG ACGTACACGC

-251  CAGTGGGACG TAGCTTCTTC AGTTCCCCGG AGGGTTACTA CCATCCCCTG

-201  GGTGGTGGAC GCGAGGTTTG GTTCGGTTTC CATCAGAGCG TAAGGCCCTC

-151  GCAGTGGAAG ATGATGCTCA ATATCGATGT CTCGGCCACC GCTTTCTACA

-101  AGGCTCAACC AGTCATTGAC TTCATGTGCG AGGTGCTGGA CATTCGCGAC

 -51  ATCAACGAGC AGCGCAAACN CGCTCACCGA TTCGCAGCGC GTCAAGTTCA

   1  CCGGAGATCA AGGGTCTCAA GATCGAGATC ACCCACTGCG GCCAGATGCG

  51  TCGCAAGTAT CGTGTGTGCA ACGTCACTCG CCGCCCCGCT CAGATGCAAT

 101  CATTCCCACT GCAGCTGGAG AACGGACAGA CCGTATGGTG CACCGTGGCC

 151  AAGTACTTCC TGGACAAGTA CCGCATGAAG TTGCGCTACC CGCACTTGCC

 201  CTGCCTGCAG GTTGGCCAAG AGCACAAGCA CACTTACCTG CCTCTAGAGG

        <<CGTTGTA ACACCGGCCT GTC| PKOUT1
 251  TGTGCAACAT TGTGGCCGGA CAGCGGTGCA TTAAAAAGCT GACCGATATG

 301  CAGACGTCNA CCATGATCAA GGCCACAGCT CGTTCAGCTC CGGATCGTGA

 351  GCGTGAGATT AACAATTTGG TAAAGCGCGC CGACTTCAAC AACGATTCTT

 401  ATGTGCAAGA GTTTGGCCTG ACCATCTCCA ATTCGATGAT GGAGGTACGA

 451  GGACGCGTCT TGCCTCCTCC CAAGCTTCAG TATGGGGGAG GTGTGTCTAC

                                        <<GTCTTGTTC CACTCGAACC
 501  CGGCCTCACC GGCCAGCAGC TGTTCCCGCC ACAGAACAAG GTGAGCTTGG

      G| PGSP6OUT
 551  CCTCGCCCAA CCAGGGTGTT TGGGATATGC GCGGCAAGCA GTTCTTCACT

       T7C3 >>
 601  GGCGTCGAGA TCCGCATCTG GGCCATCGCC TGTTTTGCCC CACAGCGCAC

 651  GGTGCGCGAG GATGCGCTGC GTAATTTCAC CCAGCAGCTG CAGAAGATCT

 701  CAAACGATGC AGGCATGCCG ATAATTGGAC AGCCGTGCTT CTGTAAGTAC

 751  GCCACCGGGC CGGATCAAGT GGAACCCATG TTCCGTTACN TGAAGATCAC

 801  NTTCCCCGGC CTGCAGNTNG TCGTGGTTGT GCTGCCCGGC AAGACTCCAG

 851  TGTACGCCGA GGTGAAGCGT GTAGGTGACA CCGTTCTGGG TATGGCCACA

 901  CAGTGTGTAC AGGCCAAGAA CGTGAACAAG ACATCGCCAC AGACGCTCTC

 951  TAATCTGTGT CTGAAGATCA ACGTCAAGTT GGGCGGCATC AATTCAATTC
```

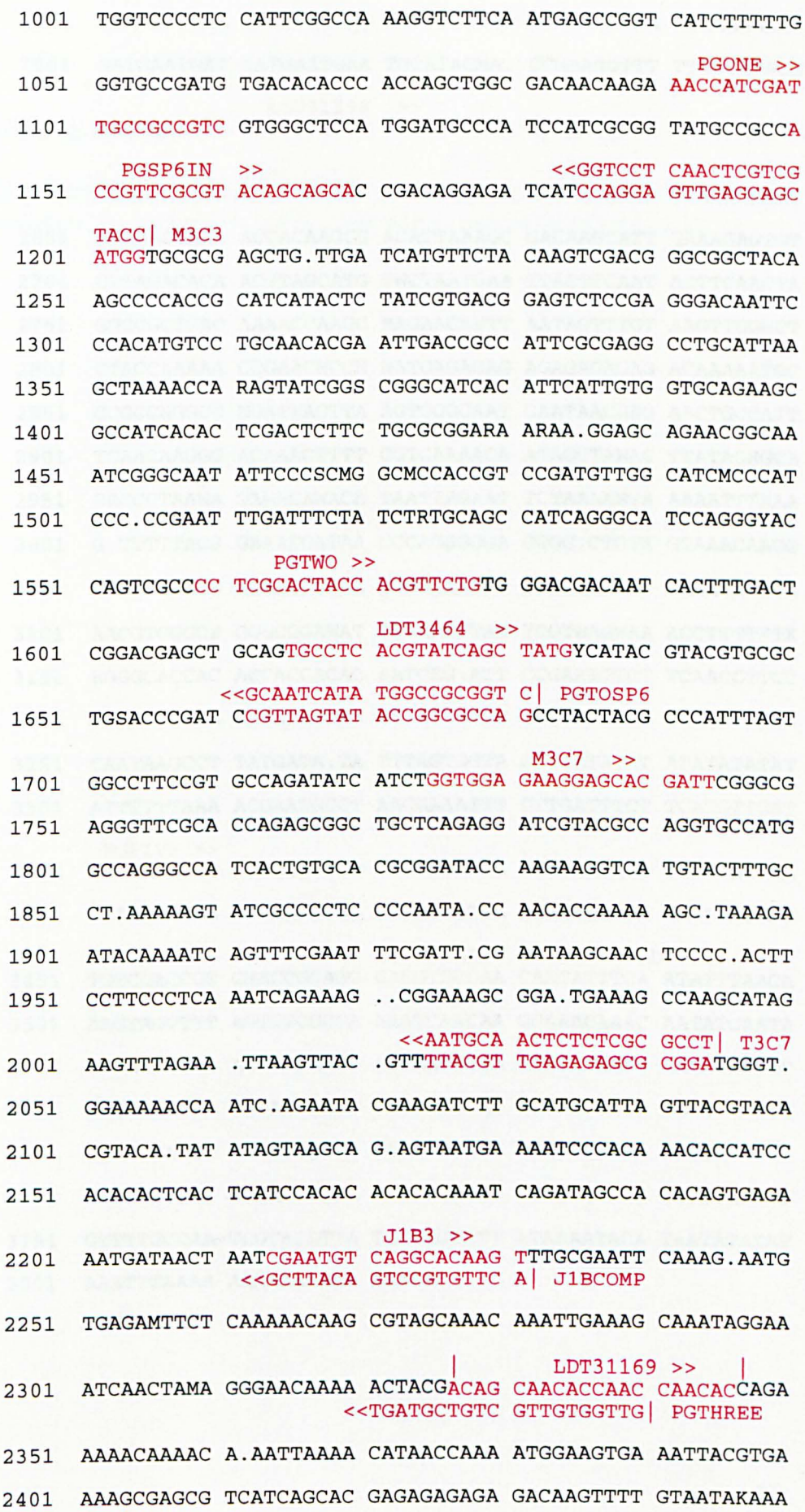
1001 TGGTCCCCTC CATTCGGCCA AAGGTCTTCA ATGAGCCGGT CATCTTTTTG
PGONE >>
1051 GGTGCCGATG TGACACACCC ACCAGCTGGC GACAACAAGA AACCATCGAT
1101 TGCCGCCGTC GTGGGCTCCA TGGATGCCCA TCCATCGCGG TATGCCGCCA
PGSP6IN >> <<GGTCCT CAACTCGTCG
1151 CCGTTCGCGT ACAGCAGCAC CGACAGGAGA TCATCCAGGA GTTGAGCAGC
TACC| M3C3
1201 ATGGTGCGCG AGCTG.TTGA TCATGTTCTA CAAGTCGACG GGCGGCTACA
1251 AGCCCCACCG CATCATACTC TATCGTGACG GAGTCTCCGA GGGACAATTC
1301 CCACATGTCC TGCAACACGA ATTGACCGCC ATTCGCGAGG CCTGCATTAA
1351 GCTAAAACCA RAGTATCGGS CGGGCATCAC ATTCATTGTG GTGCAGAAGC
1401 GCCATCACAC TCGACTCTTC TGCGCGGARA ARAA.GGAGC AGAACGGCAA
1451 ATCGGGCAAT ATTCCCSCMG GCMCCACCGT CCGATGTTGG CATCMCCCAT
1501 CCC.CCGAAT TTGATTTCTA TCTRTGCAGC CATCAGGGCA TCCAGGGYAC
PGTWO >>
1551 CAGTCGCCCC TCGCACTACC ACGTTCTGTG GGACGACAAT CACTTTGACT
LDT3464 >>
1601 CGGACGAGCT GCAGTGCCTC ACGTATCAGC TATGYCATAC GTACGTGCGC
<<GCAATCATA TGGCCGCGGT C| PGTOSP6
1651 TGSACCCGAT CCGTTAGTAT ACCGGCGCCA GCCTACTACG CCCATTTAGT
M3C7 >>
1701 GGCCTTCCGT GCCAGATATC ATCTGGTGGA GAAGGAGCAC GATTCGGGCG
1751 AGGGTTCGCA CCAGAGCGGC TGCTCAGAGG ATCGTACGCC AGGTGCCATG
1801 GCCAGGGCCA TCACTGTGCA CGCGGATACC AAGAAGGTCA TGTACTTTGC
1851 CT.AAAAAGT ATCGCCCCTC CCCAATA.CC AACACCAAAA AGC.TAAAGA
1901 ATACAAAATC AGTTTCGAAT TTCGATT.CG AATAAGCAAC TCCCC.ACTT
1951 CCTTCCCTCA AATCAGAAAG ..CGGAAAGC GGA.TGAAAG CCAAGCATAG
<<AATGCA ACTCTCTCGC GCCT| T3C7
2001 AAGTTTAGAA .TTAAGTTAC .GTTTTACGT TGAGAGAGCG CGGATGGGT.
2051 GGAAAAACCA ATC.AGAATA CGAAGATCTT GCATGCATTA GTTACGTACA
2101 CGTACA.TAT ATAGTAAGCA G.AGTAATGA AAATCCCACA AACACCATCC
2151 ACACACTCAC TCATCCACAC ACACACAAAT CAGATAGCCA CACAGTGAGA
J1B3 >>
2201 AATGATAACT AATCGAATGT CAGGCACAAG TTTGCGAATT CAAAG.AATG
<<GCTTACA GTCCGTGTTC A| J1BCOMP
2251 TGAGAMTTCT CAAAAACAAG CGTAGCAAAC AAATTGAAAG CAAATAGGAA
| LDT31169 >> |
2301 ATCAACTAMA GGGAACAAAA ACTACGACAG CAACACCAAC CAACACCAGA
<<TGATGCTGTC GTTGTGGTTG| PGTHREE
2351 AAAACAAAAC A.AATTAAAA CATAACCAAA ATGGAAGTGA AATTACGTGA
2401 AAAGCGAGCG TCATCAGCAC GAGAGAGAGA GACAAGTTTT GTAATAKAAA

```
2451  TTACGATTAA ATTGTACAAT ATATTTTTAC ACGATACGAA ATGAAGACAT
2501  GATGAATGAT AATGAATGAA TGCATACMA. CCMAAGGTTT TTAGTATACM

                      LDT31398  >>
2551  AAATGAATAC GTTGCTGATC GACTCACACA GCAAACACCA CATG.AACAC

        PGFOUR    >>
2601  CAACCACTCG GATTCTCTGT A..CTGTG.A ACGAAGACCA CCACCCMAAT
2651  ATAAACCAAA ACCACAAGCG ACATTAAAGC GACAAGCATT GAAAGAGTGT
2701  GTTAGACACA ACTTAGCATG TWCTAATGAA TTACTTCAAT ACTTCAACTA
2751  GGGCGCTGAC AAAACCAAGC MAGAACATTT AATAGTTTGT AAGTTGGGCT
2801  CTACCAAAAA CCGAACMCCN NATGAGAGAG AGAGAGAGAG AGAAAAATGC
2851  CCGCCNGGCC NGATWAGTTA AGTGGGCAAT GAATAACGAG AACTGCCATT
2901  TCAACAAGGG ACAAACTTTT GGTCAAAACA ATAGCTAWAC TTATAGRGCA
2951  GRCCCTAAWA TAWACAWACA TAATTRGAAT TCTAAAAMTA AAAATTTAAA
3001  G.TTTTTACG GAAASGATAA CCCAGSGGGA GGGG.CTGTK GTAAACAAGG
3051  TGGATAAATT AAAATTCAAA GGGGCAAATA ACACGGWAGC AGAACACGTA
3101  AACGTGGGCR GGGCGGAWAT TAAARGTTAK YCGTWAGWAA ACCTTTTKTK
3151  RGGGCACCAC ACCACCACAC AATCRG.ATT CCGAATTTCT TCAACCTTCC
3201  TGGAGTCCAA GGCATATCAY TCAA.TGTCT TCTTATTAAG GAACCTCCAA
3251  CAATAAGCCT TATGATA.TA TTTAGTGGTA CCTTATATAT ATATATATAT
3301  ATTTTTTAAA ACGAATGCCT AACGAAATTT GTTGATTTCT TCATGTTGAT

       PGFIVE >>
3351  GCTTCGAATT GGCTTCTTCG CTGCTTTTCG TTGTAATAAT TTCGTATTAA
3401  TTAACTTTAG ATCAAAGTGG TGTACGGGTA ATAATAAACA AGGTAATTGT

                          <<C CTCCACCGTT GTTGTAA| LDT7339
3451  TCTCCACCGT CMRCCGGAGG GAGGTGGCAA CAACATTTCA ATATTTAACA
3501  AAGTAGTTTT AGTTTCGCCA AAATCAACAA GCAAACAAAC AATATCAATA
3551  TCAATATGAA ACGTATGCTT AGTAATTGTA CTATATNGAG GACACAGTTC
3601  AAGTTAACAT TATAATGAGT TGTTATTTAT GCGGCGCGGG CGACGACGTT
3651  NTATCCACTC GGAATCGCCC GGGCCAAACC TAATTTATAA TTGTATACAT
3701  CCTTYTTCAC AGAACCTTTA ATTTAGATTT AGTTTCCAAG TTTGCAAGCT
3751  GTTTTGCCAA TCGTACATTA TGTGAGCATT ATAAAATACA TAATATATAT
3801  AAATTTAAAA AAAAAAAAAA AAAAA
```

Appendix 10.6.

The full length Pileup of amino acid sequences shown in figure 6.16. For details of the sequences see the legend accompanying figure 6.16.

```
                        *         20         *
Hyp Pombe : ------------------------------------ :   -
AGO1      : MVRKRRTDAPSEGGEGSGSREAGPVSGGGRGSQRGGFQ :  38
Zwille    : ------------------------------------ :   -
Hyp Rice  : ------------------------------------ :   -
Hyp CE    : ------------------------------------ :   -
Diomedes  : ------------------------------------ :   -
Hyp Rat   : ------------------------------------ :   -
Co-eIF-2A : ------------------------------------ :   -
Hyp Human : ------------------------------------ :   -

            40         *         60         *
Hyp Pombe : ------------------------------------ :   -
AGO1      : QGGGQHQGGRGYTPQPQQGGRGGRGYGQPPQQQQQYGG :  76
Zwille    : -----------MPIRQMKDSSETHLVIKTQPLKHHNPK :  27
Hyp Rice  : ------------------------------------ :   -
Hyp CE    : ------------------------------------ :   -
Diomedes  : ------------------------------------ :   -
Hyp Rat   : ------------------------------------ :   -
Co-eIF-2A : ------------------------------------ :   -
Hyp Human : ------------------------------------ :   -

              80         *        100         *
Hyp Pombe : ------------------------------------ :   -
AGO1      : PQEYQGRGRGGPPHQGGRGGYGGGRGGGPSSGPPQRQS :  114
Zwille    : TVQNGKIPPPSPSPVTVTTPATVTQSQASSPSPPSKNR :  65
Hyp Rice  : ------------------------------------ :   -
Hyp CE    : ---------------------------------DLEEIF :  6
Diomedes  : ------------------------------------ :   -
Hyp Rat   : ------------------------------------ :   -
Co-eIF-2A : ------------------------------------ :   -
Hyp Human : ------------------------------------ :   -

              120         *        140         *
Hyp Pombe : ------------------------------------ :   -
AGO1      : VPELHQATSPTYQAVSSQPTLSEVSPTQVPEPTVLAQQ :  152
Zwille    : SRRRNRGGRKSDQGDVCMRPSSRPRKPPPPSQTTSSAV :  103
Hyp Rice  : ------------------------------------ :   -
Hyp CE    : NSPPTQPQTFSDVPQRQAGSLAPGVPIGNTSVSIGEPA :  44
Diomedes  : --------------PRMWPLVEQLWPVQQQLPPRWPPP :  24
Hyp Rat   : ------------------------------------ :   -
Co-eIF-2A : ------------------------------------ :   -
Hyp Human : ------------------------------------ :   -
```

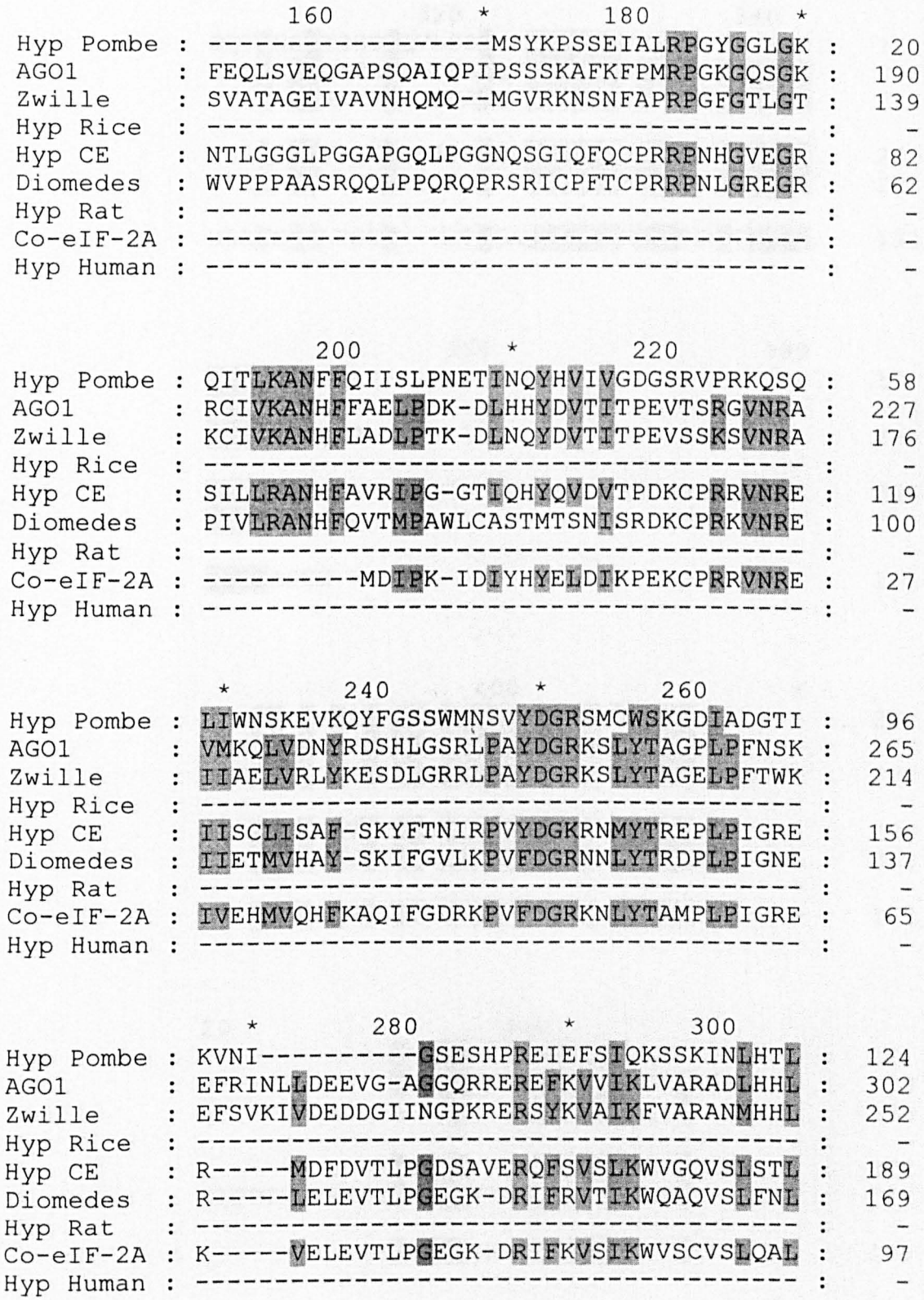
160 * 180 *
Hyp Pombe : ----------MSYKPSSEIALRPGYGGLGK : 20
AGO1 : FEQLSVEQGAPSQAIQPIPSSSKAFKFPMRPGKGQSGK : 190
Zwille : SVATAGEIVAVNHQMQ--MGVRKNSNFAPRPGFGTLGT : 139
Hyp Rice : ---------- : -
Hyp CE : NTLGGGLPGGAPGQLPGGNQSGIQFQCPRRPNHGVEGR : 82
Diomedes : WVPPPAASRQQLPPQRQPRSRICPFTCPRRPNLGREGR : 62
Hyp Rat : ---------- : -
Co-eIF-2A : ---------- : -
Hyp Human : ---------- : -
200 * 220
Hyp Pombe : QITLKANFFQIISLPNETINQYHVIVGDGSRVPRKQSQ : 58
AGO1 : RCIVKANHFFAELPDK-DLHHYDVTITPEVTSRGVNRA : 227
Zwille : KCIVKANHFLADLPTK-DLNQYDVTITPEVSSKSVNRA : 176
Hyp Rice : ---------- : -
Hyp CE : SILLRANHFAVRIPG-GTIQHYQVDVTPDKCPRRVNRE : 119
Diomedes : PIVLRANHFQVTMPAWLCASTMTSNISRDKCPRKVNRE : 100
Hyp Rat : ---------- : -
Co-eIF-2A : ----------MDIPK-IDIYHYELDIKPEKCPRRVNRE : 27
Hyp Human : ---------- : -
* 240 * 260
Hyp Pombe : LIWNSKEVKQYFGSSWMNSVYDGRSMCWSKGDIADGTI : 96
AGO1 : VMKQLVDNYRDSHLGSRLPAYDGRKSLYTAGPLPFNSK : 265
Zwille : IIAELVRLYKESDLGRRLPAYDGRKSLYTAGELPFTWK : 214
Hyp Rice : ---------- : -
Hyp CE : IISCLISAF-SKYFTNIRPVYDGKRNMYTREPLPIGRE : 156
Diomedes : IIETMVHAY-SKIFGVLKPVFDGRNNLYTRDPLPIGNE : 137
Hyp Rat : ---------- : -
Co-eIF-2A : IVEHMVQHFKAQIFGDRKPVFDGRKNLYTAMPLPIGRE : 65
Hyp Human : ---------- : -
* 280 * 300
Hyp Pombe : KVNI----------GSESHPREIEFSIQKSSKINLHTL : 124
AGO1 : EFRINLLDEEVG-AGGQRREREFKVVIKLVARADLHHL : 302
Zwille : EFSVKIVDEDDGIINGPKRERSYKVAIKFVARANMHHL : 252
Hyp Rice : ---------- : -
Hyp CE : R-----MDFDVTLPGDSAVERQFSVSLKWVGQVSLSTL : 189
Diomedes : R-----LELEVTLPGEGK-DRIFRVTIKWQAQVSLFNL : 169
Hyp Rat : ---------- : -
Co-eIF-2A : K-----VELEVTLPGEGK-DRIFKVSIKWVSCVSLQAL : 97
Hyp Human : ---------- : -

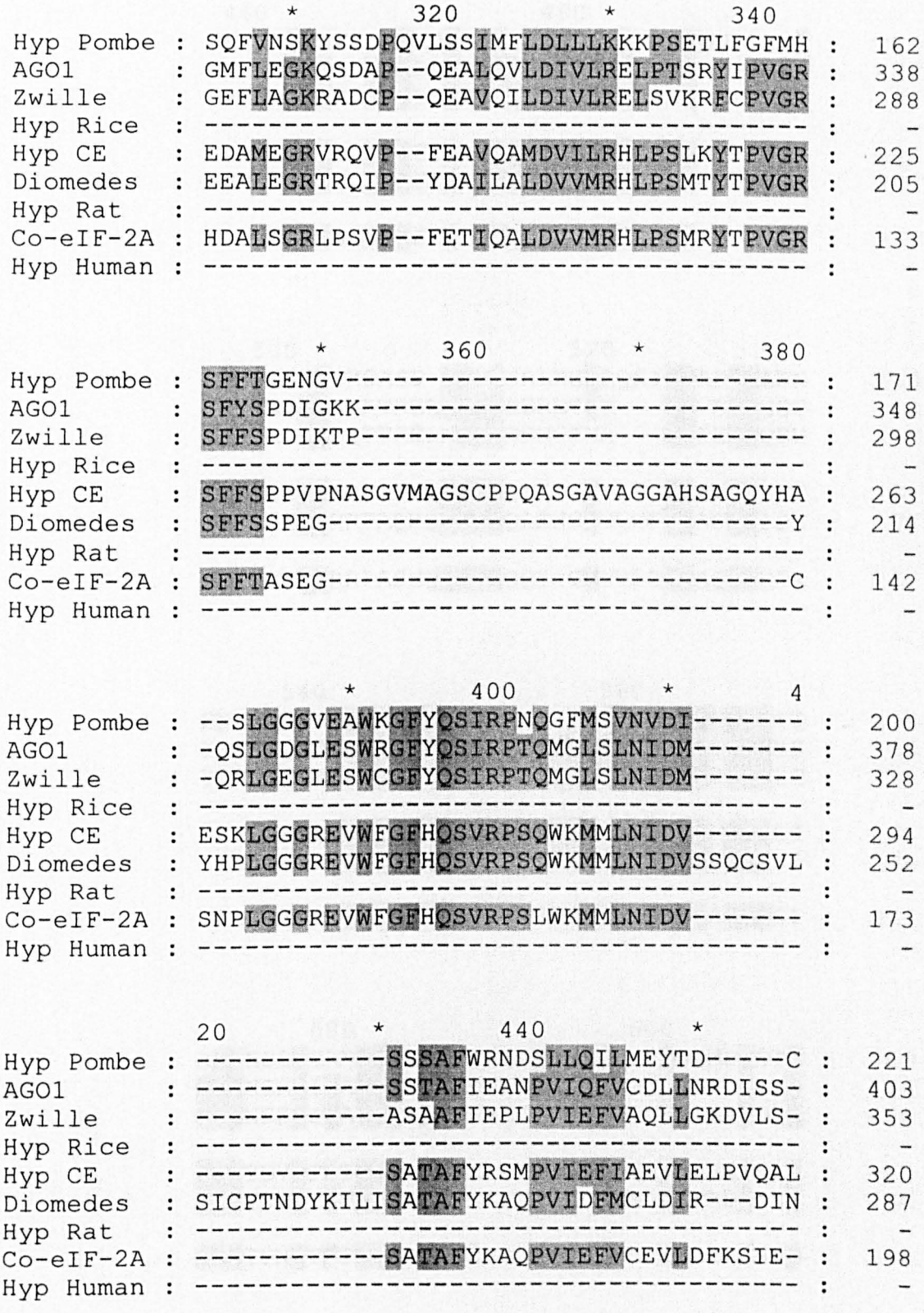
320
340
Hyp Pombe : SQFVNSKYSSDPQVLSSIMFLDLLLKKKPSETLFGFMH : 162
AGO1 : GMFLEGKQSDAP--QEALQVLDIVLRELPTSRYIPVGR : 338
Zwille : GEFLAGKRADCP--QEAVQILDIVLRELSVKRFCPVGR : 288
Hyp Rice : ---------- : -
Hyp CE : EDAMEGRVRQVP--FEAVQAMDVILRHLPSLKYTPVGR : 225
Diomedes : EEALEGRTRQIP--YDAILALDVVMRHLPSMTYTPVGR : 205
Hyp Rat : ---------- : -
Co-eIF-2A : HDALSGRLPSVP--FETIQALDVVMRHLPSMRYTPVGR : 133
Hyp Human : ---------- : -
360
380
Hyp Pombe : SFFTGENGV---------- : 171
AGO1 : SFYSPDIGKK---------- : 348
Zwille : SFFSPDIKTP---------- : 298
Hyp Rice : ---------- : -
Hyp CE : SFFSPPVPNASGVMAGSCPPQASGAVAGGAHSAGQYHA : 263
Diomedes : SFFSSPEG----------Y : 214
Hyp Rat : ---------- : -
Co-eIF-2A : SFFTASEG----------C : 142
Hyp Human : ---------- : -
400
4
Hyp Pombe : --SLGGGVEAWKGFYQSIRPNQGFMSVNVDI------- : 200
AGO1 : -QSLGDGLESWRGFYQSIRPTQMGLSLNIDM------- : 378
Zwille : -QRLGEGLESWCGFYQSIRPTQMGLSLNIDM------- : 328
Hyp Rice : ---------- : -
Hyp CE : ESKLGGGREVWFGFHQSVRPSQWKMMLNIDV------- : 294
Diomedes : YHPLGGGREVWFGFHQSVRPSQWKMMLNIDVSSQCSVL : 252
Hyp Rat : ---------- : -
Co-eIF-2A : SNPLGGGREVWFGFHQSVRPSLWKMMLNIDV------- : 173
Hyp Human : ---------- : -
20
440
Hyp Pombe : ----------SSSAFWRNDSLLQILMEYTD-----C : 221
AGO1 : ----------SSTAFIEANPVIQFVCDLLNRDISS- : 403
Zwille : ----------ASAAFIEPLPVIEFVAQLLGKDVLS- : 353
Hyp Rice : ---------- : -
Hyp CE : ----------SATAFYRSMPVIEFIAEVLELPVQAL : 320
Diomedes : SICPTNDYKILISATAFYKAQPVIDFMCLDIR---DIN : 287
Hyp Rat : ---------- : -
Co-eIF-2A : ----------SATAFYKAQPVIEFVCEVLDFKSIE- : 198
Hyp Human : ---------- : -

```
                460         *         480         *
Hyp Pombe  : SNVRDLTRFDLKRLSRKFRFLKVTCQHRNNVGTDLANR  :  259
AGO1       : ---RPLSDADRVKIKKALRGVKVEVTHRGNM-----RR  :  433
Zwille     : ---KPLSDSDRVKIKKGLRGVKVEVTHRANV-----RR  :  383
Hyp Rice   : ----------------------------------------  :    -
Hyp CE     : AERRALSDAQRVKFTKEIRGLKIEITHCGQM-----RR  :  353
Diomedes   : EQRKPLTDSQRVKFTKEIKGLKIEITHCGQM-----RR  :  320
Hyp Rat    : ----------------------------------------  :    -
Co-eIF-2A  : EQQKPLTDSQRVKFTKEIKGLKVEITHCGQM-----KR  :  231
Hyp Human  : ----------------------------------------  :    -

                500         *         520         *
Hyp Pombe  : VYSIEGFSSKSASD-SFFVRRLNGEEQKISVAEYFLEN  :  296
AGO1       : KYRISGLTAVATRELTFPVDERNTQK---SVVEYFHET  :  468
Zwille     : KYRVAGLTTQPTRELMFPVDENCTMK---SVIEYFQEM  :  418
Hyp Rice   : ----------------------------------------  :    -
Hyp CE     : KYRVCNVTRRPAQTQTFPLQLETGQTIECTVAKYFYDK  :  391
Diomedes   : KYRVCNVTRRPAQMQSFPLQLENGQTVWCTVAKYFLDK  :  358
Hyp Rat    : ----------------------------------------  :    -
Co-eIF-2A  : KYRVCNVTRRPASHQTFPLQQESGQTVECTVAQYFKDR  :  269
Hyp Human  : ----------------------------------------  :    -

                540         *         560         *
Hyp Pombe  : HNVRLQYPNLPCILVKNGAM---LPIEFCFVVKGQRYT  :  331
AGO1       : YGFRIQHTQLPCLQVGNSNRPNYLPMEVCKIVEGQRYS  :  506
Zwille     : YGFTIQHTHLPCLQVGNQKKASYLPMEACKIVEGQRYT  :  456
Hyp Rice   : ----------------------------------------  :    -
Hyp CE     : YRIQLKYPHLPCLQVGQEQKHTYLPPEVCNIVPGQRCI  :  429
Diomedes   : YRMKLRYPHLPCLQVGQEHKHTYLPLEVCNIVAGQRCI  :  396
Hyp Rat    : ----------------------------------------  :    -
Co-eIF-2A  : HKLVLRYPHLPCLQVGQEQKHTYLPLEVCNIVAGQRCI  :  307
Hyp Human  : ----------------------------------------  :    -

                580         *         600
Hyp Pombe  : AKLNSDQTANMIRFAVQRPFERVQQIDDFVHQMDWDTD  :  369
AGO1       : KRLNERQITALLKVTCQRPIDREKDILQTVQLNDYAKD  :  544
Zwille     : KRLNEKQITALLKVTCQRAEGQRNDILRTVQHNAYDQD  :  494
Hyp Rice   : ----------------------------------------  :    -
Hyp CE     : KKLTDVQTSTMIKATARSAPERERFISNLVRKAEFSAD  :  467
Diomedes   : KKLTDMQTSTMIKATARSAPDREREINNLVKRADFNND  :  434
Hyp Rat    : ----------------------------------------  :    -
Co-eIF-2A  : KKLTDNQTSTMIRATARSAPDRQEEISKLMRSASFNTD  :  345
Hyp Human  : ----------------------------------------  :    -
```

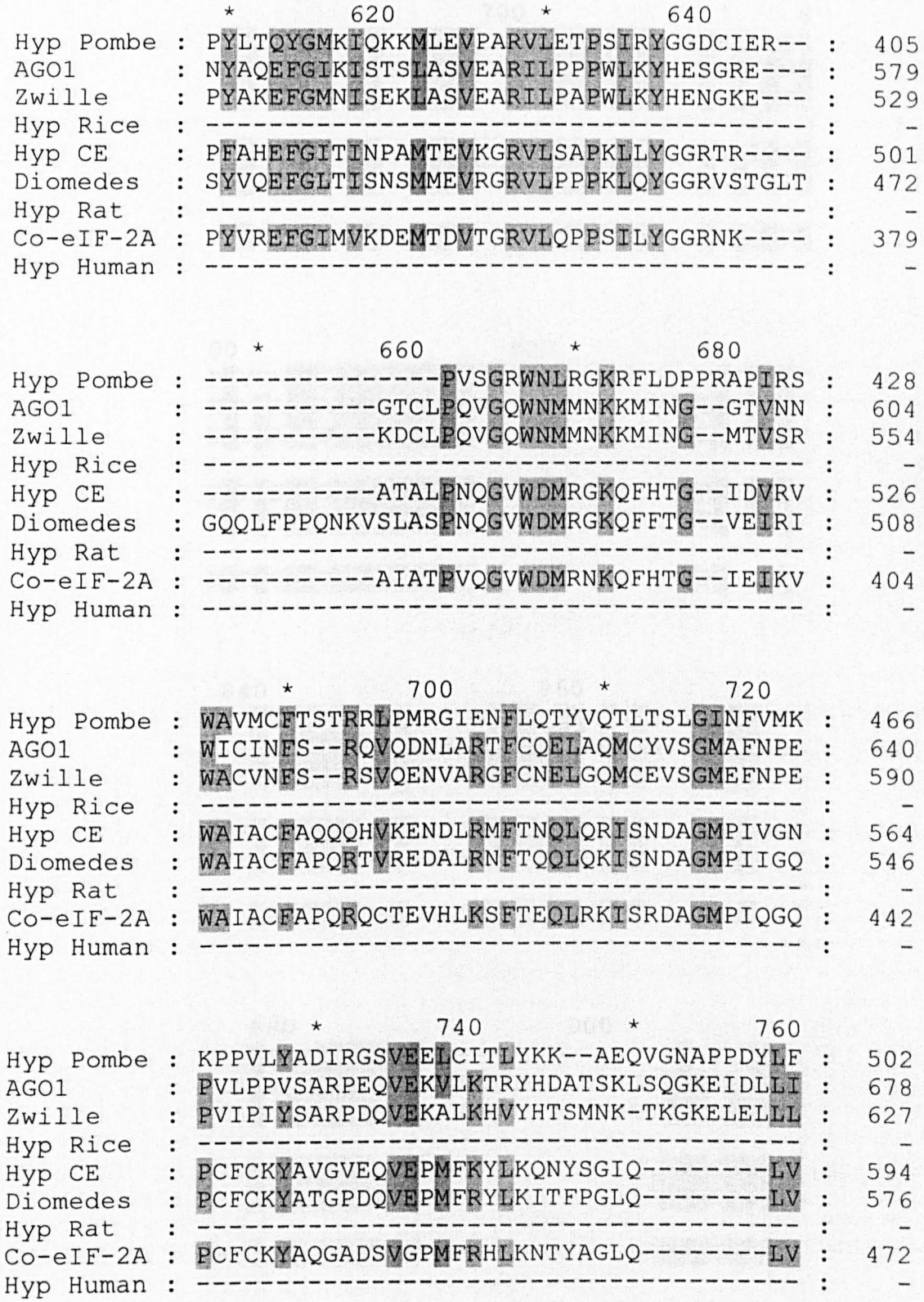
620
640
Hyp Pombe : PYLTQYGMKIQKKMLEVPARVLETPSIRYGGDCIER-- : 405
AGO1 : NYAQEFGIKISTSLASVEARILPPPWLKYHESGRE--- : 579
Zwille : PYAKEFGMNISEKLASVEARILPAPWLKYHENGKE--- : 529
Hyp Rice : ---------- : -
Hyp CE : PFAHEFGITINPAMTEVKGRVLSAPKLLYGGRTR---- : 501
Diomedes : SYVQEFGLTISNSMMEVRGRVLPPPKLQYGGRVSTGLT : 472
Hyp Rat : ---------- : -
Co-eIF-2A : PYVREFGIMVKDEMTDVTGRVLQPPSILYGGRNK---- : 379
Hyp Human : ---------- : -
660
680
Hyp Pombe : ----------PVSGRWNLRGKRFLDPPRAPIRS : 428
AGO1 : ----------GTCLPQVGQWNMMNKKMING--GTVNN : 604
Zwille : ----------KDCLPQVGQWNMMNKKMING--MTVSR : 554
Hyp Rice : ---------- : -
Hyp CE : ----------ATALPNQGVWDMRGKQFHTG--IDVRV : 526
Diomedes : GQQLFPPQNKVSLASPNQGVWDMRGKQFFTG--VEIRI : 508
Hyp Rat : ---------- : -
Co-eIF-2A : ----------AIATPVQGVWDMRNKQFHTG--IEIKV : 404
Hyp Human : ---------- : -
700
720
Hyp Pombe : WAVMCFTSTRRLPMRGIENFLQTYVQTLTSLGINFVMK : 466
AGO1 : WICINFS--RQVQDNLARTFCQELAQMCYVSGMAFNPE : 640
Zwille : WACVNFS--RSVQENVARGFCNELGQMCEVSGMEFNPE : 590
Hyp Rice : ---------- : -
Hyp CE : WAIACFAQQQHVKENDLRMFTNQLQRISNDAGMPIVGN : 564
Diomedes : WAIACFAPQRTVREDALRNFTQQLQKISNDAGMPIIGQ : 546
Hyp Rat : ---------- : -
Co-eIF-2A : WAIACFAPQRQCTEVHLKSFTEQLRKISRDAGMPIQGQ : 442
Hyp Human : ---------- : -
740
760
Hyp Pombe : KPPVLYADIRGSVEELCITLYKK--AEQVGNAPPDYLF : 502
AGO1 : PVLPPVSARPEQVEKVLKTRYHDATSKLSQGKEIDLLI : 678
Zwille : PVIPIYSARPDQVEKALKHVYHTSMNK-TKGKELELLL : 627
Hyp Rice : ---------- : -
Hyp CE : PCFCKYAVGVEQVEPMFKYLKQNYSGIQ--------LV : 594
Diomedes : PCFCKYATGPDQVEPMFRYLKITFPGLQ--------LV : 576
Hyp Rat : ---------- : -
Co-eIF-2A : PCFCKYAQGADSVGPMFRHLKNTYAGLQ--------LV : 472
Hyp Human : ---------- : -

```
                          *         780          *         8
Hyp Pombe : FILDKNSPEPYGSIKRVCNTMLGVPSQCAISKHILQSK :  540
AGO1      : VILPDNNGSLYGDLKRICETELGIVSQCCLTKHVFKMS :  716
Zwille    : AILPDNNGSLYGDLKRICETELGLISQCCLTKHVFKIS :  665
Hyp Rice  : ---------------------------------------:    -
Hyp CE    : VVVLPGKTPVYAEVKRVGDTVLGIATQCVQAKNAIRTT :  632
Diomedes  : VVVLPGKTPVYAEVKRVGDTVLGMATQCVQAKNVNKTS :  614
Hyp Rat   : ---------------------------------------:    -
Co-eIF-2A : VVILPGKTPVYAEVKRVGDTVLGMATQCVQMKNVQRTT :  510
Hyp Human : ---------------------------------------:    -

            00          *         820          *
Hyp Pombe : PQYCANLGMKINVKVGGINCSLIPKSN----PLGNVPT :  574
AGO1      : KQYMANVALKINVKVGGRNTVLVDALSRRIPLVSDRPT :  754
Zwille    : KQYLADVSLKINVKMGGRNTVLVDAISCRIPLVSDIPT :  703
Hyp Rice  : ---------------------------------------:    -
Hyp CE    : PQTLSNLCLKMNVKLGGVNSILLPNVR---PRIFNEPV :  667
Diomedes  : PQTLSNLCLKINVKLGGINSILVPSIR---PKVFNEPV :  649
Hyp Rat   : ---------------------------------------:    -
Co-eIF-2A : PQTLSNLCLKINVKLGGVNNILLPQGR---PPVFQQPV :  545
Hyp Human : ---------------------------------------:    -

             840          *         860          *
Hyp Pombe : LILGGDVYHPGVG-ATGVSIASIVASVDL-NGCKYTAV :  610
AGO1      : IIFGADVTHPHPGEDSSPSIAAVVASQDWPEITKYAGL :  792
Zwille    : IIFGADVTHPENGEESSPSIAAVVASQDWPEVTKYAGL :  741
Hyp Rice  : ---------------------------------------:    -
Hyp CE    : IFFGCDITHPPAGDSRKPSIAAVVGSMD-AHPSRYAAT :  704
Diomedes  : IFLGADVTHPPAGDNKKPSIAAVVGSMD-AHPSRYAAT :  686
Hyp Rat   : ---------------------------------------:    -
Co-eIF-2A : IFLGADVTHPPAGDGKKPSIAAVVGSMD-AHPNRYCAT :  582
Hyp Human : ---------------------------------------:    -

               880          *         900          *
Hyp Pombe : SRSQPRHQEVIEGMKD--------------IVVYLLQG :  634
AGO1      : VCAQAHRQELIQDLFKEWKDPQKGVVTGGMIKELLIAF :  830
Zwille    : VCAQAHRQELIQDLYKTWQDPVRGTVSGGMIRDLLISF :  779
Hyp Rice  : ---------------------------------------:    -
Hyp CE    : VRVQQHRQEIISDL-------------TYMVRELLVQF :  729
Diomedes  : VRVQQHRQEIIQEL-------------SSMVRELLIMF :  711
Hyp Rat   : ---------------------------------------:    -
Co-eIF-2A : VRVQQHRQEIIQDL-------------AAMVRELLIQF :  607
Hyp Human : ---------------------------------------:    -
```

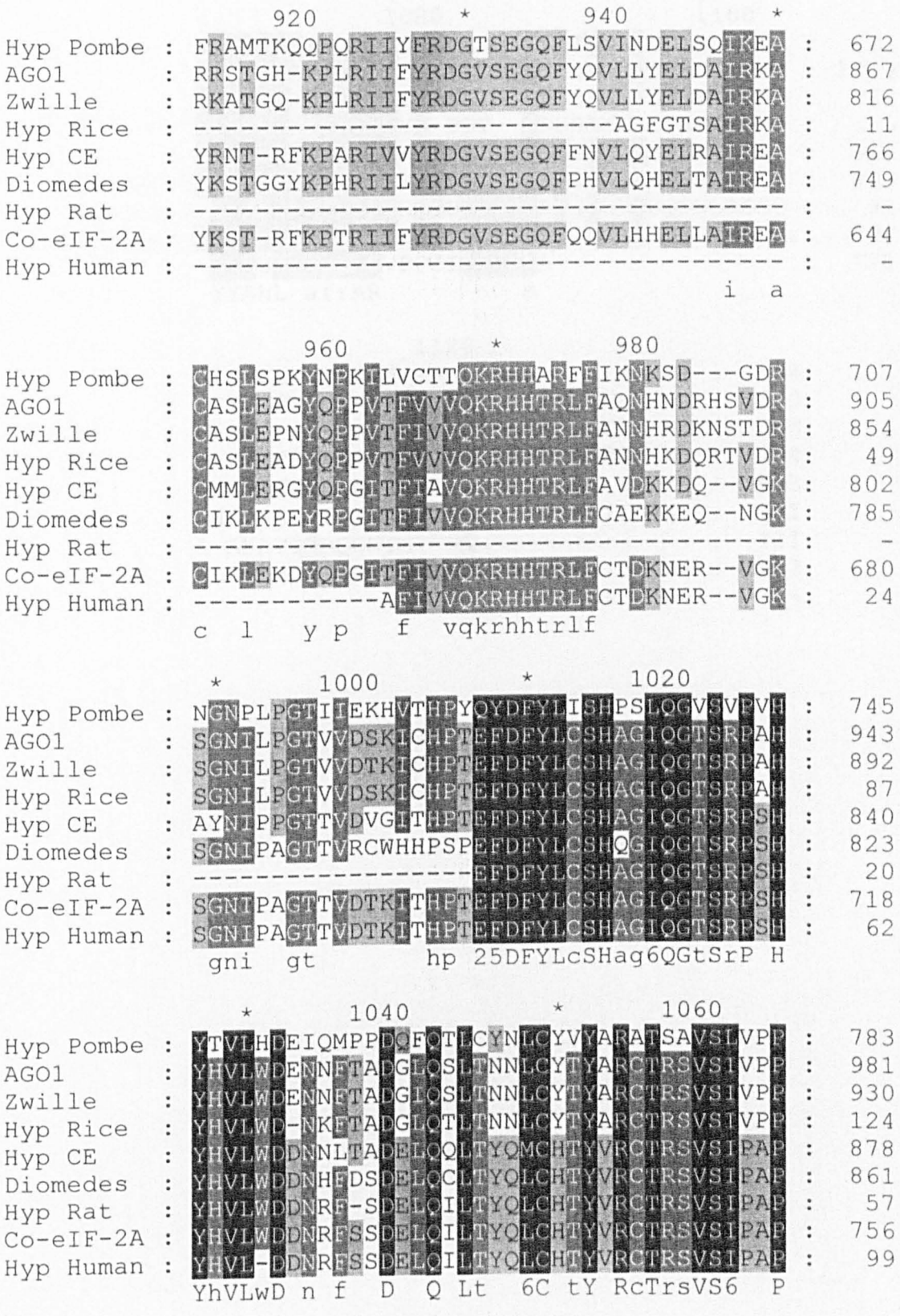
920 * 940 *
Hyp Pombe : FRAMTKQQPQRIIYFRDGTSEGQFLSVINDELSQIKEA : 672
AGO1 : RRSTGH-KPLRIIFYRDGVSEGQFYQVLLYELDAIRKA : 867
Zwille : RKATGQ-KPLRIIFYRDGVSEGQFYQVLLYELDAIRKA : 816
Hyp Rice : ----------AGFGTSAIRKA : 11
Hyp CE : YRNT-RFKPARIVVYRDGVSEGQFFNVLQYELRAIREA : 766
Diomedes : YKSTGGYKPHRIILYRDGVSEGQFPHVLQHELTAIREA : 749
Hyp Rat : ---------- : -
Co-eIF-2A : YKST-RFKPTRIIFYRDGVSEGQFQQVLHHELLAIREA : 644
Hyp Human : ---------- : -
i a
960 * 980
Hyp Pombe : CHSLSPKYNPKTLVCTTQKRHHARFFIKNKSD---GDR : 707
AGO1 : CASLEAGYQPPVTFVVVQKRHHTRLFAQNHNDRHSVDR : 905
Zwille : CASLEPNYQPPVTFIVVQKRHHTRLFANNHRDKNSTDR : 854
Hyp Rice : CASLEADYQPPVTFVVVQKRHHTRLFANNHKDQRTVDR : 49
Hyp CE : CMMLERGYQPGITFIAVQKRHHTRLFAVDKKDQ--VGK : 802
Diomedes : CIKLKPEYRPGITFIVVQKRHHTRLFCAEKKEQ--NGK : 785
Hyp Rat : ---------- : -
Co-eIF-2A : CIKLEKDYQPGITFIVVQKRHHTRLFCTDKNER--VGK : 680
Hyp Human : ----------AFIVVQKRHHTRLFCTDKNER--VGK : 24
c l y p f vqkrhhtrlf
* 1000 * 1020
Hyp Pombe : NGNPLPGTIIEKHVTHPYQYDFYLISHPSLQGVSVPVH : 745
AGO1 : SGNILPGTVVDSKICHPTEFDFYLCSHAGIQGTSRPAH : 943
Zwille : SGNILPGTVVDTKICHPTEFDFYLCSHAGIQGTSRPAH : 892
Hyp Rice : SGNILPGTVVDSKICHPTEFDFYLCSHAGIQGTSRPAH : 87
Hyp CE : AYNIPPGTTVDVGITHPTEFDFYLCSHAGIQGTSRPSH : 840
Diomedes : SGNIPAGTTVRCWHHPSPEFDFYLCSHQGIQGTSRPSH : 823
Hyp Rat : ----------EFDFYLCSHAGIQGTSRPSH : 20
Co-eIF-2A : SGNIPAGTTVDTKITHPTEFDFYLCSHAGIQGTSRPSH : 718
Hyp Human : SGNIPAGTTVDTKITHPTEFDFYLCSHAGIQGTSRPSH : 62
gni gt hp 25DFYLcSHag6QGtSrP H
* 1040 * 1060
Hyp Pombe : YTVLHDEIQMPPDQFQTLCYNLCYVYARATSAVSIVPP : 783
AGO1 : YHVLWDENNFTADGLQSLTNNLCYTYARCTRSVSIVPP : 981
Zwille : YHVLWDENNFTADGLQSLTNNLCYTYARCTRSVSIVPP : 930
Hyp Rice : YHVLWD-NKFTADGLQTLTNNLCYTYARCTRSVSIVPP : 124
Hyp CE : YHVLWDDNNLTADELQQLTYQMCHTYVRCTRSVSIPAP : 878
Diomedes : YHVLWDDNHFDSDELQCLTYQLCHTYVRCTRSVSIPAP : 861
Hyp Rat : YHVLWDDNRF-SDELQILTYQLCHTYVRCTRSVSIPAP : 57
Co-eIF-2A : YHVLWDDNRFSSDELQILTYQLCHTYVRCTRSVSIPAP : 756
Hyp Human : YHVL-DDNRFSSDELQILTYQLCHTYVRCTRSVSIPAP : 99
YhVLwD n f D Q Lt 6C tY RcTrsVS6 P

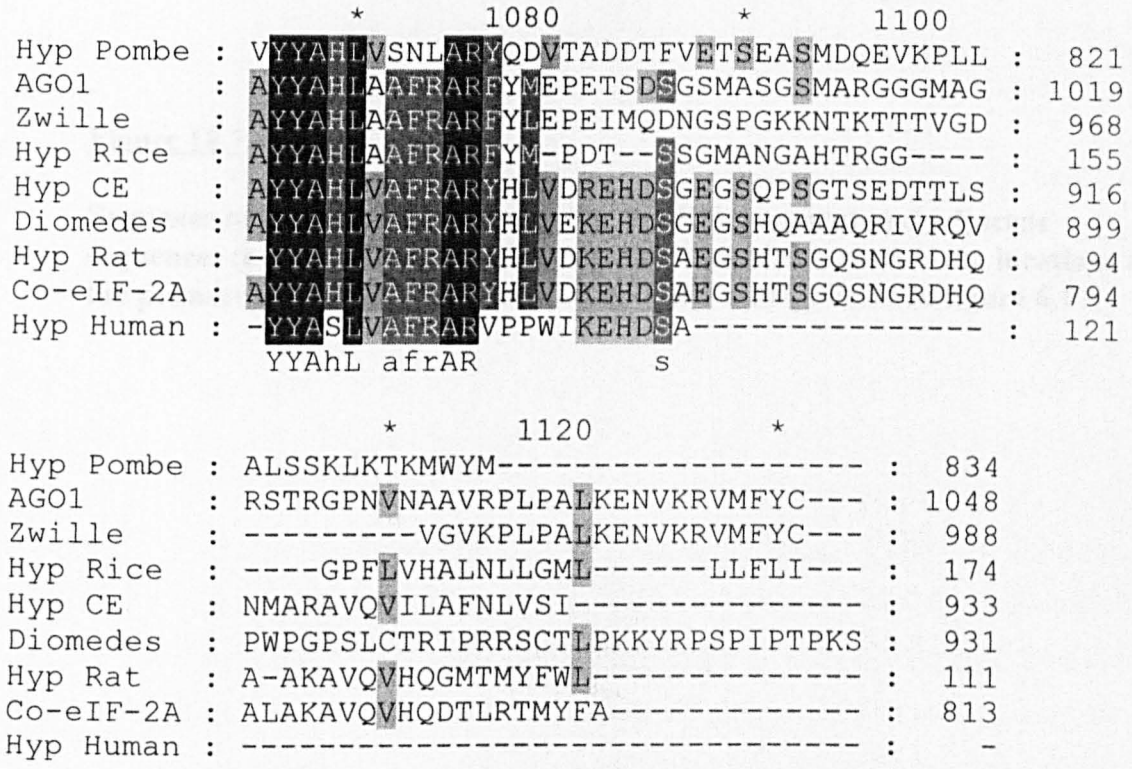
* 1080 * 1100
Hyp Pombe : VYYAHLVSNLARYQDVTADDTFVETSEASMDQEVKPLL : 821
AGO1 : AYYAHLAAFRARFYMEPETSDSGSMASGSMARGGGMAG : 1019
Zwille : AYYAHLAAFRARFYLEPEIMQDNGSPGKKNTKTTTVGD : 968
Hyp Rice : AYYAHLAAFRARFYM-PDT--SSGMANGAHTRGG---- : 155
Hyp CE : AYYAHLVAFRARYHLVDREHDSGEGSQPSGTSEDTTLS : 916
Diomedes : AYYAHLVAFRARYHLVEKEHDSGEGSHQAAAQRIVRQV : 899
Hyp Rat : -YYAHLVAFRARYHLVDKEHDSAEGSHTSGQSNGRDHQ : 94
Co-eIF-2A : AYYAHLVAFRARYHLVDKEHDSAEGSHTSGQSNGRDHQ : 794
Hyp Human : -YYASLVAFRARVPPWIKEHDSA---------- : 121
YYAhL afrAR s
* 1120 *
Hyp Pombe : ALSSKLKTKMWYM---------- : 834
AGO1 : RSTRGPNVNAAVRPLPALKENVKRVMFYC--- : 1048
Zwille : ---------VGVKPLPALKENVKRVMFYC--- : 988
Hyp Rice : ----GPFLVHALNLLGML------LLFLI--- : 174
Hyp CE : NMARAVQVILAFNLVSI---------- : 933
Diomedes : PWPGPSLCTRIPRRSCTLPKKYRPSPIPTPKS : 931
Hyp Rat : A-AKAVQVHQGMTMYFWL---------- : 111
Co-eIF-2A : ALAKAVQVHQDTLRTMYFA---------- : 813
Hyp Human : ---------- : -

Figure 10.7.

Sequence of the genomic region of the *Hin*dIII fragment and adjacent sequences (c 400bp 3' and 1500bp 5'). This figure also reveals the locations of the primers and explains the formation of the contigs listed in figure 6.17.

Genomic sequence and PRIMER list showing the location of PRIMERs. Arrows (>>) indicate direction of priming. Complementary strand primers have their sequence listed above that of the cDNA. Primer identifiers are next to the primer (in some cases where primers overlap symbols (|) denote the extent of the primer.

```
   1 AGGTGACAAT GCCGGCGTGG CTATGTGCAT CNACTATGAC ATCCAATATA

  51 CAGCCGGGAC AAGTGTCCGC GAAAGGTGAA CCGTGAGATT ATCGAGACTA

 101 TGGTGCATGC CTATAGCAAG ATCTTCGGAG TGCTCAAGCC GGTGTTCGAT

 151 GGTCGCAACA ATCTGTATAC CCGCGATCCC CCTGCCCATT GGCAACGAGC

 201 GTCTAGAGCT GGAGGTTACT CTACCCGGCG AGGGCAAAGA TCGAATCTTT

 251 CGCGTGACGA TCAAGTGGCA GGCTCAGGTC TCGCTCTTCA ATTTGGAGGA

 301 AGCTCTCGAA GGCCGCACGC GGCAGATACC CTATGATGCC ATTTTGGCGC

 351 TCGATGTGGT CATGCGCCAT CTGCCCAGCA TGACGTACAC GCCAGTGGGA

 401 CGTAGCTTCT TCAGTTCCCC GGAGGGTTAC TACCATCCCC TGGGTGGTGG

 451 ACGCGAGGTT TGGTTCGGTT TCCATCAGAG CGTAAGGCCC TCGCAGTGGA

 501 AGATGATGCT CAATATCGAT GGTGAGTTCG CAATGCTCTG TATTATCTAT

 551 TTGCCCAACT AATGATTACA AAATCCTCAG TCTCGGCCAC CGCTTTCTAC

                                                      <<CT
 601 AAGGCTCAAC CAGTCATTGA CTTCATGTGC GRGGTNCTGG ACATTCGCGA

     GTAGTTGCTC GTCGCGTT| PKOUT2
 651 CATCAACGAG CAGCGCAAAC CGCTCACCGA TTCGCAGCGC GTCAAGTTCA

 701 CGAAGGAGAT CAAGGGTTTG AAGATCGAGA TCACCCACTG CGGCCAGATG

 751 CGTCGCAAGT ATCGTGTGTG CAACGTCACT CGCCGCCCCG CTCAGATGCA

 801 ATCGTATGTA TTCAGCATTT TTAAACATTT CTGCTTTTGT TAACCAAGCT

 851 TCATCATCAT GTTAGATTCC CACTGCAGCT GGAGAACGGA CAGACCGTAG

 901 AGTGCACCGT GGCCAAGTAC TTCCTGGACA AGTACCGCAT GAAATTGCGC

 951 TACCCGCNCT TGCCCTGCCT GCAGGTTGGC CAAGAGCACA AGCACACTTA

                      <<CGT TGTAACACCG GCCTGTC| PKOUT1
1001 CCTGCCTCTA GAGGTGTGCA ACATTGTGGC CGGACAGCGG TGCATTAAAA

1051 AGCTGACCGA TATGCAGACG TCGACCATGA TCAAGGCCAC AGCTCGTTCA

1101 GCTCCGGATC GTGAGCGTGA GATTAACAAY TTGGTAAAGC GCGCCGACTT

1151 CAACAACGAT TCNTATGTGC AAGAGTTTGG CCTGACCATC TCCAATTCGA

1201 TGATGGAGGT ACGAGGACGC GTCTTGCCTC CTCCCAAGCT TCAGTATGGG

                                                     <<TGTCTT
1251 GGACGTGTGT CTACCGGCCT CACCGGCCAG CAGCTGTTCC CGCCACAGAA

     GTTCCACTCG AACCGG| PGSP6OUT
1301 CAAGGTGAGC TTGGCCTCGC CCAACCAGGG TGTNTGGGAT ATGCGNGGCA

                   PGT7C3 >>
1351 AGCAGTTCTT CACTGGCGTC GAGATCCGCA TCTGGGCCAT CGCCTGTTTT
```

```
1401 GCCCCACAGC GCACGGTGCG CGAGGATGCG GTGCGTAATT TCACCCAGCA
1451 GCTGCAGAAG ATCTCTAAAC CGATGTCAGG CATTTGCCGA TAATTGGGAC
1501 AGCCGTGCCT TCTGTAAGTA CGCCACCGGG CCGGATCAAG TGGAACCCAT
1551 GTTCCGTTAC CTGAAGATCA CCTTCCCCGG CCTGCANCTC GTCGTGGTTG
1601 TGCNGCCCGG CAAGACTCCA GTNNACGCSG AGGTGAAGCG TGTAGGTGAC
1651 ACCGTTCTGG GTATGGCCAC NCAGTGTGTR CAGGCCAAGA ACGTGAACAA
1701 GACATCGCCA CAGACGCTCT CTAATCTGTG TCTGAAGATC AACGTCAAGT
1751 TGGGCGGCAT CAATTCAATT CTGGTCCCCT CCATTCGGCC AAAGGTCTTC
1801 AATGAGCCGG TCATCTTTTT GGGTGCCGAT GTGACACACC CACCAGCTGG
                        PGONE >>
1851 CGACAACAAG AAACCATCGA TTGCCGCCGT CGTGGGCTCC ATGGATGCCC
                                 PGSP6IN >>
1901 ATCCATCGCG GTATGCCGCC ACCGTTCGCG TACAGCAGCA CCGACAGGAG
        <<GGTCC TCAACTCGTC GTACC| PGM3C3
1951 ATCATCCAGG AGTTGAGCAG CATGGTGCGC GAGCTGTTGA TCATGTTCTA
2001 CAAGTCGACG GGCGGCTACA AGCCCCACCG CATCATACTC TATCGTGACG
2051 GAGTCTCCGA GGGACAATTC CCACATGTCC TGCAACACCA ATTGACCGCC
2101 ATTCGCGAGG CCTGCATTAA GCTAGAGCCA GAGTATCGGC CGGGCATCAC
2151 ATTCATTGTG GTGCAGAAGC GCCATCATAC TCGACTCTTC TGCGCGGAGA
2201 AGAAGGAGCA GAGCGGCAAA TCGGGCAATA TTCCCGCAGG CACCACCGTC
2251 CGATGTGGGC ATCACACATN CCACCGAATT TGATTTCTAT CTCTGCAGCC
                                    PGTWO >>
2301 ATCAGGGCAT CCAGGGCACC AGTCGCCCCT CGCACTACCA CGTTCTGTGG
                                          PGLDT3 >>
2351 GACGACAATC ACTTTGACTC GGACGAGCTG CAGTGCCTCA CGTATCAGCT
                                                PGTOSP6
                                    << GCAGTCATAT GGCCGCGGTC|
2401 ATGTCATACG TACGTGCGCT GCACCCGATC CGTCAGTATA CCGGCGCCAG
2451 CCTACTACGC CCATTTAGTG GCCTTCCGTG CCAGGTAAGC CATTGGATTC
2501 GATTACCCTT CAATTCGACT TTGCGTTAAT GTTATGTAAT TCGTTTGCAG
                        PGM3C7 >>
2551 ATATCATCTG GTGGAGAAGG AGCACGATTC GGGCGAGGGT TCGCACCAGA
2601 GCGGCTGCTC AGAGGATCGT ACGCCAGGTG CCATGGCCAG GGCCATCACT
2651 GTGCACGCGG ATACCAAGAA GGTCATGTAC TTTGCCTAAA AAGTATCGCC
2701 CCTCCCCAAT ACCAACACCA AAAAGCTAAA GAATACAAAA TCAGTTTCGA
2751 ATTTCGATTC GAATAAGCAA CTCCCCACTT CCTTCCCTCA AATCAGAAAG
```

```
                                                                  <<A
2801 CGGAAAGCGG ATGAAAGCCA AGCATAGAAG TTTAGAATTA AGTTACGTTT

     ATGCAACTCT CTCGCGCCT| PGT3C7
2851 TACGTTGAGA GAGCGCGGAT GGGTGGAAAA ACCAATCAGA ATACGAAGAT

2901 CTTGCATGCA TTAGTTACGT ACACGTACAT ATATAGTAAG CAGAGTAATG

2951 AAAATCCCAC AAACACCATC CACACACTCA CTCATCCACA CACACACACA

                                                  <<GCTT ACAGTCCGTG
3001 AATCAGATAG CCACACAGTG AGAAATGATA ACTAATCGAA TGTCAGGCAC
                                                    J1B3 >>

     TTCA| J1B3C
3051 AAGTTTACGA AATCAAAGAA ATGTGAGAAT TCTCAAAAAC AAGCGTAGCA

                                                          <<TGATGCT
3101 AACAAATTGA AAGCAAATAG GAAATCANCT AAAGGGAACA AAAACTACGA
                                                             |

     GTCGTTGTGG TTG| PGTHREE
3151 CAGCAACACC AACCAACACC AGAAAAACAA AACAAATTAA AACATAACCA
     PGLDT31169 >>      |

3201 AAATGGAAGT GAAATTACGT GAAAAGCGAG CGTCATCAGC ACGAGAGAGA

3251 GAGACAAGTT TTGTAATAGA AATTACGATT AAATTGTACA ATATATTTTT

3301 ACACGATACG AAATGAAGAC ATGATGAATG ATAATGAATG AATGCATACC

                                                PGLDT313 >>
3351 ACCAAAGGTT TTTAGTATAC AAAATGAATA CGTTGCTGAT CGACTCACAC

                                        PGFOUR >>
3401 AGCAAACACC ACATGAACAC CAACCACTCG GATTCTCTGT ACTGTGAACG

3451 AAGACCACCA CCNAAATATA AACNAAAACC ACAAGCGACA TTAAAGCGAC

3501 AAGCATTGAA AGAGTGTGTT AGACACAACT TAGCATGTAC TAATGAATTA

3551 CTTCAATACT TCAACTAGGG CGCTGACAAA ACCAAGCAAG AACATTTAAT

3601 AGTTTGTAAG TTGGGCTCTA CCAAAAACCG AACACAAAAT GAGAGAGAGA

3651 GAGAGAGAAA AATGCAAGCA AGGCCAGATA AGTTAAGTGG GCAATGAATA

3701 ACGAGAACTG CAATTTCAAC AAGGGACAAA CTTTTGGTCA AAACAATAGC

3751 TATACTTATA GAGCAGAGCC TAATATATAC ATACATAATT AGAATCTAAA

3801 ACTAAAATTT AAAGTTTTTA CGAAACGATN ACCAAGCGGC GGAGCTGTTG

3851 TACAATGTAG ATTCTTAAAA TTCAAAAGTG CAATACACGG TAGCAGACAC

3901 GTAAACGTGG GCNGGGCGGA NATTAAANGT TANNCGTNAG NAAACCTTTT

3951 NTNNGGGCAC CACACCACCA CACAATCAGA TTCCGGAATT TNTTCAACCN

4001 TCCTNGAGTC CAAGGCATAT CACTCAATGT CNTCTTATTA ANGNACCTCC

4051 NACAATAAGC CTTATGATAT ATTTAGTNGT ACCTTATATA TATATATATA

4101 TATATTTTTT AAAACGAATG CCTAACGAAA TTTGTTGATT TCTTCATGTT

     PGFIVE >>
4151 GATGCTTCGA ATTGGCTTCT TCGCTGCTTT TCGTTGTAAT AATTTCGTAT

4201 TAATTAACTT TAGATCAAAG TGGTGTACGG GTAATAATAA ACAAGGTAAT
```

```
                                        <<CCTCCACCG TTGTTGTAA| PGLDT7
4251 NTTCTCCACC GTCCGCCGGA GGGAGGTGGC AACAACATTT CAATATTTTA

4301 CTAAGTAGTT TTAGTTTCGC CAAAATCAAC AAGCAAACAA ACAATATCAA

4351 TATCAATATG AAACGTATGC TTAGTAATTG TACTATATCG AGGACACAGT

4401 TCAAGTTAAC ATTATAATGA GTTGTTATTT ATGCGGCGCG GGCGACGACG

4451 TTCTATCCAC TCGGAATCGC CCGGGCCAAA CCTAATTTAT AATTGTATAC

4501 ATCCTTCTTC ACAGAACCTT TAATTTAGAT TTAGTTTCCA AGTTTGCAAG

4551 CTGTTTTGCC AATCGACATT ATGTGAGCAT TATAAAATAC ATAATATATA

4601 TAAATCTATA TGCTTATATT TAATCATTTA CTGCACTTAC AAATTAGTTG

4651 GTAATCCTCA AGAATATATG TATAAAGAAA AAAAGGGAAC AGAACGGCAG

4701 GAAGGAGGTC GCACGCGGTC CCTCAAAATG TTGAATCGAA CTCTTAGAAA

4751 TCTCTTTGGA TTTGAAATCA TATACAAACT GGTGGAACTT CAAGAATGAT

4801 TTCAAATCCC TTGATATTTC AGTGGTGGCA AAAAATTTTT AAATCTGCAT

4851 TCTCAATGCC TGTTTTTAAA CTTCTCGATG TTTATCATTT AGTCAACTAC

4901 TTCGAGTGCA ATGATATCTT TTGCAGAAAT TTTAAAACCA GAGTTAATAT

                                                    <<ATCAGG
4951 ANAAAAGTCT TCAAATAAAG TTTTTTTTTT GTCTAAATTT TGACTAGTCC

     AAGGTTGCTC CGAG| PGSIX
5001 TTCCAACGAG GCTCAACATA GCTGATATTA ATAGCTTATT AATTAATTAA

5051 TATTAATTGG TAATGCGTTT AAATGCGATT AACATTTTGT GGGGCTGTGC

5101 AATTAATTGT GTGGGCGTAT TTGTGGACTT ATTCATTTTC CATTTGTTTT

5151 TCTAATAACG TTTCTACACA AGGGATTAAA ATTTTAAACT TATGTCTTAA

5201 TTTTTACTTA AAGCAACCCG ATGCAAAAAA AAAACAAACA AACAAAAACA

5251 AACAAAAAAA CGAATCAAAC AATTTTAGTT ATAAGAAAAA AAAAACAAGA

                                <<TTCCTCAAG CGCTAAGCC| PGT7IN
5301 AAACGAAAAC GAAACAATGC AAAGGAGTTC GCGATTCGGG GCTCGATTTT

5351 TGAGATCGGC CAGAAAGAAC CAACATTTAC ATTATATATT CACTTAGTTT

                                PGT7OUT >>
5401 AAGCTGAAGC TGAAATGTGT GCCGACAATG AATGCATCTN GTAGTTGTAA

5451 AATGAGCGAA ATATTCAACA ATAATTTACT TTACCACACA ATACATGAGA

5501 AAGTCCAAAG CTTTAACTTA CTCGCAAGAT GAATGAAGCG GAAATATCGT

5551 TGGGAAAACC CTTATCACTA ATGAAAATGC CAATAACAAG CTGCTATCTC

5601 CTCCCATCCA AGAAAAATGG GCTGTNACAG TTGTCCCTAT ATACACGCGT

5651 AAAACTTATA CATATATAGT AAAGCTGGAT AACTCCGATT TTCCCAAGAA

5701 CTCAAGAAAA CTACTACTCA CNCACGCTAC AATTTCAATG GTTTCTTCAG

5751 TGTCGTGCAG CTAAGTTACA AGGAAAACAA GTTGGAGGAG AAGATTGAAG

5801 ATCGTGGATG GCCCTAGATA TCATTTCCCA ACTATGTTCT GCTCAGAAGC
```

5851 GACGGCCAAA TTAAAAAGTA CACAAANCCG GGATATCCCA ATGGGGAAC

5901 TTNCATTTTT ATCTGTC

Contig: g42sp6

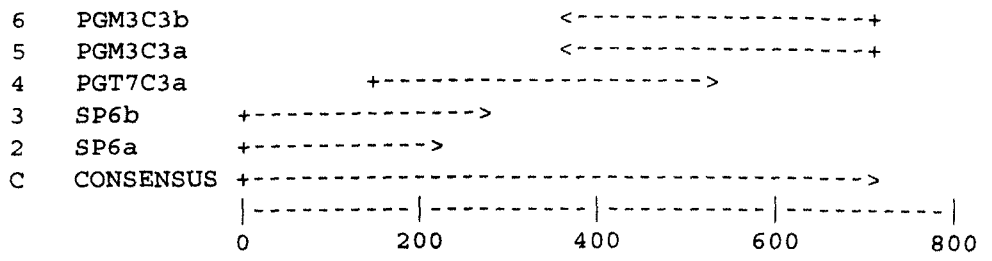

Contig: pg42t7

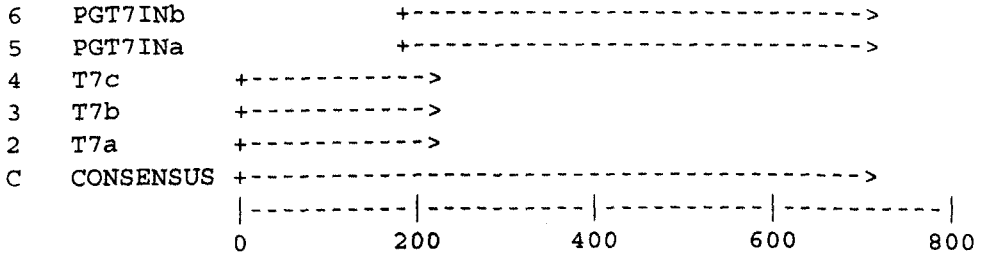

Contig: pgjib3a

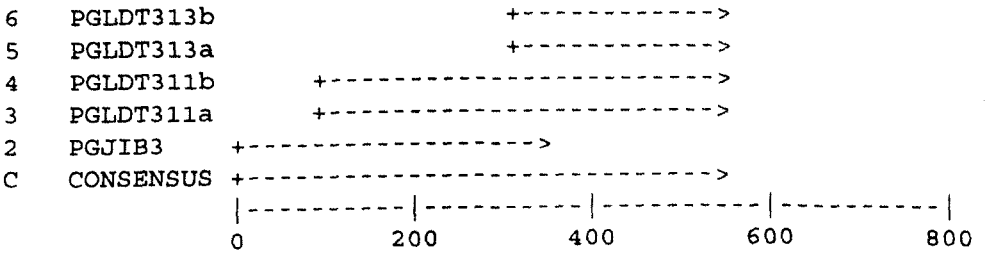

Contig: pgjibca

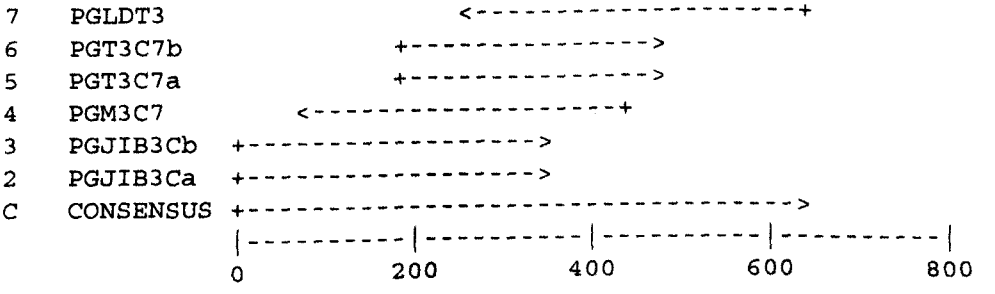

Contig: pgsp6ina

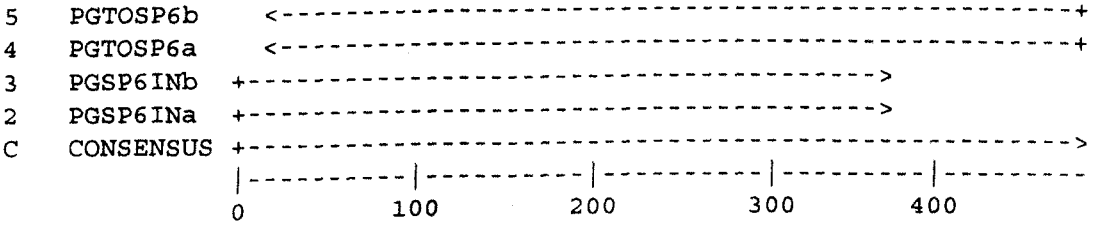

Appendix 10.8.

The sequence of LD07701 and the location of the primers used to sequence it.

LD07701 sequence and PRIMER list. Arrows (>>) indicate direction of priming. Complementary strand primers have their sequence listed above that of the cDNA. Primer identifiers are next to the primer.

```
   1  TTAACTTACT CGCAAG.ATG .AATG.AAGC GG.AAATATC GGTGGG.AAA
  51  ACCCTTATCA CTAATGGAAA ATGCCAATAA CAAGCTGCTA TCTCCTCCCA
 101  TCCAARAAAA ATGGGCTGTA ACAGTTGTCC CTATATACAC GCGTAAAACT
 151  TATACATATA TAGTAAAGCT GGATAACTCC GATTTTCCCA AGAACTCAAG
 201  AAAACTACTC ACACACGCTA CAATTTCAAT GGTTTCTTCA GTGTCGTGCA
                                                 LD77A >>
 251  GCTAAGTAAA AGGGAAAACA AGTTGGAGGG AGAAGATTGA AGATCGTGGA
 301  TGGCCTTAGA TATCATTTCC AAACTATGTT CTGCTCAGAG SMAAGGCCCA
 351  AATAAAAGGA CAAAARGCCG GGATATCCAA ATGGG.AACT TACATTTTTA
 401  TCTGTCAAAA TTCAATTGAG CTTTAAACTA AAGNATAGAT CGAGCAAAAA
 451  ACGAAAATAA AAAAAAAACA AAAAAAAAAT GGGAAGTAAA AACTTGNAAC
 501  AAAAAAAAGA AGGAG.AAGA GTAAGAAATA CAGNAAAGGG AATCGCATTG
 551  TTTCTACATA TTACTTATAA ATGTGCCGTT TATAGGATGT CTACAATTAT
 601  ATACAACAAA TATAGGATAT ATACCTAGGA TATATAATCA GGATCGAAAT
 651  CGAAGCTAGG AACAGCAATT TGCACAACTC TTCCTAAAGG GAAATAAAAG
 701  GATAAAAATA CAAATCTAAA TCTAACTAAC GATTAAATTA CATATATGCC
        LD77B >>
 751  ACAATTACCG AGATTTCAAG RAGTGGACGG ACTAACTCCA AGCAATT.AA
 801  AACGTTATAT TTGAAATAAC TTATGAACTT ATGATMCCAT ATATGTATGT
 851  GTGTACTCTA TACTCTTCCA ACTAGACCCA GAGTCCCACT CGAACCCGGA
 901  CCACATGCGC GATCCACATA GCCATTAGCC CACAAACACT CAATCCACAC
 951  AATACACACA ATCCACACTC GACTTAGTGT TCCAAATGCG CATCGGATCA
1001  GATCGGATAA CGAACCCCTT AGCTGAAATT CGACTAGCAA AATCAATACG
1051  TTAGTAACAC TTATTCGTGC GTTAAGATTA GGGAGATCAT CTGGTACATA
                <<AGTTGG TTTTACGGCC CA| LD77C
1101  CCTTACTTTA AAAATCAACC AAAATGCCGG GTAATTAATC AATAAAATAC
1151  ATATTATTAG TTCTAATCTA AGAGGAGTAA ACAAAAACAA AACAAAAACA
1201  AAAGGAAAAC AAAAATACAT CAACATTATG AATAAAGAAA AATAAGCAAC
1251  GTGAGCAACG TAATATGGGA AAT.CTGTAA CTTTGGTGAT CTTTTTAAAT
1301  GTTATTAGTA AAAGAAGGCA AAACAAAATC AAGTTTAATG ACGAATACAA
1351  ATCAAACCAG TTTTAAATGT GACTTAAATT ACGACGTAAA CGACATTTTT
1401  CCNCAACATT ATATGTGTAA ACAAGACGAA AAAAAAAAAA AAAAAA
```